

Utah State University

DigitalCommons@USU

Reports

Utah Water Research Laboratory

January 1982

Salt Loading from Efflorescence and Suspended Sediments in the Price River Basin

David S. Bowles

Hooshang Nezafati

Rao K. Bhasker

J. Paul Riley

R. J. Wagenet

Follow this and additional works at: https://digitalcommons.usu.edu/water_rep



Part of the [Civil and Environmental Engineering Commons](#), and the [Water Resource Management Commons](#)

Recommended Citation

Bowles, David S.; Nezafati, Hooshang; Bhasker, Rao K.; Riley, J. Paul; and Wagenet, R. J., "Salt Loading from Efflorescence and Suspended Sediments in the Price River Basin" (1982). *Reports*. Paper 585.

https://digitalcommons.usu.edu/water_rep/585

This Report is brought to you for free and open access by the Utah Water Research Laboratory at DigitalCommons@USU. It has been accepted for inclusion in Reports by an authorized administrator of DigitalCommons@USU. For more information, please contact digitalcommons@usu.edu.



SALT LOADING FROM EFFLORESCENCE AND SUSPENDED SEDIMENTS
IN THE PRICE RIVER BASIN

by

David S. Bowles, Hooshang Nezafati, Bhasker Rao K.,
J. Paul Riley, and R. J. Wagenet

The work on which this report is based was supported with funds provided by the State of Utah and by the U.S. Department of the Interior, Office of Water Research and Technology under P.L. 95-467, Project No. B-172-Utah, Grant No. 14-34-0001-9099.

WATER RESOURCES PLANNING SERIES
UWRL/P-82/05

Utah Water Research Laboratory
College of Engineering
Utah State University
Logan, Utah 84322

May 1982

Contents of this publication do not necessarily reflect the views and policies of the Office of Water Research and Technology, U.S. Department of the Interior, nor does mention of trade names or commercial products constitute their endorsement or recommendation for use by the U.S. Government.

ABSTRACT

Salinity control is a major component of water management in arid climates and irrigated areas and one of particular concern in the Colorado River Basin. The salts enter the water as it flows over land or moves through the soil or geologic formations. The principal salt collection processes are 1) dissolution from the soil surface during runoff events, 2) transpiration of soil water leaving salt residuals, 3) efflorescence left by evaporating seepage and then dissolved by subsequent runoff, 4) dissolution with weathering of fixed bed channels, 5) salts released by sediments entering the channel from sheet, gully, and bank erosion, and 6) deep percolation through saline aquifer reaching the stream as base flow. This study examined processes 3 and 5.

Salt efflorescence was examined by field observation and instrumentation, laboratory experiments, and mathematical modeling. The field data showed near saturation conditions of sodium sulfate waters below crusts of densities between 0.14 and 0.36 g/cm² and which formed over about a 10-day period following channel cleaning by storm runoff. Laboratory data on salt crusting in soil columns were also used in developing a model which when applied to the Price River Basin estimated that no more than 7.5 percent of the total salt loading comes from salt efflorescence being carried away in the stream flow. The conditions favorable to the accumulation of salt efflorescence are highly saline water just below the soil surface and a source of heat for vaporizing the water.

Salt release from suspended sediments was studied by laboratory experimentation with sediment material obtained from various locations in the Price River Basin. The Buckingham Pi Theorem was employed to derive relationships expressing the EC of a sediment water system as a function of the controlling factors. The results were presented in two salt release equations, one excluding the effect of initial EC and the other providing for initially saline solutions. The salt release equations were incorporated into an adapted version of the Watershed Erosion and Sediment Transport (WEST) model and applied to a small tributary of Coal Creek. Extrapolation to the entire Price River Basin led to an estimate that about 0.50 percent of the total annual salt load is released from suspended sediments.

This study concludes that surface salt sources produce a relatively small fraction of the total loading. Future studies need to go underground. They need to quantify and examine the flow lines of water movement from mountain source and valley floor recharge areas to points of emergence as base flow in the larger stream channels. They need to investigate the aquifers and their soluble salt content.

TABLE OF CONTENTS

| Chapter | | Page |
|---------|--|------|
| I | THE PRICE RIVER BASIN AND THE COLORADO RIVER SALINITY PROBLEM | 1 |
| | Introduction | 1 |
| | Salt Sources | 1 |
| | Salt Loading by Natural Processes | 1 |
| | Salt Loading by Human Activity | 3 |
| | Problems Caused by River Salinity | 3 |
| | Data on the Problem | 3 |
| | Response to the Problem | 3 |
| | Future Threat | 5 |
| | Potential Control Measures | 5 |
| | Specific Introduction to the Present Study | 5 |
| | The Problem | 5 |
| | Study Objectives | 6 |
| II | STUDY AREA | 9 |
| | General | 9 |
| | Climate | 9 |
| | Streamflow | 11 |
| | Fluvial Sediment | 11 |
| | Geology | 11 |
| III | LITERATURE REVIEW | 13 |
| | Salinity Processes and Sources in the Price River Basin | 13 |
| | Importance of Price River Salinity | 13 |
| | Salinity Studies in the Price River Basin | 13 |
| | Salt Efflorescence | 14 |
| | Solute Transport Models | 16 |
| | Unsaturated Soil Moisture Flow | 16 |

TABLE OF CONTENTS (CONTINUED)

| Chapter | | Page |
|---------|--|------|
| | Vertical Flow Studies | 17 |
| | Solute Movement According to the Theory of Miscible Displacement. | 17 |
| | Salt-Sediment Relationships | 20 |
| | Sediment Yield. | 22 |
| | Sediment Transport | 23 |
| | Modes of Sediment Transport | 23 |
| | The Bed Load Transport | 23 |
| | Suspended Sediment Transport | 23 |
| | Total Sediment Load | 25 |
| | Role of Dimensional Analysis | 26 |
| | Buckingham Pi Theorem | 26 |
| | Characteristics of the Pi Terms | 26 |
| | Conclusion | 27 |
| IV | SALT EFFLORESCENCE EXPERIMENTS | 29 |
| | Field Studies | 29 |
| | Laboratory Experiment | 30 |
| | Aerial Observation and Photography | 32 |
| V | MODEL OF SALT EFFLORESCENCE GROWTH | 33 |
| | Introduction | 33 |
| | Water Flow | 33 |
| | Equation | 33 |
| | Top and Bottom Boundary Flux of Water | 34 |
| | Salt Transport | 35 |
| | Equation | 35 |
| | Top and Bottom Boundary Conditions for Solute Concentration | 37 |
| | Chemical Equilibrium | 37 |
| | Ion-Pair Formation | 39 |
| | Modeling Principle | 39 |
| | Model Limitations | 39 |
| | Recommendations | 40 |
| VI | RESULTS OF SALT EFFLORESCENCE STUDY | 41 |

TABLE OF CONTENTS (CONTINUED)

| Chapter | | Page |
|---------|--|------|
| | Field Data | 41 |
| | Laboratory Data | 43 |
| | Model Results | 44 |
| | Contribution of Salt Efflorescence to Overall Salinity | 55 |
| VII | LABORATORY COLLECTION OF SALT SEDIMENT DATA | 57 |
| | Introduction | 57 |
| | Sediment Materials | 57 |
| | Salinity Measurement Procedure | 57 |
| | Structure of Laboratory Experiments | 57 |
| | Recirculating Flume Experiments | 57 |
| | Mixing Tank Experiments | 58 |
| | Multiple Stirrer Experiments | 60 |
| VIII | SALT RELEASE CHARACTERISTICS OF PRICE RIVER BASIN SEDIMENTS | 61 |
| | Introduction | 61 |
| | Salt Release Characteristics by Sediment Source | 61 |
| | Factors Controlling Salt Release from Upland Soil Material | 61 |
| | Laboratory Approach | 61 |
| | Effect of Dilution | 62 |
| | Effect of Particle Size | 64 |
| | Effect of Mixing Velocity | 68 |
| | Interaction between Mixing Velocity and Particle Size | 71 |
| | Effect of Initial EC | 72 |
| IX | SALT-RELEASE EQUATIONS | 77 |
| | Introduction | 77 |
| | Application of Buckingham Pi Theorem | 77 |
| | Inclusion of Initial EC (EC_0) | 80 |
| | Testing the Equations | 81 |
| | Performance of Equation 74 with Higher Dilution Factors | 82 |
| | Performance of Equation 74 with Smaller Particle Sizes | 85 |
| | Extrapolation of Equation 74 to Larger Systems | 87 |
| | Performance of Equation 74 in Initially Saline Solutions | 88 |

TABLE OF CONTENTS (CONTINUED)

| Chapter | | Page |
|---------|--|------|
| | Testing Equation 79 and Its Comparison with Equation 74 | 88 |
| | Chapter Summary | 89 |
| X | SALT-SEDIMENT MODEL: DEVELOPMENT AND APPLICATION | 91 |
| | Introduction | 91 |
| | General Requirements of the Salt-Sediment Model | 91 |
| | Selection of the Watershed Erosion and Sediment Transport (WEST) Model | 91 |
| | Modification of the WEST Model | 95 |
| | Salt-Release Submodel | 95 |
| | Basic Assumptions for the Salt-Release Submodel | 96 |
| | Considerations in Applying the Salt-Sediment Model | 97 |
| | General | 97 |
| | Land Simulation Phase (LANDHYD) | 97 |
| | Channel Phase Simulation (CHANNEL) | 98 |
| | Application of the Salt-Sediment Model in the Price River Basin | 98 |
| | General | 98 |
| | Subwatershed Selection | 99 |
| | Model Calibration | 100 |
| | Model Results | 100 |
| | Comparison of Results | 102 |
| XI | SUMMARY, CONCLUSIONS, AND RECOMMENDATIONS | 105 |
| | Summary | 105 |
| | Overview | 105 |
| | Study of Salt Efflorescence | 105 |
| | Study of Salt Release from Sediment | 106 |
| | Conclusions | 106 |
| | Study of Salt Efflorescence | 106 |
| | Study of Salt Release from Sediment | 107 |
| | Recommendations | 108 |

TABLE OF CONTENTS (CONTINUED)

| Chapter | Page |
|--|------|
| SELECTED BIBLIOGRAPHY | 111 |
| APPENDIX A: WATER CONTENT AND CHEMICAL ANALYSIS DATA FOR THE 27-COLUMN EXPERIMENT | 119 |
| APPENDIX B: EXPERIMENTAL DATA | 127 |
| APPENDIX C: DATA FOR ANALYSIS OF SUMMER STORMS IN THE PRICE RIVER BASIN | 141 |

LIST OF FIGURES

| Figure | | Page |
|--------|--|------|
| 1 | Weighted average dissolved solids concentration, Colorado River at Imperial Dam | 4 |
| 2 | Sketch of a typical salt efflorescence crust | 7 |
| 3 | The Price River Basin of east-central Utah | 10 |
| 4 | Taxonomy of solute transport models | 16 |
| 5 | Simulation of solar heat input using infrared lamps | 31 |
| 6 | Sketch of an experimental column for growing salt efflorescence | 31 |
| 7 | Electrical conductivity-total dissolved solids relationship | 38 |
| 8 | Accumulation of salt efflorescence with time, as measured by efflorescence density | 42 |
| 9 | Effect of salt crust formation on evaporation of saline soil water | 44 |
| 10 | Comparison of accumulative evaporation from soil columns saturated with distilled and saline waters | 45 |
| 11 | Electrical conductivity of saturation extract versus depth for soil columns saturated with distilled and saline waters after drying for 14 days | 46 |
| 12 | Moisture content vs depth for soil columns initially saturated with distilled and saline waters after drying for 14 days | 46 |
| 13 | Predicted and measured profiles for total calcium at various time periods | 47 |
| 14 | Predicted and measured profiles for total magnesium at various time periods | 48 |

LIST OF FIGURES (CONTINUED)

| Figure | | Page |
|--------|---|------|
| 15 | Predicted and measured profiles for total sodium at various time periods | 49 |
| 16 | Predicted and measured profiles for total potassium at various time periods | 50 |
| 17 | Predicted and measured profiles for total chloride at various time periods | 51 |
| 18 | Predicted and measured profiles for total sulfate at various time periods | 52 |
| 19 | Predicted and measured profiles for volumetric water content at various time periods | 53 |
| 20 | Cross-section of the mixing tank | 58 |
| 21 | Comparison of the salt release characteristics of channel bank and valley floor sediments | 62 |
| 22 | Effect of dilution factor on salt release in the mixing tank apparatus | 63 |
| 23 | Effect of dilution factor on salt release in the multiple stirrer system | 64 |
| 24 | Plot of log EC versus log t showing how the slope of the regression lines are in increasing order for decreasing soil to water ratios | 65 |
| 25 | Effect of particle size on salt release from channel bank material | 66 |
| 26 | Effect of particle size on salt release from channel bank material | 67 |
| 27 | Effect of mixing velocity on salt release | 69 |
| 28 | Effect of mixing velocity on salt release from soil material in the multiple stirrer apparatus. | 70 |
| 29 | Effect of initial EC on salt release | 73 |
| 30 | Effect of initial EC on salt release rate as compared with the rate in deionized water | 74 |
| 31 | Effect of initially saline solutions on the salt release | 75 |

LIST OF FIGURES (CONTINUED)

| Figure | | Page |
|--------|--|------|
| 32 | Cumulative dilution effect on salt release from soil samples in the mixing tank experiment . . . | 75 |
| 33 | Plots of Π_1 versus Π_2 with Π_3 held constant at six different values | 78 |
| 34 | Plot of Π_1 versus Π_3 with Π_2 held constant . . . | 78 |
| 35 | Plot of $\log \Pi_1$ versus $\log \Pi_2$ with Π_3 held constant at six values | 79 |
| 36 | Plot of $\log \Pi_1$ versus $\log \Pi_3$ | 80 |
| 37 | Comparison of the predicted and measured EC using Equation 74 | 82 |
| 38 | The linear regression of predicted and measured values of EC using Equation 74 | 83 |
| 39 | The linear regression of predicted and measured values of EC using Equation 74 | 83 |
| 40 | The linear regression of predicted and measured values of EC using Equation 74 | 84 |
| 41 | Comparison of predicted and measured EC using Equation 74 on data from a replicated run . . . | 84 |
| 42 | Comparison of predicted and measured EC values using Equation 74 over a higher dilution factor range of 0.05-0.2 | 85 |
| 43 | Comparison of predicted and measured EC using Equation 74 on dilution factor range 0.1-2.0 . . . | 86 |
| 44 | Comparison of predicted and measured EC using Equation 74 with coefficients: $k = 0.09$, $a = 0.604$, and $b = 0.123$ | 87 |
| 45 | Comparison of the predicted and measured EC using Equation 74 applied to data obtained from the mixing tank apparatus | 88 |
| 46 | Comparison of measured EC with values predicted using Equation 74 for deionized water solutions with initial ECs of 602, 1125, and 2125 $\mu\text{mho/cm}$ at 25°C | 89 |

LIST OF FIGURES (CONTINUED)

| Figure | | Page |
|--------|--|------|
| 47 | Comparison of predicted and measured EC using Equations 74 and 78 | 90 |
| 48 | Comparison of predicted and measured EC using Equation 78 in the four different saline solutions | 90 |
| 49 | General requirements of the salt sediment model | 92 |
| 50 | WEST model data management system | 93 |
| 51 | Source-zones superimposed on the infiltration capacity function | 94 |
| 52 | Processes simulated in a research | 95 |
| 53 | Organization of the LANDHYD (land phase) of the salt-sediment model | 97 |
| 54 | Organization of CHANNEL (channel phase) of the salt-sediment model | 98 |
| 55 | Subwatershed in the Coal Creek subbasin | 99 |
| 56 | Comparison of observed and simulated flows from a storm on August 25, 1980 | 101 |
| 57 | Comparison of observed and simulated flows from a storm on July 18, 1978 | 101 |
| 58 | Flow, suspended sediment, TDS, and salt load predicted by model for storm on August 25, 1980 | 103 |
| 59 | Flow, suspended sediment, TDS, and salt load predicted by model for storm on July 18, 1978 | 103 |

LIST OF TABLES

| Table | | Page |
|-------|--|------|
| 1 | Water and salt budgets of the central Price River Basin | 14 |
| 2 | Annual water and salt yields for the Price River at Woodside, Utah, for selected years | 15 |
| 3 | Saturation extract analysis of soil used in experimental columns | 30 |
| 4 | Composition of saline water used in experimental columns | 32 |
| 5 | Results of soil water analysis in ephemeral channel bed | 41 |
| 6 | Results of chemical analysis of efflorescence. | 41 |
| 7 | Accumulation of salt efflorescence as measured by salt efflorescence density, with time, in Bitter Creek. | 42 |
| 8 | Soil solution EC measurements in Bitter Creek | 43 |
| 9 | Chemical analysis of the soil material upland of the channel | 58 |
| 10 | Summary of the laboratory experiments | 59 |
| 11 | Experimental data on increase in conductivity with time for various dilution factors | 68 |
| 12 | Summary of curve fitting analyses of data on increasing salinity concentration with time | 69 |
| 13 | The apparent equilibrium EC in solutions with different particle size fraction and dilutions as affected by mixing process | 71 |
| 14 | The result of sieve analysis to determine the grinding effect of mixing | 72 |

LIST OF TABLES (CONTINUED)

| Table | | Page |
|-------|---|------|
| 15 | Results of chemical analysis of water samples taken from two major creeks within the Price River Basin | 73 |
| 16 | Cumulative salinity concentrations with five soil sample additions in the mixing tank experiment | 76 |
| 17 | The measured and predicted values of EC in $\mu\text{mho/cm}$ at 25°C using Equation 74 | 81 |
| 18 | Coefficients in Equation 74 as determined for different ranges of the dilution factor | 86 |
| 19 | Data on predictability of EC from Equation 74 for smaller particle sizes | 86 |
| 20 | Coal Creek flow, sediment and salinity data for two storms | 100 |
| 21 | Parameter values calibrated for LANDHYD | 102 |
| 22 | Comparison of the estimated percentage of total annual salt load at Woodside with respect to source | 103 |

CHAPTER I

THE PRICE RIVER BASIN AND THE COLORADO RIVER SALINITY PROBLEM

Introduction

The growing spectre of increasing river salinity causing increasing economic losses to users of the Lower Colorado River has intensified interest in salinity control programs in the Upper Basin. Much of the salinity loading occurs through natural processes. Additional loading results from human water development; 1) placing water flow paths in greater contact with natural salt sources, and 2) increasing evapotranspiration or consumptive use. A salinity control program requires identification of the major salt sources (locations where water accumulates salts) and quantitative understanding of the major salt loading processes (expressions of how salt loading at a given location is influenced by various factors and changes over time). From this information, one can formulate effective designs for reducing salt loadings.

This study examines salt loading by natural processes on the valley floor of the Price River Basin of Central Utah. Particular emphasis is given to salts entering the stream with the sediment load, and salts dissolved from crusts of salt efflorescence that form in ephemeral channels and elsewhere on the ground surface between storms.

Salt Sources

Salt Loading by Natural Processes

The Price River, typical of many Colorado tributaries, flows out of the

relatively small mountainous fraction of the basin and across a desert valley to its junction with the Green River. The streamflow emerging from the mountains enters the valley with an average salinity concentration of about 1000 mg/l. On the valley floor, additional flows entering the stream add to the salt load even as evapotranspiration and infiltration reduce flows by about 35 percent. The combined effect is an average salinity concentration of about 2500 mg/l at the mouth of the river (Riley et al. 1982b).

The salinity, whether from the mountains or the valley, originates in salts leached from underlying soils and rocks. The relatively high annual precipitation on the weather-resistant igneous and metamorphic rocks of mountain areas produces greater runoff with relatively lower dissolved solids concentrations. In spite of the low concentrations, high runoff volumes from large areas make these uplands a major salt source, measured in tons, in the Price River Basin and other Colorado tributaries.

Underground runoff also occurs from the mountains into aquifers underlying the valley areas. The amount of such runoff, its salt content when entering the valley, the salt loading it collects from valley formations, and how these natural flowpaths and loadings are altered by human development are all unknowns and deserve greater attention than has been given them in previous work (CH2M Hill 1982).

The relatively low precipitation on the valley floor produces much less

runoff, but the runoff that occurs has much higher dissolved solids concentrations. Even though the valleys produce less salt tonnage than do the mountains, the higher concentrations promise greater economy for salinity control measures. Hence, valley salt sources need to be identified and examined in planning a salinity control program.

Nearly 25 percent of the valley floor of the Price River Basin is underlain by Mancos Shales. These marine formations are erodable sediments with a high soluble salt content. Other soils contribute lesser but still significant salt loadings.

The principal processes loading salinity from the soil to the stream are:

1. Salts dissolve from the soil surface during surface runoff from cloud-burst storms.

2. Evapotranspiration brings salts to the surface with the soil water and leaves them there.

3. Water infiltrates saline formations, return to small ephemeral streams with dissolved salts, and evaporates under the desert sun to leave a white salt efflorescence crust that is dissolved and carried away by the next runoff event.

4. Salts are dissolved from fixed-bed channels during runoff events at rates that are greatest at the beginning and decline over the course of a hydrograph. Between storms, natural weathering of the bed material sets the stage for increased mineral dissolution at the beginning of the next storm.

5. Salts are exposed and dissolved during runoff events as erosion eats into the surface of soil formations and the grinding action of flowing water makes the particles progressively finer, exposing additional minerals to dissolution. This exposure and dissolution

occur with the sheet erosion from the soil surface, the gulley erosion that forms microchannels, and the degrading of the bed and cutting of the banks in larger streams. As flows increase downstream, the channels become more deeply entrenched, causing undercutting and mass wasting from the sides of the channels, and greater sediment and salt loads.

6. Waters infiltrating more deeply into underlying saline formations dissolve salts, travel longer distances underground, and emerge as the sustained low flows of the larger streams. Also on these larger streams during high flows, water enters bank storage and dissolves soluble salts contained in the bank material. Afterward, the waters draining from bank storage, which now contain salts dissolved from the surrounding alluvium (perhaps deposited there since the last storm by processes mentioned above), emerge and add salinity to the base flow. Recharge and water use changes can substantially alter the depth of flow lines underground, and, thereby, the formations penetrated, and the salinity of the base flow.

Of these six processes, the first two are diffused over the land surface. The third occurs in ephemeral streams of a size large enough to intercept interflow but not large enough to have permanent base flow. The fourth and fifth occur in channels of all sizes from the small rills left after a storm by gulley erosion to the largest streams. The sixth process is associated with only a few large perennial streams.

Studies have pursued better understanding of the workings of these processes and sought to estimate their relative magnitude. According to studies of land processes contributing to diffuse salinity production, less than 5 percent of the total salt load comes from the summed contributions of overland flow (Ponce 1975), natural vegetation transpiration (Malekuti

1975), and the sediments eroded by microchannel flow (White 1977). According to Dixon (1978), salt loadings from larger channels (Process 4) are unlikely to be more than another 5 percent. Riley et al. (1982b) list the formation and dissolution of efflorescence, salt release during sediment transport, and deep percolation as the primary salinity sources remaining unquantified. Since the above quantities are small, one or more of these last three must be the primary natural salinity sources from the valley floor of the Price River Basin.

This study examines the first two of these. Should they, too, prove relatively minor, effluent base flow would be left as the primary natural salinity source.

Salt Loading by Human Activity

Man's ability to manage hydrogeochemical processes within the waters of a river system to reduce salt transport is limited by the constraints imposed by nature. On the other hand, human activity (agriculture, mining, industry, urban development, etc.) can have far reaching effects on river salinity.

The effects of salinity on water users and natural aquatic systems are associated with the concentration of solids dissolved in the flow more than with the total salt load of a river system. Concentrations can be increased either by water losses or by salt loading. Water losses occur as a result of man's consumptive use of water.

Salt loading occurs with the discharge into stream systems of the additional mineral salts in municipal and industrial wastes and in irrigation return flows. Overall, water resources developments in the Colorado River Basin in the forms of municipal and industrial uses, irrigation, construction of reservoirs, and diversions out of the basin have added to salinity concentrations.

Human activity, however, is not the primary focus of this study.

Problems Caused by River Salinity

Data on the Problem

The earliest concerns about the water quality of the Colorado River were over its suitability for irrigated agriculture. As far back as 1903, limited sampling was performed in order to determine salinity levels and evaluate their acceptability for maintenance of crop production. Since 1941, fairly complete records of flow and water quality conditions have been maintained at 17 stations throughout the basin by the U. S. Geological Survey.

The institutionalized reference point for salinity control on the Colorado River is Imperial Dam, where irrigation water is diverted into the Imperial Valley just north of the Mexican border. Average annual salinity concentrations since 1941 are plotted on Figure 1. These show a long term trend (tested as statistically significant at the 5 percent level) toward greater salinity concentrations even though considerable fluctuation occurs as new irrigation development or reservoirs come on line.

Response to the Problem

A water quality condition becomes a problem when something valued by individuals or society is harmed. Damages are experienced through loss of crop production, degradation of environmental quality, corrosion of plumbing, and the like. In the Lower Colorado River Basin, significant damages are occurring (Andersen and Kleinman 1978). Society acts to protect these values (reduce these damages) through the adoption of water quality standards which are aimed at maintaining water quality at levels that are acceptable for various beneficial uses.

The Colorado River water quality problem took on an international dimen-

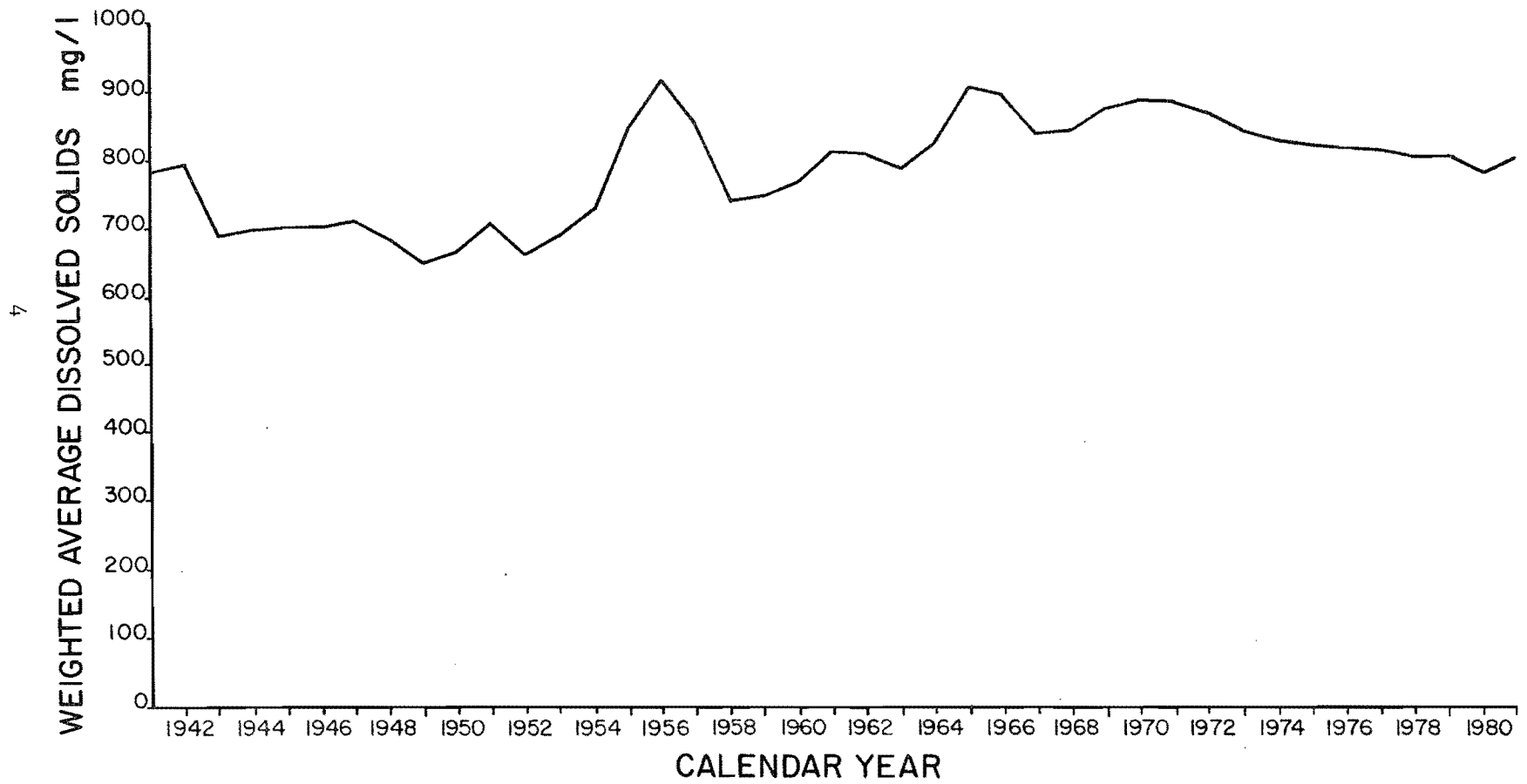


Figure 1. Weighted average dissolved solids concentration, Colorado River at Imperial Dam.

sion in the mid-sixties. The average annual salinity of the water delivered to Mexico at the Northerly International Boundary (NIB) under the treaty signed in 1944, had increased to the point where an action plan was negotiated, between the United States and Mexico. Some projects have been successfully implemented. The Colorado River International Salinity Control Project in the Gila Project area is attributed as having reduced the salt concentration of Colorado water at the NIB from 1641 mg/l in 1962 to 739 mg/l in 1979 (Clinton 1980).

Future Threat

Further river development is expected, in the absence of mitigating measures, to increase salinity concentrations. Several major projects are now under construction in the Upper Colorado River Basin (USDI 1979). The Colorado River Board of California (CRB), the Environmental Protection Agency (EPA), and the U.S. Bureau of Reclamation (USBR) have all developed models to simulate the impact on salinity of future basin development. For example, USBR developed a Colorado River Simulation Model (CRSM) and an Interim Water Quality Simulation Model for the Colorado River. Specific predicted concentrations for the year 2000 at Imperial Dam by the three agencies are respectively 1,340 mg/l, 1,165 mg/l, and 1,250 mg/l (Maletic 1972). All agree that, unless control measures are undertaken, river salinity will substantially increase. Without salinity control measures, damages in the Lower Colorado River Basin are predicted to reach \$45-\$60 million/year.

Potential Control Measures

Many methods have been proposed to reduce salinity in the Colorado River waters. Some would import large quantities of low salinity water from other river basins, desalt deep groundwater brines or sea water and transport the fresh water to the Colorado River,

or augment snow packs through cloud seeding to increase runoff. However, technical and economic analyses show that the most promising approach is to reduce the quantities of salt entering the river system. Specific projects are classified, depending on the source of salt, as 1) irrigation source control projects, 2) point source control projects, and 3) diffuse source control projects.

Irrigation source control projects modify irrigation scheduling and the construction of water conveyance and drainage systems to reduce deep percolation. The salinity control project undertaken in the Wellton-Mohawk Irrigation District is an example.

Point source control projects deal with localized salt sources such as mineral springs or outcrops of soluble formations adjacent to or underlying surface water sources. The Crystal Geyser and Paradox Valley projects are good examples of point source control projects in Utah and Colorado respectively.

Diffuse source control projects are targeted to reduce salt contributions that accumulate over large areas. These conceptual projects have not been sufficiently formulated to have tentative plans or rough cost estimates. Some areas being examined for diffuse source salinity control are the 1) Big Sandy River Unit, 2) Price, San Rafael, and Dirty Devil River Units, 3) McElmo Creek Unit, etc. The purpose of this study is to add to the understanding of the physical processes causing diffuse salt loading and thereby work toward a technology for its successful control at a reasonable cost.

Specific Introduction to the Present Study

The Problem

The specific area examined for sources of diffuse salt loading is the

portion of the Upper Colorado River Basin within the Price River diffuse source control project. The Price River Basin encompasses 4921 square kilometers and is located principally in Carbon and Emery Counties of east-central Utah. Traditionally, Mancos Shales, marine shale deposits which underlie nearly 25 percent of the area, have been considered the prime source of salt in the basin. The Price River contributes approximately 3 percent of the salt load of the Colorado River in less than 1 percent of the water (Iorns et al. 1965).

As presented above, previous studies have eliminated all the identified salt loading processes except efflorescence, salt-sediment transport, and deep percolation as major loading sources. This study examines the first two of these three sources.

Salt efflorescence. Water enroute downstream in a channel may be lost by seepage or evapotranspiration and precipitate appreciable amounts of dissolved solids. Extensive salt deposits are left as flows recede in ephemeral stream channels. Other deposits are left by waters seeping through the banks and evaporating shortly after being exposed to the desert sun. These deposits, called efflorescence, form a crust on the soil surface. The efflorescence crust has irregular thickness but typically rises above the soil surface an average of a few millimeters (Figure 2). The conditions most favorable to the growth of salt efflorescence are highly saline water just below and moving toward the soil surface and a source of heat above vaporizing the soil water. Salt efflorescence accumulates in nearly all the stream channels in the central part of the Price River Basin. It covers the bars, banks, and exposed pebbles within the streams as well as a few areas of land surface away from the streams.

Salt efflorescence grows in thickness between runoff events in an ephem-

eral stream. When storms occur, the flow picks up the easily soluble salt crust. Higher salt concentrations often occur after high water periods when water from bank storage and containing salts dissolved from bank material returns to the stream.

Salt sediment transport. Sediments accumulate from sheet erosion and eroding tributary gullies, erosion of the stream bed, and the sloughing of channel banks. Flows collect salts from the sediments. Whitmore (1976) observed that the rate of salt release from Mancos Shale derived saline sediments in the first two minutes of the water/sediment contact time is as high as 80 to 90 percent of the total salt release. However, the churning action of the flow grinds the sediments progressively finer exposing more salts to dissolution and causing some salt loading to continue. White (1977) found that the salt load resulting from the suspended sediments is directly proportional to the amount of suspended sediment and that "microchannels contribute 3.4 percent of the total salt load of the Price River at Woodside." Dixon (1978) modeled the salinity uptake in natural channels transversing Mancos Shales, found a strong salt-sediment relationship, and recommended further studies.

Study Objectives

The objectives of this study are to identify and quantify 1) the physical and chemical processes of the growth of salt efflorescence in stream channels and subsequent release of salt from this source to the flow, and 2) the major processes involved in the release of salts from suspended sediments. Both objectives were pursued using data from the Price River Basin as input to mathematical models for quantitative process understanding. Both were targeted to assess overall process importance in contributing salt loading to the Colorado River.

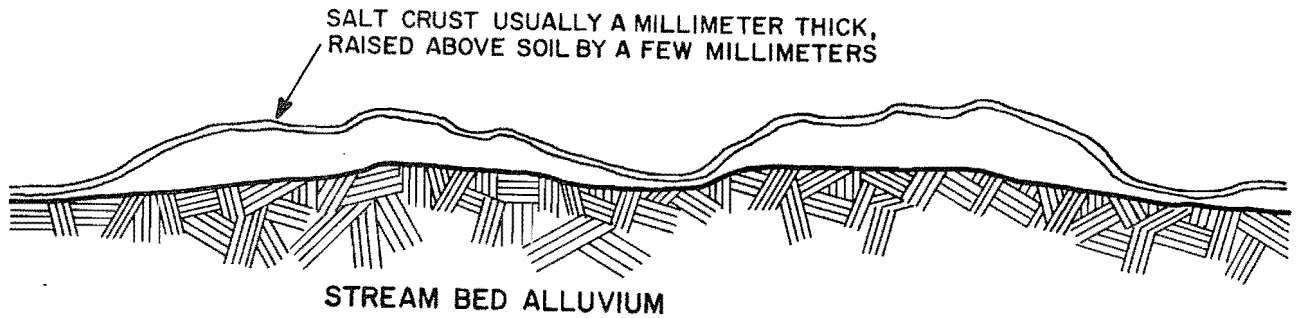


Figure 2. Sketch of a typical salt efflorescence crust.

The growth of salt efflorescence was examined by field instrumentation and data collection, artificial growth of salt efflorescence in soil columns in laboratory, and mathematical modeling techniques using digital computers. Aerial photographs and field observations were employed to assess the aerial extent and pattern of formation of efflorescence.

Salt release from suspended sediments was examined in seven steps:

1. Identify the sediments contributing significant salinity to the Price River Basin.

2. Perform laboratory experiments to identify the important processes of salt release from the sediment material and the factors controlling the rates of those processes.

3. Develop mathematical relationships to express salt release rates from suspended sediments as a function of the controlling factors (identified in 2).

4. Model the process of salt release from suspended sediments utilizing the mathematical relationships (developed in 3).

5. Incorporate the submodel (developed in 4) into a land erosion and sediment transport model to simulate total salt release from suspended sediments in a catchment.

6. Demonstrate the applicability of the model by using it to estimate salt release from suspended sediments for a stream in the Price River Basin.

7. Extrapolate the model results to estimate salt release from suspended sediments for the entire basin.

CHAPTER II

STUDY AREA

General

The Price River Basin (Figure 3), located principally in Carbon and Emery Counties of east-central Utah, encompasses nearly 4,921 km² (1900 mi²). The Price River flows in a generally southeasterly direction and enters the Green River above the town of Green River, Utah. The basin elevation ranges from 3,182 m (10,433 ft) at Monument Peak in the west portion of the basin to approximately 1,280 m (4,200 ft) at the confluence of the Price and Green Rivers.

Vegetation in the basin varies with elevation, amount of precipitation, and soil characteristics. The principal plant communities in the headwaters area are subalpine forest and sagebrush. A mixture of pinyon-juniper, shadscale, and greasewood dominates in the middle and lower portions of the basin (Mundorff 1972).

The principal industry of the Price River Basin is coal mining. The upland areas contain numerous underground mines which serve as the source of coking coal for the western United States. Farming and ranching are concentrated in the central and lower basin. However, low precipitation and poor soils restrict both activities. A total of about 18,600 ha (46,000 acres), or 3 percent of the basin, is irrigated (Mundorff 1972). The irrigated lands are primarily used to raise hay, feed corn, and grains. The range lands are grazed by both cattle and sheep.

Climate

The climate of the basin is continental and semiarid. Weather records show that daily and seasonal temperatures vary over a wide range, with extreme values of 108°F (42°C) and -42°F (-41°C) reported (Mundorff 1972). In the higher elevations of the mountainous area, the growing seasons are short and precipitation is high, leading to an almost alpine climate. In the central part of the basin, precipitation and natural vegetation are sparse and the growing season is much longer.

Normal annual precipitation ranges from 630 to 760 mm (25 to 30 inches) in the headwaters area, to 250 mm (10 inches) at Price and 200 mm (8 inches) in the lower basin (Jeppson et al. 1968). On the highest 30 percent of the area, about 65 percent of the precipitation falls from October through April, and most of it is snow. Summer storms are typically high intensity, short duration thunderstorms, while winter precipitation comes from low intensity frontal storms.

The precipitation in the central and lower basin from May through September is generally associated with convective thunderstorms. These storms, occurring most frequently in August, are generally isolated and produce high intensity events, 25-76 mm/hr (1 to 3 in/hr) for a short duration, 15 to 60 minutes. These high intensity summer and fall storms produce almost all of the surface runoff and erosion on the valley floor.

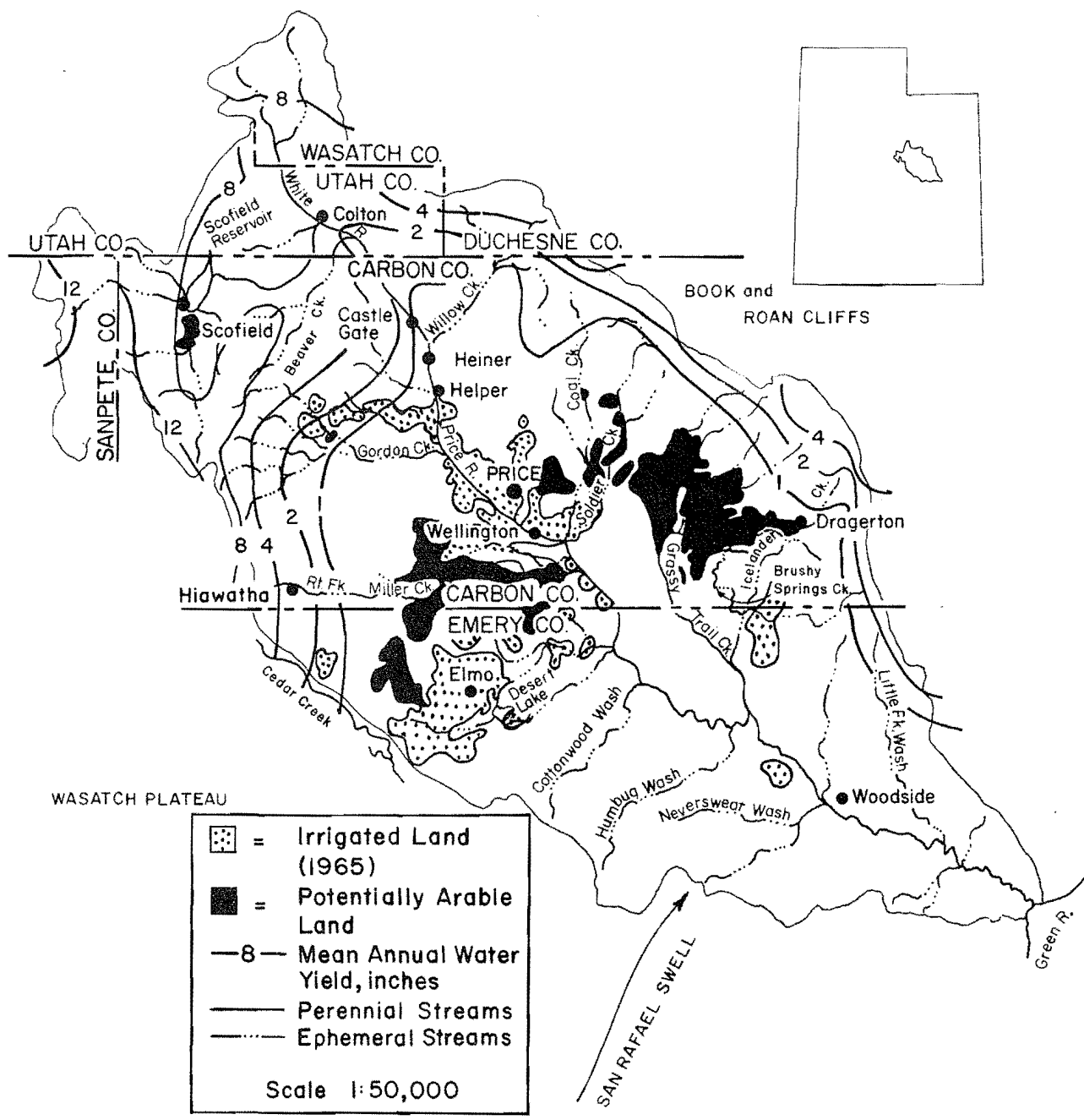


Figure 3. The Price River Basin of east-central Utah. (1 mile = 1.61 km)

Streamflow

The Price River is approximately 214 km (133 mi) long with an average annual discharge of $91.1 \times 10^6 \text{ m}^3$ (73,900 ac-ft). Average annual runoff for the Price River Basin ranges from less than 25 mm (1 inch) in the valley to over 305 mm (12 inches) in the mountains (Figure 3). The majority of the flow from the upper one-third of the watershed originates from snowmelt runoff. Many tributaries that drain the central and lower basin flow only during the early spring and for brief periods following rainstorms. Streamflow declines in the downstream direction because of infiltration and evapotranspiration losses, and irrigation diversions in the central part of the basin.

Fluvial Sediment

Most sediment movement in the Price River Basin occurs during a short period of time each year. Most of the movement is caused by high intensity runoff from thunderstorms. Sediment concentrations and discharge during snowmelt runoff increase significantly from concentrations and discharges during base flow periods, but amounts are low relative to those during runoff from high-intensity thunderstorms (Mundorff 1972).

Sediment concentrations may range from a few hundred to more than 100,000 mg/l (gm^{-3}) during short periods. The

wide range is illustrated with data collected at a sampling site on the Price River. At 9:20 a.m. the sediment concentration at a discharge of 2.5 cfs ($0.07 \text{ m}^3 \text{ s}^{-1}$) was only 408 mg/l (gm^{-3}), and almost 3 hours later during a flash flood the sediment concentration at a discharge of about 150 cfs ($4.24 \text{ m}^3 \text{ s}^{-1}$) was 186,000 mg/l (gm^{-3}) (Mundorff 1972).

Geology

Surface rocks and soils of marine shale origin have a predominant influence on streamflow salinity in the Price River Basin (Mundorff 1972). The Mancos Shales, the major marine shale deposit and an important salt source, cover nearly 25 percent of the basin (Ponce 1975). The Mancos Shales are classified in three main members: Masuk, Blue Gate, and Tununk, which are generally separated by sandstone layers. When separating layers of sandstone are missing, the shale is termed "undivided." These strata have a dip of about 10 degrees to the north and west and each member is consequently exposed at some point in the central Price River Basin (Ponce 1975).

Other bedrock units, in descending order, which are potential sources of salinity are the Morrison Formation, Summerville Formation, Curtis Formation, Carmel Formation, Chinle Formation, and Moenkopi Formation (CH2M-Hill 1982). All seven formations outcrop within the basin.

CHAPTER III

LITERATURE REVIEW

Salinity Processes and Sources in the Price River Basin

Importance of Price River Salinity

The Price River is a major salt contributor to the Colorado River system. Of the 90 sampling points in the Colorado River Basin above Lake Powell, the ratio of salt load to flow was highest from the Price River (Blackman et al. 1973). Iorns et al. (1965) reported that the Price River contributes approximately 3 percent of the salt load of the Colorado River but less than 1 percent of the water.

The sources of salt in the Price River Basin are widely diffused. Mundorff (1972), following a detailed survey of salinity in the basin, reported a relatively good quality surface water in the headwater areas and increasing salinity concentrations as flows move downstream. In its headwaters, the total dissolved solids content of the Price River is normally less than 400 mg/l and is predominantly of the calcium bicarbonate type. In the valley, the river crosses various Mancos Shale members; and the average salt concentration increases from 600 to 2400 mg/l. At Woodside, near the confluence of the Price and Green Rivers, the annual average total dissolved solids concentration over a period of 18 years has varied between 2000 and 4000 mg/l and is predominantly sodium sulfate. Mundorff (1972) attributes this deterioration in water quality to drainage from the Mancos Shales, depletions from irrigation which concentrate the salt load, and the

discharge of municipal and irrigation return flows into the river. White (1977) reported suspended sediment and salt loads to be highly correlated, thus suggesting a need to investigate suspended sediments as a source of salinity.

Salinity Studies in the Price River Basin

A large number of investigators have attempted water and salt balances of the Price River Basin hydrosalinity system. Hyatt et al. (1970) modeled water and salt movement through the Price River Basin, using an analog computer, with results presented in Table 1. In contrast, in a report to the U.S. Bureau of Land Management (BLM) and the U.S. Bureau of Reclamation (USBR), Gifford et al. (1975) estimated that agricultural practices account for one-third of the salt outflow from the basin. They also estimated that point sources, such as salt wells and springs, contribute another one-third, and the remaining one-third was assumed to come from natural diffuse sources.

In still another report (USDI 1978), BLM estimated that nearly 40 percent of the salt contribution occurred during spring runoff, 35 percent was from irrigation return flow, and the remaining 25 percent was associated with base flow (see Table 2). Riley et al. (1982b) estimated that nearly 60 percent of the salt loading in the Price River Basin originates in the mountains and the remaining 40 percent on the valley floor area. CH2M Hill (1982) stated that agricultural areas on the valley floor are the primary salt source based

Table 1. Water and salt budgets of the central Price River Basin.

| | Water (Ac ft/yr) | | Salt (Tons/yr) | |
|------------------------------|------------------|----------|----------------|----------|
| | Inflows | Outflows | Inflows | Outflows |
| Measured Surface | 70,000 | 68,000 | 20,000 | 220,000 |
| Unmeasured Surface | 28,000 | | 45,000 | |
| Precipitation | 15,000 | | | |
| Natural Loading | | | 168,000 | |
| Agricultural Loading | | | 15,000 | |
| Subsurface | | 4,000 | | 28,000 |
| Phreatophyte Consumptive Use | | 5,000 | | |
| Evapotranspiration of Soil | | 36,000 | | |
| Total | 113,000 | 113,000 | 248,000 | 248,000 |

Source: Hyatt et al. (1970).

on the premise the subsurface flow from the mountain areas is negligible. The conflicts among these estimates need to be resolved if effective diffuse source salinity management is to be formulated.

Other investigators have studied specific salt loading mechanisms. Ponce (1975) found that the salinity in the runoff was highly correlated with the salt content of the upper one-tenth inch of the soil crust. He developed salt loading functions which relate the total dissolved solids to the precipitation and runoff rates and concluded that overland flow accounts for about 0.5 percent of the salt produced in the basin. Malekuti and Gifford (1978) estimated that saline soil water brought to the ground surface by plants contributes between 0.01 and 0.02 percent of the total annual salt load to the Price River. The salinity pickup characteristics of small channels (called micro-channels and defined as streams of the highest order which receive negligible interflow) were studied and reported by White (1977). He concluded that "micro-channels contribute 3.4 percent of the total salt load of the Price River at Woodside." Based on extrapolations from intensive analysis of salt loading

from channel beds and banks in the Coal Creek drainage on the valley floor, Riley et al. (1982b) estimated the combined loading from overland and channel flow to be certainly less than 10 percent and probably less than 5 percent of the average total.

Salt Efflorescence

Deposits known as salt efflorescence form wherever unsaturated flow carries salt from the soil matrix to a surface where the water evaporates leaving a salt crust behind. Most salt efflorescence forms on channel beds where it can be picked up and carried downstream by subsequent flows. Salts leached from the soil, in part by the emergence of bank storage accumulated during previous high flows, are a source of salt loading. This is a different source than the salt which enters the stream in saturated flow and provides a base flow source to perennial or intermittent streams.

In quantifying salt efflorescence, a distinction is made between salt efflorescence crust density and salt efflorescence density. The first refers to the mass of crust per unit area expressed in $g\ cm^{-2}$. The latter refers to the total mass of salt found

Table 2. Annual water and salt yields for the Price River at Woodside, Utah, for selected years.

| Year | Spring Runoff ^a | | Base Flow ^b | | Irrigation Return Flow ^c | | Annual Total | |
|---------------------------|----------------------------|---------------------|------------------------|---------------------|-------------------------------------|---------------------|----------------------|---------------------|
| | Discharge (ac-ft) | Salt Load (tons) | Discharge (ac-ft) | Salt Load (tons) | Discharge (ac-ft) | Salt Load (tons) | Discharge (ac-ft) | Salt Load (tons) |
| 1966 | 22,530 | 76,900 | 44,090 | 185,200 | 16,250 | 75,700 | 66,620 | 262,200 |
| 1967 | 44,320 | 110,400 | 32,230 | 138,670 | 24,830 | 86,800 | 76,550 | 248,900 |
| 1968 | 61,670 | 109,400 | 39,450 | 166,500 | 34,710 | 122,900 | 101,120 | 275,800 |
| 1969 | 100,950 | 151,100 | 61,460 | 218,530 | 37,400 | 137,000 | 162,410 | 369,500 |
| 1970 | 30,070 | 113,200 | 33,690 | 153,500 | 21,710 | 83,400 | 63,760 | 266,800 |
| 1971 | 23,920 | 69,600 | 28,690 | 112,450 | 18,270 | 67,900 | 52,610 | 182,050 |
| 1972 | 14,820 | 54,580 | 30,730 | 115,710 | 30,380 | 84,000 | 45,550 | 170,290 |
| 1973 | 84,240 | 156,700 | 54,760 | 182,080 | 23,760 | 84,800 | 139,000 | 338,780 |
| 1974 | 14,860 | 51,100 | 24,260 | 99,130 | 11,550 | 44,630 | 39,120 | 150,230 |
| 1975 | 61,970 | 114,400 | 35,570 | 131,320 | 31,790 | 91,500 | 97,540 | 245,720 |
| Average | 45,940 | 100,730 | 38,490 | 150,300 | 25,065 | 87,860 | 84,430 | 251,030 |
| Percent of Annual | 54 | 40 | 46 | 60 | 30 | 35 | 100 | 100 |
| Average Concentration | | 1,612 | | 2,871 | | 2,577 | | 2,186 |
| Average Monthly Discharge | 11,490 | | 4,811 | | 6,270 | | 7,040 | |
| Average Monthly Salt Load | | 25,180 | | 18,790 | | 21,970 | | 20,920 |

^aSpring runoff period used is April, May, June, and July.

^bBase flow period is remainder of year.

^cIrrigation return flow period is July, August, September, and October.

Source: U.S. Department of the Interior (1978).

in a specified depth of soil and is measured in the same units.

A parametric model for simulating the formation of salt efflorescence needs to cover both water movement and salt transport in the unsaturated zone. If water reaches the surface at rates less than the evaporation rate, all the water evaporates leaving the salts behind to form a crust. As the crust impedes movement to the surface and evaporation of continuing unsaturated flow, the formation of salt efflorescence may slow and eventually halt. These latter processes, however, are poorly understood and were a subject of this study.

Solute Transport Models

Unsaturated Soil Moisture Flow

A number of approaches to modeling solute transport has been proposed as shown in Figure 4. The continuity relationship provides a starting point for all of them. The equation of continuity for one-dimensional vertical flow of water in an unsaturated soil is

$$\frac{\partial \theta}{\partial t} = -\frac{\partial v}{\partial Z} \dots \dots \dots (1)$$

in which

θ = volumetric water content (L³/L³)

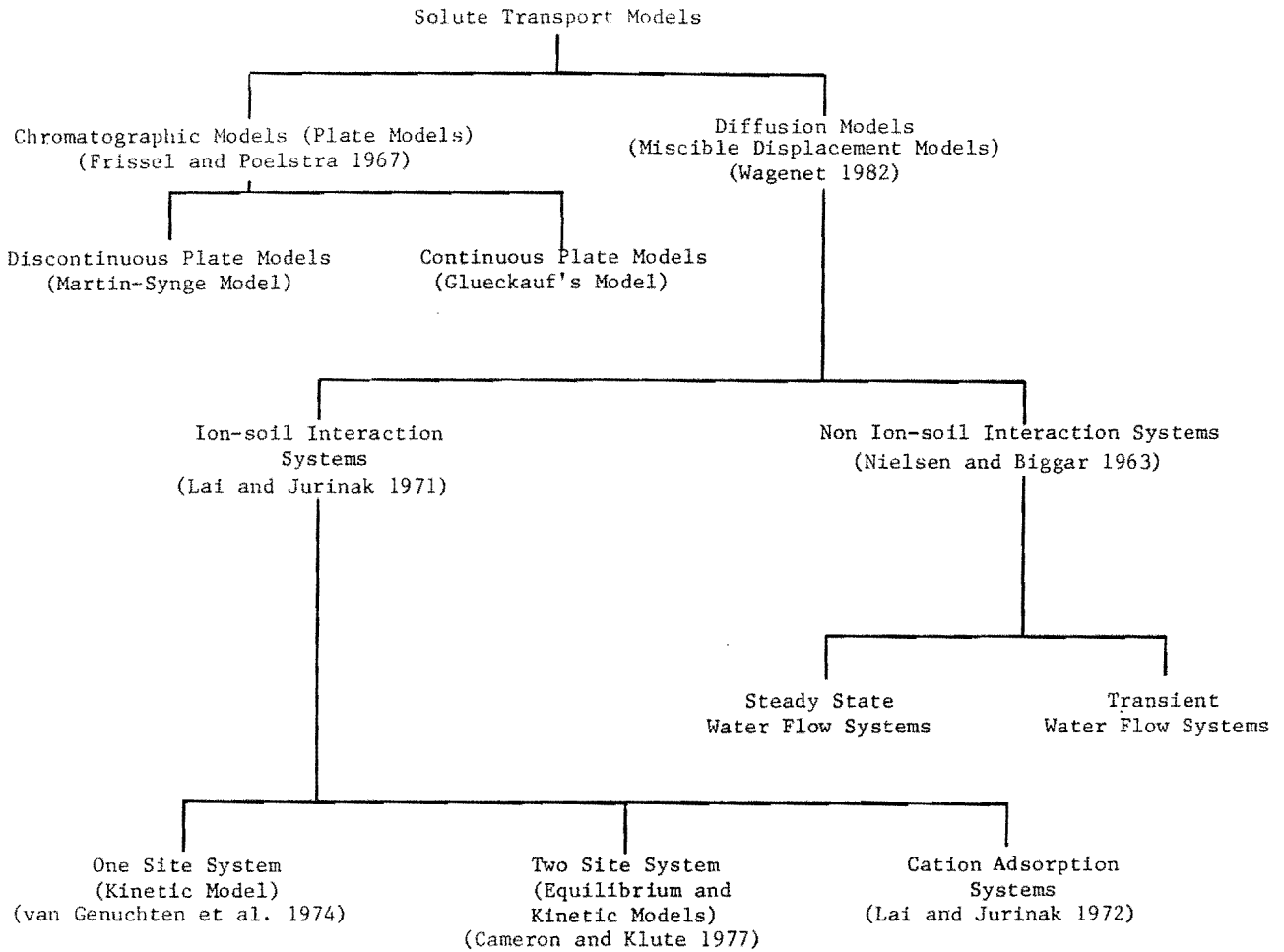


Figure 4. Taxonomy of solute transport models.

t = time

Z = distance

v = volumetric flux of water given by Darcy's equation

$$= - K(\theta) \frac{\partial H}{\partial Z} \dots \dots \dots (2)$$

in which

K(θ) = hydraulic conductivity (L/T)

H = hydraulic head (L)

Let H = ψ + g, where ψ = soil water potential and g = gravity potential. Equation 1 can now be written as

$$\frac{\partial \theta}{\partial t} = \frac{\partial}{\partial Z} \left[K(\theta) \frac{\partial}{\partial Z} (\psi + g) \right] \\ \frac{\partial}{\partial Z} \left[K(\theta) \frac{\partial \psi}{\partial Z} + K(\theta) \frac{\partial g}{\partial Z} \right] \dots (3)$$

Since $\frac{\partial g}{\partial Z} = 1$, and $\frac{\partial \psi}{\partial Z} = \frac{\partial \psi}{\partial \theta} \cdot \frac{\partial \theta}{\partial Z}$ by chain rule, Equation 3 can be rewritten as

$$\frac{\partial \theta}{\partial t} = \frac{\partial}{\partial Z} \left[K(\theta) \frac{\partial \psi}{\partial \theta} \frac{\partial \theta}{\partial Z} + K(\theta) \right] \dots (4)$$

But, $K(\theta) \frac{\partial \psi}{\partial \theta}$ is the diffusion coefficient D(θ). Therefore,

$$\frac{\partial \theta}{\partial t} = \frac{\partial}{\partial Z} \left[D(\theta) \frac{\partial \theta}{\partial Z} \right] + \frac{\partial K(\theta)}{\partial Z} \dots (5)$$

Equation 5 is the nonlinear diffusion equation for vertical unsaturated flow.

Vertical Flow Studies

Vertical movement of water in unsaturated soils has been extensively studied to predict salinity profiles of irrigated soils (Warrick et al. 1971), rate of drainage from soils (Remson et al. 1965), drying of soils (Gardner 1959), and evaporation from soils (Gardner and Fireman 1957).

Gardner and Fireman (1957) conducted some experiments and found that one of two factors controls the rate of evaporation from a soil with a water

table. One is the potential evaporation rate determined by external conditions and approximated by the rate of evaporation from a free-water surface. The other is the rate at which water can be transmitted upward through the soil from the water table to the surface. Obviously, evaporation is limited by the lesser of these two rates. It may be further reduced by a barrier at the soil surface. Gardner and Fireman (1957) showed that the evaporation rate is inversely proportional to the thickness of a surface mulch when the rate of vapor movement through the mulch is less than the potential evaporation rate.

Solute Movement According to the Theory of Miscible Displacement

Miscible displacement theory considers solute movement to be jointly governed by the processes of convection (movement of the bulk soil solution) and diffusion (thermal motion within the soil solution). A substantial number of experimental studies (reviewed by, e.g., van Genuchten and Cleary 1979; Nielsen et al. 1980) have given credibility to this theory. The basic equations can be used in derivations that include many combinations of sources and sinks of solute (i.e., biological and chemical transformations, ion-soil interactions, plant extraction). Depending on the factors included and the assumptions made, the resultant equations vary greatly in complexity. Different ones are solvable by different analytic or numeric methods, with the result that a wide variety of equations and solutions exist in the literature.

According to miscible displacement theory, the flux of solute is the result of the combined effects of diffusion and convection. That is:

$$J_S = J_D + J_C \dots \dots \dots (6)$$

where J = the mass of solute transported through a cross sectional area in a unit time (ML⁻² T⁻¹) and the subscripts S, D, and C represent total solute, that

solute transported by diffusion, and that by convection, respectively.

Fick's first law states that

$$J_D = -D_o \frac{dc}{dx} \quad \dots \quad (7)$$

in which

c = the solute concentration (ML⁻³)

x = distance (L)

D_o = the ionic diffusion coefficient in a pure water system (L² T⁻¹)

The frame of reference for Fick's law in a soil system can be taken as either the entire bulk soil or the solution phase within which diffusion occurs. Considering the entire soil volume, Equation 7 becomes

$$J_D = -D_p \frac{dc}{dx} \quad \dots \quad (8)$$

in which

D_p = the effective diffusion coefficient for any given ion (L² T⁻¹)

and is related to D_o by,

$$D_p = D_o \theta \left(\frac{L}{L_e}\right)^2 \gamma \alpha \quad \dots \quad (9)$$

in which

θ = the volumetric soil water content (L³/L³)

$\left(\frac{L}{L_e}\right)^2$ = a tortuosity factor (Olsen and Kemper 1968)

and γ and α contain the effects of anion exclusion and the charged soil matrix on water viscosity. Values of D_p are always less than D_o . Estimation of D_p for soils has been the subject of a number of studies (e.g., Porter et al.

1960; Kemper and Van Schaik 1966). One empirical representation of D_p (Kemper and Van Schaik 1966) is

$$D_p(\theta) = D_o a e^{b\theta} \quad \dots \quad (10)$$

where a and b are empirical constants reported (Olsen and Kemper 1968) to be approximately $b = 10$ and $0.005 < a < 0.01$. Using Equation 9, Equation 8 can be rewritten as

$$J_D = -D_o \theta \left(\frac{L}{L_e}\right)^2 \gamma \alpha \frac{dc}{dx} = -D_p(\theta) \frac{dc}{dx} \quad \dots \quad (11)$$

Assuming steady, water movement through a homogeneous soil of uniform water content, the total amount of solute transported by convection across a unit area in the direction of flow is given by

$$J_C = -\theta D_m(v) \frac{dc}{dx} + v \theta c \quad \dots \quad (12)$$

where

v = the average interstitial flow velocity (LT⁻¹)

D_m = the mechanical dispersion coefficient (depending only on v)

The first term represents flow by mechanical dispersion and the second term considers transport due to the flow velocity. For one-dimensional flow in a simple nonaggregated porous material, D_m can be considered proportional to the first power of the average velocity,

$$D_m(v) = \lambda |v| \quad \dots \quad (13)$$

where

$|v|$ is the absolute value of v , and $\lambda \approx 0.4$.

At high pore water velocities, D_m is much larger than D_p , and diffusion is completely obscured (Kirida et al. 1973).

Combining Equations 11 and 12 into Equation 6 sums the effects of diffusion and convection as:

$$J_S = - \left[\theta D_m(v) + D_p(\theta) \right] \frac{dc}{dx} + v \theta c$$

$$= -\theta D(v, \theta) \frac{dc}{dx} + qC \quad . \quad . \quad . \quad (14)$$

in which

D = the apparent diffusion coefficient (L^2T^{-1})

q = the volumetric water flux (LT^{-1})

The continuity equation (Kirkham and Powers 1972) states that the rate of change of solute within a finite volume element must equal the difference between the amounts of solute that enter and leave the element. Applying these relationships to Equation 14, and including considerations of ion-soil interaction (i.e., cation adsorption) and sources or sinks of solute (i.e., chemical precipitation-dissolution reactions) one obtains

$$\frac{\partial}{\partial t} (S + \theta C) = \frac{\partial}{\partial Z} \left[\theta D(v, \theta) \frac{\partial C}{\partial Z} \right]$$

$$- \frac{\partial (qC)}{\partial Z} + \phi \quad . \quad . \quad . \quad . \quad (15)$$

in which

S = the concentration of solute in the "adsorbed" phase (ML^{-1})

ϕ = solute movement from source or to sink ($ML^{-3}T^{-1}$)

t = time (T)

Z has replaced x to specifically designate a positive downward coordinate

Equation 15 is the fundamental representation of miscible displacement theory. If the solute does not interact

with the soil ($S = 0$) and solute is neither gained nor lost ($\phi = 0$) the equation may be simplified by dropping these terms.

Solutions generally require a knowledge of one or more of 1) the relationship between soil water content and soil water matric potential energy, 2) the hydraulic conductivity-water content relationship, 3) the functional form of the apparent diffusion coefficient, and 4) the magnitude of the source or sink processes. In laboratory experiments, these relationships have been measured quite accurately, yet the implications of temporal and spatial variations of these relationships in the field are only beginning to be studied. Accurate predictions of solute flux on a field basis from miscible displacement theory is presently limited by this lack of technique for handling variability in field processes.

Nevertheless, several models for describing solute transport under field conditions from the relationships of Equation 15 have been proposed (e.g., Bresler 1973, Warrick et al. 1971; VanDePol et al. 1977). Some consider ion-soil interactions. Adsorption-desorption models generally assume either an equilibrium of the ions adsorbed on the soil with the concentration of the solution (e.g., Lapidus and Amundson 1952; Lai and Jurinak 1971) or at least a situation approaching equilibrium conditions (e.g., Hornsby and Davidson 1973; Cameron and Klute 1977). Some adsorption-desorption models consider only one or two cations interacting with the soil surface at a time. The more realistic representation is to model cation exchange with four (Ca, Mg, Na, K) cations competing for interaction with a negatively charged clay mineral surface. Robbins et al. (1980a) present a cation exchange model for estimating the $\partial s / \partial t$ term in Equation 15.

Soil chemical regimes are usually transient. Irrigation water quality

varies and precipitation supplies water of different ion content. Plant extraction of water concentrates ions in the soil solution, producing changes in ion solubility and the composition of the exchange phase. Description of solute transport must consider these processes, particularly in cases where gypsum or lime are present in the soil profile.

An empirical representation of the soil chemistry for estimating the ϕ term in Equation 15 (Melamed et al. 1977) is

$$\phi = \alpha K (R - C) \quad (16)$$

where K is a transfer coefficient related to salt composition and soil properties, R is the maximum soil solution concentration at which there is no precipitation or dissolution, and $\alpha = 0$ for $S = 0$; $\alpha = 1$ when $S > 0$ or $R > C$. Values of K were determined by curve-fitting to match calculated solute distributions with observed. The value used for K combines the effects of many processes, including cation exchange and precipitation-dissolution reactions. Each application of this model requires recalibration of K for local conditions.

Mechanistic models of soil chemistry have been developed and coupled to descriptions of solute transport (e.g., Tanji et al. 1972; Dutt et al. 1972; Oster and Rhoades 1975; Jury and Pratt 1980; Robbins et al. 1980b). These models are constructed upon the general principles of chemical equilibrium. They usually consider ionic strength to calculate ion activities, represent CaCO_3 -pH- CO_2 relationships, and precipitate and dissolve various solid phases depending upon solubility relationships. These models are constructed to be used as subroutines in numerical solutions of Equation 15, so that solution ion concentrations predicted by transport alone can be adjusted for chemical equilibrium. A good summary of principles and models of

cation and salt movement in soils is available in Wagenet (1982).

In order to use the water flow and salt transport equations to develop digital computer simulation models, it is necessary to write the partial differential equations in numerical form. Finite difference techniques have been widely used for this purpose. Hanks and Bowers (1962) developed a numerical solution to be used in computer simulation of soil moisture flow. Bresler (1973) presented a numerical solution for noninteracting salt transport by approximating the terms in the diffusion-convection equation. Childs and Hanks (1975) incorporated a growing root zone and a growing plant cover as functions of time. Tillotson (1979) numerically approximated the equations describing transient one-dimensional transport of soil-water, nitrogen, and heat.

The literature survey of water flow and salt transport in the unsaturated zone has shown that past work has emphasized transport within the soil profile. In contrast, salt efflorescence occurs at the soil surface. Extrapolation of existing water flow-salt transport models to predict the formation of salt efflorescence requires information on the processes through which efflorescence develops and on the physical and chemical characteristics of the crust that affect those processes.

Salt-Sediment Relationships

In examining the kinetics of salt release from a Mancos Shale derived soil, Jurinak, Whitmore, and Wagenet (1977) found that the initial 72 hours of salt release can be described by three first-order, diffusion controlled reactions. They applied the concept in investigating the applicability of two sets of assumptions in the description of the soil mineral dissolution process. Equation 8 (see also Crank 1975) was rewritten to describe the dissolution of

a soil particle into a rapidly stirred solution with the results:

$$\frac{dC}{dt} = \frac{DA}{L} [C_S - C] \dots (17)$$

in which

A = the total surface area of the material undergoing dissolution per unit volume of water (L²)

L = the thickness of a stagnant boundary layer surrounding the particle and through which diffusion occurs (L)

C_S = the concentration at the surface of the particle which is assumed to be the equilibrium solubility (ML⁻³)

C = the concentration of the uniformly stirred bulk solution into which the particle is dissolving (ML⁻³)

Equation 17 assumes an isothermal closed system with the source material undergoing dissolution being present in amounts well in excess of that required to saturate the solution. This assumption was used by these authors to integrate Equation 17 between appropriate boundary conditions with the results:

$$\ln \left(1 - \frac{C}{C_S} \right) = -kt \dots (18)$$

in which

$$k = DA/L$$

Accordingly, a plot of $-\ln(1 - (C/C_S))$ vs t should produce a line with slope of k if dissolution is a simple diffusion controlled reaction.

Jurinak et al. (1977) also considered concentration as being time and distance dependent during diffusion across a boundary layer of width L . Fick's second law of diffusion:

$$\frac{\delta C}{\delta t} = D \left(\frac{\delta^2 C}{\delta x^2} \right) \dots (19)$$

was integrated to describe the rate of transfer of material across the distance X where $0 < X < L$ and ultimately the rate of change of the concentration of the bulk solution. They used Crank's solution to Equation 19 which expresses the mass M_t of diffusing substance leaving the outer edge of the boundary layer and entering the bulk solution as:

$$M_t = k'' (t)^{1/2} \dots (20)$$

in which

$$k'' = 2 C_S (D/\pi)^{1/2} \dots (21)$$

Since M_t is directly proportional to the concentration of the bulk solution, they further stated that:

$$C = k' (t)^{1/2} \dots (22)$$

in which

k' = a new constant including k'' and additional factors relating concentration to mass

A plot of C vs $t^{1/2}$ should produce a line with a slope equal to k' . The two rate Equations (18 and 22) fit experimental data equally well in describing salt release.

Laronne and Schumm (1977) studied salt release from sediment samples of Mancos Shales in dilutions up to 1:99 (sediment to water ratio). Their data suggested that many mineral particles react as if covered by a slightly soluble coating of iron or silica oxide. A rate expression was derived which provides for more rapid dissolution of sodium and magnesium hydrated sulfates than of gypsum or calcite.

Dixon (1978) studied the salt pickup from flow induced in an ephemeral channel in the Coal Creek subbasin near Price (Riley et al. 1982a). A plot of salt load versus the square root of time indicated a linear relationship, suggesting that the diffusion controlled reaction, reported by Jurinak et al.

(1977) for salt release from soil suspensions, also operates in natural channel systems.

Peterson (1979) monitored the kinetics of salt release from Mancos Shale derived soils by electrical conductivity measurements. The data were analyzed to find mathematical relations that describe how salt release varies with parameters such as particle size and soil to water ratio. He also studied the effect of ionic strength on the kinetics of salt release. The best fitting curves were of the logarithmic form:

$$Y = a t^b \dots \dots \dots (23)$$

Y = EC

t = contact time

a,b = coefficients

Sediment Yield

Sediment yield equals soil erosion less upstream deposition. Erosion is the detachment of soil particles and their movement to a nearby channel. After reaching a channel, the particles are transported downstream as suspended sediment and bed load.

Estimating sediment yield requires study of 1) the geographical variability of precipitation, 2) the amount of runoff, 3) the detachment of soil particles by raindrop impact, or runoff or both, and 4) the transport and storage of sediment on the watershed. There are two major approaches.

The first uses relationships, such as those describing the effect of raindrop energy on erosion, antecedent soil moisture and infiltration on soil erodibility, the mechanisms of rill formation and interrill erosion, and sediment transport by overland flows (Shen 1979). The fundamental processes are expressed for quantitative application to a watershed. Considerable additional

research is needed before a satisfactory operational equation can be proposed.

Examples of needed relationships are the rill and interrill erosion equations of Onstad and Foster (1975), Foster and Meyer (1975), and Foster, Meyer, and Onstad (1977). Negev (1967) developed a model which simulated the entire erosion process including sheet, gully, and channel erosion. Smith (1976) discussed the capabilities and limitations of a deterministic distributed-parameter watershed model to simulate sediment production. He used hypothetical examples to illustrate the effects of erosion on rainfall patterns, slope convergence, and comparative sediment-production, rainfall, overland flow, and channel flow.

Shirley and Lane (1978) derived analytical solutions by solving equations of rill and interrill erosion, sediment concentration (continuity), and the kinematic flow equation by methods of characteristics for the rising, equilibrium, and recession limbs of the hydrograph. Woolhiser and Blinco (1975) modeled erosion from a fallow field by hypothesizing relationships for detachment, entrainment, transport, and deposition of sediment. Williams (1978) developed a model to predict sediment production from agricultural watersheds from an instantaneous burst of rainfall.

Simons, Li, and Stevens (1975), Simons and Li (1976), Simons, Li, and Ward (1977), and Li (1979) developed the most comprehensive model to date. Their model incorporates raindrop erosion, interception, infiltration, ground-surface irregularities, and water-sediment routing. Kinematic routing was used for both overland and channel flows.

The second approach to estimating sediment yield is by regression. Numerous equations have been developed, but by far the most popular is the universal soil loss equation (USLE)

derived by Wischmeier and Smith (1965). This equation has been tested, extended, and modified with data collected from many regions of the United States. Wischmeier and Smith (1978) have revised and extended their earlier handbook on the USLE.

Sediment Transport

Modes of Sediment Transport

The processes of sediment transport have been described by a variety of empirical and semi-theoretical relationships based on the physical and hydrodynamic characteristics of the flow system. Sediment particles are transported by:

1. Surface-creep; rolling or sliding on the bed
2. Saltation; bouncing along the bed
3. Suspension; being carried by the surrounding, fluid

Sediments moving as surface-creep and saltation are supported by the river bed and called bedload. Sediments which are supported by flow are called the suspended load. The "total sediment load" is the summation of the bed load and the suspended load.

A given particle may continually shift among these transport modes as it moves downstream. For example, sediments may be transported by saltation and then suddenly be caught by the flow turbulence and transported in suspension. Experiments have also shown a definite exchange between the moving sediments and sediments on the bed (Einstein 1950).

Water flowing over sediment exerts hydrodynamic forces that tend to move or entrain the grains. The forces that resist entrainment vary with the grain size, grain size distribution, and plasticity of the sediment. When the

hydrodynamic forces reach a value that begins to move the bed grains, a "critical shear stress" or "critical velocity" is said to be reached. Many investigators have presented formulas for defining these critical conditions. In fact, Lelliavsky (1955) reports that Brahms presented a formula for critical velocity in 1753.

The Bed Load Transport

Sediment transport studies prior to 1930 dealt almost exclusively with bed load. Numerous equations were proposed, and they can be categorized among three approaches (Graf 1971):

1. The DuBoys-type equations which are based on shear stress (DuBoys 1879; Shields 1936; Kalinske 1947).
2. The Schoklitsch-type equations which are based on using discharge to estimate the lift force (Schoklitsch 1914 and 1930; Gilbert 1914).
3. The Einstein-type equations which use regression incorporating various factors to estimate the lift force (Einstein 1942 and 1950; Shen 1970).

Suspended Sediment Transport

By integrating concentrations. The discharge of suspended sediment per unit width of channel for uniform two-dimensional flow is given by

$$q_s = \gamma_s \int_0^D U_y C_y dy \quad \dots (24)$$

in which

q_s = the weight rate of suspended sediment discharge between the streambed, $y = 0$, and the water surface, $y = D$ (kg/s)

γ_s = the average weight of the water-sediment mixture (kg/m³)

D = total depth of flow (m)

U_y = the velocity at the level y (m/s)

C_y = the concentration by weight of suspended sediment at the level y (ppm)

y = a measured distance above the streambed (m)

The suspended sediment discharge rate for the entire stream cross-section, Q_s , is obtained by integrating Equation 24 over the cross section to give

$$Q_s = \gamma_s Q \bar{C} \quad . \quad . \quad . \quad . \quad . \quad (25)$$

in which

Q = water discharge (m³/s)

\bar{C} = a velocity weighted average sediment concentration (ppm)

To integrate Equation 24, U_y and C_y must be expressed as functions of y. The customary approach is to describe the velocity distribution by a logarithmic equation and the relative concentration distribution by a gradient-type diffusion equation (Nordin 1970).

The vertical distribution of velocity for fully turbulent flow over a rough boundary is given by

$$\frac{U}{U_*} = 8.5 + 2.5 \ln \left(\frac{y}{K_S} \right) \quad . \quad . \quad (26)$$

in which

U_* = shear velocity (m/s)

K_S = a representative height of roughness elements (m)

An equation for the vertical distribution of concentration was first introduced by Rouse (1937):

$$\frac{C}{C_a} = \left[\frac{a}{(D-a)} \frac{(D-y)}{y} \right]^Z \quad . \quad . \quad (27)$$

in which

Z = empirical exponent expressed as

$$Z = W/(KU_*)$$

W = the fall velocity of sediment (m/s)

K = a universal constant equal to 0.4

C_a = a reference concentration at level y (ppm)

Combining Equations 26 and 27, the equation for transport of suspended sediment per unit width of channel between the level a and the water surface is given by:

$$q_s = \gamma_s U_* C_a \int_a^D \left[\frac{a}{(D-a)} \frac{(D-y)}{y} \right]^Z 2.5 \ln \left(\frac{y}{K_S} \right) + 8.5 dy \quad . \quad . \quad . \quad (28)$$

Einstein (1950) integrated Equation 28 by taking the lower limit of integration to be two grain diameters from the bed, $a = 2d$, and equating the suspended sediment concentration at that level to the concentration of material with diameter d moving as bed load. Einstein tabulated his solution (Einstein 1950). Colby and Hembree (1955) solved Equation 28 in graphical form.

Lane and Kalinske (1941) integrated Equation 24 by calculating an average value for the exchange coefficient (which is required in determining the

concentration profile) and by assuming a logarithmic velocity distribution. They presented the results graphically in the form of Equation 25.

From energy expended. The relationship between the energy in a stream and the quantity of sediment transported was considered by researchers even before the suspended load equations were formulated (Nordin 1970). Bagnold (1966) noted that the sediment transport rate could be equated to a work rate by multiplying by the ratio of the tractive stress needed to maintain transport of the load to the normal stress due to the immersed weight of the load. The resulting equation, after consideration of turbulence measurements, was

$$i = W \left(\frac{e_b}{\tan \alpha} + 0.01 \frac{\bar{u}}{V} \right) \dots (29)$$

or for suspended load only

$$i_s = W \frac{e_s \bar{U}_s}{V} (1 - e_b) \dots (30)$$

in which

i = sum of the bed load and suspended load transport rates (kg/s/m)

i_s = the suspended load transport rate (kg/s/m)

\bar{U}_s = mean velocity of suspended solids (m/s)

\bar{u} = mean stream velocity (m/s)

e_b = efficiency factor for bed load transport

e_s = suspended load efficiency

$$= \frac{\text{suspended load rate}}{\text{stream power}}$$

α = the average angle of encounter between sediment grains

V = the weighted mean fall velocity for suspended material (m/s)

d = flow depth (ft)

S = slope

W = stream power = $\rho d S \bar{u}$ (kg/m/s)

From hydrodynamic concepts.

Hydrodynamic models also have been developed for computation of suspended sediment transport. Owens and Odd (1970) developed a two layer flow and sediment transport model. Computer simulation of unsteady flow and transport was undertaken by Tywoniuk (1969). Based on DeVries model, Kerksen et al. (1977) employed morphological computations to investigate the effects of human interference or geometrical changes in a river or estuary. The model is partly based on the two-dimensional sediment diffusion-convection equation and restricted to non-cohesive and nearly uniform sediment material (Kerksen, Ad Prins, and van Rijn 1979).

Total Sediment Load

There are two methods of computing the total sediment load:

1. Indirect method: computing bed load and suspended load separately and then summing the two components.
2. Direct method: by the equations developed for computation of total sediment load directly.

An example of the direct method is the Watershed Erosion and Sediment Transport (WEST) model developed by HYDROCOMP Inc. for the Environmental Protection Agency (Leytham and Johanson 1979). This model simulates the movement of water and sediment through the land and channel phases of the hydrologic cycle. The WEST model is composed of two separate models, the

ARM model and the CHANL model, linked by a data management system. The ARM model (Donigian and Crawford 1976; Donigian et al. 1977) simulates land phase processes, and CHANL model simulates the instream or channel processes. Hydraulic routing is performed by using kinematic equations. Sediment routing is performed by explicitly modeling the component processes such as scour, deposition, and armoring. Ackers and White's technique (Ackers and White 1973) is used for calculating the potential or ultimate concentration of the cohesionless material, and the works of Camp (1943) and Brown (1967) are used to estimate deposition of the fine cohesion material. The model gave promising results when tested using laboratory data.

Role of Dimensional Analysis

When theoretical methods fail to provide sufficient ordering of the independent variables to set up a successful field measurement program or laboratory experiment, dimensional analysis provides a convenient starting point for structuring experimentation.

Buckingham Pi Theorem

Ancient mathematicians represented multiplication by Π , just as they represented summation or addition by Σ . The Buckingham Pi Theorem (Buckingham 1915) states that the outcome of any complete physical process can be expressed by multiplying independent dimensionless products (Pi terms) combining the variables shaping the physical phenomenon. That is:

$$\Pi_1 = f[\Pi_2, \Pi_3, \Pi_4, \dots] \quad (31)$$

For example,

$$R = K X^{C_1} Y^{C_2} Z^{C_3} \dots \quad (32)$$

where R represents the effect of any set of causes, X, Y, and Z, as their product when raised to some power C_i and multiplied by a dimensionless

coefficient K which may or may not be constant depending on the outcome of the experiment. Field or laboratory experiments are designed to collect data, and the data are used to place numerical values on the coefficients.

Characteristics of the Pi Terms

The pi-terms have the following characteristics:

1. The number of Pi terms equals the number of fundamental variables (measurable physical factors influencing process outcome) minus the number of basic dimensions (distance, mass, time, etc.).

2. Pi terms are mutually independent. This is assured if each Pi term contains a fundamental variable which no other Pi term contains. The fundamental variables in any subset of variables must also be mutually independent.

3. Pi terms are dimensionless.

Pi terms have two distinct advantages for finding a general relationship among pertinent fundamental variables:

1. Pi terms reduce the number of variables to be investigated. This is important because the work required to find the relationship among variables is proportional to the cube of the number of variables. For example, reducing six fundamental variables to three pi-terms reduces the amount of work to 27/216 or about 12.5 percent of its former value.

2. Because Pi terms are dimensionless, regardless of the size of the phenomenon, they apply equally to model and prototype.

Derivation of individual Pi terms.
The Buckingham Pi Theorem is applied by first listing the pertinent fundamental variables and their basic dimensions. Then Pi terms are assembled by inspection in a pattern that satisfies the

three characteristics listed above. In a three Pi terms experiment, for example, we have:

$$\Pi_1 = f[\Pi_2, \Pi_3] \dots \dots \dots (33)$$

A functional relationship such as:

$$\Pi_1 = f[\Pi_2] \dots \dots \dots (34)$$

is found by regressing Π_1 vs Π_2 , while Π_3 is held constant at different values. Adopting a different notation Equation 34 can be expressed as:

$$\Pi_{123}^- = f[\Pi_1, \Pi_2] \dots \dots \dots (35)$$

in which the Π_{123}^- is a functional relationship of three Pi terms obtained by varying Π_1 and Π_2 , and holding Π_3 at a constant value of say Π_3 . The functional relationships between Π_1 and Π_3 , while holding Π_2 constant, can also be determined by regression and expressed as:

$$\Pi_{123} = f[\Pi_1, \Pi_3] \dots \dots \dots (36)$$

The third functional relationship is a constant Π_{123}^- determined by holding both Π_2 and Π_3 constant. The ordering of experiments requiring more than three Pi terms requires a Latin square design (Murphy 1950).

Combination of the Pi terms. The three individual functional relationships described above can be combined by either addition or multiplication. As explained by Murphy (1950), the combination by addition is valid if the difference between ordinates is constant. In the above notation,

$$\Pi_{123}^- - \Pi_{123}^= = \text{constant}$$

or

$$\Pi_{123}^- - \Pi_{123}^= = \text{constant}$$

If two sets of data are taken, each at a different value for a constant Pi term

(i.e. one set with Π_2 and the other set with Π_2^-), then the vertical distance between the two curves must be equal for all values of the Pi term used as the independent variable. For example, if the data plot as straight lines, they must be parallel. The general form of combination for Pi terms by addition is (Murphy 1950):

$$\Pi_1 = \Pi_{123}^- + \Pi_{123}^- - \Pi_{123}^- \dots \dots (37)$$

The combination by multiplication is valid only if the ratio of the ordinates is constant. That is:

$$\frac{\Pi_{123}^-}{\Pi_{123}^=} = \text{constant}$$

or

$$\frac{\Pi_{123}^-}{\Pi_{123}^=} = \text{constant}$$

This means parallel lines on log-log plots of Π_1 versus Π_2 or, as an alternative, on log-log plots of Π_1 versus Π_3 . The combination of Pi terms is performed by (Murphy 1950):

$$\Pi_1 = \frac{\Pi_{123}^- \Pi_{123}^-}{\Pi_{123}^-} \dots \dots \dots (38)$$

The K value in Equation 32 is determined mathematically as a result of combination by multiplication using Equation 37.

Conclusion

Suspended sediments and salt efflorescence are potentially significant sources of salinity loading of the Price River. The literature review, however, found little descriptive information that could be used in quantitative evaluation of these two sources. Experimentation was thus necessary.

CHAPTER IV

SALT EFFLORESCENCE EXPERIMENTS

Field Studies

In the summer of 1979, field sites were visited to study conditions favorable to the formation of salt efflorescence. During the spring and early summer, soluble salt efflorescence accumulates in nearly all stream channels in the central basin. In addition, efflorescence occurs in low lying poorly drained areas, stagnant water ditches, and shallow water table areas.

The conditions observed as favorable for the growth of salt efflorescence are a highly saline water table near the soil surface and a high rate of solar radiation for vaporizing the soil water. Other factors that increase evaporation rates, such as high wind speed and low humidity, may also enhance accumulation of efflorescence.

Soil salinity sensors (Soil Moisture Equipment Corporation, Santa Barbara, California, Cat. No. 5000 A) were installed in the channel bed of Bitter Creek, a small ephemeral drainage near Price, Utah, at 10, 20, and 30 cm depths to monitor changes in electrical conductivity (EC) of the soil moisture during wetting and drying cycles.

Both the water and the efflorescence crust were analyzed in the laboratory for chemical composition. Samples of water saturating the channel bed were collected from small depressions on the ephemeral channel beds of Miller Creek and Bitter Creek. Samples of efflorescence were taken using cookie-cutters. These samples contained varying amounts of nonefflorescent soil material. This

dry sample was powdered by hand. Twenty grams of dry sample were mixed with 350 cc of distilled water. The mixture was shaken for 15 minutes and then allowed to stand for 72 hours. The supernatant liquid was decanted, filtered, and analyzed.

Salt efflorescence crust densities were also measured at several places on channel beds. Large pieces of crust were carefully lifted from the soil surface and brought to the laboratory. They were weighed, and their surface areas were measured. The densities varied between 0.14 grams per cm^2 and 0.36 grams per cm^2 .

The accumulation of salt efflorescence was carefully monitored in a selected area on the Bitter Creek channel bed by taking samples and analyzing them in the laboratory. A small metallic pipe of 1.25 cm diameter with a cutting edge was pushed into the soil and a sample 2.5 cm deep was removed. This sample was mixed with 40 ml of distilled water, shaken well, and then allowed to stand for 24 hours. The supernatant liquid was decanted, filtered and its EC measured. Three samples each were taken on August 20 and 30 and on September 9 and 18, 1979. A storm had occurred on August 16, but there were no storms during the period efflorescence growth was monitored. For $\text{EC} < 5 \text{ mmho cm}^{-1}$ in the Price River Basin (USDA 1969),

$$\text{ppm salt in solution} = 640 \text{ EC}$$

$$\dots \dots \dots (39)$$

in which EC is in mmho cm^{-1} . Using

this approximation, EC measurements were converted into salt efflorescence density measurements in grams per cm² in the upper 2.5 cm of soil crust.

Laboratory Experiment

Knowledge and understanding obtained from field studies helped in designing a laboratory experiment to produce salt efflorescence under controlled conditions. The major laboratory objective was to duplicate natural channel bed conditions in soil columns where efflorescence, soil water, and salt content could be continuously monitored. The data collected could be used in developing and verifying a water flow-salt transport model for predicting salt efflorescence formation.

Soil was obtained from the bed of the Service Berry Creek tributary near the Wattis instrumentation site (Township T 15 S, Range R 9 E, Latitude 39°30'22"N., Longitude 110°55'27"W). More information on this subwatershed is provided by Riley et al. (1982b). The air dried soil was sieved through a Taylor series sieve no. 9 (opening size of 1.981 mm). PVC pipes of 10 cm diameter were used to form soil columns by filling them with sieved soil samples. The bulk density of the soil was estimated to be 1.26 gms/cc.

The columns were initially saturated with saline water matching the EC and chemical composition found in the field. Infrared heat lamps were used for evaporating water from the soil. The lamps were calibrated using an electrically calibrated pyroelectric radiometer (RS 3960, Laser Precision Corp.). Their distances from the soil surfaces were varied during the experiment to simulate diurnal variation of incoming solar heat (Figure 5). A sketch of the experimental arrangement is given in Figure 6.

The experiment was conducted in two stages. In the first stage, only four soil columns, each 25 cm long, were

used. Two soil columns were saturated with saline water, and the other two were saturated with distilled water. Small columns were used so that they could be accurately weighed to monitor daily evaporation. The experiment was continued for 14 days. At the end of the experiment, all four columns were cut into sections, and the soil at different depths was analyzed for water content and the EC of the saturation extract.

In the second stage, 27 columns, each 50 cm long, were used in an experiment lasting 13 days. The initial soil and saline water analyses are given in Tables 3 and 4. On the first, second, third, fourth, fifth, seventh, ninth, eleventh, and thirteenth days, sections varying between 2 cm and 10 cm in thickness were cut from the three columns. Water content measurements, chemical analysis of the saturation extracts, and EC measurements were obtained for sections on each of the columns. The data obtained are given in Appendix A.

Table 3. Saturation extract analysis of soil used in experimental columns.

| | |
|---|------------------------|
| Sodium, as Na ⁺ | 13,500. (mg/l) |
| Calcium, as Ca ⁺⁺ | 200. |
| Magnesium, as Mg ⁺⁺ | 1,080. |
| Chloride, as Cl ⁻ | 1,505. |
| Bicarbonate as HCO ₃ ⁻ | 153. |
| Sulfate, as SO ₄ ⁼ | 30,816. |
| Percent gypsum by weight | 28.0 |
| Percent lime by weight | 9.80 |
| Cation exchange capacity | 5.40 me/100 g |
| Saturation percentage | 30.8 |
| EC of saturation extract | 44.2 mmho/cm @ 25°C |
| pH | 8.9 |
| Soil is classified as Sandy Loam based on hydrometer/screen analysis | |

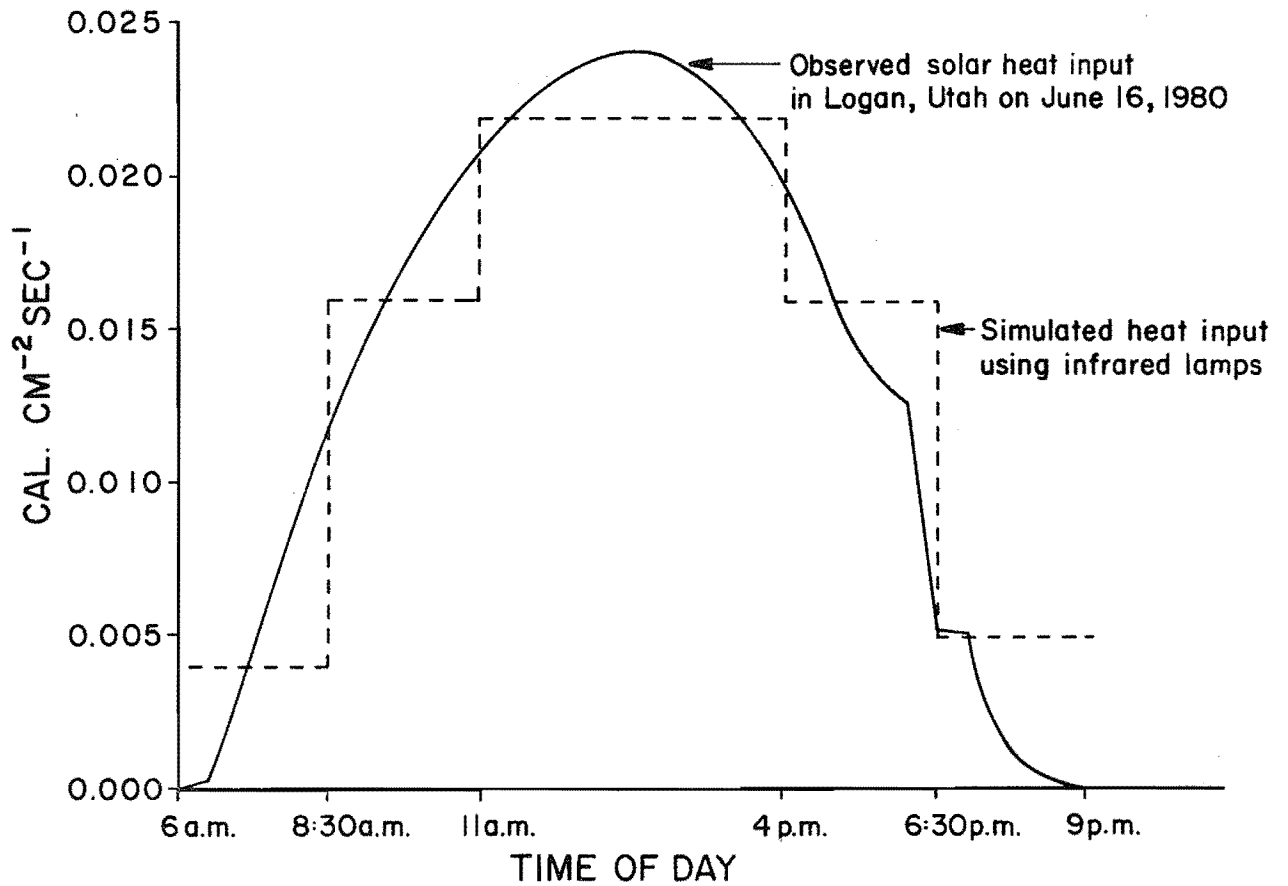


Figure 5. Simulation of solar heat input using infrared lamps.

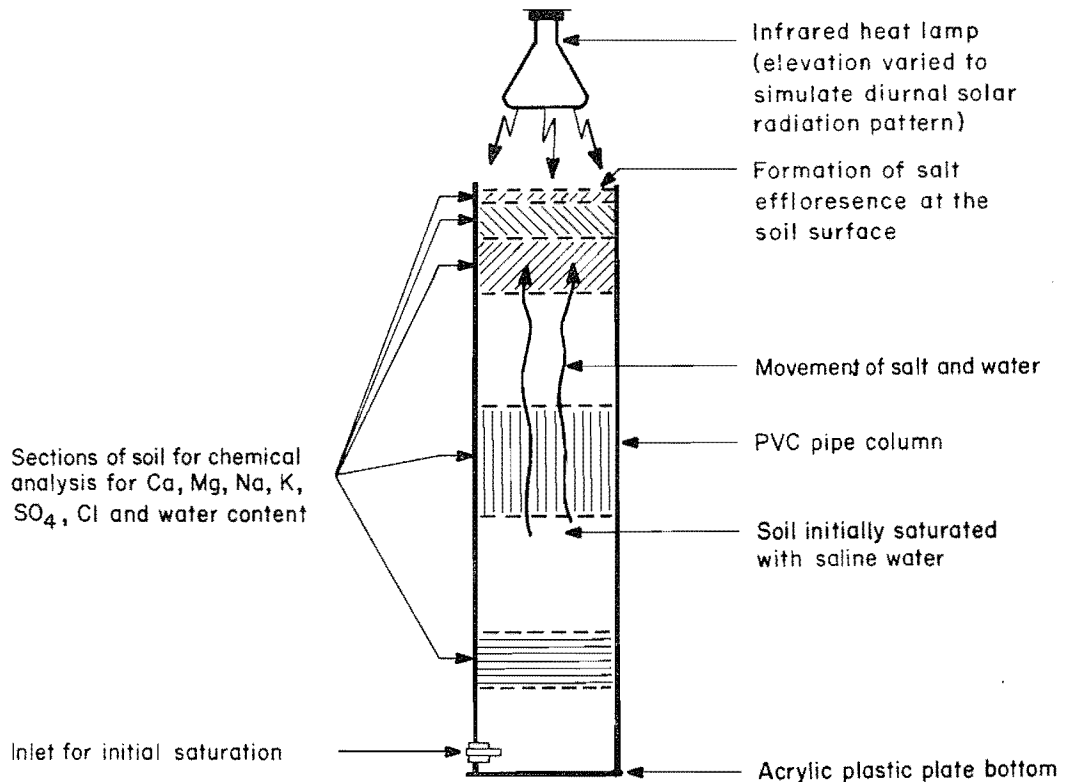


Figure 6. Sketch of an experimental column for growing salt efflorescence.

Table 4. Composition of saline water used in experimental columns.

| | |
|---|---------------|
| Sodium sulfate (Na_2SO_4) | 21,000 (mg/l) |
| Sodium carbonate (Na_2CO_3) | 200 |
| Sodium chloride (NaCl) | 700 |
| Magnesium sulfate (MgSO_4) | 7,500 |
| Magnesium carbonate (MgCO_3) | 100 |
| Magnesium chloride (MgCl_2) | 200 |
| Calcium sulfate (CaSO_4) | 2,200 |
| Calcium carbonate (CaCO_3) | 100 |
| Calcium chloride (CaCl_2) | 100 |
| Potassium sulfate (K_2SO_4) | 8,500 |
| Potassium chloride (KCl) | 200 |

Aerial Observation and Photography

On August 4, 1980, Price River and some of its tributaries were observed from the air in a plane under favorable weather conditions. The objective was to examine the extent and evidence on pattern of growth of efflorescence in

the channels. Aerial photographs were taken.

Stream channels observed in a flight time of about 3 hours included Price River from Helper to the point of confluence of Grassy Trail Creek, part of Grassy Trail Creek, Desert Seep Wash, Coal Creek, Soldier Creek, and Miller Creek. All the streams except Miller Creek were flowing, and little efflorescence was observed. On the other hand, Miller Creek, the dry channels of many small tributaries, and many land depressions were completely covered with efflorescence.

No correlation was observed between efflorescence and reaches receiving irrigation return flows. If a stream bed was covered with efflorescence, it seemed to extend over long distances with uniform density, suggesting that the salts were deposited during flow recession after a storm hydrograph rather than by direct evaporation of subsurface inflow.

CHAPTER V

MODEL OF SALT EFFLORESCENCE GROWTH

Introduction

The mathematical model developed for predicting the growth of salt efflorescence consists of three main components. Subroutines WATER, SOLUTE, and CHEM deal with water flow, salt transport, and chemical equilibrium, respectively. The theoretical approaches to water flow, salt transport, and chemical equilibrium used in developing the mathematical model are described in this chapter. Subroutines IONPAR and EFFL, which represent the salt efflorescence process, will also be discussed. Further annotations are available in the computer program listing (Rao 1982, Appendix E).

Water Flow

Equation

Equation 3 uses two variables to represent H (ψ and g). Rubin (1966) described three possible transformations for reducing the equation to a single dependent variable. The one used was developed by Richards (1931) and makes use of the relationship:

$$C(\theta) = \frac{\partial \theta}{\partial h} \dots \dots \dots (40)$$

where $C(\theta)$ is the soil water differential capacity (L^{-1}). By the chain rule of calculus,

$$\frac{\partial \theta}{\partial t} = \frac{\partial \theta}{\partial h} \frac{\partial h}{\partial t} = C(\theta) \frac{\partial h}{\partial t} \dots \dots (41)$$

The substitution of Equation 41 into Equation 3 yields:

$$C(\theta) \frac{\partial h}{\partial t} = \frac{\partial}{\partial z} \left(K(\theta) \frac{\partial H}{\partial z} \right) \dots \dots (42)$$

where the hydraulic head ($H = h - z$) is the only dependent variable. Depth z is positive measured downwards from the soil surface.

When written in the finite-difference form (Rao 1982), Equation 42 becomes

$$\begin{aligned} & \left(- \frac{2 K_{i-1/2}^{j+1/2}}{\Delta z_1} \right) h_{i-1}^{j+1} + \left(\frac{C(\theta) \Delta z_3}{\lambda \Delta t} + \frac{2 K_{i-1/2}^{j+1/2}}{\Delta z_1} \right. \\ & \left. + \frac{2 K_{i+1/2}^{j+1/2}}{\Delta z_2} \right) h_i^{j+1} + \left(- \frac{2 K_{i+1/2}^{j+1/2}}{\Delta z_2} \right) h_{i+1}^{j+1} \\ & = \left(\frac{C(\theta) \Delta z_3}{\Delta t} h_i^j + \frac{2 K_{i+1/2}^{j+1/2}}{\Delta z_2} \right. \\ & \left. \left[(1 - \lambda) (h_{i+1}^j - h_i^j) - \Delta z_2 \right] \right. \\ & \left. + \frac{2 K_{i-1/2}^{j+1/2}}{\Delta z_1} \left[(1 - \lambda) (h_{i-1}^j - h_i^j) + \Delta z_1 \right] \right) \frac{1}{\lambda} \end{aligned} \dots \dots \dots (43)$$

The Crank-Nicolson (1947) implicit method for solving a finite difference equation was used with an approximation at the intermediate ($j + 1/2$) time interval. This is of a form with 0.5 as the coefficient preceding the h^{j+1} and h^j terms. The Laasonen (Richtmyer 1957) implicit method of evaluation only uses the h^{j+1} terms. The explicit method, solving for h^{j+1} directly, uses only the h^j terms. Several solution forms for Equation 43 can therefore be envisioned. A general form can be

established by using a "weighting" factor, λ , that can take on any value in the range $0 \leq \lambda \leq 1$. The Crank-Nicolson method in which $\lambda = 0.5$ and the Laasonen method in which $\lambda = 1$ are stable for all values of Δz and Δt . The computer program is written such that λ can be given any value, but only the Crank-Nicolson solution ($\lambda = 0.5$) was used in this study.

To solve Equation 43 for vertical flow in an unsaturated soil, it is necessary to estimate K (the hydraulic conductivity) and C (the change in soil water content with head). The value of C can be found by fitting a cubic spline function to the θ vs h data and differentiating (Erh 1972). Tillotson (1979) developed a computer subroutine SPLINE to do this. The hydraulic conductivity, K , can be estimated from water content-pressure head relationships by one of the methods of Jackson (1972), Brooks and Corey (1964), and Campbell (1974). The θ - h data and corresponding C and K values used in this study were taken from Tillotson (1979).

Instead of establishing a constant time increment, a variable increment was computed from volumetric water content changes in the soil profile. If the absolute value of the greatest simulated change in the volumetric water content over the entire soil profile is greater than a predetermined amount, the time increment is halved, and the pressure heads are recalculated using the smaller time increment. This prevents rapid changes in water content and solute concentration from masking the behavior of the water and solute movement. A predetermined value of 0.03 cm^3 water per cm^3 soil was used. Time increments range from 0.024 hr to 6 hr.

Equation 43 is of the form

$$A h_{i-1}^{j+1} + B h_i^{j+1} + C h_{i+1}^{j+1} = D \quad (44)$$

For a given time, each depth boundary excluding the top and bottom, also produces an equation of this form. The linear system of equations produced at a given time is solved using the Thomas algorithm (Bruce et al. 1953) which converts the tridiagonal coefficient matrix to an upper triangular matrix and solves for the pressure heads by back substitution.

Conversion of pressure heads to volumetric water contents is performed by approximating the soil moisture curve with a straight line over pressure head intervals. The appropriate intervals (0.01 in this study) are used to calculate the dependent variable, θ .

Top and Bottom Boundary Flux of Water

The top boundary condition can be changed with time to simulate either rainfall or evaporation. Rainfall is represented by a positive flux of water, and evaporation by a negative flux. This surface flux (EOR) is incorporated into the numerical solutions of the water flow equation. Numerically approximating Darcy's law gives:

$$EOR = \frac{K_{i-\frac{1}{2}}^{j+\frac{1}{2}}}{2 \Delta z_1} \left(h_{i-1}^j + h_{i-1}^{j+1} - h_i^j - h_i^{j+1} + 2 \Delta z_1 \right) \quad (45)$$

Using this approximation in developing the finite difference water flow equation gives:

$$C(\theta) \left(\frac{h_i^{j+1} - h_i^j}{\Delta t} \right) = \frac{2 EOR}{\Delta z_2} - \frac{K_{i+\frac{1}{2}}^{j+\frac{1}{2}}}{\Delta z_2 \Delta z_3} \left[\left(h_i^j + h_i^{j+1} - h_{i+1}^j - h_{i+1}^{j+1} \right) + 2 \Delta z_2 \right] \quad (46)$$

Since there is no $(i-1)$ depth increment at the surface, the assumption is made that $\Delta z_3 = 2 \Delta z_2$. Substituting for Δz_3 in Equation 46 and simplifying gives:

$$\left(\frac{C(\theta)}{\Delta t} + \frac{K_{i+\frac{1}{2}}^{j+\frac{1}{2}}}{2 \Delta z_2^2} \right) h_i^{j+1} - \left(\frac{K_{i+\frac{1}{2}}^{j+\frac{1}{2}}}{2 \Delta z_2^2} \right) h_{i+1}^{j+1}$$

$$= \frac{C(\theta)}{\Delta t} h_i^j + \frac{EOR}{\Delta z_2} - \frac{K_{i+\frac{1}{2}}^{j+\frac{1}{2}}}{2 \Delta z_2} \left(\frac{h_i^j}{\Delta z_2} - \frac{h_{i+1}^j}{\Delta z_2} + 2 \right) \dots \dots \dots (47)$$

Equation 47 provides values for the coefficient matrix and a vector corresponding to the unknown pressure head at the soil surface. If more water is applied than the soil can absorb, the surface soil-water pressure head equals the saturated soil-water pressure with runoff being calculated. During evaporation, the surface soil-water pressure head cannot go below the dry air soil-water pressure head. For the bottom boundary condition, the model can simulate no flux ((∂H/∂z) = 0), a unit gradient ((∂H/∂z) = 1), a constant soil-water pressure head, or a water table.

The actual surface flux (WFDD) is calculated as the potential amount estimated from Equation 45.

$$WFDD = \frac{K_{i-\frac{1}{2}}^{j+\frac{1}{2}}}{2 \Delta z_1} \left(h_{i-1}^j + h_{i-1}^{j+1} - h_i^j - h_i^{j+1} + 2 \Delta z_1 \right) \dots \dots \dots (48)$$

Salt Transport

The model for salt transport represents Ca, Mg, Na, K, Cl, and SO₄ ions as independent species in order to facilitate the interfacing with the CHEM subroutine.

Equation

The diffusion-convection equation for a noninteracting solute is:

$$\frac{\partial(\theta c)}{\partial t} = \frac{\partial}{\partial z} \left(D(\theta, q) \frac{\partial c}{\partial z} \right) - \frac{\partial}{\partial z} (q c) \dots \dots \dots (49)$$

in which

- c = concentration of solute
- θ = volumetric water content
- t = time
- z = depth

D(θ, q) = apparent diffusion coefficient

q = water flux

The second-order finite difference approximation of the left-hand side of Equation 49 is:

$$\frac{\partial(\theta c)}{\partial t} = \left(\frac{\theta_i^j + \theta_i^{j+1}}{2} \right) \left(\frac{c_i^{j+1} - c_i^j}{\Delta t} \right) \dots \dots \dots (50)$$

The second-order finite difference approximation of the right-hand side is:

$$\begin{aligned} & \frac{\partial}{\partial z} \left(D(\theta, q) \frac{\partial c}{\partial z} \right) - \frac{\partial}{\partial z} (q c) \\ &= \left[D_{i+\frac{1}{2}}^{j+\frac{1}{2}} \left(\frac{c_{i+1}^{j+\frac{1}{2}} - c_i^{j+\frac{1}{2}}}{z_{i+1} - z_i} \right) - D_{i-\frac{1}{2}}^{j+\frac{1}{2}} \left(\frac{c_i^{j+\frac{1}{2}} - c_{i-1}^{j+\frac{1}{2}}}{z_i - z_{i-1}} \right) \right] \left(\frac{z_{i+1} - z_i}{2} \right) \\ &+ \left(\frac{z_i - z_{i-1}}{2} \right) \left[\left(\frac{q_i^j + q_i^{j+1}}{2} \right) \left(\frac{c_{i+1}^{j+\frac{1}{2}} - c_{i-1}^{j+\frac{1}{2}}}{z_{i+1} - z_{i-1}} \right) \right] \dots \dots \dots (51) \end{aligned}$$

Substituting

$$\Delta z_1 = z_i - z_{i-1}$$

$$\Delta z_2 = z_{i+1} - z_i$$

$$\Delta z_3 = z_{i+1} - z_{i-1}$$

in Equation 51 and simplifying:

$$\begin{aligned} \frac{\partial}{\partial z} \left(D(\theta, q) \frac{\partial c}{\partial z} \right) - \frac{\partial}{\partial z} (qc) \\ = \frac{2 D_{i+\frac{1}{2}}^{j+\frac{1}{2}}}{\Delta z_2 \Delta z_3} \left(c_{i+1}^{j+\frac{1}{2}} - c_i^{j+\frac{1}{2}} \right) \\ - \frac{2 D_{i-\frac{1}{2}}^{j+\frac{1}{2}}}{\Delta z_1 \Delta z_3} \left(c_i^{j+\frac{1}{2}} - c_{i-1}^{j+\frac{1}{2}} \right) \\ - \left(\frac{q_i^j + q_i^{j+1}}{2 \Delta z_3} \right) \left(c_{i+1}^{j+\frac{1}{2}} - c_{i-\frac{1}{2}}^{j+\frac{1}{2}} \right) \quad (52) \end{aligned}$$

Substituting:

$$c_i^{j+\frac{1}{2}} = \frac{c_i^j + c_i^{j+1}}{2}, \quad c_{i+1}^{j+\frac{1}{2}} = \frac{c_{i+1}^j + c_{i+1}^{j+1}}{2}, \text{ etc.}$$

in Equation 52 and simplifying:

$$\begin{aligned} \frac{\partial}{\partial z} \left(D(\theta, q) \frac{\partial c}{\partial z} \right) - \frac{\partial}{\partial z} (qc) \\ = \frac{D_{i+\frac{1}{2}}^{j+\frac{1}{2}}}{\Delta z_2 \Delta z_3} \left(c_{i+1}^j + c_{i+1}^{j+1} - c_i^j - c_i^{j+1} \right) \\ - \frac{D_{i-\frac{1}{2}}^{j+\frac{1}{2}}}{\Delta z_1 \Delta z_3} \left(c_i^j + c_i^{j+1} - c_{i-1}^j - c_{i-1}^{j+1} \right) \\ - \left(\frac{q_i^j + q_i^{j+1}}{4 \Delta z_3} \right) \left(c_{i+1}^j + c_{i+1}^{j+1} - c_{i-1}^j - c_{i-1}^{j+1} \right) \\ \dots \dots \dots (53) \end{aligned}$$

Substituting Equations 50 and 53 in Equation 49 and placing unknowns to the left and knowns to the right, the diffusion-convection equation can be written in the finite-difference form as:

$$\begin{aligned} c_{i-1}^{j+1} \left(- \frac{D_{i-\frac{1}{2}}^{j+\frac{1}{2}}}{\Delta z_1 \Delta z_3} - \frac{q_i^j + q_i^{j+1}}{4 \Delta z_3} \right) \\ + c_i^{j+1} \left(\frac{\theta_i^j + \theta_i^{j+1}}{2 \Delta t} + \frac{D_{i+\frac{1}{2}}^{j+\frac{1}{2}}}{\Delta z_2 \Delta z_3} \right. \\ \left. + \frac{D_{i-\frac{1}{2}}^{j+\frac{1}{2}}}{\Delta z_1 \Delta z_3} \right) + c_{i+1}^{j+1} \left(- \frac{D_{i-\frac{1}{2}}^{j+\frac{1}{2}}}{\Delta z_2 \Delta z_3} \right. \\ \left. + \frac{q_i^j + q_i^{j+1}}{4 \Delta z_3} \right) = c_{i-1}^j \left(\frac{D_{i-\frac{1}{2}}^{j+\frac{1}{2}}}{\Delta z_1 \Delta z_3} \right. \\ \left. + \frac{q_i^j + q_i^{j+1}}{4 \Delta z_3} \right) + c_i^j \left(\frac{\theta_i^j + \theta_i^{j+1}}{2 \Delta t} \right. \\ \left. - \frac{D_{i+\frac{1}{2}}^{j+\frac{1}{2}}}{\Delta z_2 \Delta z_3} - \frac{D_{i-\frac{1}{2}}^{j+\frac{1}{2}}}{\Delta z_1 \Delta z_3} \right) + c_{i+1}^j \left(\frac{D_{i+\frac{1}{2}}^{j+\frac{1}{2}}}{\Delta z_2 \Delta z_3} \right. \\ \left. - \frac{q_i^j + q_i^{j+1}}{4 \Delta z_3} \right) \dots \dots \dots (54) \end{aligned}$$

where $D_{i-\frac{1}{2}}^{j+\frac{1}{2}}$ is a modified form of Bresler's (1973) apparent diffusion coefficient (combined diffusion-dispersion coefficient). That is,

$$D_{i-\frac{1}{2}}^{j+\frac{1}{2}}(\theta, q) = D_0 a e^{b\theta_{i-\frac{1}{2}}^{j+\frac{1}{2}}} + \lambda \left| \frac{q_{i-\frac{1}{2}}^{j+\frac{1}{2}}}{\theta_{i-\frac{1}{2}}^{j+\frac{1}{2}}} \right| \dots \dots \dots (55)$$

in which

- D_0 = diffusion coefficient in a free water system (L^2T^{-1})
- a and b = empirical constants characterizing the soil

λ = experimental constant depending on the characteristics of the porous medium

$\theta_{i-\frac{1}{2}}^{j+\frac{1}{2}}$ = average volumetric water content over the space and time increment

$q_{i-\frac{1}{2}}^{j+\frac{1}{2}}$ = average flux of water over the space and time increment

C_t = solute concentration in rain or irrigation water at time, t

WC_t = water content at soil surface at time, t

During evaporation, the

$$SC_t = \frac{\sum_{i=1}^d S_{t-1,i} - \sum_{i=2}^d S_{t,i}}{W_{t,1}} \quad . \quad . \quad (57)$$

Olsen and Kemper (1968) found that Equation 55 fit data collected on soils reasonably well when $b = 10$ and $a = 0.001$ to 0.005 . In this study a was assumed to be 0.001 . Model predictions were found to be fairly insensitive to the values of a and b . λ was given a value of 0.4 based on Bresler (1973). The fluxes of water were calculated using Darcy's law with pressure heads obtained from the solution of the water flow equation.

in which

$S_{t,i}$ = salt in the system at time increment t and depth increment i

$W_{t,i}$ = water in the system at time increment t and depth increment i

d = number of depth increments

Equation 54 is of the same form as Equation 44. The linear system of equations produced for a given time was solved for the solute solution concentrations using the same method as described in solving the water flow equation for the soil-water pressure heads.

The bottom boundary solute concentration was best estimated as the soil-water solute concentration at depth $d-1$ for the time increment $t-1$.

Chemical Equilibrium

Top and Bottom Boundary Conditions for Solute Concentration

After the transport model executes a predetermined number of salt and water movement calculations, the model can 1) print the salt profile without considering chemical precipitation or dissolution, 2) call the chemistry subroutines, bring the solution salts into chemical equilibrium with lime and gypsum, and print the soil profile description, or 3) call the chemistry and the exchange subroutines which model cation exchange equilibrium and print the soil profile description. In the present study, the exchange subroutine was not used as the soil had a low cation exchange capacity of 5.4 me/100 g of soil.

The model was sensitive to the boundary conditions. The best result for the simulation of salt efflorescence was obtained by a top boundary solute concentration during rain or irrigation (positive flux of water) given by:

$$SC_t = \frac{C_t + SC_{t-1} \left(\frac{WC_{t-1}}{WC_t} \right)}{2} \quad . \quad . \quad (56)$$

in which

SC_t = soil-water solute concentration at surface at time, t

The chemical equilibrium subroutine (CHEM) used in this study was developed by Robbins (1979) and listed in Rao

(1982), who validated it at normal soil salinity range (EC of 4 to 5 mmho/cm) using lysimeter data. The original model used a method described by McNeal et al. (1970) which calculated EC from individual ion concentrations. Since this method does not give good results at the high EC values encountered in this study (60-70 mmho/cm), a new relationship was established between EC and total dissolved solids (TDS) using data pertaining to this study. Figure 7 plots the data and shows the best fit line of

$$EC = 0.6902 \text{ TDS}^{0.6312} \dots (58)$$

Solution ionic strength (I, mole/liter) was calculated (Griffin and Jurinak 1973) from:

$$I = 0.0127 \text{ EC} \dots (59)$$

which is corrected for ion pair formation in the EC range of 0 to 35 mmho/cm.

The mono- and divalent ion activity coefficients (γ_1 and γ_2) were calculated from the Davies relationship which has been shown to be valid up to $I = 0.5$ moles/liter (Stumm and Morgan 1981):

$$\log \gamma_i = -0.509 z_i^2 \left(\frac{I^{1/2}}{1.0 + I^{1/2}} - 0.3 I \right) \dots (60)$$

in which

z_i is the ionic charge

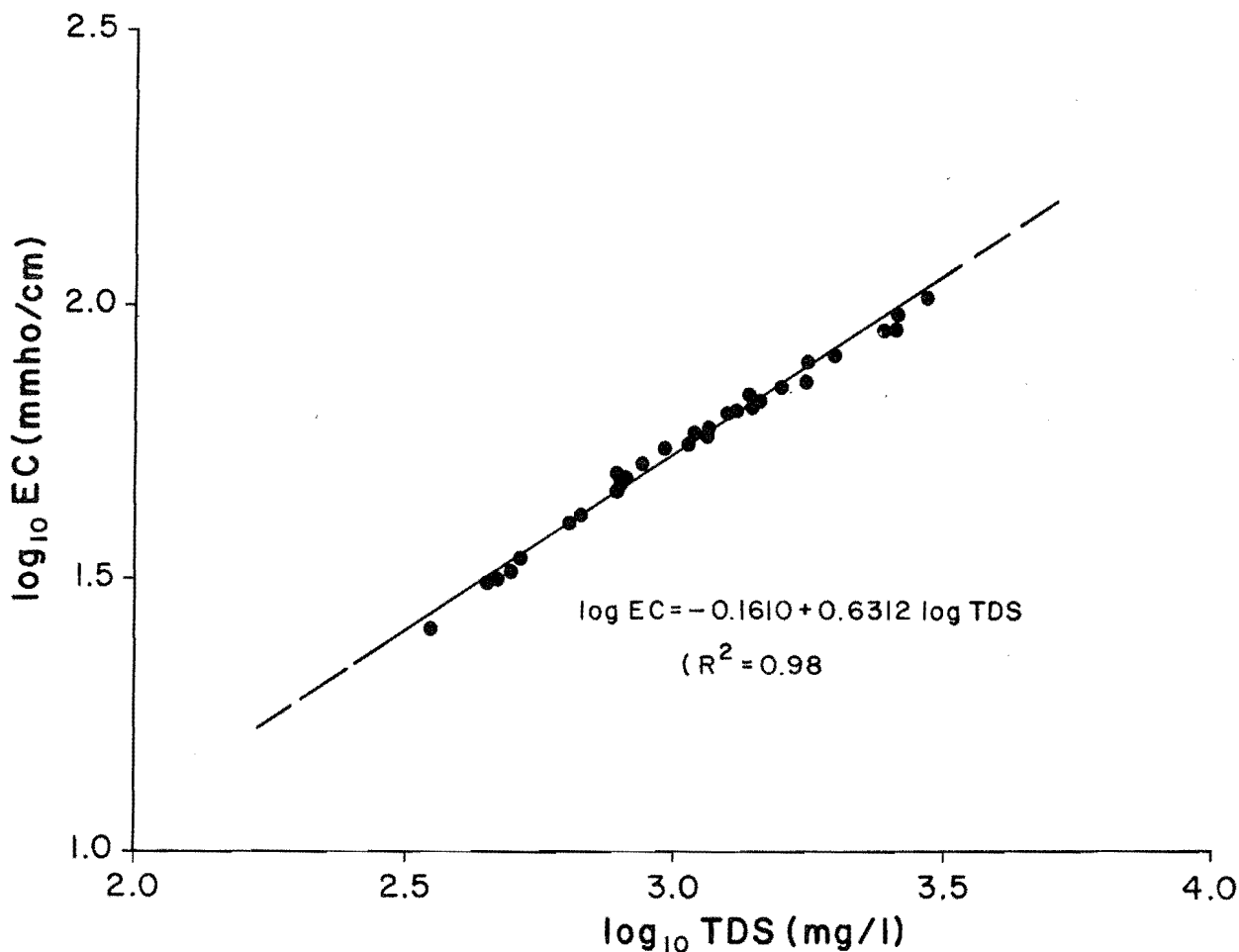


Figure 7. Electrical conductivity-total dissolved solids relationship.

The ionic strength in the column experiment varied from 0.5 to 6.5 moles/liter. Other details of the chemical equilibrium submodel are available in Robbins (1979).

Ion-Pair Formation

The high concentrations of solute used in salt efflorescence modeling result in ion-pair formations and cause the EC-TDS relationship to be nonlinear. A method of successive approximations (Adams 1971) was used to write the subroutine IONPAR for computing ion-pair formations. But in this application, negative ion concentrations were obtained as intermediate values in its iterative solution. The same ion may participate in several ion associations in mixed salt solutions. An intermediate negative value for ion concentration is therefore more common with increased salt concentrations and more intense ion-pair formation. To overcome difficulties with negative values, Darab et al. (1980) modified the method by calculation of the weighted averages of ion concentrations after each iterative step. The negative deviation was eliminated by introduction of a function containing the ratio of the ion-pair concentration to the analytical concentration of the related ion.

The concentration of the ion i in the n -th step of iteration was determined by the relationship:

$$c_{i(n)\text{reduced}} = \frac{[c_{i(n-1)} \cdot \text{HF}] + c_{i(n)}}{\text{HF} + 1} \quad \dots \quad (61)$$

in which

$c_{i(n)}$ = the analytical concentration of ion i at the n th iteration

$$\text{HF} = \frac{\sum_{j=1}^y (c_i A_j)}{c_i} \quad \dots \quad (62)$$

in which

$(c_i A_j)$ = the concentration ion-pairs formed by ions c_i and A_j

Since the iterations converged slowly, it was necessary to make another averaging as follows:

$$(c_i)_n = \frac{c_{i(n)} + c_{i(n-1)}}{2} \quad \dots \quad (63)$$

Subroutine IONPAR then converged quickly for total dissolved solids concentrations up to 6,000 me/liter.

Modeling Principle

Formation of salt efflorescence was simulated based on the observation that the salt left behind at the soil surface forms a crust that is not in physical contact with the soil water. The water evaporated in a given day was multiplied by the concentration of the soil solution at the top depth increment to estimate the amount of salt deposited and contributing to the accumulation of efflorescence. The rate of accumulation is measured in grams of salt per unit area per day.

Model Limitations

The water flow-salt transport model developed to predict the rate of accumulation of salt efflorescence crust contains a number of assumptions that should be considered before its use as a basin-wide salinity management tool. The model neglects the spatial variability of soil physical properties and temporal variability of soil-water quality. The model does not provide for the situation when the soil is dry and water movement is primarily via the vapor phase which does not transport salt to the soil surface. At high electrical conductivities of the soil solution, including the 60-70 mmho/cm encountered in this study, the chemical equilibrium model does not predict accurately because of

the limitations of the Davies equation in calculating activity coefficients beyond the range of validity of the theory of a dilute electrolyte (Stumm and Morgan 1981).

The accuracy of water flow and salt transport predictions is limited by the numerical approximation techniques used. The model is very sensitive to boundary condition formulations and moisture-release curve input data for the soil under consideration. These relationships are very difficult to accurately obtain from laboratory experiments and represent in empirical equations.

Recommendations

The model is a useful tool to study the effects of soil properties, water quality, and evaporation rates on salt efflorescence crust formation at a given location. For basinwide applications, the spatial variability of soil properties and temporal variability of soil-water quality should be considered and results summed. A statistical analysis of the spatial variability of efflorescence crust densities may provide a more meaningful estimate of the contribution of salt efflorescence to overall salinity.

CHAPTER VI

RESULTS OF SALT EFFLORESCENCE STUDY

Field Data

The chemical analyses of soil water collected from the beds of Miller and Bitter Creeks are given in Table 5. Magnesium and sulfate ions predominate in Miller Creek. Sodium and sulfate ions predominate in Bitter Creek.

dominance of sodium and sulfate. Similar results were obtained by Mundorff (1972), who analyzed efflorescence samples from Drunkards Wash and five other sites in the central basin. The dominance of sodium sulfate is probably due to the exchange of sodium by calcium resulting from solubilized gypsum.

The chemical analyses of the salt efflorescence samples (Table 6) show a

accumulation of salt efflorescence in

Table 5. Results of soil water analysis in ephemeral channel bed.

| | Miller Creek | Bitter Creek |
|----------------------------------|--------------|--------------|
| Date of Collection | 7/17/79 | 7/19/79 |
| Carbonate, as $\text{CO}_3^{=}$ | 0. (mg/l) | 38. (mg/l) |
| Bicarbonate, as HCO_3^- | 672. | 1,109. |
| Calcium, as Ca^{++} | 215. | 506. |
| Chloride, as Cl^- | 81. | 1,113. |
| Magnesium, as Mg^{++} | 230. | 4,042. |
| Potassium, as K^+ | 10. | 123. |
| Sodium, as Na^+ | 170. | 10,616. |
| Sulfate, as $\text{SO}_4^{=}$ | 1,331. | 40,616. |

Table 6. Results of chemical analysis of efflorescence.

| | Desert Seep Wash | Bitter Creek | Wattis |
|----------------------------------|------------------|--------------|------------|
| Date of Collection | 7/17/79 | 7/19/79 | 7/19/79 |
| Carbonate, as $\text{CO}_3^{=}$ | 43. (mg/l) | 23. (mg/l) | 40. (mg/l) |
| Bicarbonate, as HCO_3^- | 365. | 183. | 276. |
| Calcium, as Ca^{++} | 375. | 144. | 419. |
| Chloride, as Cl^- | 84. | 519. | 241. |
| Magnesium, as Mg^{++} | 1,228. | 925. | 1,044. |
| Potassium, as K^+ | 1,150. | 1,400. | 2,700. |
| Sodium, as Na^+ | 5,500. | 3,350. | 4,550. |
| Sulfate, as $\text{SO}_4^{=}$ | 18,472. | 11,872. | 17,385. |

Bitter Creek was monitored by measuring the EC of the salt-crust solution and then converting into salt efflorescence density measurements in a gram per cm⁻² in the upper 2.5 cm of soil crust. The results (Table 7) show that the three

field samples gave efflorescence density values within a reasonable range of sampling and analysis error.

Table 7. Accumulation of salt efflorescence as measured by salt efflorescence density, with time, in Bitter Creek.

| Salt Efflorescence Density (Grams Per cm ² in the Upper 1 Inch of Soil Crust) | | | | |
|--|-----------|-----------|-----------|---------|
| Date | Sample #1 | Sample #2 | Sample #3 | Average |
| 8/20/79 | 0.04 | 0.04 | 0.05 | 0.04 |
| 8/30/79 | 0.08 | 0.12 | 0.12 | 0.11 |
| 9/9/79 | 0.09 | 0.10 | 0.12 | 0.10 |
| 9/18/79 | 0.08 | 0.11 | 0.12 | 0.10 |

The data are plotted in Figure 8. Since very limited field studies were conducted, only four sets of data points are available. It is believed that the physical and chemical processes of salt accumulation are the same though density of salt crust may vary spatially. Hence, an attempt is made to interpret these limited data to draw some general information about the accumulation of efflorescence. From the measurements made, the process of efflorescence appears to occur within the first 10 days after a storm runoff had dissolved the previous efflorescence. Beyond 10 days the accumulation of efflorescence seems to be very slow. This behavior can be explained either by the fact that no more soil moisture was available to evaporate or that the salt efflorescence crust already formed considerably de-

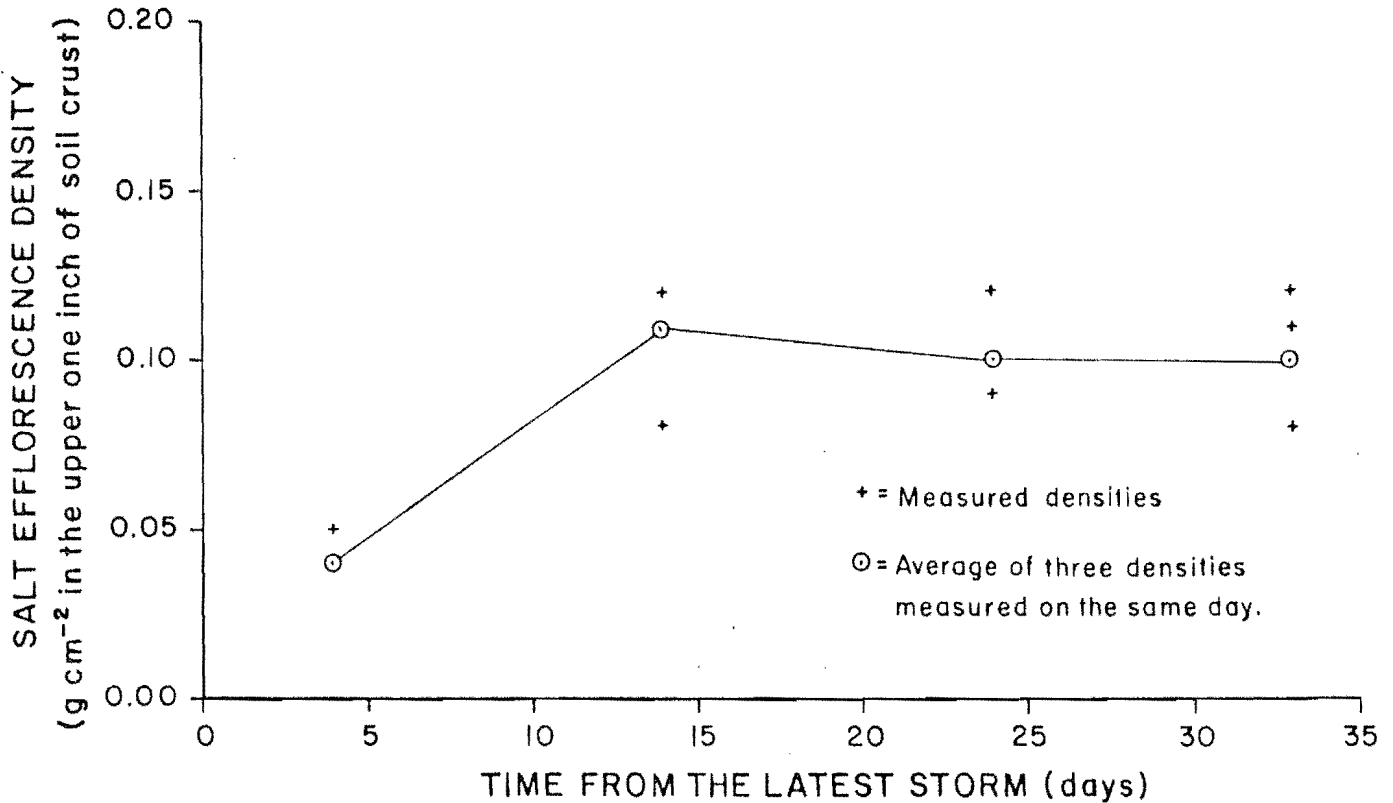


Figure 8. Accumulation of salt efflorescence with time, as measured by efflorescence density.

creased further evaporation of soil water. From the observation that the moisture content varied only between 22 percent and 25 percent by weight during the period of data collection, the first reason is less likely. However, it should be noted that a slight deviation of water content from saturation may reduce hydraulic conductivity value and thus decrease the upward flux of water. Also, near saturation moisture contents were commonly found to exist below existing salt efflorescence crusts. Thus, it is deduced that, once formed, the salt efflorescence crust may act as a physical barrier for vapor flow or prevent heat radiation from reaching the soil surface. Also, precipitated salts may clog the soil pores. Both processes may reduce evaporation and the upward flux of water.

The effect of salt efflorescence on the evaporation of soil water is not well understood. The structure of the efflorescence crust needs to be examined to determine how the crust might restrict evaporation. The reflectivity of efflorescence needs to be studied to determine the amount of solar radiation that is lost to the atmosphere and thus unavailable to evaporate soil moisture. In the Price River Basin the color of efflorescence varies from pure white to brownish white depending on the amounts of dissolved organic matter and wind-blown soil particles that are deposited along with the salts.

The electrical conductivities of soil solution measured in the bed of Bitter Creek are given in Table 8. EC values ranged from 35 mmho/cm to above 45 mmho/cm.

Laboratory Data

An empirical function was needed for the water flow model to represent the reduction in evaporation rate caused by the growing salt crust. Laboratory data for the two soil columns saturated

Table 8. Soil solution EC measurements in Bitter Creek.

| Date | EC (mmho/cm @ 25°C) Measured at Depths of | | |
|----------|--|-------|-------|
| | 10 cm | 20 cm | 30 cm |
| 8/12/79 | 36.0 | 35.0 | 35.0 |
| 8/20/79 | >45.0 | 38.0 | 38.0 |
| 8/30/79 | 41.0 | 40.0 | 40.0 |
| 9/9/79 | 40.0 | 40.0 | 40.0 |
| 9/18/79 | 38.0 | 40.0 | 40.0 |
| 10/13/79 | 37.0 | 40.0 | 40.0 |

with saline water were examined. The ratio of actual to potential evaporation (E/EP) was plotted against time (t) since the start of formation of salt efflorescence (Figure 9). The curve fit to the data had an R² = 0.92 and the equation

$$\frac{E}{EP} = 0.9243 t^{-0.5214} \quad . \quad . \quad (64)$$

The cumulative evaporation was also plotted against time for four soil columns (Figure 10). Two had been initially saturated with distilled water and the remaining two with saline water. The columns saturated with distilled water evaporated about 7-8 mm more water over the 14-day period than did the columns saturated with saline water. This observation further indicates that the salt crust restricts soil-water evaporation and slows the accumulation of efflorescence.

It should also be noted that the soil-water in columns saturated with distilled water had an EC of approximately 20-25 mmho/cm due to the salt content of the soil itself (Figure 11). Otherwise, the difference in the cumulative evaporation could have been much larger.

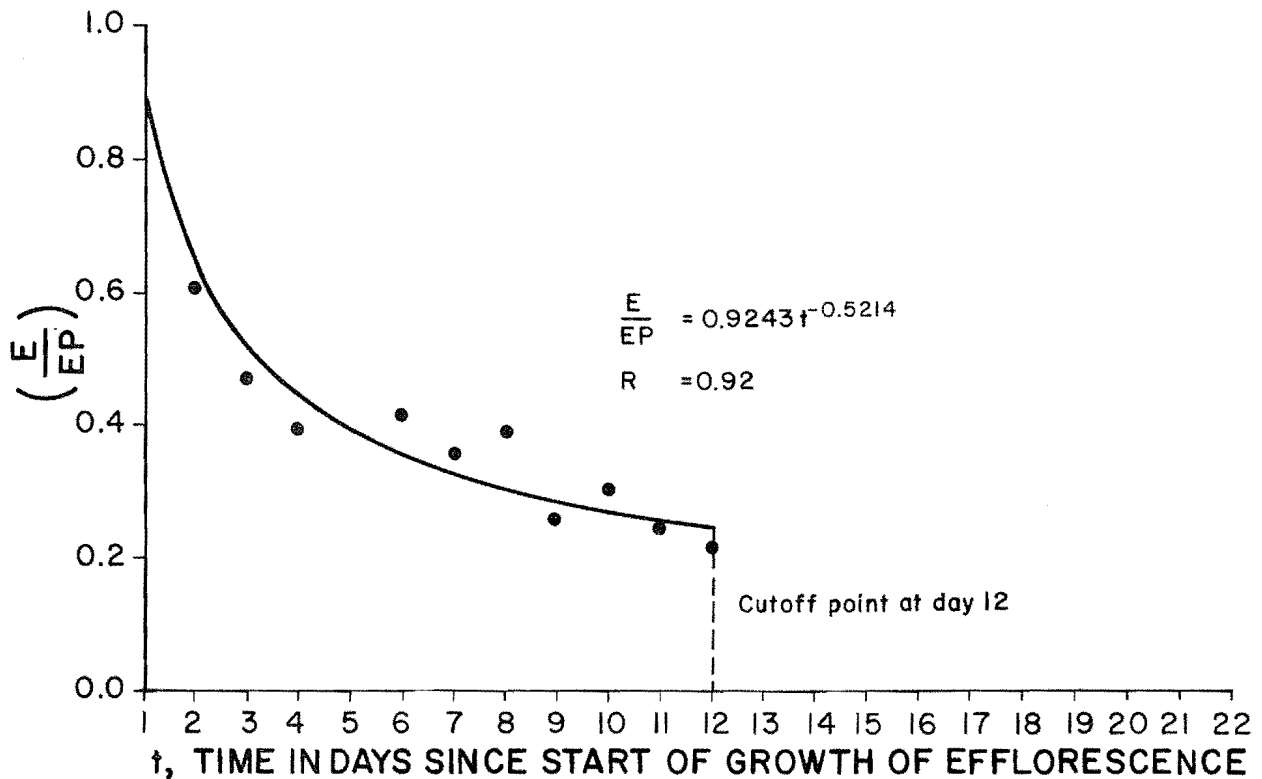


Figure 9. Effect of salt crust formation on evaporation of saline soil water.

The moisture content profiles at the end of the experiment are plotted in Figure 12 for all the four soil columns. This plot provides laboratory verification of the availability of moisture below salt crusts observed qualitatively in the field studies.

In the second stage of the experiment, water content measurements, chemical analysis of the saturation extracts, and EC measurements were made at five sections on each of the 27 columns with the results given in Appendix A. These data were used in verifying the water flow-salt transport model developed for simulating the growth of salt efflorescence.

Model Results

The water flow-salt transport-chemical equilibrium model developed

for simulating the growth of salt efflorescence was verified in three stages. First, the model was verified as to water flow and salt transport by measuring and plotting predicted and measured water content and solute concentration profiles against time. The measured profiles are plotted as bands indicating the range of the values measured at a depth. The wide bands are caused by some combination of natural variability and errors or inconsistencies in measurement. The 27 columns may not have been good replicates of each other because of a lack of uniformity in filling the columns or saturating the soil. Some leakage of soil solution was noted in the bottom plate joints of a few columns, and the lower boundary condition for the water flow model was zero flux. Care was taken during the experiment to place the columns below infrared lights such that each column received an equal amount of

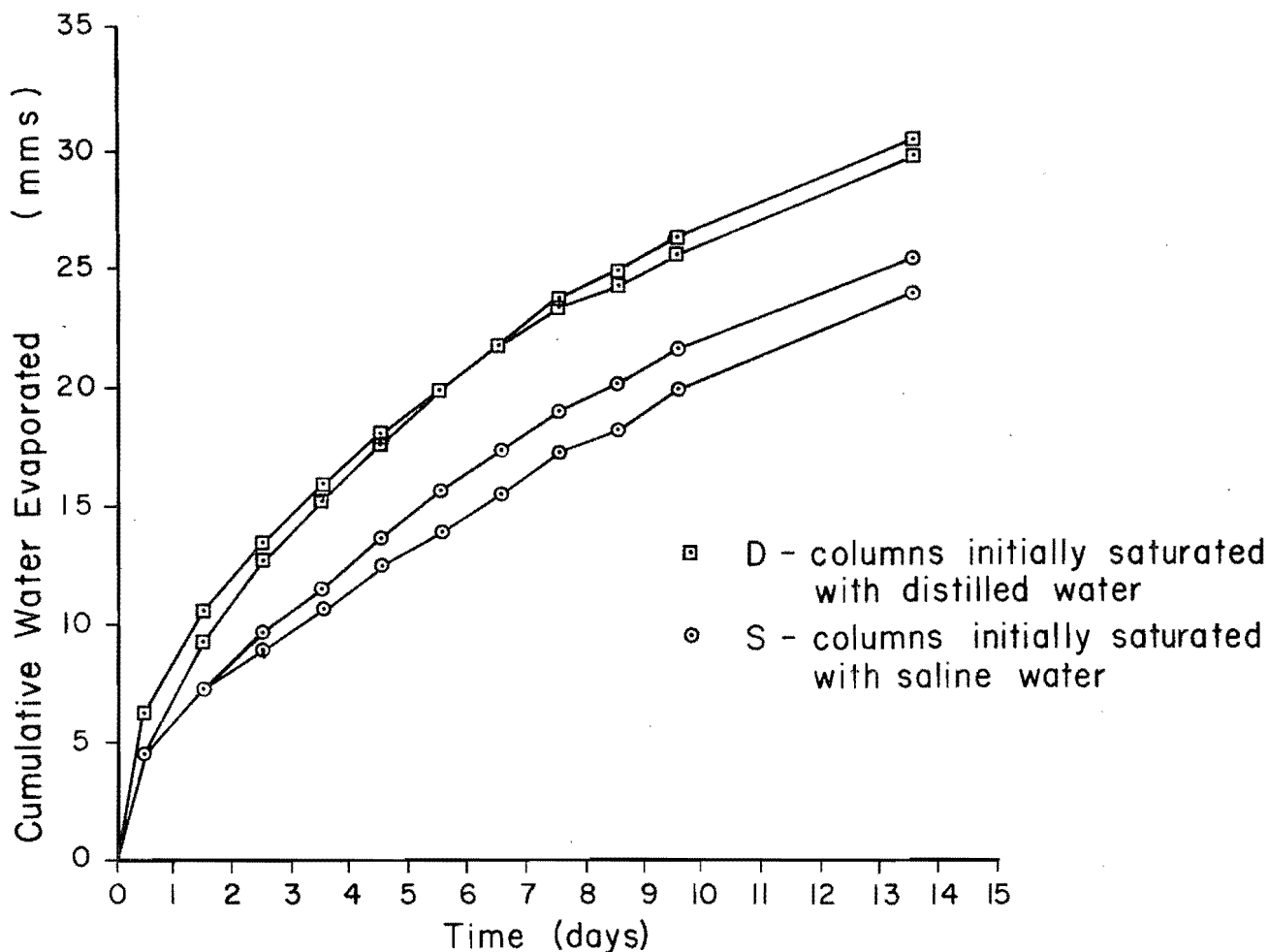


Figure 10. Comparison of accumulative evaporation from soil columns saturated with distilled and saline waters.

radiant heat. The columns were grouped closely together and subjected to the same air movement conditions.

The predicted and measured profiles are plotted for 24, 48, 72, 96, 144, and 240 hours for calcium, magnesium, sodium, potassium, chloride, sulfate, and water content in Figures 13 through 19, respectively. Most predicted profiles lie entirely within the measured bands. There is a good agreement between the predicted and measured Ca^{++} concentration profiles. The predicted concentrations at the top boundary are at the maximum or little above the maximum of observed value. During test runs of the model it was observed that the top boundary salt

concentrations were very sensitive to the way in which top boundary conditions were modeled.

The agreement is also generally good for the predicted and measured concentration profiles for magnesium (Mg^{++}). However, the concentrations are overpredicted at the second and third depths. Since this was also observed corresponding in the profiles of sodium and chloride, it is thought to be caused by over estimation of water content.

For sodium (Na^+), there is a general agreement between the observed and predicted profiles except that the concentrations at second and third

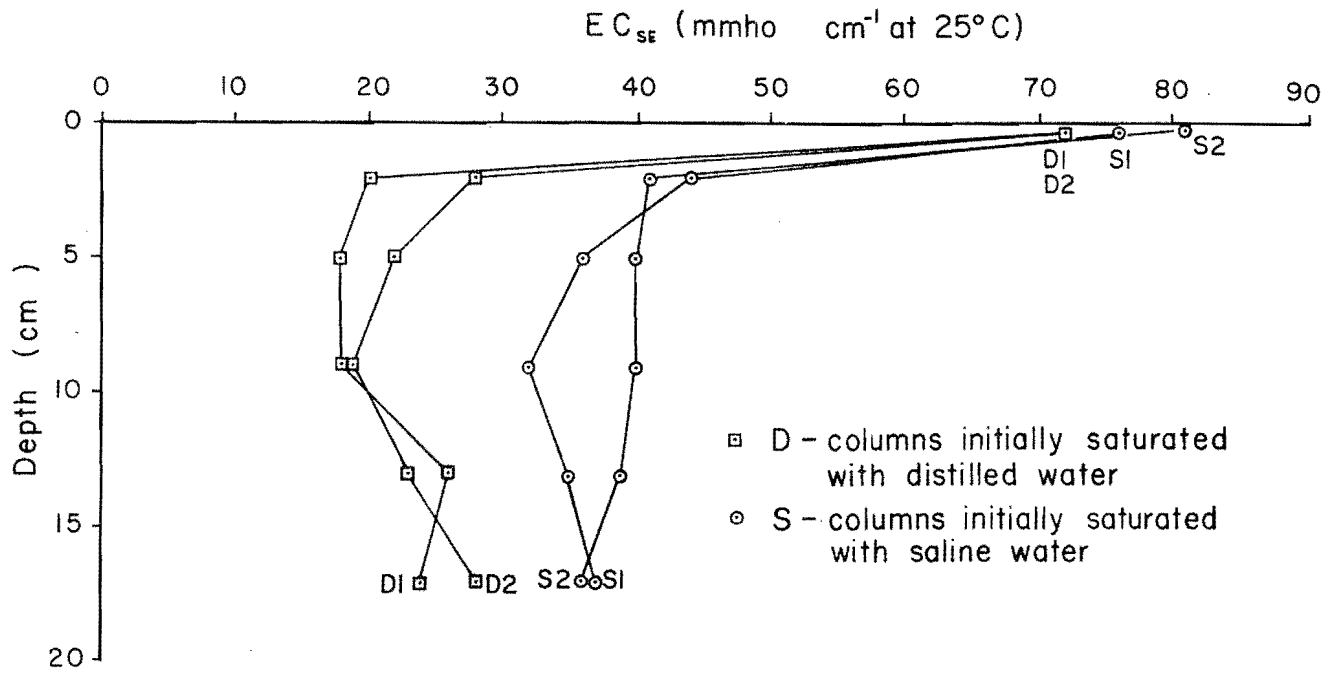


Figure 11. Electrical conductivity of saturation extract versus depth for soil columns saturated with distilled and saline waters after drying for 14 days.

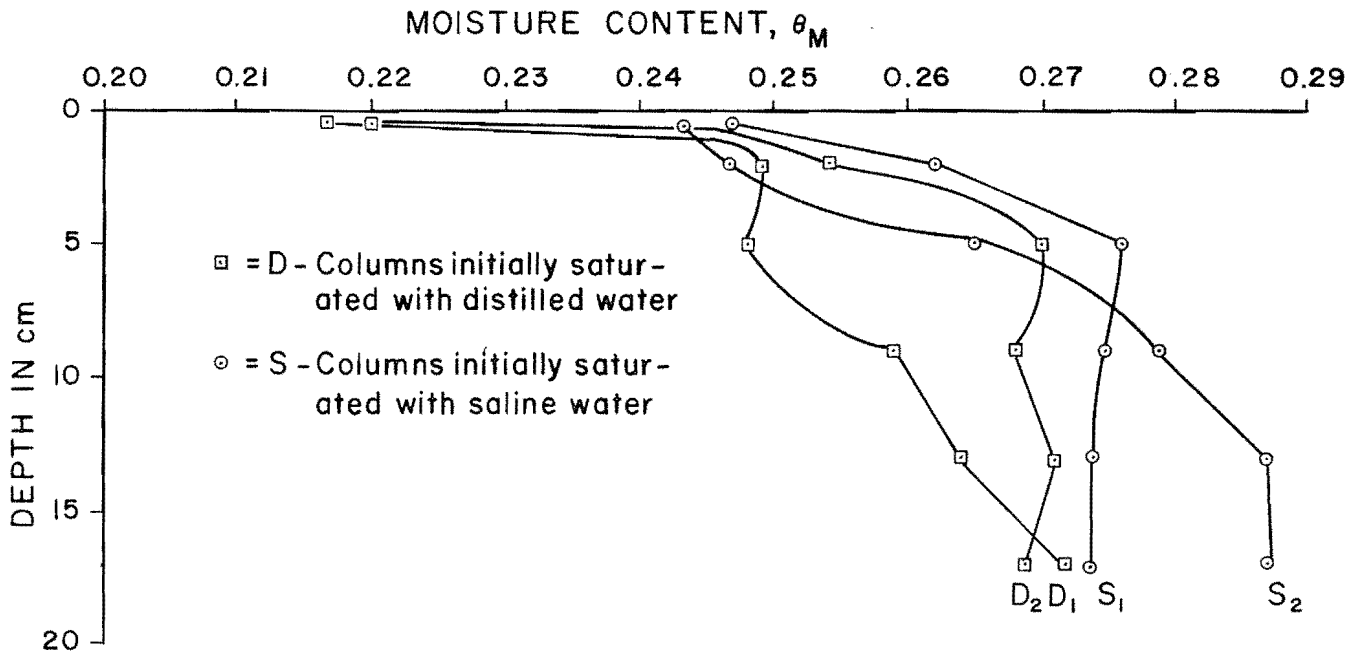


Figure 12. Moisture content vs depth for soil columns initially saturated with distilled and saline waters after drying for 14 days.

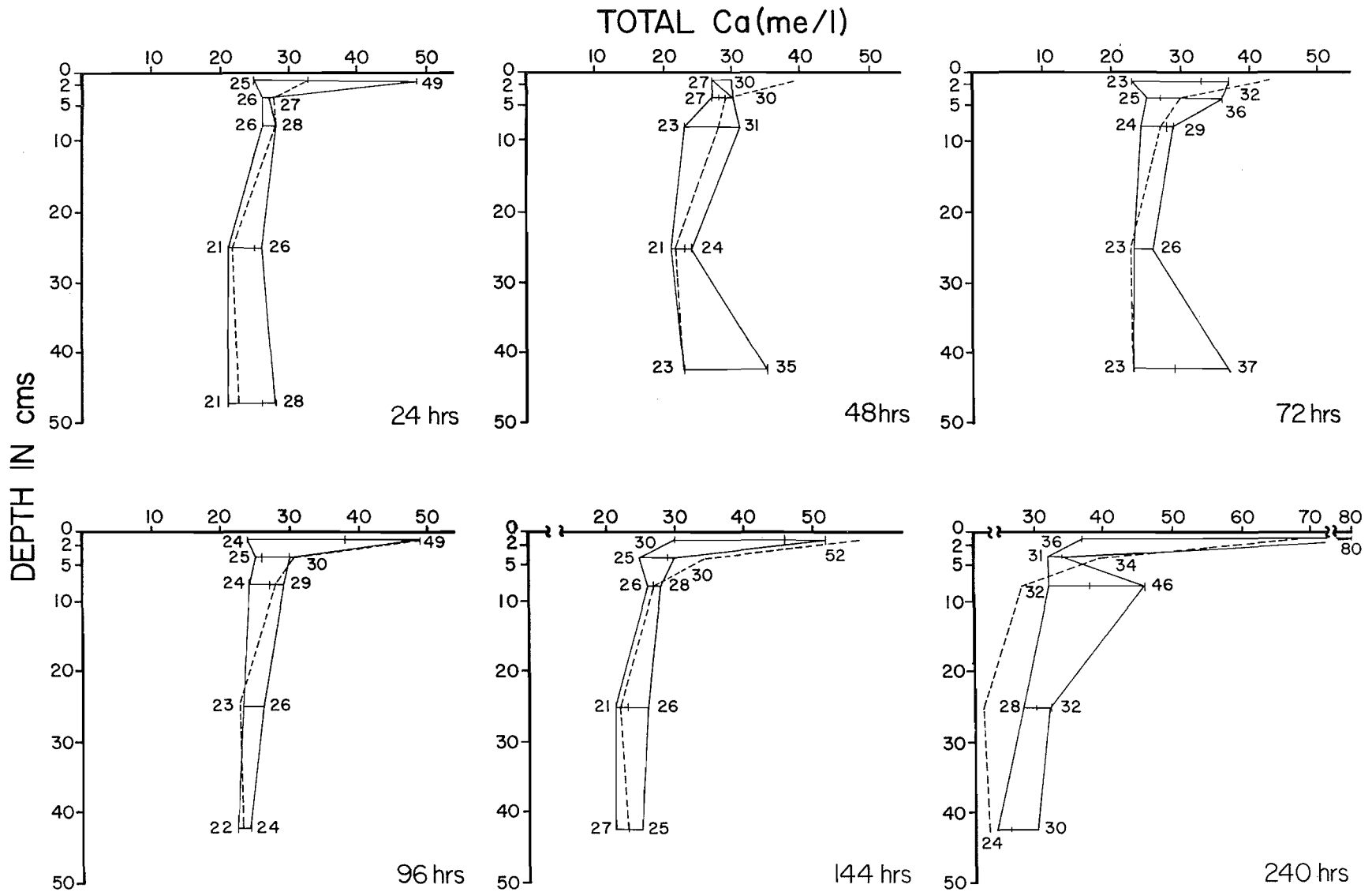


Figure 13. Predicted and measured profiles for total calcium at various time periods (dashed line predicted; solid line measured).

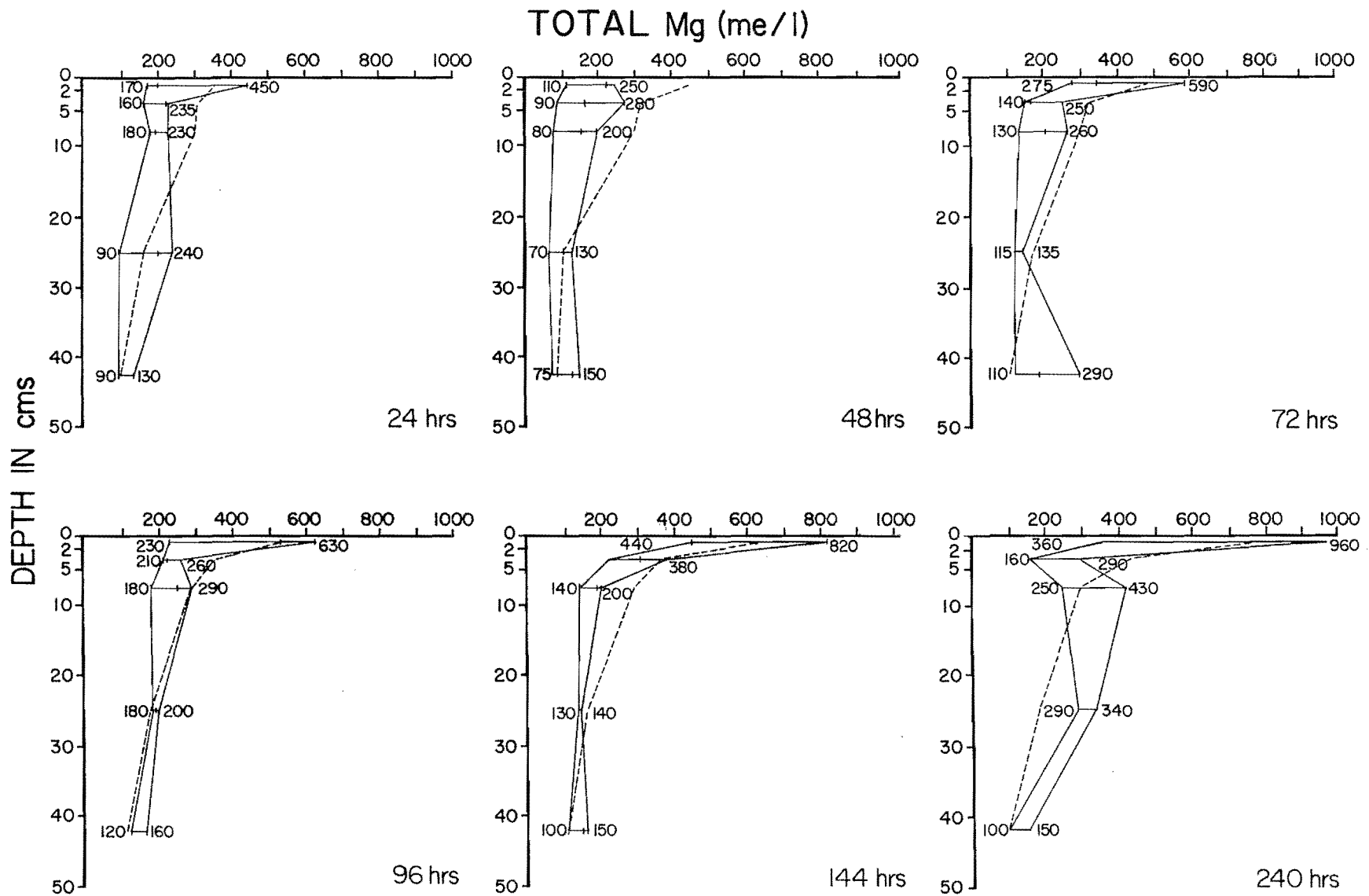


Figure 14. Predicted and measured profiles for total magnesium at various time periods (dashed line predicted; solid line measured).

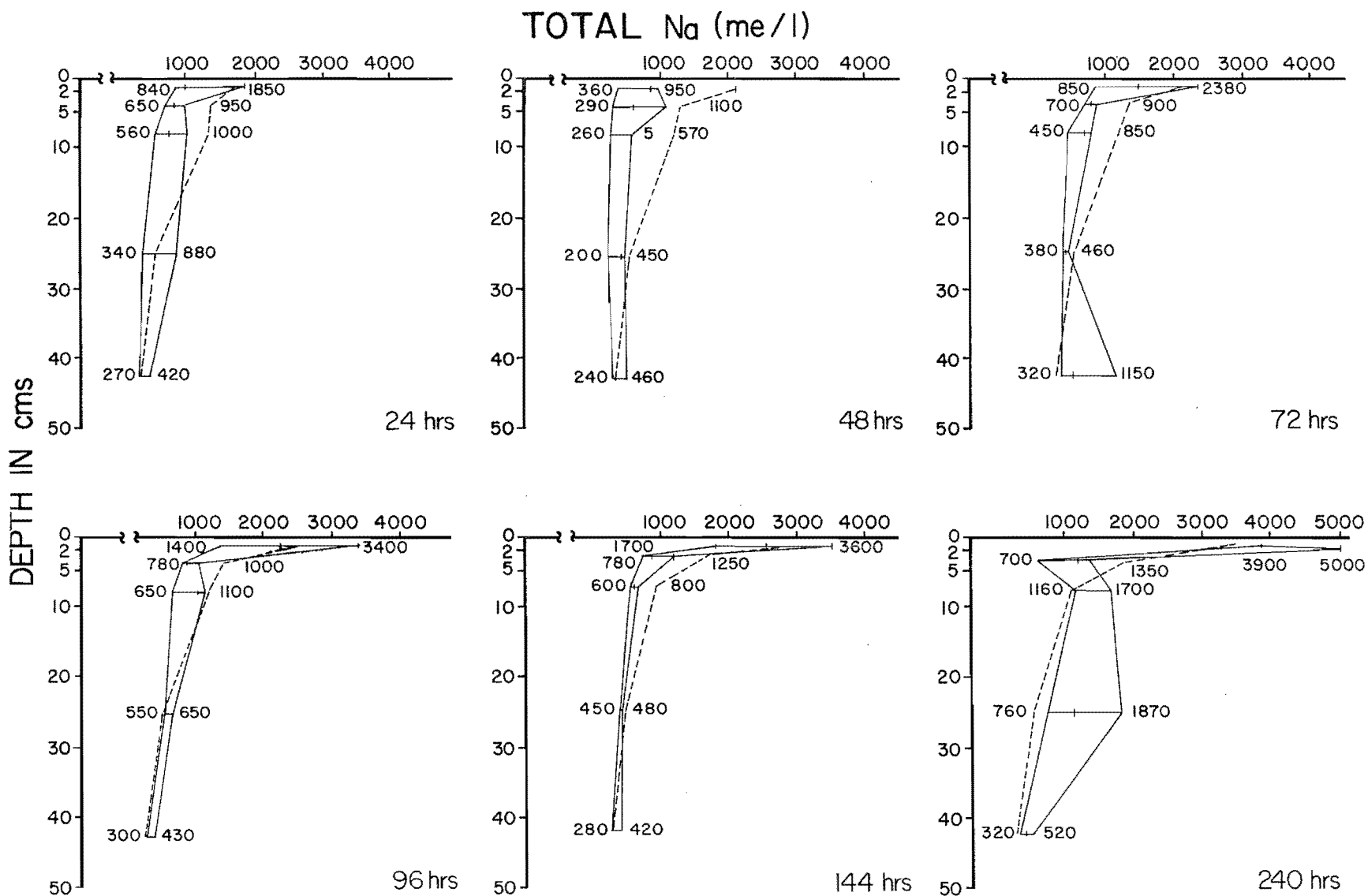


Figure 15. Predicted and measured profiles for total sodium at various time periods (dashed line predicted; solid line measured).

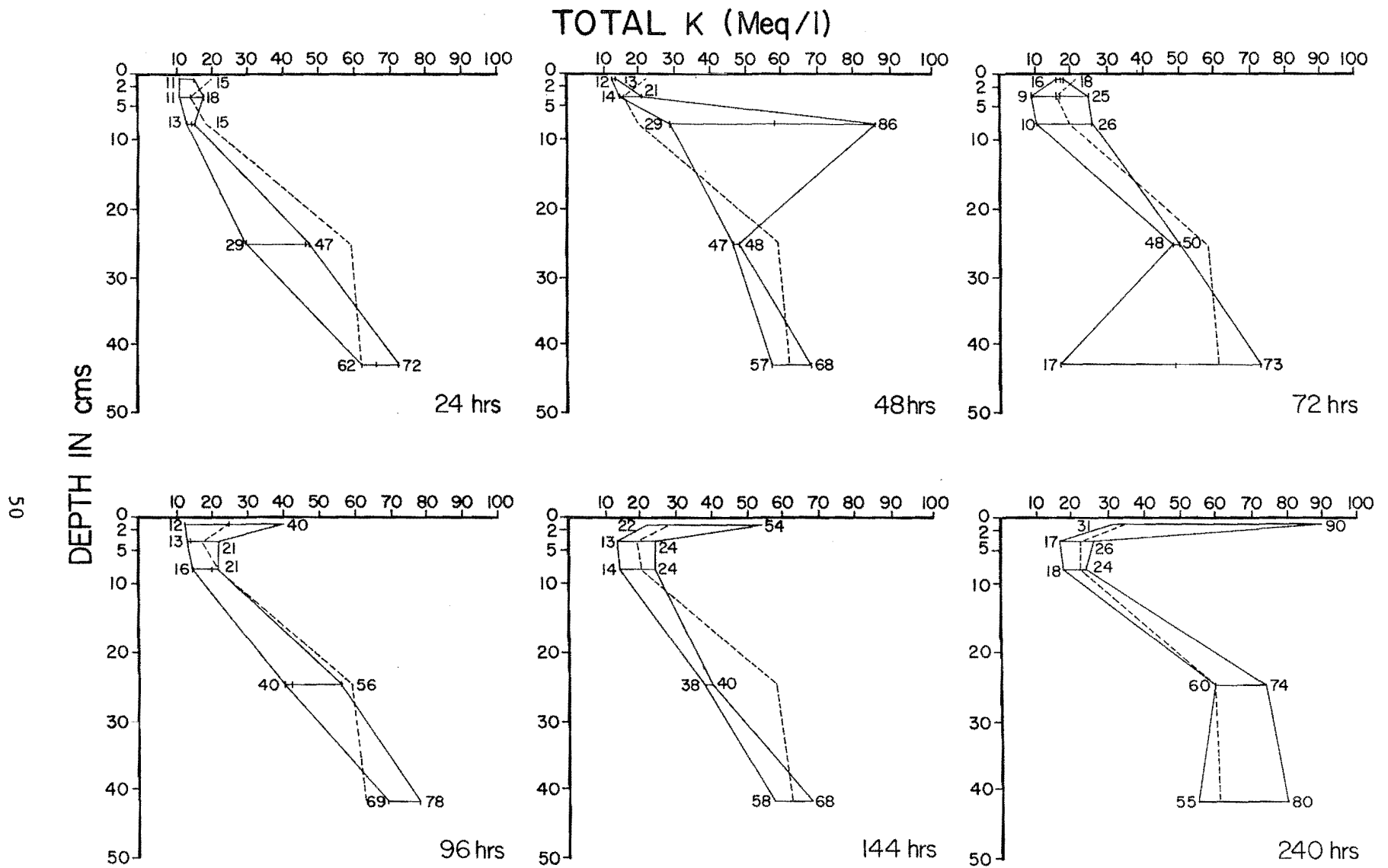


Figure 16. Predicted and measured profiles for total potassium at various time periods (dashed line predicted; solid line measured).

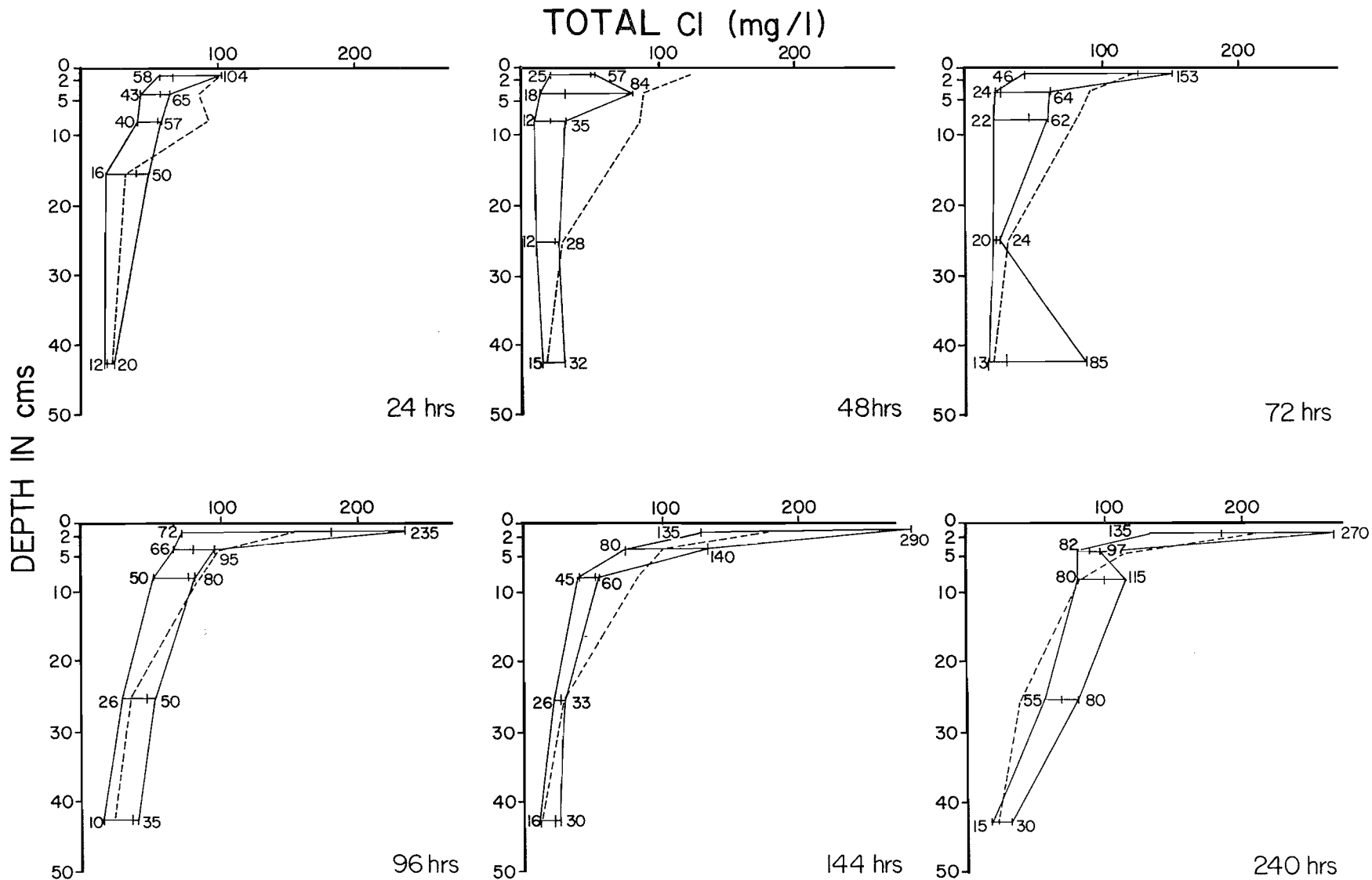


Figure 17. Predicted and measured profiles for total chloride at various time periods (dashed line predicted; solid line measured).

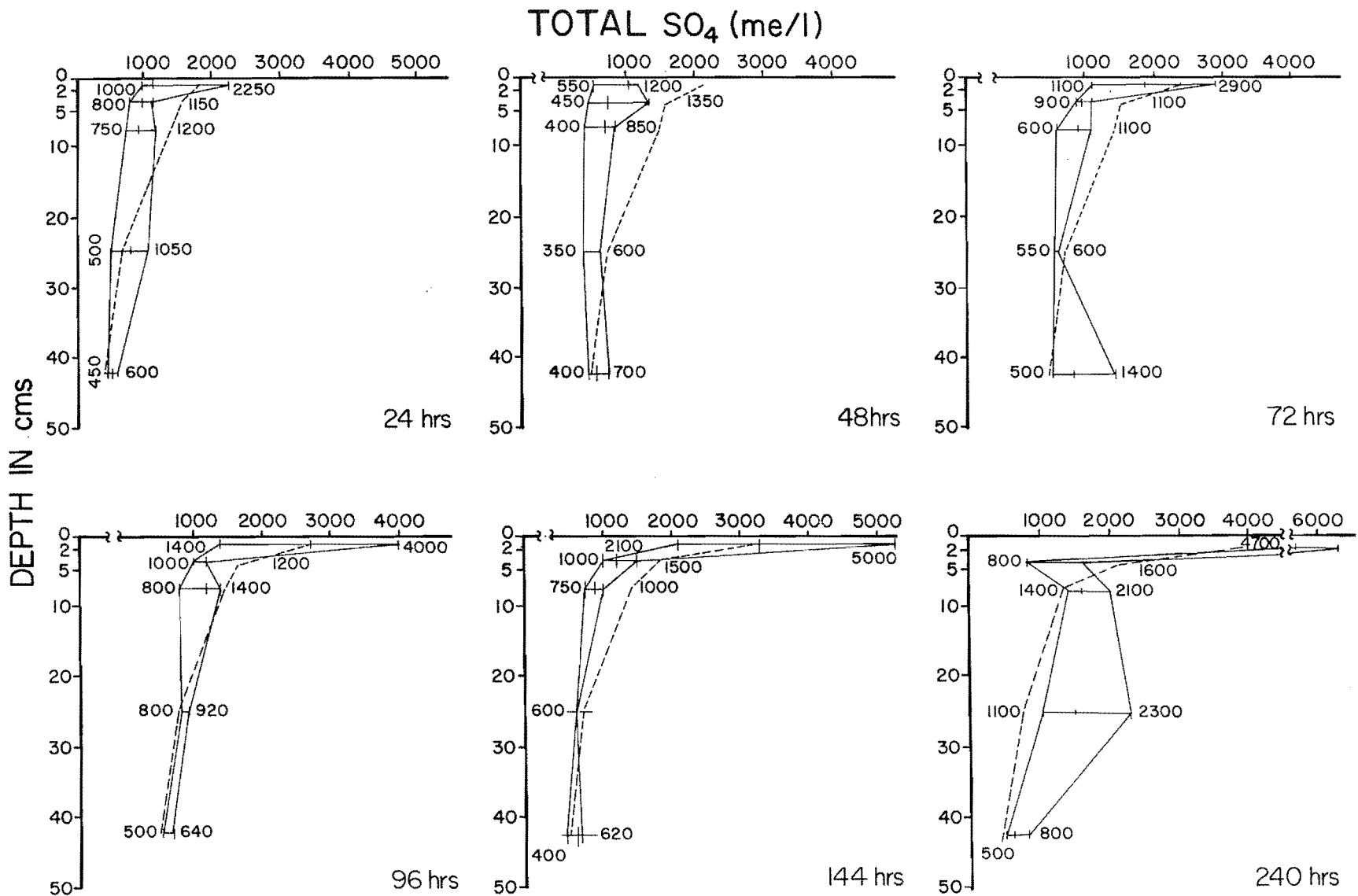


Figure 18. Predicted and measured profiles for total sulfate at various time periods (dashed line predicted; solid line measured).

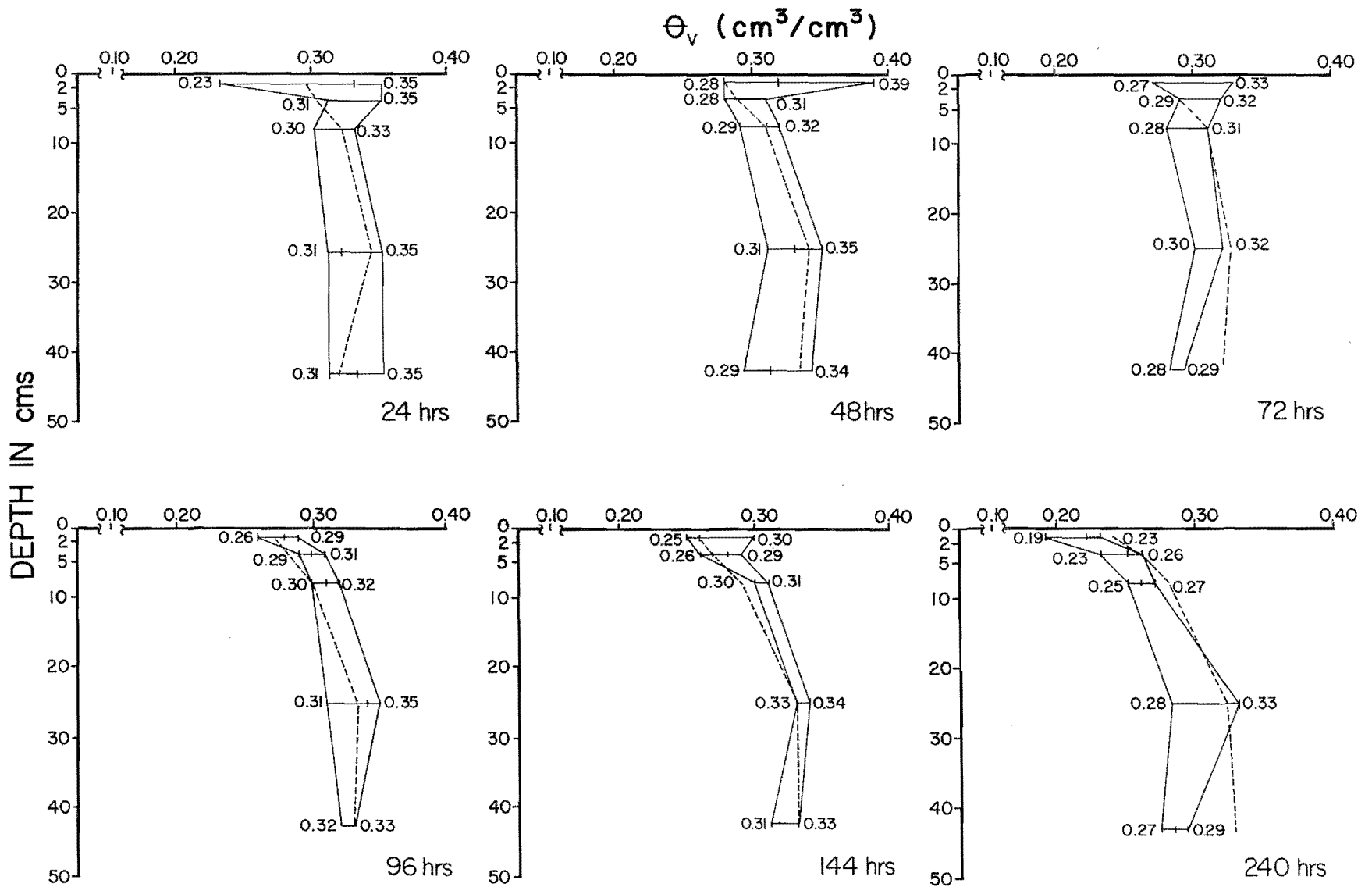


Figure 19. Predicted and measured profiles for volumetric water content at various time periods (dashed line predicted; solid line measured).

depths are overpredicted. In general, the band widths of the measured profiles decrease with time as the initial variability among the columns is damped.

Potassium (K^+) had larger band widths on measured profiles than did the other ions. For example, the predicted profiles at 240 hrs lie completely within the measured profile.

Profiles for chloride (Cl^-) show good agreement for periods of 96 hours and longer. Shapes generally agree for shorter periods. Sulfate (SO_4) profiles also show satisfactory agreement.

Overall, the profile comparisons suggest reasonable model performance. The model performs within the range of accuracy found in the laboratory data, suggesting that more precise measurements would be required to develop a better model. The fact that the subroutine CHEM was found to give reasonable concentrations for calcium, sulfate and carbonate is somewhat surprising considering that the original subroutine was developed for much lower electrolyte concentrations.

Model validity was next examined by comparing the amount of salt efflorescence on the soil surface predicted by the model with that measured in the field or laboratory, as part of this study or by others. Model densities are calculated in grams per square centimeter and based on an assumption of uniform efflorescence thickness. Actual densities vary over small areas (Figure 1), and this variability requires that a number of measurements be made to get an average.

In this study, the laboratory measurements of efflorescence crust density varied between 0.14 g/cm^2 and 0.36 g/cm^2 . In the literature, Riley et al. (1979) report salt efflorescence densities between 0.0001 g/cm^2 and 0.11 g/cm^2 in the upper 2 cm of soil crust. Riley et al. (1982a) report salt efflorescence densities varying between

0.002 g/cm^2 and 0.94 g/cm^2 in the upper 1 cm of soil crust. The model predicted 0.19 g/cm^2 on the 13th day after the efflorescence started to form.

The salt efflorescence densities predicted for each day of accumulation, starting on the second day, are 0.02, 0.04, 0.05, 0.07, 0.09, 0.11, 0.13, 0.14, 0.16, 0.18 and 0.19 g/cm^2 . According to the model, the rate of efflorescence formation remains constant even though the evaporation rate decreases with the formation of efflorescence crust. This can be at least partially explained by increases in the solute concentration of the evaporating soil water causing more salt to be left per unit volume of water evaporated.

The observed stoppage of efflorescence crust formation after 12 days could either be due to the salt crust growing to a thickness that prevents evaporation or due to the clogging of soil pores by precipitating salts at high concentrations. Overall, the present model prediction of salt efflorescence density seems reasonable compared with measured salt efflorescence densities. The variation in measured efflorescence densities is probably due to variation in the salinity of the soil-water which is the source of salt for efflorescence, spatial variation in the physical properties of the soil matrix, and the time of collection with respect to the formation stage of the efflorescence.

In the third and final validity check, the model prediction of ion-pair formation was examined. The percentages of ions involved in ion-pair formation were predicted by the model as 55-75 percent of calcium ions, 59-79 percent of magnesium ions, 7-19 percent of sodium ions and 13-29 percent of potassium ions. The percentage of ion-pair formation increases with increasing concentration (EC from 30-100 mmho/cm). The degree of ion-pair formation by different ions agrees with those report-

ed by Darab et al. (1980) as 15-65 percent of calcium ions, 15-75 percent of magnesium ions and 1-6 percent of sodium ions.

Contribution of Salt Efflorescence
to Overall Salinity

In the estimation of salt loading from efflorescence in the Price River Basin, it was assumed that 1) efflorescence loading occurs mainly during the months of May, June, July and August, 2) every runoff-producing storm carries away all salt efflorescence in the channel bed, 3) the time between storms is the period for growth of efflorescence, and 4) the maximum density of salt efflorescence is reached in 12 days.

Thus, if the time between storms exceeds 12 days, a maximum salt loading is predicted to occur. When the time between two storms is less than 12 days, the salt loading due to efflorescence is less than the maximum amount. Peckins (1981) wrote of a "cleansing effect that occurred between storm flows. There was evidence to indicate that the water quality of a storm flow was improved if it occurred shortly after another storm event. There are several instances when this phenomenon occurred during the study period."

In order to model the variation in the interval between storms, a probabilistic approach was chosen. Data for summer storms and intervals between consecutive storms are given in Appendix A for each year from 1941 to 1977. In assembling these data, it was assumed that a daily precipitation of 0.25 inch or more would produce runoff (Riley et al. 1982b). An exponential distribution (Haan 1977) was fitted to the time interval data by the method of moments. The resulting probability density distribution of the time interval between storms was

$$f(t) = 0.0564 e^{-0.0564t} \quad . \quad . \quad (65)$$

where t is the number of days between consecutive storms.

Salt efflorescence crust density was expressed as a function of time since the last storm from data collected on the rate of accumulation of efflorescence,

$$g(t) = 0.0158t \quad \text{for } 0 \leq t \leq 10 \\ = 0.158 \quad \text{for } t > 10 \quad . \quad . \quad (66)$$

where g(t) is the density of salt efflorescence crust in g/cm² and t is the time in days since the previous storm.

Thus, the expected salt efflorescence density for a storm is expressed as:

$$E(g(t)) = \int_0^{10} g(t) f(t) dt \\ + 0.158 \int_{10}^{\infty} f(t) dt \\ = \int_0^{10} 0.0158t (0.0564e^{-0.0564t}) dt \\ + 0.158 \int_{10}^{\infty} (0.0564e^{-0.0564t}) dt \\ . \quad . \quad . \quad (67)$$

$$= 0.12 \text{ g/cm}^2 \quad (12 \times 10^5 \text{ kg/km}^2)$$

To estimate the basinwide salt load from a storm, the expected value of salt efflorescence crust density was multiplied by the ephemeral channel bed area in the central basin of the Price River, where most efflorescence occurs due to the outcrop of Mancos Shales. The ephemeral channel drainage densities in three subwatersheds (Service Berry Tributary, Soldier Creek and Coal Creek) are 6.79, 9.79, and 9.45 km/km² respectively. Taking an average drainage

density of 8.67 km/km^2 over an area of approximately 907 km^2 , the total length of ephemeral channels is approximately $1,172 \text{ km}$. With an average channel width of 300 cm (10 ft), total area of efflorescence is approximately 5.7 km^2 .

By combining the area of ephemeral channel beds in the central basin with the expected salt efflorescence density at the time of storm occurrence, the expected value of salt loading for a storm is $6.9 \times 10^6 \text{ kg}$. From the 37 years of data in Appendix A, the average number of storms per year is four. Therefore, the expected value of salt loading from efflorescence in the Price River Basin is approximately $27.5 \times 10^6 \text{ kg/yr}$. Taking the total annual salt load at Woodside as $3.7 \times 10^8 \text{ tons}$ (Ponce 1975), the estimated contribution of efflorescence to the overall

salt loading in Price River Basin at Woodside is approximately 7.5 percent.

This estimate of basinwide average annual salt loading from efflorescence is based on several assumptions, some of which bias the estimate toward being too high and others toward being too low. Assumptions that cause bias toward a high estimate are that none of the salt crust is leached back into the soil and that all of it is carried all the way to the mouth of the Price River by each storm. Assumptions biasing toward a low estimate are that no efflorescence loading is associated with channel cleansing during spring snowmelt or other storms outside the four summer months. If one assumes that winter and spring runoff carries away summer storm residuals, the estimate becomes reasonable.

CHAPTER VII

LABORATORY COLLECTION OF SALT SEDIMENT DATA

Introduction

The experimental procedure used to study salt release from suspended sediments was designed:

1) To examine the sources (land, channel bank, or in-channel) of suspended sediment material in the Price River Basin.

2) To perform laboratory experiments with sediment material in order to identify factors controlling the rate of salt release.

3) To develop quantitative relationships for salt release from suspended sediments based on the laboratory data.

Sediment Materials

Sediment samples were taken 1) from lands on the valley floor near the channel, 2) from the channel banks, and 3) from the channel bottom. Valley floor samples were taken from a site near Woodside, and channel bank and bed samples were taken from the Price River at Woodside, Wellington, and Price (Figure 3). An analysis of the saturation extract of the soil sample is provided in Table 9.

Salinity Measurement Procedure

The laboratory work was performed by the Soil Testing Laboratory of the Department of Soil Science and Biometeorology, Utah State University. The samples were mixed with water, and the electrical conductivity (EC) of the solutions was monitored using a Yellow

Springs salinity-conductivity-temperature meter (YSI Model 33). Electrical conductivity is expressed as $\mu\text{mho/cm}$.

All EC's were corrected to a standard temperature of 25°C using temperature correction factors provided by Richards (1954). All experiments were replicated two times for the entire range of the controlling factors. The data presented are the average results from the two replications. The values between replicates never varied by more than $210 \mu\text{mho/cm}$.

Structure of Laboratory Experiments

Experiments were conducted over ranges of the controlling factors matching observed ranges in the Price River Basin. These were dilution (1:1000 to 1:5), particle size (less than 0.074 mm to 2 mm for soil samples and less than 0.074 mm to 7.92 mm for channel material), mixing velocity (0.3 to 2 fps) (0.09 to 0.62 m s^{-1}), and initial EC of solutions containing NaCl and Na_2SO_4 (600 to $8000 \mu\text{mho/cm}$ @ 25°C). Table 10 lists the laboratory experiments.

Saturation extract electrical conductivity measurements, as recommended by U. S. Salinity Laboratory (Richards 1954), were made using a Beckman Model RC 19 conductivity meter incorporating a pipette solution cell and having a precision of $\pm 20 \mu\text{mho/cm}$. The experimental procedure was to record the increase of EC with time.

Recirculating Flume Experiments

The initial experimental design to identify and quantify the factors

Table 9. Chemical analysis of the soil material upland of the channel.

| <u>Texture</u> | | <u>% Gypsum</u> | <u>% Lime CaCO₃</u> | |
|--------------------|----------------|------------------------------|--------------------------------|----------------|
| Silty loam | | 3.9 | 24.3 | |
| -----meq/l----- | | | | |
| <u>Sodium</u> | <u>Calcium</u> | <u>Magnesium</u> | <u>Chloride</u> | <u>Sulfate</u> |
| 135 | 20.6 | 5.2 | 2.4 | 158.1 |
| meq/l | | <u>Saturation Percentage</u> | <u>mmho/cm ECe</u> | <u>pH</u> |
| <u>Bicarbonate</u> | | 42 | 16 | 8.2 |

controlling salt release from suspended sediment utilized a 15.25 m long recirculating flume for channel flow and the transport of suspended sediments. However, nonuniform flows, with high turbulence intensities, were generated at the diffuser. The fact that a constant velocity could not be maintained throughout the length of the flume made it impossible to study the effect of velocity on salt release. In addition, the impact of the recirculating pump blades upon the sediment particles affected the salt release process. Therefore, the laboratory experiments were shifted to a mixing tank and subsequently to a multiple stirrer, in which the flow regime could be more closely controlled.

Mixing Tank Experiments

A 55 gallon (208 l) steel drum was used to mix sediment and water at various mixing velocities. A rectangular 152 mm wide by 508 mm long steel paddle, located at the center of the 559 mm diameter and 914 mm deep tank, was rotated using a variable speed motor (Figure 20). The motor speed was adjusted so that the average velocity measured with a current meter at two points, 152 mm and 229 mm from the center of the tank, was equal to the desired velocity.

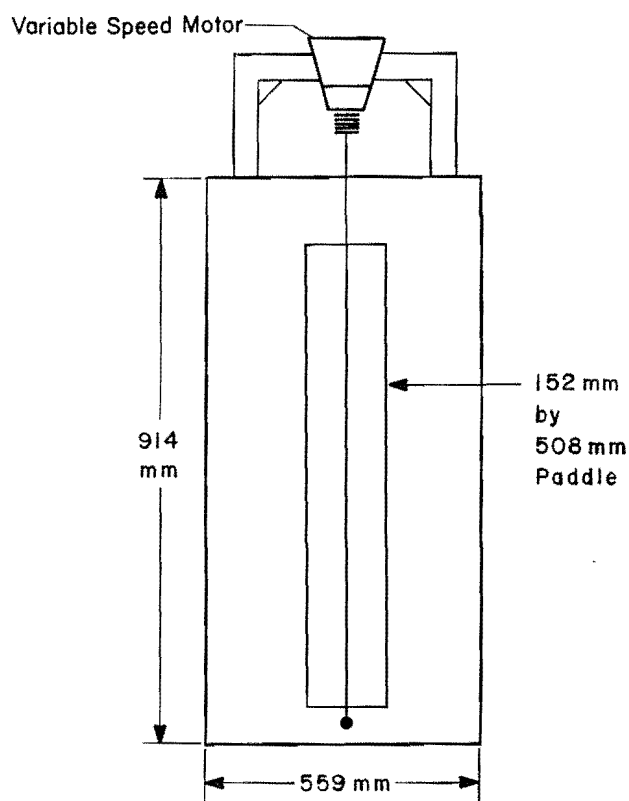


Figure 20. Cross-section of the mixing tank.

Table 10. Summary of the laboratory experiments.

| Experimental Apparatus | Experimental Set | Purpose of the experiments | No. of experiments for each set | Factors which were varied | Levels of factors varied | Factors which were held constant | No. of replicates | |
|------------------------|------------------|--|---------------------------------|--|--|--|-------------------|-----|
| Mixing Tank | A | To study the effect of dilution | 8 | Dilution | Dilution (1:10, 1:20, 1:40, 1:60, 1:80, 1:125, and 1:250) | Mixing velocity and particle size | 8 | |
| | B | To study the effect of mixing velocity | 5 | Mixing velocity | Mixing velocity (.3, .7, 1, and 2 feet per second) | Particle size and dilution | 5 | |
| Multiple Stirrer | C | Comparison of various sediment material | 6 | Dilution and particle size | Dilution (1:5, 1:10, 1:50, 1:100) particle size $d < 2$ mm, $0.125 < d < 0.5$, and $0.074 < d < 0.125$ mm) | Mixing velocity | 6 | |
| | D | To study the effect of dilution | 6 | Dilution | Dilution factor (1:100, 1:75, 1:50, 1:20, 1:10, and 1:5) | Particle size and mixing velocity | 6 | |
| | E | To study the effect of particle size | 6 | Particle size | Particle size fraction ($3.71 < d < 7.92$ mm, $1.651 < d < 3.79$ mm, $d < 2$ mm, $1.0 < d < 1.651$ mm, $0.5 < d < 1.0$ mm, and $d < 0.074$ mm) | Mixing velocity | 6 | |
| | F | To study the effect of mixing velocity | 14 | Mixing velocity | Mixing velocity (0.96 and 0.43 fps) ($d < 0.074$ mm, $0.175 < d < 0.5$ mm, $0.85 < d < 1.651$, and $d < 1.981$ mm) | Particle size and dilution | 14 | |
| | G | To study the interaction of mixing velocity and the particle size | 4 | Mixing velocity and particle size | Mixing velocity (0.43 and 0.96 fps) ($0.175 < d < 0.417$ mm, $0.104 < d < 0.175$ mm) | Dilution | 4 | |
| | H | To study the effect of initial EC (NaCl and Na ₂ SO ₄ solutions) | 24 | Initial EC and dilution | Initial EC (602, 1125, 2102, 2658, 3484, 5851, and 7773 umho/cm @ 25°C) Dilution (1:100, 1:75, 1:50) | Mixing velocity and particle size | 24 | |
| | I | Verification of Equations 28 and 32 | 30 | Dilution, mixing velocity, and particle size | Dilution (1:1000, 1:500, 1:250, 1:100, 1:75, 1:50, 1:20, 1:10, 1:5) Mixing velocity (0.96 and 0.43 fps) Particle size fraction ($0.5 < d < 1$ mm, $0.125 < d < 0.5$ mm, and $0.074 < d < 0.125$ mm) | Initial EC, mixing velocity, particle size, and dilution | 30 | |
| | Total | | | 103 | | | | 103 |

The soil samples were mixed with water varying the dilution factor (sediment:water ratio) and the mixing velocity. The particle sizes of the sediment material were not varied and were less than 2 mm for all the experiments. Tap water with an EC of about 350 $\mu\text{mho/cm}$ ($\mu\text{S cm}^{-1}$) was used; and, the tank was filled several days before each run to give the water time to reach ambient room temperature. During the experiments, the observed water temperature was about $25 \pm 1^\circ\text{C}$. The EC measurements were made at about 14 time intervals, ranging from 5 seconds to several hours. The probe of the EC meter was lowered to approximately the middle depth of the mixing tank and the electrical conductivity was monitored. The probe was taken out of the mixing tank and prepared for the next reading after careful rinsing in deionized water. The mixing tank was also emptied and washed with tap water after each experimental run.

Multiple Stirrer Experiments

For greater efficiency and more control, a multiple stirrer with six

stirring units was used. Each unit had a 25 mm wide by 75 mm long steel paddle which mixed the sediment-water solution in a 1000 ml glass beaker. The paddles were lowered into the beakers, and their depths were adjusted so that the velocity of the moving water closely approximated the parabolic distribution found in channel flow, a velocity maximum at the water surface and close to zero at the bottom. The mixing speed of the steel paddles, controlled by a powerstat and indicated by a centrally located tachometer, was set to match the velocity of the moving water when averaged over the depth of the beaker.

The initial experiments used deionized water. To study the effect of initial EC upon the rate of salt release, experiments (Set H, Table 10) were conducted using initially saline solutions. Sodium sulfate (Na_2SO_4) and sodium chloride (NaCl) were used to prepare solutions with the desired initial EC. Sodium salts, and sodium sulfate in particular, are the most common salts in the water system of the Price River Basin.

CHAPTER VIII

SALT RELEASE CHARACTERISTICS OF PRICE RIVER BASIN SEDIMENTS

Introduction

This chapter describes the results of the experiments to determine the salt release characteristics of the suspended sediments in the Price River Basin. First the salt release characteristics of sediment materials from various sources were examined in a search for the material with the greatest salt release potential. This material was then examined to determine the important factors affecting salt release.

Salt Release Characteristics by Sediment Source

The laboratory experiments examined sediments from the bottoms of perennial streams, the banks of perennial streams, and the surface of the valley floor. Representative samples were mixed with deionized water, and the electrical conductivity of each solution was monitored until there was little or no change in the EC. The last EC measurement was assumed to be the equilibrium EC of the sediment-water suspension.

The channel bottom material released its salts quickly with little increase upon mixing. The saturation extract, EC, indicative of the low salt release potential of in-channel sediments, was in the order of 500 to 1000 $\mu\text{mho/cm}$.

The channel bank material was collected from the unwetted exposed cross-section of the Price River channel during low flows. This material had a saturation extract EC of 1000 to 3000 $\mu\text{mho/cm}$ two to three times that of

the bed material. Similar experiments were conducted with the soil material taken from the valley floor near the Price River channel. Figure 21 compares the salt release rates between bank and valley floor materials. The increase in EC for the channel material is quite rapid in the first few minutes (suggesting a spike on a halograph of dissolved salts) and decreases to almost zero soon thereafter. In contrast the soil samples taken upland of the Price River channel showed lower rates of salt release for about the first 12 minutes but larger rates thereafter, with the total EC reaching two to three times bank values. It took 1 to 4 hours for the EC of the solutions to approach equilibrium. The rapid initial salt release from the channel bank materials can probably be attributed to salt efflorescence.

The apparent equilibrium EC can be assumed to give a good indication of the potential salt release from the sediment. The greater equilibrium EC from the soil material taken from the uplands is undoubtedly because these materials are less weathered. This sediment material was selected for detailed further study of salt release characteristics. However, the channel bank material was also examined to probe the effects of the factors controlling salt release from suspended sediments.

Factors Controlling Salt Release from Upland Soil Material

Laboratory Approach

The selected upland soil material was a composite sample taken from the

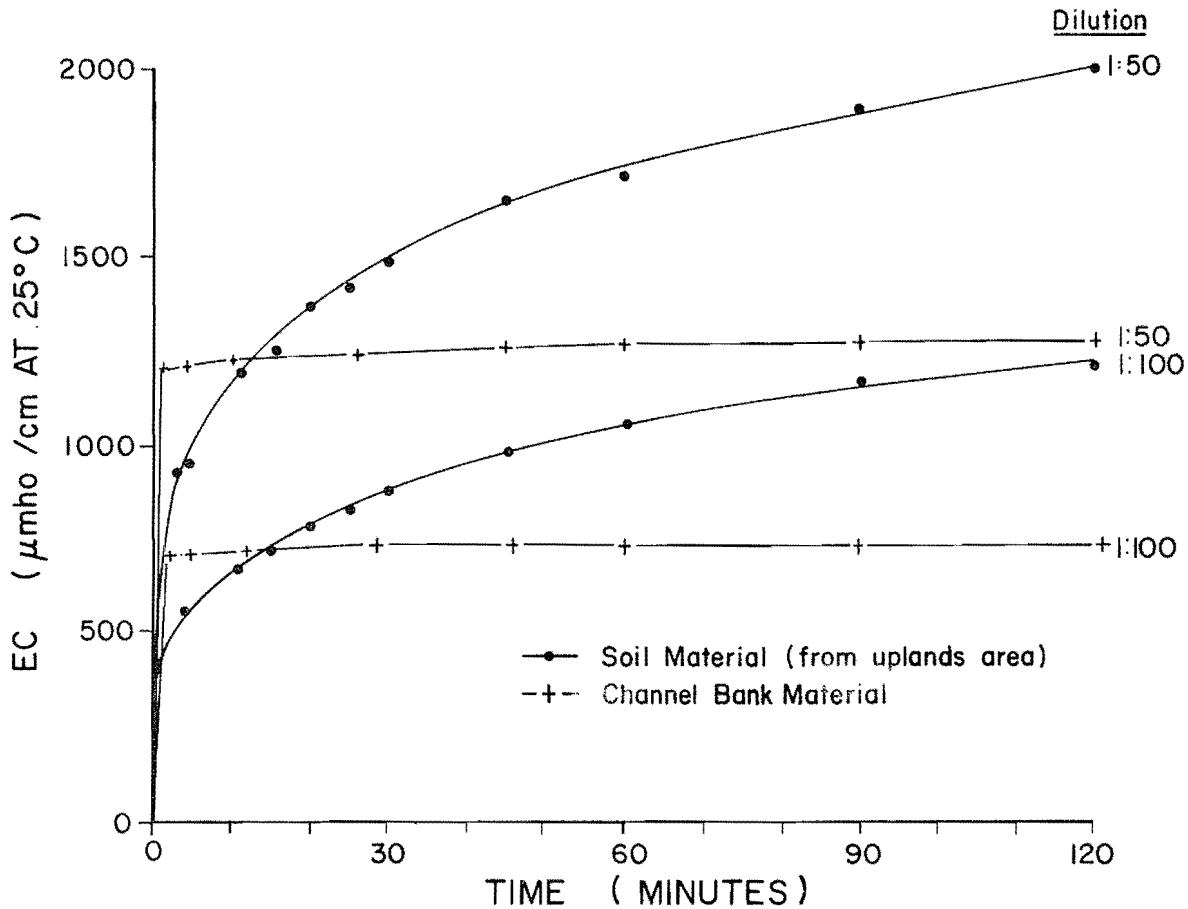


Figure 21. Comparison of the salt release characteristics of channel bank and valley floor sediments (Experimental Set C, Table 10).

surface (0-15 cm) at a site near Woodside (Figure 3). The soil had a silty loam texture, and its saturation extract indicated a $Ca^{2+} - Na^+ - SO_4^{2-}$ system (Table 9). To determine their effects on the salt release characteristics of dilution, particle size, mixing velocity, and the initial EC of the solution, adjusted by adding sodium salts, were varied in the experimental runs. The effect of each of these factors is discussed individually below.

Effect of Dilution

The dilution factor is defined as the ratio of sediment to water on a weight basis. Figures 22 and 23 show the relationships between the dilution

factor and salt release from soil-water suspensions in the mixing tank and the multiple stirrer systems, respectively. For both apparatuses, the initial dissolution rate increased with the soil to water ratio; however, the dissolution continued longer with smaller ratios.

The pattern can be shown for different soil to water ratios by comparing the salt release rates as indicated by slopes of the lines tangent to the salt release curves at given contact times. For example, at 1 minute of contact time and a 1:5 soil to water ratio, the salt release rate is 5.09 mmho/cm/min, whereas it is 0.69 mmho/cm/min at a soil to water ratio of 1:50. After 30 minutes contact time, the salt release rates are 1.46 and 10.4 µmho/cm/min

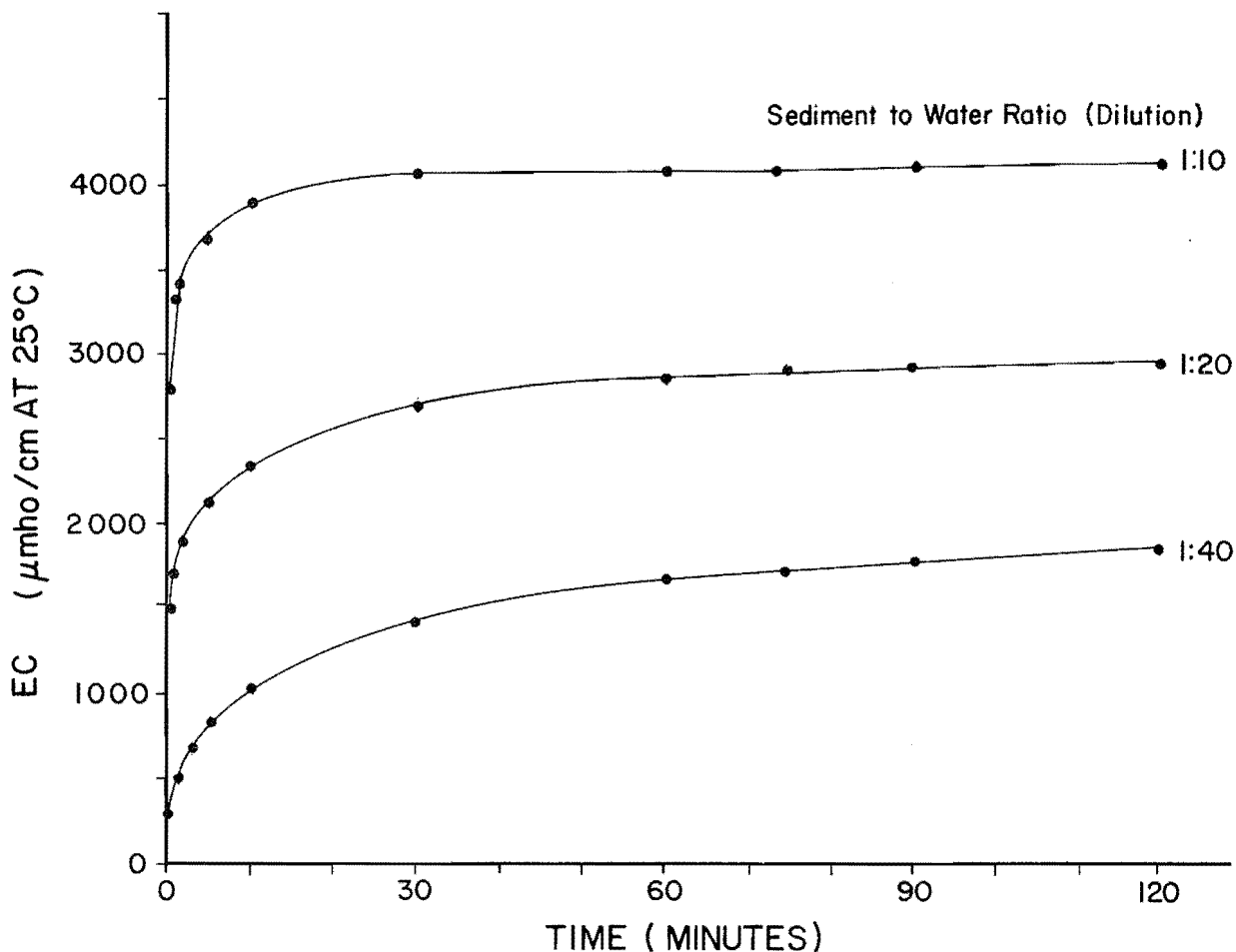


Figure 22. Effect of dilution factor on salt release in the mixing tank apparatus (Experimental Set A, Table 10).

for the 1:5 and 1:50 soil to water ratios, respectively, and the ratio of the two rates has approximately reversed.

Another perspective of the relationship is seen when best fit lines are constructed through salt release data presented on a log-log plot (Figure 24). The intercepts are higher at the larger soil to water ratios, representing initial rapid dissolution, whereas the slopes decrease with increasing soil to water ratios.

From still another perspective, the dilution factor also affects the time

required to reach apparent equilibrium. At the larger soil to water ratios, the salt release reaction approaches equilibrium after a few minutes of contact time. In contrast, at the smaller soil to water ratios (higher dilutions), the reaction proceeds for hours before it approaches equilibrium. The time was less than 60 minutes for dilutions 1:5 and 1:10 and about 4 hours for dilutions of 1:20 to 1:100.

These differences can be explained by molecular diffusion, which is usually considered to be the rate limiting factor in a dissolution process (Stumm and Morgan 1970). The concentration gradient is defined as the difference

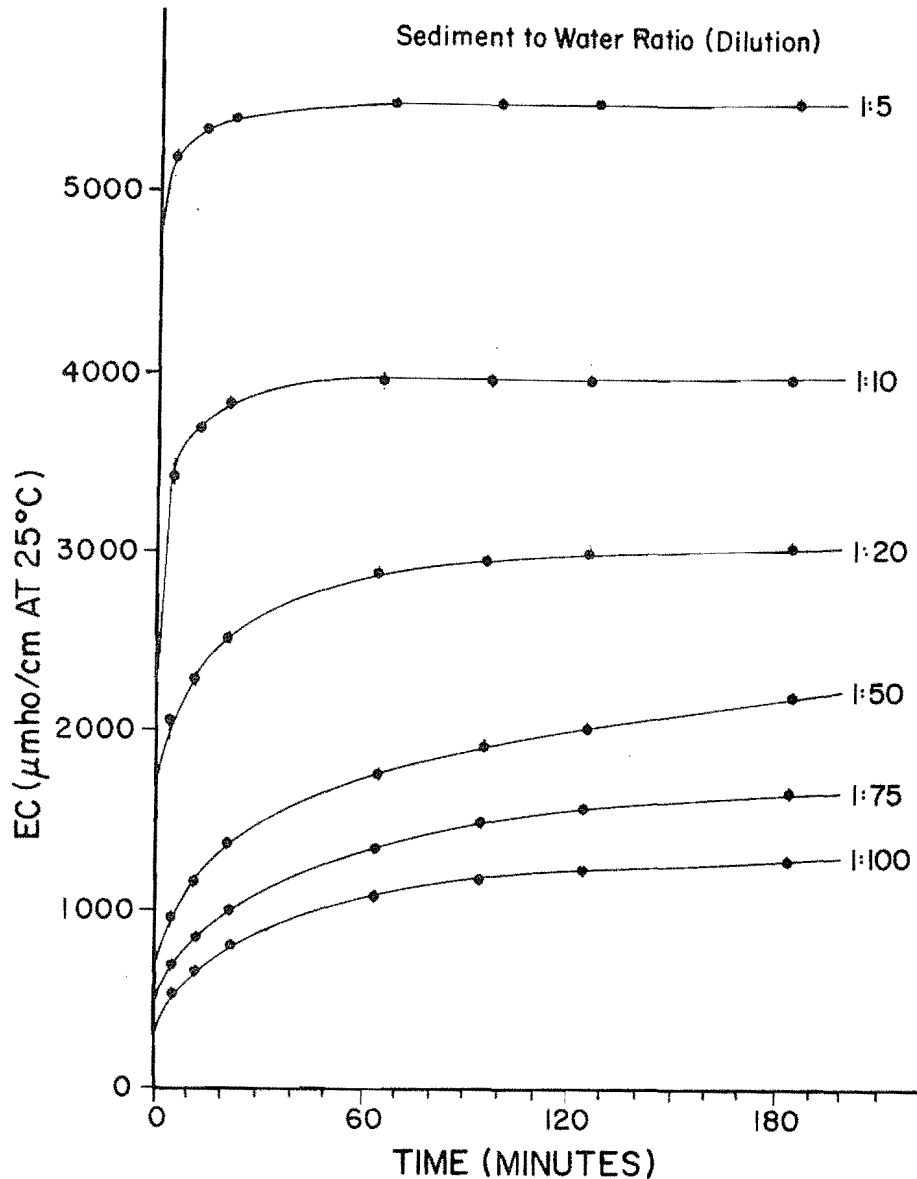


Figure 23. Effect of dilution factor on salt release in the multiple stirrer system (Experimental Set D, Table 10).

between the equilibrium concentration of the soil-water system and the concentration of the uniformly mixed bulk solutions. At higher soil to water ratios, the concentration gradient is less than that at lower soil to water ratios where the gradient remains relatively large throughout the dissolution process. Therefore, the system approaches equilibrium more rapidly at higher soil to water ratios.

Effect of Particle Size

Figures 25 and 26 show relationships between particle size and salt release from channel bank and soil materials, respectively. The trend was for higher salt release from smaller sizes than from the coarser material. The effect was more distinct in channel bank than in soil material, where higher EC sometimes resulted from a coarser

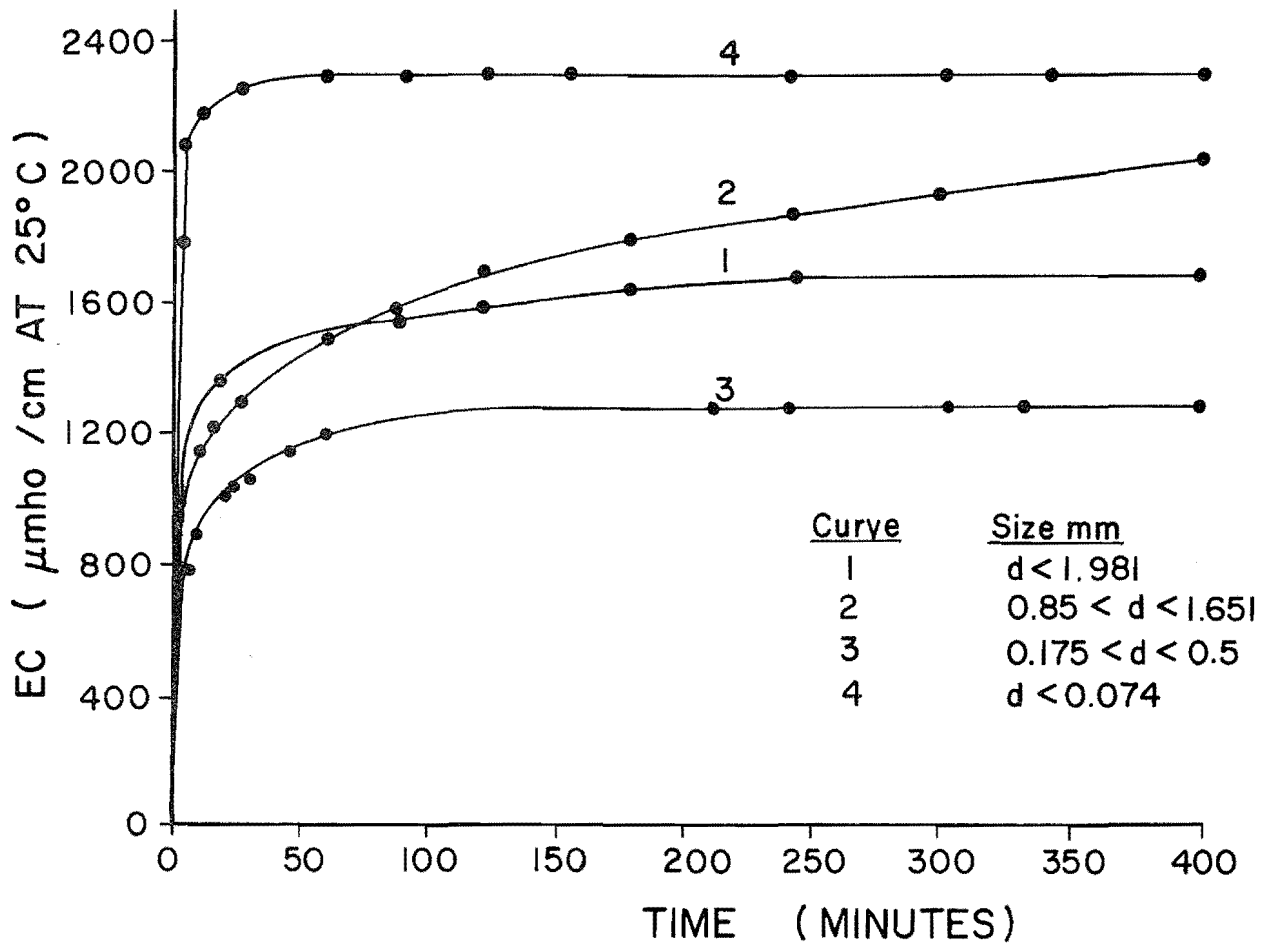


Figure 26. Effect of particle size on salt release from channel bank material (Experimental Set E, Table 10).

the consistently high r^2 values. The k value increased as the sediment to water ratio increased.

Equation 22, judging by r^2 values only, seemed to predict salt release more closely in high than in low dilutions. However, the test of r values provided by Snedecor (1967) failed to establish a significant difference among the coefficients of determination for different dilution factors. Consequently, the equation originally tested in solutions of 1:1 dilution (Jurinak, Whitmore, and Wagenet 1977) can be applied up to dilutions as high as 1:100. A relationship between k' and the sediment to water ratio was sought by regressing k' against the dilution factor, δ , with the results:

$$k' = 1626.40 \delta^{1/2} \dots \dots \dots (69)$$

The r^2 value was 0.972, and the strong relationship between k' and the dilution factor suggests that k can be decomposed into factors controlling salt release and that the dilution factor is one of these.

Equation 68 had the highest overall r^2 values, but the Snedecor (1967) test did not show a significant improvement from Equation 22. However, in fitting data to Equation 22, only k' was evaluated and n was fixed at a value of 2. In the case of Equation 68, both J and n were evaluated, which resulted in slightly higher r^2 values. Both J and n values increased with a greater sediment to water ratio. The n values varied from 4.42 to 56.0 compared to the value of 2 reported by Jurinak, Whitmore, and Wagenet (1977).

Table 11. Experimental data on increase in conductivity with time for various dilution factors.

| Time (Min) | Dilution Factor | | | | | |
|------------------|-----------------|------|------|------|------|-------|
| | 1:5 | 1:10 | 1:20 | 1:50 | 1:75 | 1:100 |
| 0.5 | -- | -- | -- | -- | -- | 363 |
| 1. | 5089 | -- | -- | 690 | 547 | -- |
| 2. | -- | 3068 | 1748 | -- | -- | -- |
| 2.5 | -- | -- | -- | -- | 606 | -- |
| 3. | 5118 | -- | -- | 927 | -- | -- |
| 3.5 | -- | 3424 | 2056 | -- | -- | -- |
| 4. | -- | -- | -- | -- | -- | 559 |
| 4.5 | -- | -- | -- | 951 | 690 | -- |
| 5. | 5231 | -- | -- | -- | -- | -- |
| 6. | -- | -- | 2176 | -- | -- | -- |
| 6.5 | -- | 3555 | -- | -- | -- | -- |
| 10. | 5327 | -- | -- | -- | -- | -- |
| 10.5 | -- | -- | 2348 | -- | -- | 656 |
| 11. | -- | 3656 | -- | 1189 | 820 | -- |
| 15. | -- | -- | -- | -- | 892 | 713 |
| 15.5 | 5350 | -- | -- | 1248 | -- | -- |
| 16. | -- | 3745 | 2450 | -- | -- | -- |
| 20. | 5406 | -- | -- | 1368 | 960 | 780 |
| 21. | -- | 3816 | 2556 | -- | -- | -- |
| 25. | -- | -- | -- | 1416 | 1026 | 822 |
| 30. | 5436 | -- | 2664 | 1488 | 1056 | 876 |
| 31. | -- | 3840 | -- | -- | -- | -- |
| 45. | 5472 | -- | 2796 | 1650 | 1206 | 984 |
| 46. | -- | 3936 | -- | -- | -- | -- |
| 60. | -- | -- | 2856 | 1716 | 1296 | 1056 |
| 61. | 5480 | 3976 | -- | -- | -- | -- |
| 90. | 5480 | 3980 | 2952 | 1896 | 1416 | 1170 |
| 120. | 5480 | 3984 | 3014 | 2046 | 1535 | 1206 |
| EC _{eq} | 5481 | 3980 | 3045 | 2296 | 1632 | 1285 |

EC's are in $\mu\text{mho/cm}$ @ 25°C.

Effect of Mixing Velocity

Soil samples of particle size less than 2 mm were prepared to investigate the effect of mixing on salt release (Experiment Set B, Table 10). The dilution of 1:20 was kept constant. First the soil sample was weighed and poured into the mixing tank, containing a measured volume of water, without starting the motor (velocity = 0.0 fps),

and EC was recorded. Then a set of five experiments was conducted with average mixing velocities ranging from 0.3 up to 2 fps (0.09 to 0.61 m s⁻¹). Figure 27 is a plot of the results. The lowest curve corresponds to the experiment performed without mixing, and therefore, salt movement principally by diffusion.

An increased mixing velocity accelerated the salt release rate up to a velocities of 1 fps (0.31 m s⁻¹). This velocity is approximately that required for suspension of material of the particle size used, i.e., $d < 2$ mm. The explanation suggested is that the thickness of the stagnant boundary layer formed during dissolution depends on the turbulence (mixing) of the system. At high turbulence this thickness is decreased and the rate of salt release (dc/dt) is increased (Equation 17). In other words the slow Fickian diffusion toward the liquid/solid interface is replaced by more rapid turbulent diffusion away from the suspended particles.

The reason that the rate of salt release did not increase for mixing velocities beyond that required for suspension of the sediment might also be that the turbulence is sufficient to limit the thickness of the stagnant layer to a lower bound. Beyond this point, increased turbulence would neither reduce the boundary layer thickness nor increase dc/dt in Equation 17. To investigate whether or not the mixing velocity was affecting the total amount of salt released, another set of experiments (Set F, Table 10) was conducted using the multiple stirrer. Soil samples of different size fractions were prepared and mixed with deionized water at a mixing speed of 100 rpm (revolutions per minute) for about 6 hours, and the EC of the solutions was recorded. Then the mixing was stopped and the suspensions were covered to minimize evaporation. After 2 days a final EC was recorded as the apparent equilibrium EC.

Table 12. Summary of curve fitting analyses of data on increasing salinity concentration with time.

| Eq. No. | Equation | | Dilution | | | | | | Average Values |
|---------|---|----------|----------|--------|--------|--------|--------|--------|----------------|
| | | | 1:100 | 1:75 | 1:50 | 1:20 | 1:10 | 1:5 | |
| 18 | $\ln \left(1 - \frac{C}{C_s} \right) = kt$ | k | 0.0275 | 0.0254 | 0.0247 | 0.0515 | 0.0807 | 0.0993 | 0.0515 |
| | | r^{2a} | 0.946 | 0.935 | 0.911 | 0.931 | 0.911 | 0.830 | 0.910 |
| 22 | $C = k' t^{1/2}$ | k' | 137 | 172 | 234 | 389 | 551 | 772 | 375.8 |
| | | r^2 | 0.952 | 0.945 | 0.937 | 0.863 | 0.808 | 0.754 | 0.876 |
| 68 | $C = J t^{1/n}$ | J | 407.3 | 501.1 | 691.8 | 1698.2 | 3548.0 | 5128.6 | 1995.8 |
| | | n | 4.42 | 4.44 | 4.48 | 8.0 | 17.45 | 56.0 | 15.82 |
| | | r^2 | 0.991 | 0.985 | 0.996 | 0.968 | 0.877 | 0.930 | 0.957 |

^ar values were tested for significance, and all were found to be significant at 99 percent level.

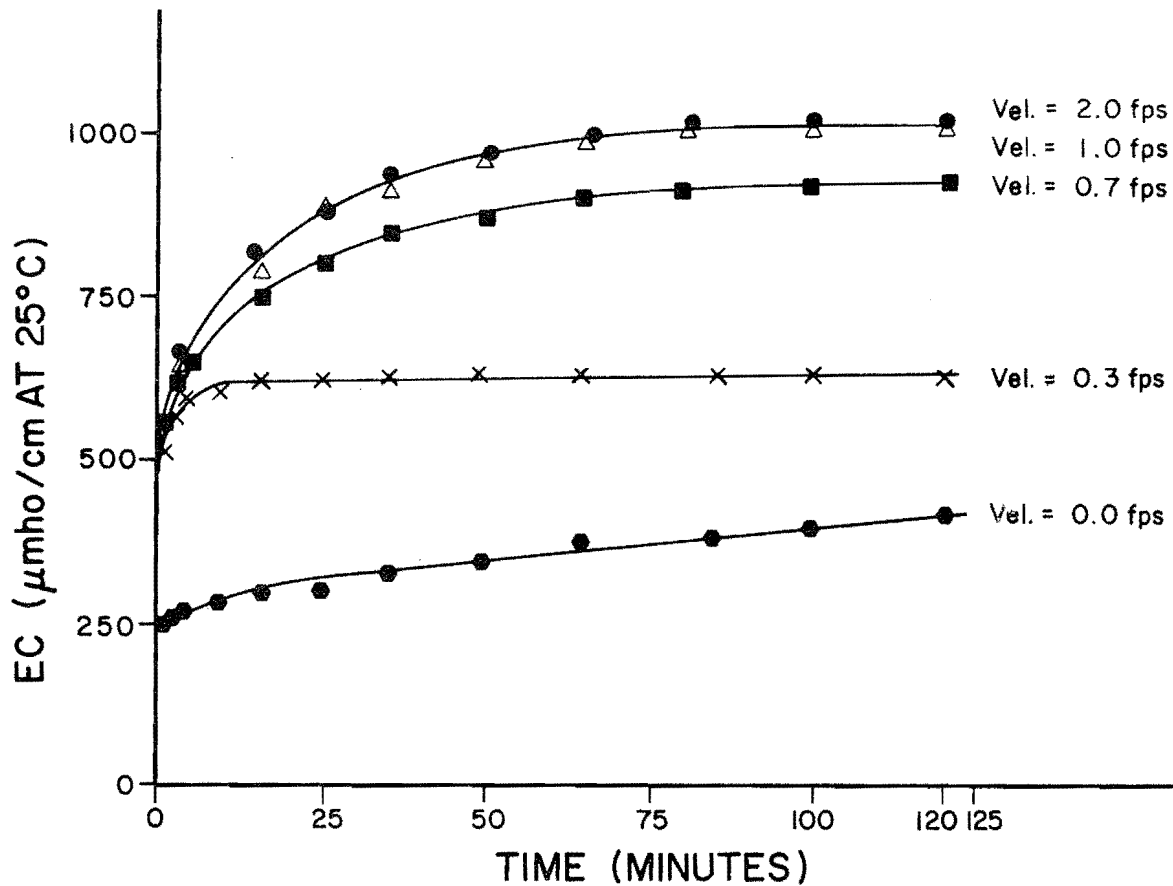


Figure 27. Effect of mixing velocity on salt release (Experimental Set B, Table 10).

The experiments were repeated at a speed of 50 rpm. Figure 28 contains the salt release curves. It was interesting that solutions mixed at different velocities converged to the same apparent equilibrium EC in three of the four cases.

The anomaly between curves 7 and 8 might have been caused by the presence of white material which X-ray diffraction showed to be gypsum. It was suspected that the particles are coated with a less soluble mineral, such as iron or silica oxide, which retarded the salt release rate. A subsample of gypsum, when analyzed by the Soil Science Department at Utah State University for chemical content, had 2-3 percent silica (SiO₂) and 1-2 percent

iron (Fe). This contamination could possibly retard dissolution.

In a similar set of experiments (Set F, Table 10), different size fractions of the channel material were diluted to various sediment/water ratios using deionized water without mixing. The solutions were covered to minimize concentration by evaporation, and the ECs of the solutions were monitored up to 12 days to investigate whether higher mixing velocities would cause the sediments to yield more salt. The same solutions were also mixed at the highest speed attainable with the multiple stirrer, 100 rpm. The mixing was stopped after 6 hours. Table 13 shows the apparent equilibrium ECs of the six solutions as measured after 12 days in

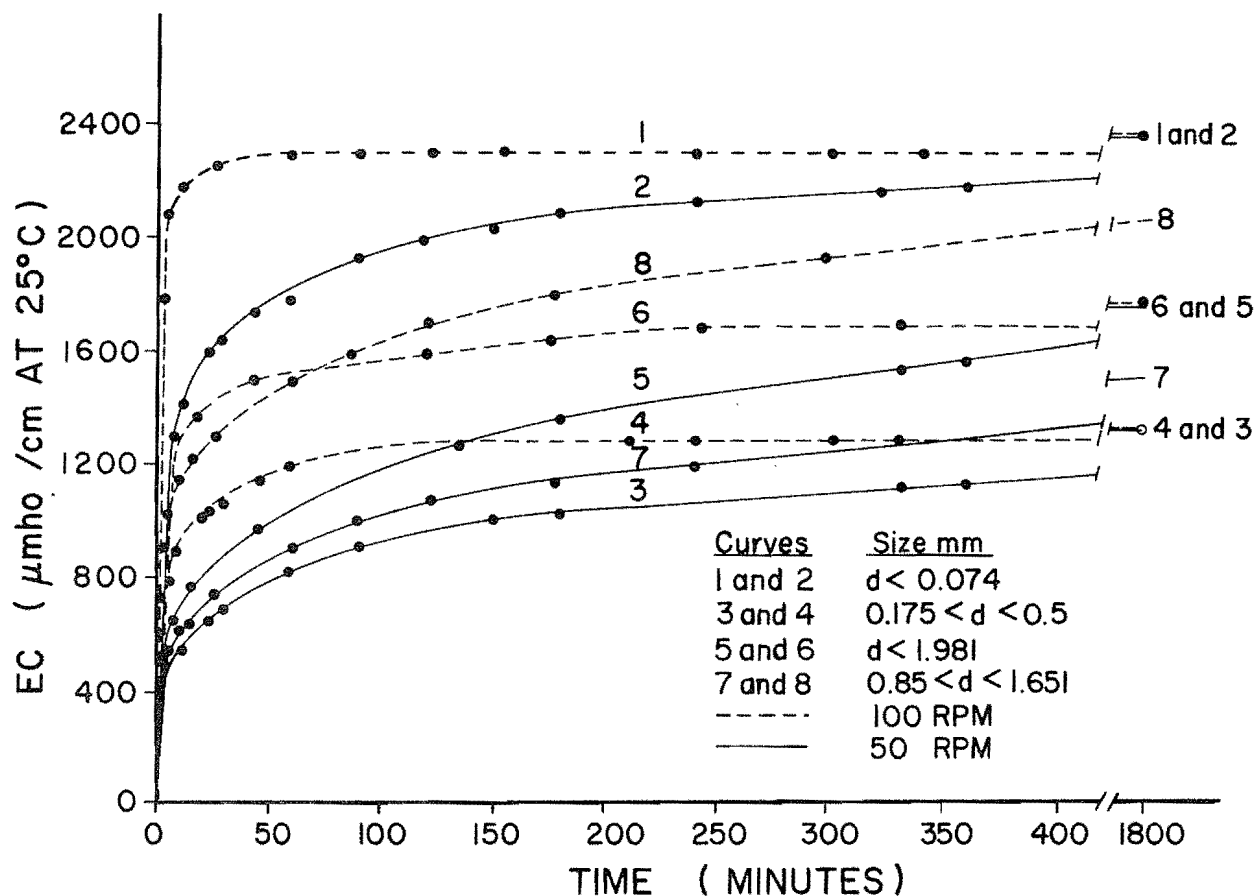


Figure 28. Effect of mixing velocity on salt release from soil material in the multiple stirrer apparatus (Experimental Set F, Table 10).

Table 13. The apparent equilibrium EC in solutions with different particle size fraction and dilutions as affected by mixing process (Experimental Set F, Table 10).

| Particle size fraction (mm) | | d < 0.074 | | 0.074 < d < 0.125 | | 0.125 < d < 0.5 | |
|---------------------------------------|-------------|-----------|------|-------------------|------|-----------------|------|
| | | 1:10 | 1:5 | 1:10 | 1:5 | 1:10 | 1:5 |
| After 12 days without mixing | Mean | 1051 | 1750 | 852 | 1636 | 1363 | 2385 |
| | Replicate 1 | 1155 | 1810 | 910 | 1715 | 1426 | 2465 |
| | Replicate 2 | 947 | 1690 | 794 | 1557 | 1300 | 2305 |
| After additional 6 hours of mixing | Mean | 1081 | 1686 | 872 | 1512 | 1361 | 2093 |
| | Replicate 1 | 1205 | 1785 | 925 | 1610 | 1400 | 2150 |
| | Replicate 2 | 957 | 1595 | 819 | 1414 | 1522 | 2036 |

EC in $\mu\text{mho/cm}$ @ 25°C.

still water and then after undergoing mixing for another 6 hours. The mixing did not increase the ECs, and in fact the ECs at the end of the mixing are a little less. However, this difference is within the precision limits of the electrical conductivity meter.

The logical inference from these results is that mixing accelerates the salt release rate but does not increase the ultimate salt loading from suspended material. The magnitude of the acceleration can be seen from the fact that it took about 50 hours for sediment/water solutions mixed at a speed of 50 rpm to reach the same apparent equilibrium EC which they reached in 18 hours with a mixing speed of 100 rpm (Figure 28).

Interaction between Mixing Velocity and Particle Size

Mixing appeared to break the particles into smaller sizes. Such grinding would contribute to an increased salt release rate at higher velocities by increasing the particles'

surface areas. To quantify this grinding effect, soil samples of different size fractions were mixed with deionized water at two different mixing speeds. The samples were then dried and sieved to determine whether any reduction in particle size had occurred.

Table 14 shows the results of sieve analysis of the soil samples of size fraction $0.175 < d < 0.417$ mm, and $0.104 < d < 0.175$ mm after being mixed at 100 rpm. About 10 percent by weight shifted to the next smaller size fraction. Sieve analysis, however, was found to be a poor means of checking for particle size degradation because:

1. Separation of cohesive from cohesionless particles was not possible without washing the sample, which reduced the release of salt from the soil samples.

2. The fine cohesive material was attached to the coarser particles during the wetting-drying cycle, and this was complicating preparation of samples within desired particle size fractions.

Table 14. The result of sieve analysis to determine the grinding effect of mixing (Experimental Set G, Table 10).

| 1. Size fraction $0.175 < d < 0.417$ mm weight before the experiment (30 g). | | | |
|---|---------------|-------------|-------------------|
| Sieve Opening mm | Retained g | Passed g | Percent Passed |
| 0.175 | 25.2 | 2.6 | 9.35 |
| 0.147 | 1.6 | 1.0 | 3.6 |
| 0.104 | 0.4 | 0.6 | 2.15 |
| 0.074 | 0.3 | 0.3 | 1.07 |
| pan | 0.3 | - | - |
| Total weight after the experiment 27.8 g | | | |
| 2. Size fraction $0.104 < d < 0.175$ mm weight before the experiment (30 g). | | | |
| Sieve Opening mm | Retained g | Passed g | Percent Passed |
| 0.104 | 18.1 | 2.9 | 10.35 |
| 0.088 | 2 | 0.9 | 3.2 |
| 0.074 | 0.4 | 0.5 | 1.7 |
| pan | 0.5 | - | - |
| Total weight after the experiment 28 g | | | |

3. Upon contact with water the fine particles were detached from the cohesionless particles. This made it difficult to find out whether the size shift of the cohesionless material was due to a breakdown of particle size during the mixing process or the detachment of fine particles.

4. Drying of the wet samples prior to the second sieve analysis caused heat-sensitive particles to break due to expansion.

Hydrometry and pipet analysis were also tried to check for particle

size degradation of the fine cohesive materials, but neither method was successful.

Effect of Initial EC

Saline solutions were prepared and used in place of deionized water in experimental runs (Set H, Table 10) conducted to study the effect of initial electrical conductivity on salt release. Sodium chloride (NaCl) and sodium sulfate (Na_2SO_4) were used to make the solutions. Table 15 gives the results of chemical analysis of water samples taken from Miller and Bitter Creeks; the latter shows a particular predominance of sodium and magnesium sulfates. Sodium sulfate was also reported to be the predominant salt by Mundorff (1972) and White (1977) in related studies in the Price River Basin.

Figures 29 and 30 show the effect of initial electrical conductivity, EC_0 , on the salt release rate from a soil sample with a size fraction, $0.5 < d < 1$ mm, and for three dilutions (1:50, 1:75, 1:100). Initial EC varied from about 600 to 8000 $\mu\text{mho/cm}$.

The salt release rate did not show a significant change until the initial EC passed a threshold of about 2100 $\mu\text{mho/cm}$ for all dilutions. This implies that the EC of the salt release curve is additive to the initial EC. The point is better demonstrated in Figure 31 which shows the salt release curves for the entire spectrum of initial salinities for a dilution of 1:50.

The additive effect is also evident from the results of the experiments conducted in the mixing tank. Here, the saline solutions resulting from placing the soil material in tap water were used for investigating the effect of EC_0 on salt release characteristics. The experiments started by mixing the soil sample in the mixing tank and by monitoring the EC of the solution. When

Table 15. Results of chemical analysis of water samples taken from two major creeks within the Price River Basin.

| | Miller Creek | | Bitter Creek | |
|----------------------------------|--------------|-------|--------------|--------|
| | mg/l | meq/l | mg/l | meq/l |
| Alkalinity, as CaCO_3 | 551. | - | 941. | - |
| Carbonate, as CO_3^{2-} | 0. | 0 | 38. | 1.27 |
| Bicarbonate, as HCO_3^- | 672. | 11.02 | 1,109. | 18.18 |
| Calcium, as Ca^{2+} | 215. | 10.75 | 506. | 25.30 |
| Chloride, as Cl^- | 81. | 2.28 | 1,113. | 31.35 |
| Magnesium, as Mg^{2+} | 230. | 19.17 | 4,042. | 336.83 |
| Potassium, as K^+ | 10. | 0.26 | 123. | 3.15 |
| Sodium, as Na^+ | 170. | 7.39 | 10,805. | 469.78 |
| Sulfate, as SO_4^{2-} | 1331. | 27.73 | 40,616. | 846.17 |

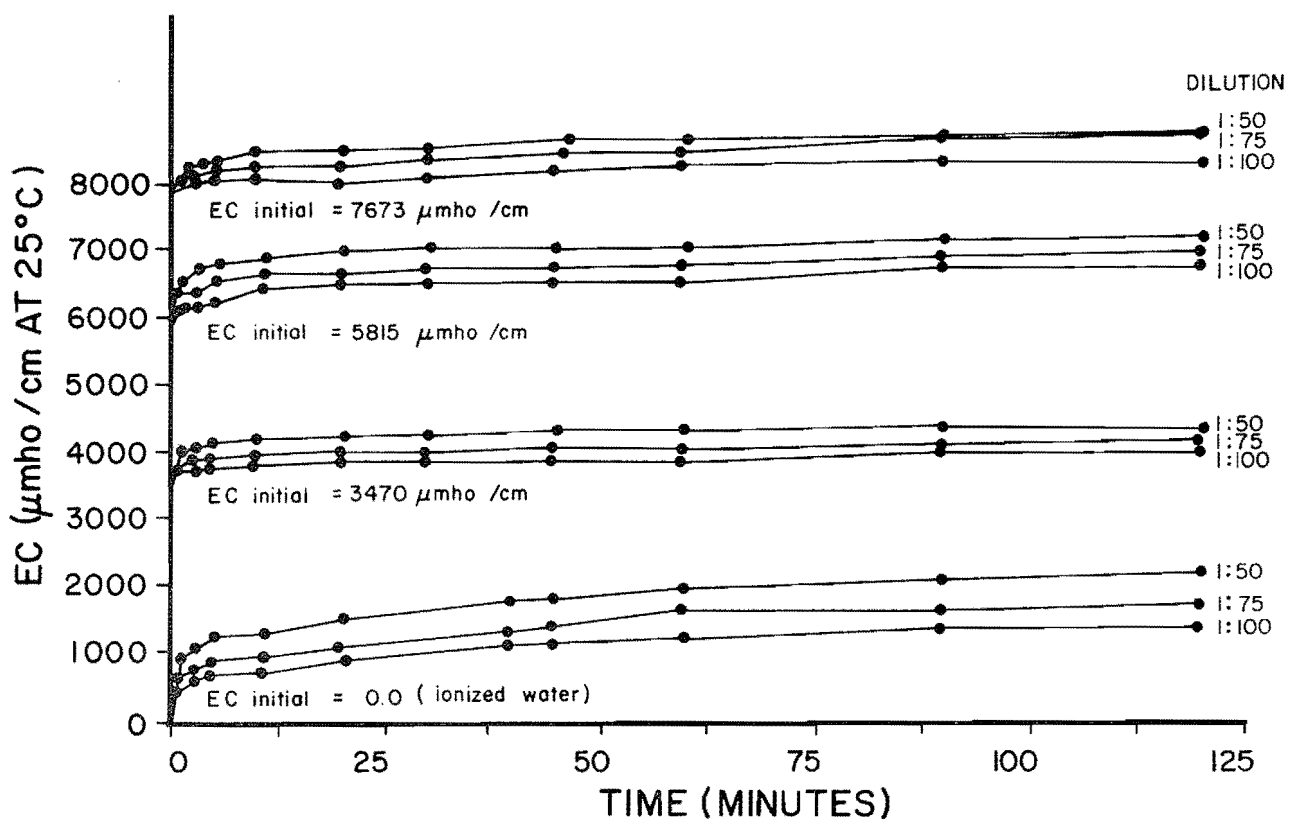


Figure 29. Effect of initial EC on salt release (Experimental Set H, Table 10).

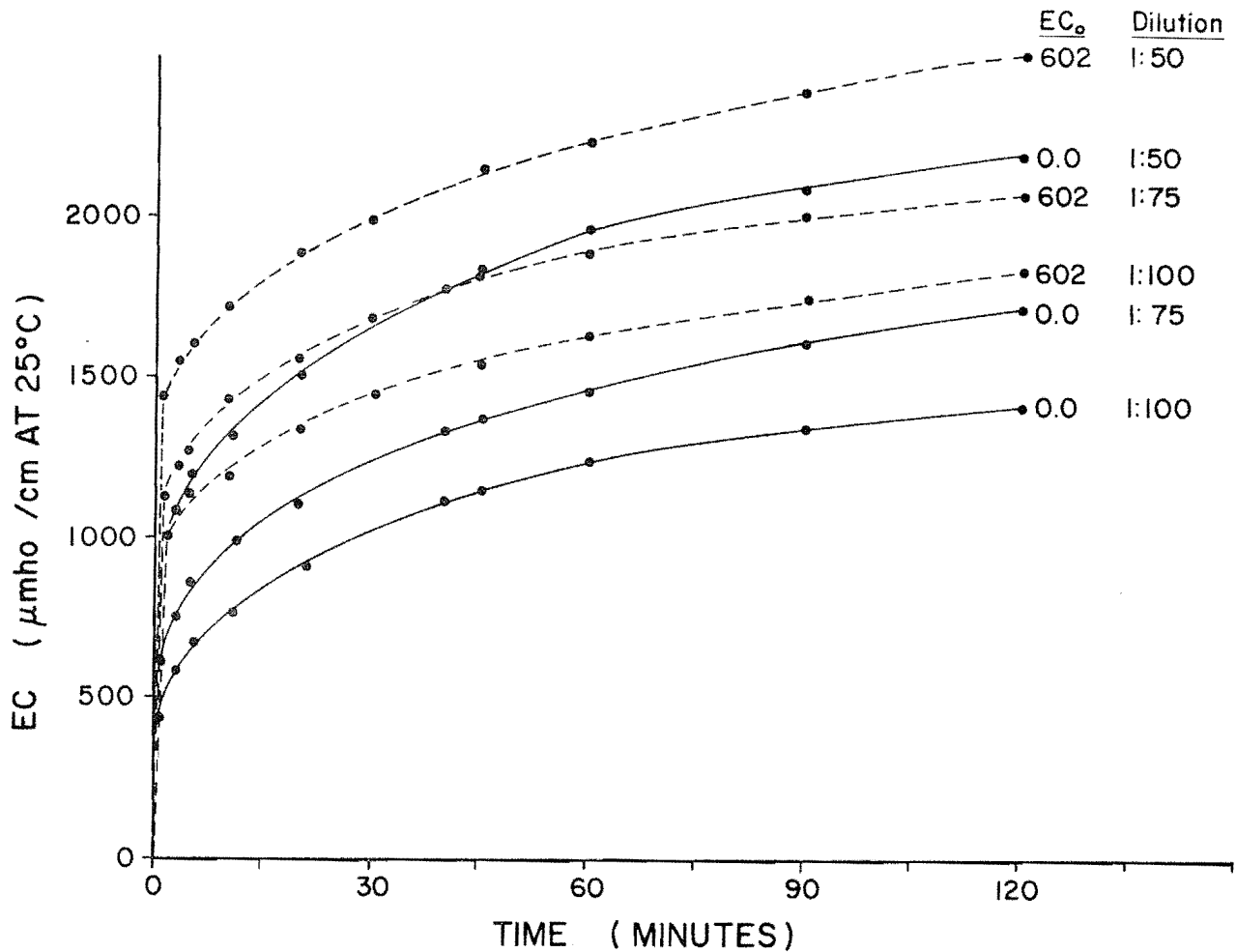


Figure 30. Effect of initial EC on salt release rate as compared with the rate in deionized water (i.e., $EC_0 = 0.0$) (Experimental Set H, Table 10).

an apparent equilibrium EC was reached, the concentration of the solution was doubled by adding a second soil sample of equal weight, and the EC measurements were continued until a new apparent equilibrium EC was reached. This process was reported five times with concentrations increasing to about 25,000 mg/l ($g\ m^{-3}$). Figure 32 presents the experimental data, and Table 16 is a summary of the results. The net increase in EC did not vary among the five soil additions by more than 8 percent. Furthermore, the percent of apparent equilibrium EC reached in different time increments (Table 16) is almost the same for different initial EC's up to about 1400 $\mu\text{mho/cm}$.

The effect of higher initial salinity is similar to that of higher dilution factors, that is, the system approaches equilibrium more rapidly. Furthermore, the net increase in EC was less in runs with higher EC_0 's and higher dilution factors than in runs with lower EC_0 's and lower dilution factors. It should be recalled that the initial analysis of the selected soil material indicated a highly saline $Ca^{2+} - Na^+ - SO_4^{2-}$ system (Table 16). Ca^{2+} was low in saturation extract, probably because of the fraction of gypsum; and when Na_2SO_4 was added to the soil-water suspension, the high SO_4^{2-} concentration further lowered the Ca^{2+} concentration.

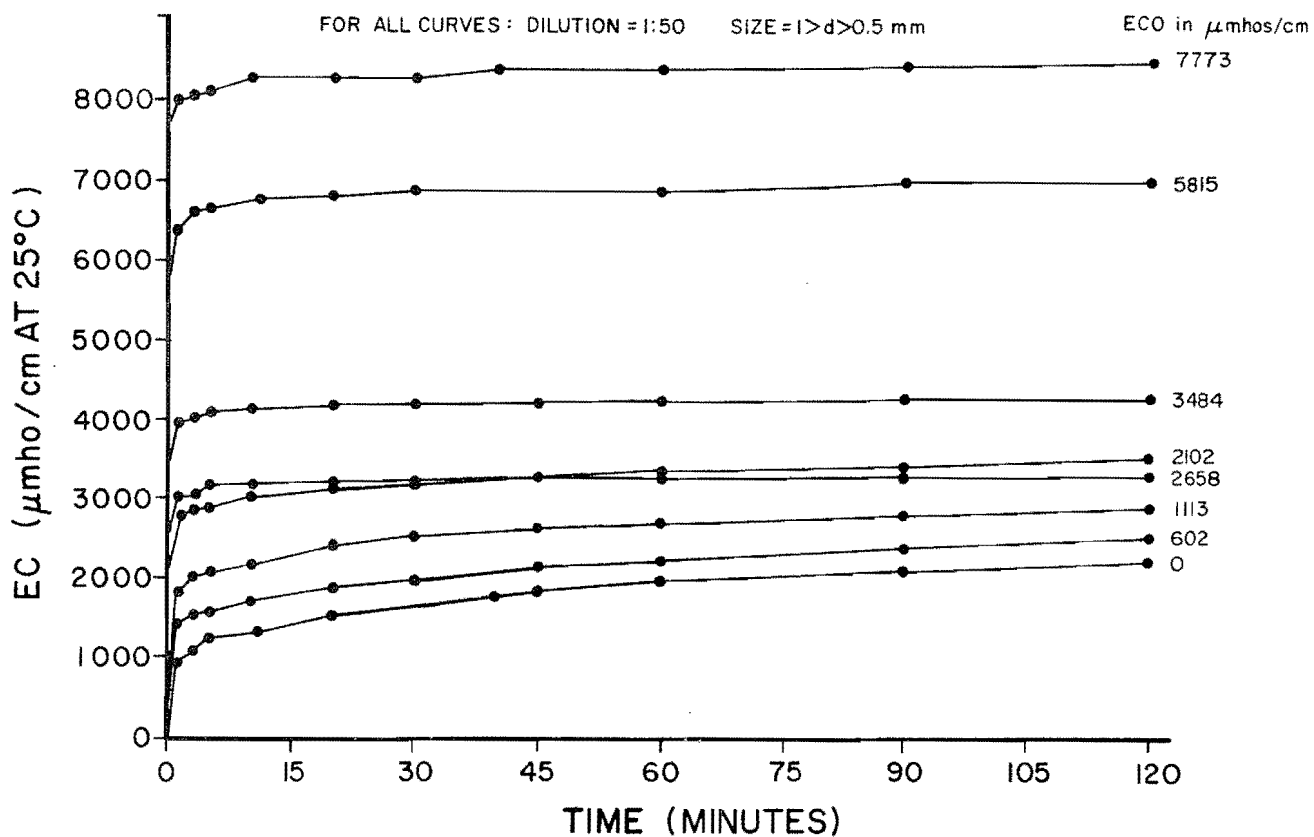


Figure 31. Effect of initially saline solutions on the salt release (Experimental Set H, Table 10).

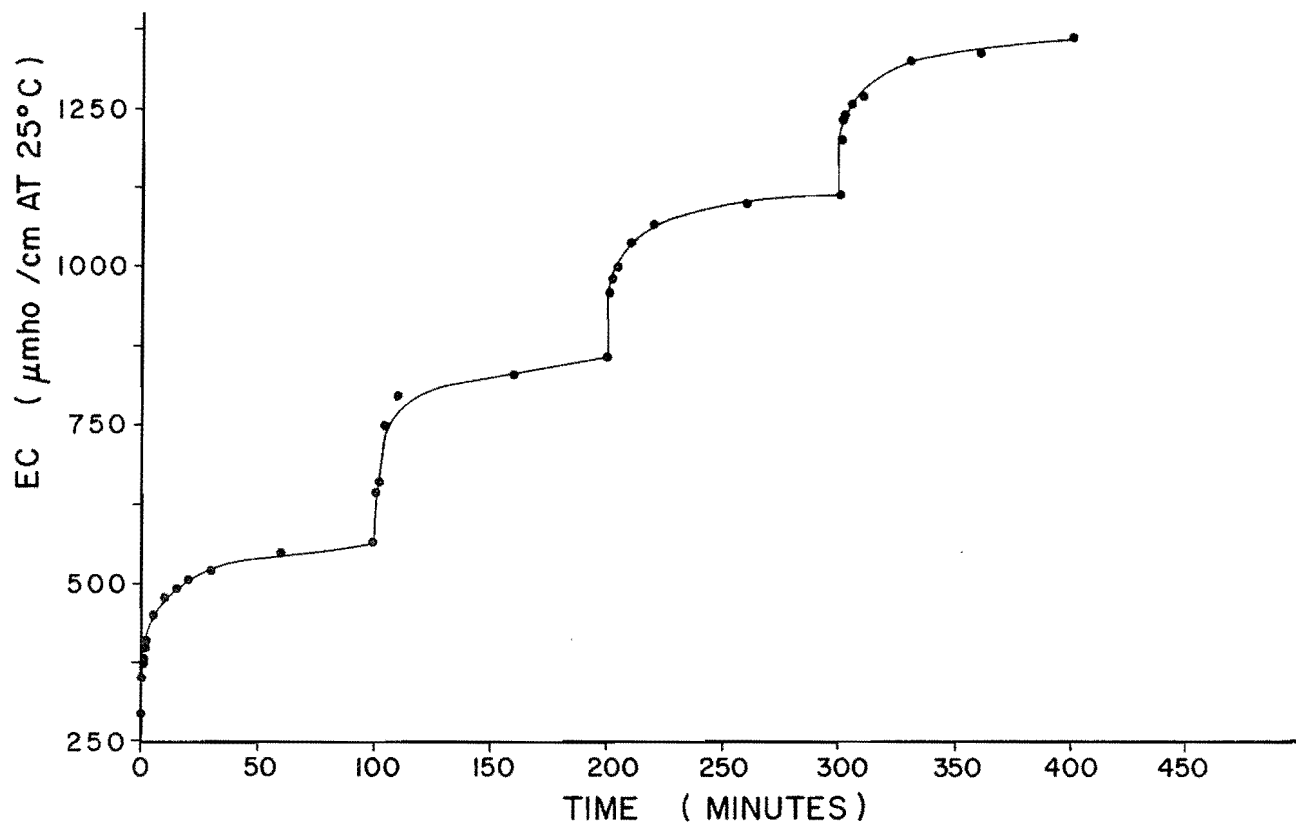


Figure 32. Cumulative dilution effect on salt release from soil samples in the mixing tank experiment (Experimental Set A, Table 10).

Table 16. Cumulative salinity concentrations with five soil sample additions in the mixing tank experiment (Experimental Set A, Table 10).

| Experimental Set A No. | Velocity Range (fps) | Initial EC ($\mu\text{mho/cm}$ @ 25°C) | Cumulative Dilution | Cumulative Concentration (ppm) | Apparent Equilibrium EC ($\mu\text{mho/cm}$ @ 25°C) | Net Increase in EC ($\mu\text{mho/cm}$ @ 25°C) | Percent of Equilibrium EC (EC_{eq}) Reached in Different Elapsed Time (Minutes) | | | | | |
|------------------------|----------------------|---|---------------------|--------------------------------|--|---|---|------|------|------|------|------|
| | | | | | | | 1 | 2 | 5 | 10 | 30 | 60 |
| 1 | 0.917 - 1.028 | 296 | 1:250 | 3981 | 566 | 270 | 31.4 | 42.9 | 52.8 | 67.0 | 84.3 | 94.0 |
| 2 | 1.028 - 1.119 | 563 | 1:125 | 7932 | 858 | 295 | 27.3 | 33.2 | 63.6 | 79.3 | - | 90.9 |
| 3 | 0.937 - 1.028 | 854 | 1:80 | 11975 | 1108 | 255 | 39.5 | 47.4 | 55.2 | 71.0 | - | 94.7 |
| 4 | 0.937 - 1.028 | 1120 | 1:60 | 16240 | 1362 | 243 | 46.1 | 49.7 | 56.4 | 61.5 | 84.2 | 89.7 |
| 5 | 0.937 - 1.028 | 1362 | 1:40 | 24592 | 1773 | 410 | 31.8 | 34.8 | 53.0 | 68.1 | 87.9 | 98.5 |

CHAPTER IX

SALT-RELEASE EQUATIONS

Introduction

This chapter describes application of the Buckingham Pi Theorem to quantify salt release from suspended sediments using the experimental data of Chapter VIII. The purpose was to develop mathematical equations describing the release of salt from suspended sediments as a function of dilution, particle size, mixing velocity, and initial EC. The salt release equations thus developed were verified using additional experimental data, and the predictive applicability and limitations of the equations are discussed at the end of this chapter.

Application of Buckingham Pi Theorem

The Buckingham Pi Theorem was applied to develop an empirical relationship for estimating the electrical conductivity of a sediment-water solution (EC dimensions: $D^{-1}L^{-1}T$) from

EC_e = saturation extract EC of a particular particle size fraction ($D^{-1}L^{-1}T$)

D_{50} = average size of a particle size fraction (L)

V = mixing velocity (LT^{-1})

t = contact time (T)

δ = dilution factor (dimensionless)

The dimensions of EC are based on the fact that EC is the reciprocal of the

electrical resistance (ohms) which has dimensions of DT^{-1} , where D is the electrical inductance (Murphy 1950). By inspecting the dimensions of the fundamental variables and satisfying the three characteristics of the Pi terms, three independent dimensionless Pi terms were formed as follows:

$$\Pi_1 = \left(\frac{EC}{EC_e} \right),$$

$$\Pi_2 = \left(\frac{Vt}{D_{50}} \right)$$

and

$$\Pi_3 = (\delta)$$

and combined by

$$\Pi_1 = f[\Pi_2, \Pi_3]$$

The individual Pi terms were calculated, according to Equations 70 through 73, by using laboratory data obtained from experimental set D (Table 10 and Appendix B), and arbitrarily selected values of the controlling factors of:

$$D_{50} = 0.029 \text{ in (0.75 mm)}$$

$$EC_e = 29 \text{ mmho/cm at } 25^\circ\text{C}$$

$$V = 0.96 \text{ fps (0.29 m s}^{-1}\text{)}$$

$$\delta = 0.01, 0.01333, 0.02, 0.05, 0.1, \text{ and } 0.02$$

The range of dilution factors (δ) was used to establish criteria for

combination of the Pi terms as discussed in the literature review chapter. Π_1 was plotted against Π_2 with Π_3 held constant at six different values (Figure 33). A similar plot of Π_1 versus Π_3 with Π_2 held constant was also constructed (Figure 34). By reading values of Π_3 from Figure 34 with Π_2 being held constant at nine convenient values of $\Pi_2 = 2.34 \times 10^5$ (corresponding to $t = 10$ min). The functional relationships between Π_1 and Π_2 , and Π_1 and Π_3 were developed using Equations 35 and 36. That is, log-log plots of Π_1 versus Π_2 and Π_3 , respectively were constructed (Figures 35 and 36), and using a regression analysis the equations which best described the experimental data were calculated.

The following functional relationships resulted:

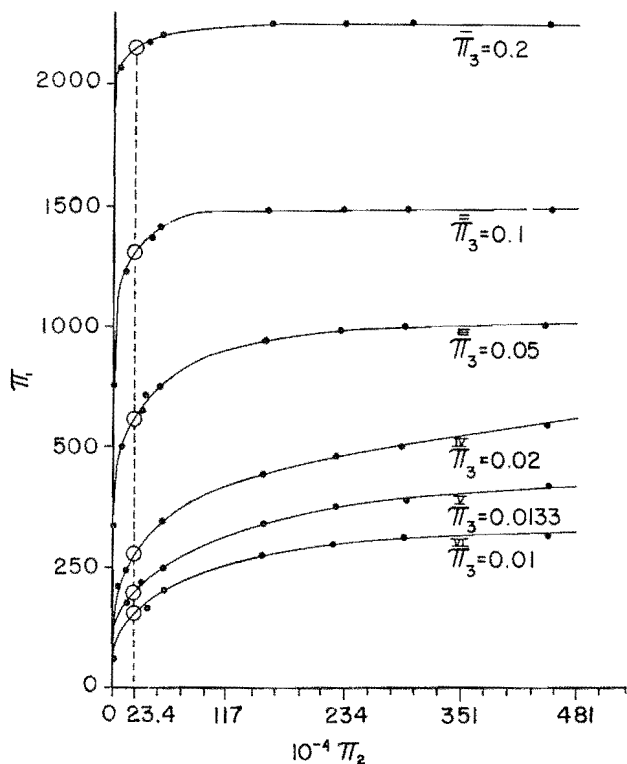


Figure 33. Plots of Π_1 versus Π_2 with Π_3 held constant at six different values (Experimental Set D, Table 10).

$$\Pi_{12\bar{3}} = 1.5453 \times 10^{-3} \Pi_2^{0.222}$$

with Π_3 held constant at 0.01, and

$$\Pi_{1\bar{2}3} = 1.3838 \Pi_3^{0.745}$$

with Π_2 held constant at 2.34×10^5 . The constant of Equation 36 was determined by inserting the values at which Π_3 and Π_2 constant into the above functional relationships, respectively, averaging the two values. This resulted in:

$$\Pi_{1\bar{2}\bar{3}} = 4.455 \times 10^{-2}$$

The following values of $\Pi_{12\bar{3}}$ were used for the validity check.

$$\Pi_{12\bar{3}} = 1.545 \times 10^{-3} \Pi_2^{0.222},$$

$$\Pi_{1\bar{2}\bar{3}} = 2.726 \times 10^{-3} \Pi_2^{0.195}, \text{ and}$$

$$\Pi_{12\bar{3}} = 2.602 \times 10^{-3} \Pi_2^{0.222}$$

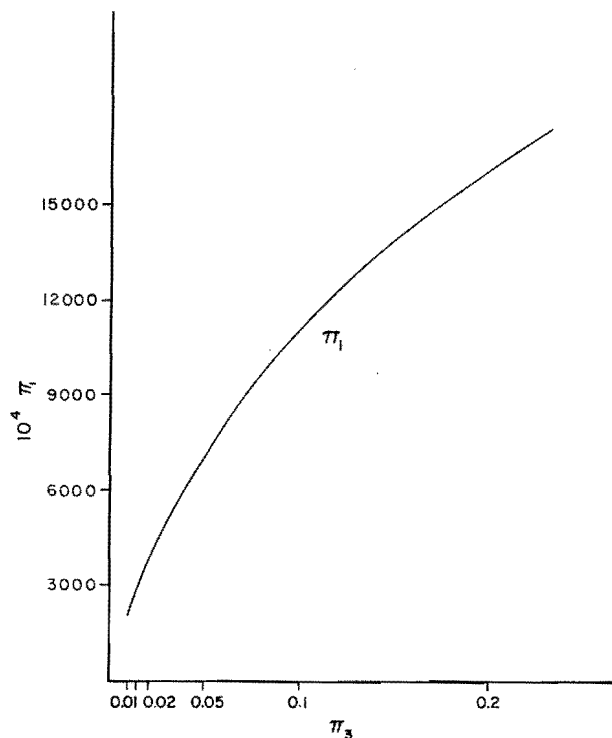


Figure 34. Plot of Π_1 versus Π_3 with Π_2 held constant (Experimental Set D, Table 10).

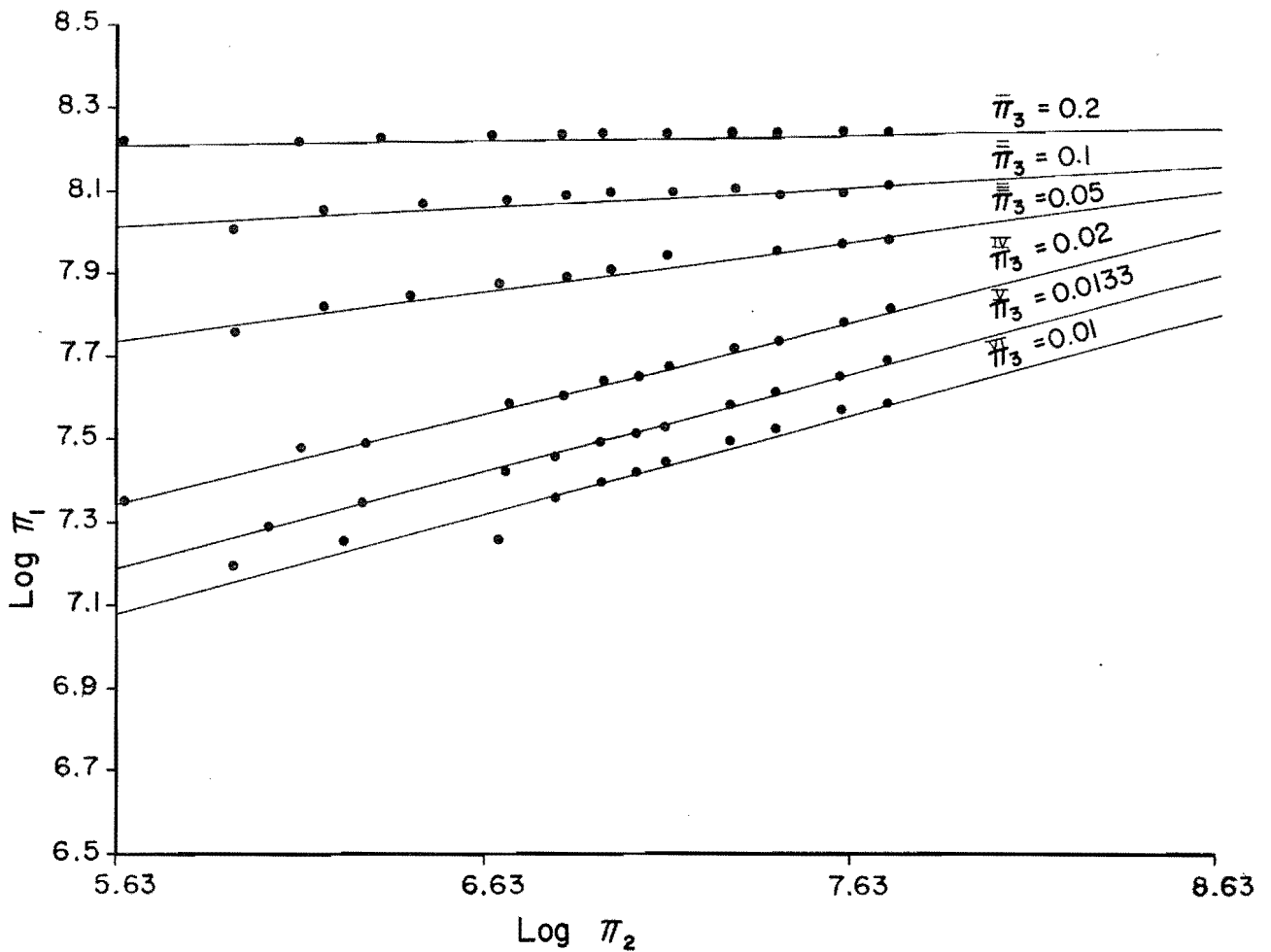


Figure 35. Plot of $\log \pi_1$ versus $\log \pi_2$ with π_3 held constant at six values (Experimental Set D, Table 10).

The ratios of $\frac{\pi_{12\bar{3}}}{\pi_{12\bar{3}}}$ and $\frac{\pi_{12\bar{3}}}{\pi_{12\bar{3}}}$ were found to be equal to a constant. That is,

$$\frac{\pi_{12\bar{3}}}{\pi_{12\bar{3}}} = \frac{\pi_{12\bar{3}}}{\pi_{12\bar{3}}} = 0.78 \dots (70)$$

This is also evidenced by the parallel lines on the log-log plots of π_1 versus π_2 (Figure 35). Consequently, the validity check revealed that the combination should be by multiplication. Based on Equation 38:

$$\pi_1 = \frac{\pi_{12\bar{3}} \pi_{12\bar{3}}}{\pi_{12\bar{3}}} \dots (71)$$

The following equation resulted:

$$\pi_1 = 0.048 (\pi_3)^{0.745} (\pi_2)^{0.222} \dots (72)$$

Substituting for the pi terms we have:

$$\left(\frac{EC}{EC_e}\right) = 0.048 (\delta)^{0.745} \frac{Vt}{D_{50}}^{0.222} \dots (73)$$

or

$$EC = k (\delta)^a \left(\frac{Vt}{D_{50}}\right)^b EC_e \dots (74)$$

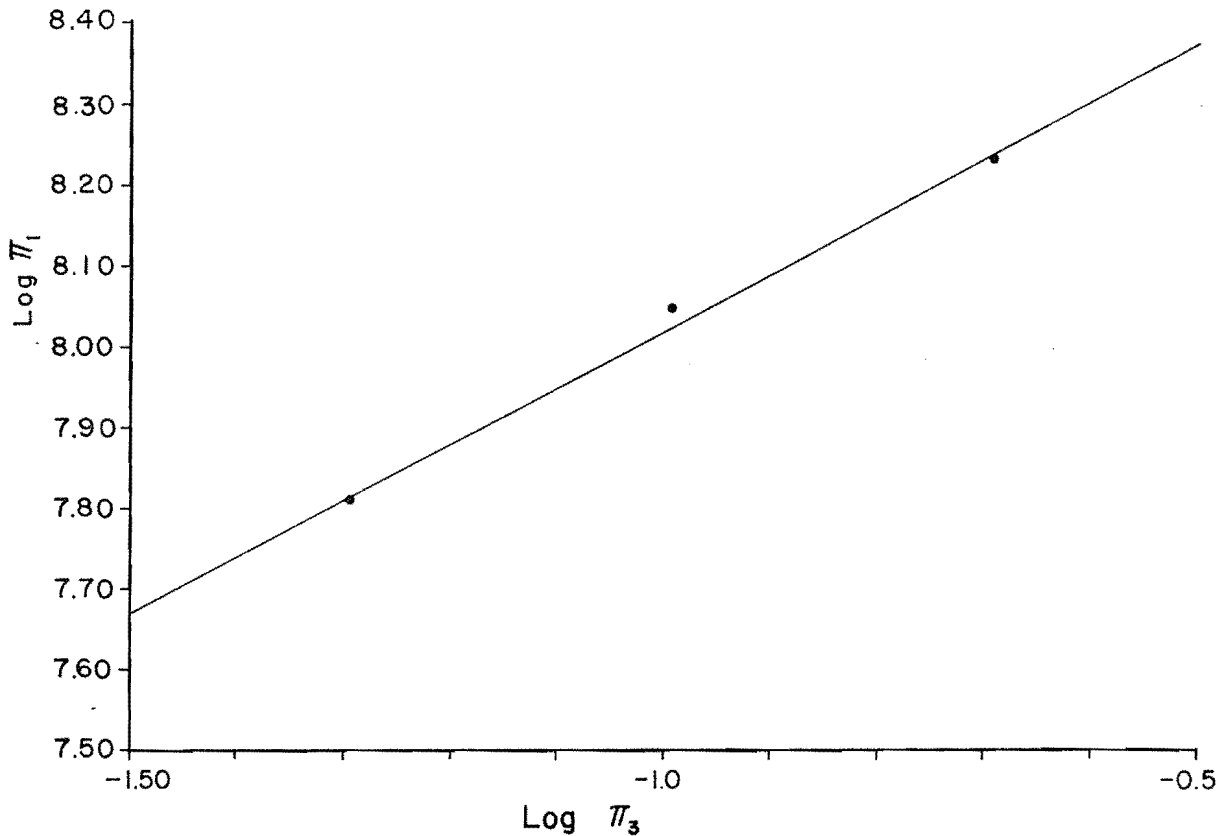


Figure 36. Plot of $\log \Pi_1$ versus $\log \Pi_3$ (Experimental Set D, Table 10).

in which

$$K = 0.048$$

$$a = 0.745$$

$$b = 0.222$$

Inclusion of Initial EC (EC_0)

An attempt was next made to add the initial electrical conductivity (EC_0) to provide a more general empirical salt sediment relationship. Addition of another fundamental variable, however, would necessitate a fourth dimensionless independent Pi term and consequently a Latin-square design approach.

A fourth Pi term was assembled as:

$$\Pi_4 = \frac{EC_o}{EC_e} \dots \dots \dots (75)$$

This Π_4 , however, violates the independency requirement of the Buckingham Pi Theorem in that both Π_1 and Π_4 must include EC_e in order to make both Pi terms dimensionless. Furthermore, the Latin square design is required to hold the Pi terms constant, one at a time, while varying the others. It would not be possible to hold Π_1 constant because of the fact that it includes EC, a dependent fundamental variable, which would change upon change of the other fundamental variables.

A preferred approach was to redefine the fundamental variable as:

$$EC_a = EC - EC_0 \dots \dots \dots (76)$$

in which

$$EC_a = \text{increase in electrical conductivity in the solution}$$

The Π_1 term was thus modified to

$$\Pi_1 = \left(\frac{EC_a}{EC_e} \right) \dots \dots \dots (77)$$

range of 600-8000 $\mu\text{mho/cm}$ at 25°C , the coefficient values were

$$k = 0.818$$

$$a = 1.273$$

$$b = 0.153$$

and the other Π terms remained unchanged. The procedure used to obtain Equation 74 led to:

$$\frac{EC_a}{EC_e} = k (\delta)^a \left(\frac{Vt}{D_{50}} \right)^b \dots \dots (78)$$

Testing the Equations

or

$$EC = EC_0 + k (\delta)^a \left(\frac{Vt}{D_{50}} \right)^b EC_e \dots (79)$$

Additional laboratory experiments (Experimental Set I, see Table 10) were performed to verify Equations 74 and 79. The results for Equation 74 are listed on Table 17 and plotted on Figure 37. The average prediction errors are 22, 34, and 11 $\mu\text{mho/cm}$ at 25°C for $\delta = 0.01$, 0.0133, and 0.02, respectively.

For the same experimental data used to calibrate Equation 74 and for the EC_0

Table 17. The measured and predicted values of EC in $\mu\text{mho/cm}$ at 25°C using Equation 74 (Experimental Set I, Table 10).

| Time in Minutes | Dilution Factor | | | | | |
|-----------------|-----------------|--------|---------|--------|--------|--------|
| | 0.01 | | 0.01333 | | 0.02 | |
| | EC_m | EC_p | EC_m | EC_p | EC_m | EC_p |
| 0.5 | 363 | 360 | - | - | - | - |
| 1 | - | - | 547 | 521 | 690 | 704 |
| 2 | 487 | 490 | - | - | - | - |
| 2.5 | - | - | 606 | 638 | - | - |
| 3 | - | - | - | - | 927 | 899 |
| 4 | 559 | 571 | - | - | - | - |
| 4.5 | - | - | 690 | 727 | 951 | 984 |
| 10.5 | 665 | 708 | - | - | - | - |
| 11 | - | - | 820 | 887 | 1189 | 1199 |
| 15 | 713 | 766 | 892 | 950 | 1248 | 1285 |
| 20 | 780 | 817 | 960 | 1012 | 1368 | 1370 |
| 25 | 822 | 858 | 1026 | 1064 | 1416 | 1439 |
| 30 | 876 | 894 | 1056 | 1108 | 1488 | 1499 |
| 45 | 984 | 978 | 1206 | 1212 | 1650 | 1640 |
| 60 | 1056 | 1043 | 1296 | 1292 | 1716 | 1748 |
| 90 | 1170 | 1141 | 1416 | 1414 | 1896 | 1913 |
| 120 | 1206 | 1216 | 1635 | 1508 | 2046 | 2039 |

Note: EC_m = measured EC in $\mu\text{mho/cm}$ at 25°C .

EC_p = predicted EC by Equation 71.

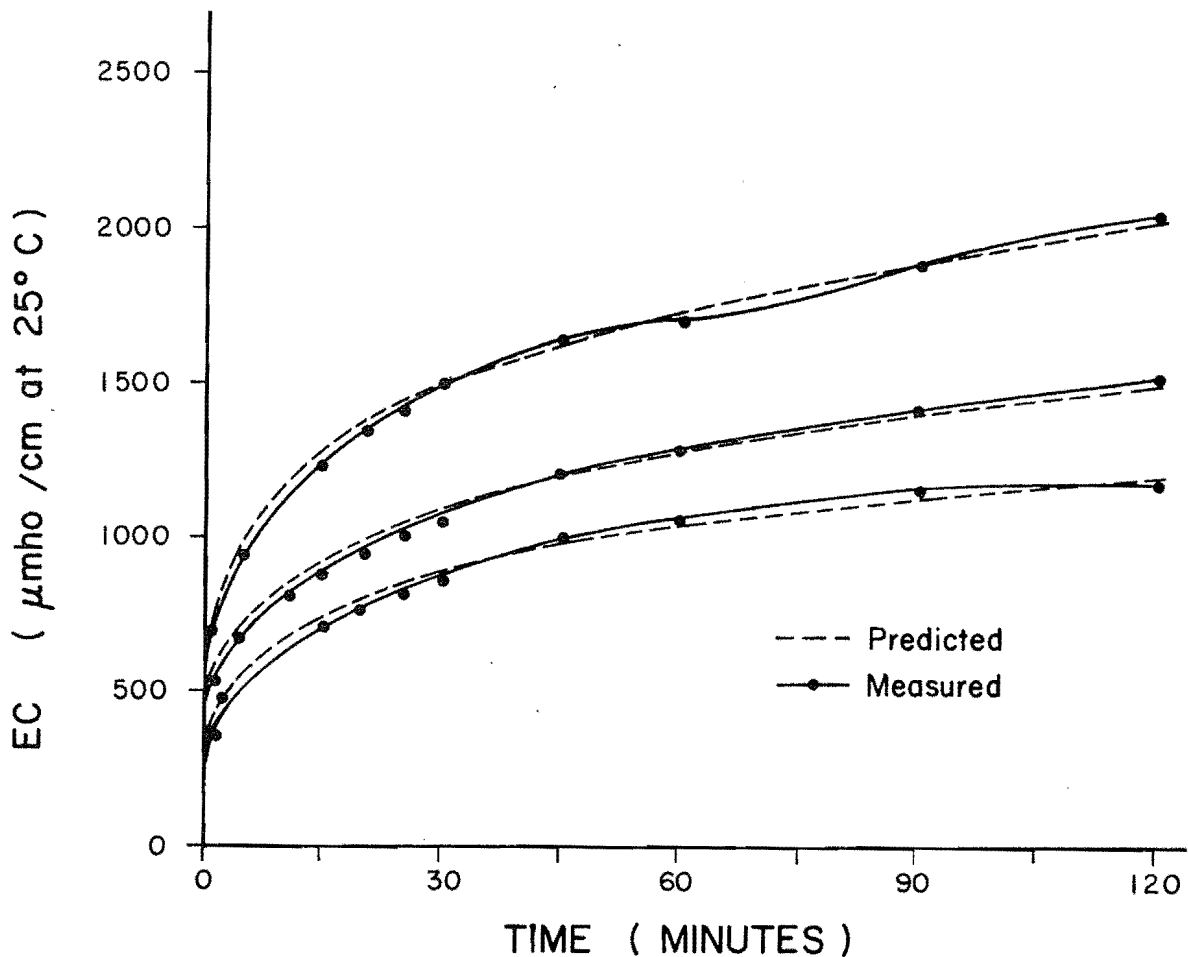


Figure 37. Comparison of the predicted and measured EC using Equation 74 (Experimental Set I, Table 10).

Figures 38, 39, and 40 are plots of measured versus predicted EC's for the dilution factors of 0.01, 0.0133, and 0.02, respectively. The solid lines were obtained by regressing EC_p on EC_m . The coefficients of determination, r^2 , varied between 0.990 and 0.998.

These experimental runs were repeated (Experimental Set I, Table 10), and Equation 74 was used to estimate the results. All the experimental variables were kept at their former values except the EC_e value of particle size fraction $0.5 < d < 1$ mm was 32 mmho/cm at 25°C for the replicates as compared with 29 mmho/cm at 25°C in the previous runs. The difference was due to natural variability among the soil samples. Figure 41 shows the measured and predicted values of EC using Equation 74

for the replicate runs. The r^2 in this varied between 0.950 and 0.971.

Performance of Equation 74 with Higher Dilution Factors

Figure 42 shows that for higher dilution factors, ranging from 0.05 up to 0.2, the predicted EC's were higher than the measured EC's. The physical explanation probably lies in the difference in concentration gradient. Specifically, the slopes of the log-log plots of EC versus t (Figure 24) are flatter for these higher dilution factors than they are in the dilution factor range of 0.01-0.02.

For empirical analysis of this relationship, one can again turn to the Buckingham Pi Theorem, where the validity check for combining Pi terms by

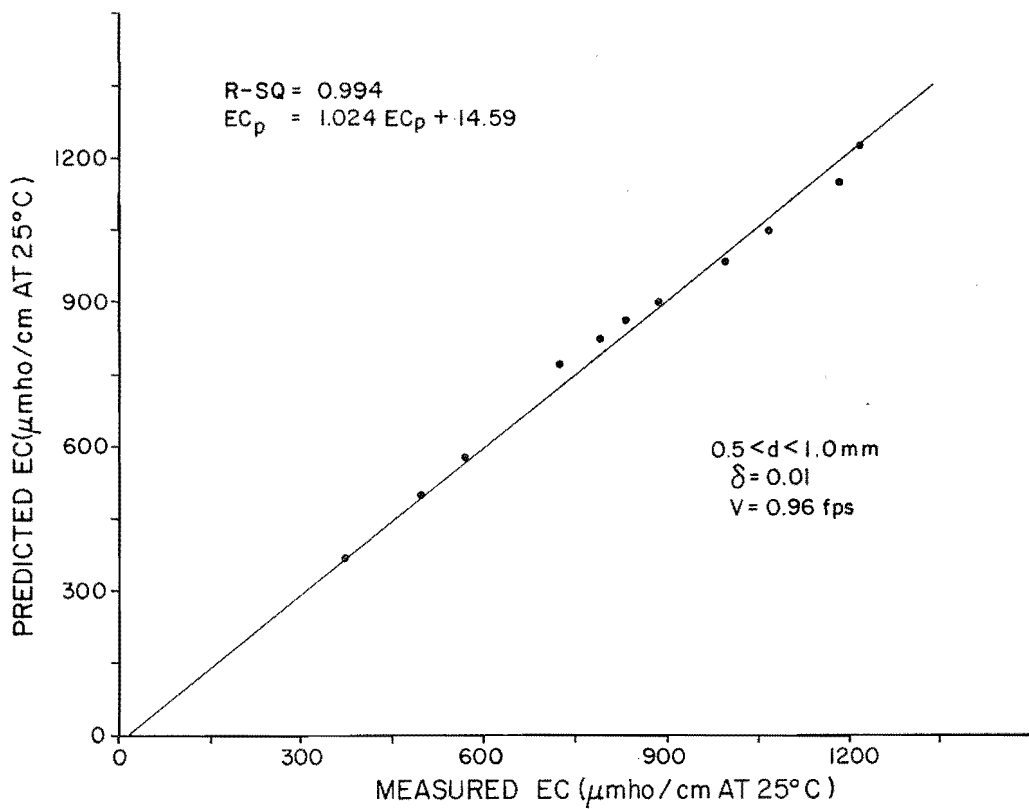


Figure 38. The linear regression of predicted and measured values of EC using Equation 74 (Experimental Set I, Table 10).

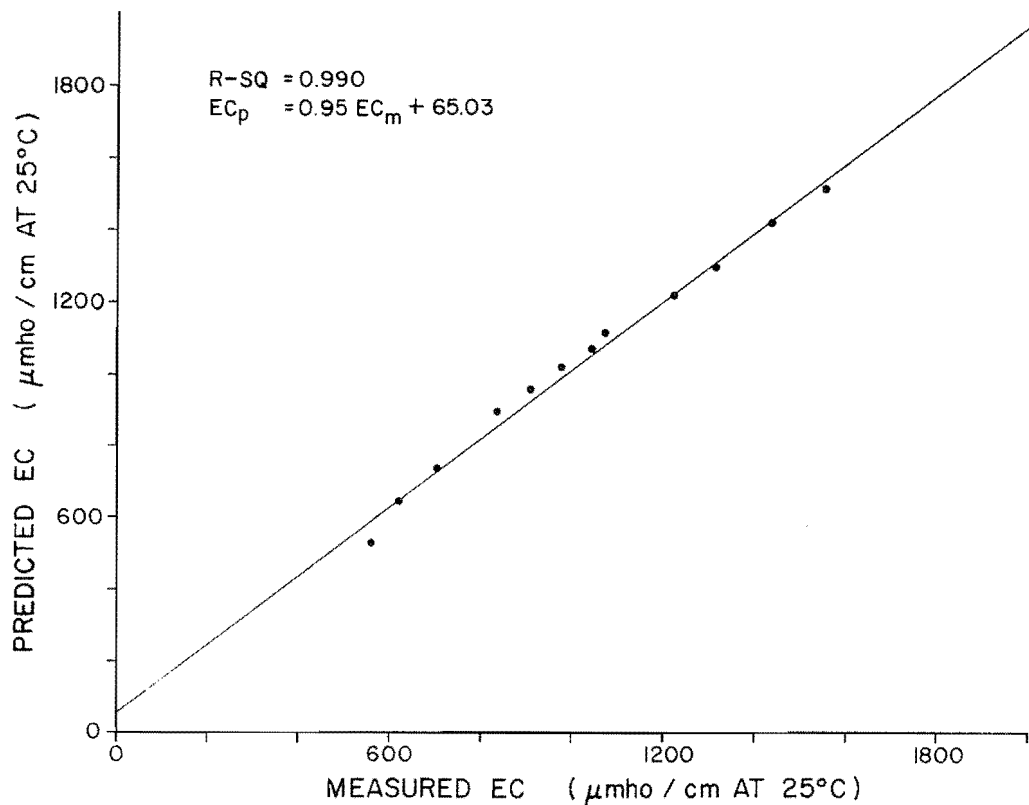


Figure 39. The linear regression of predicted and measured values of EC using Equation 74 (Experimental Set I, Table 10).

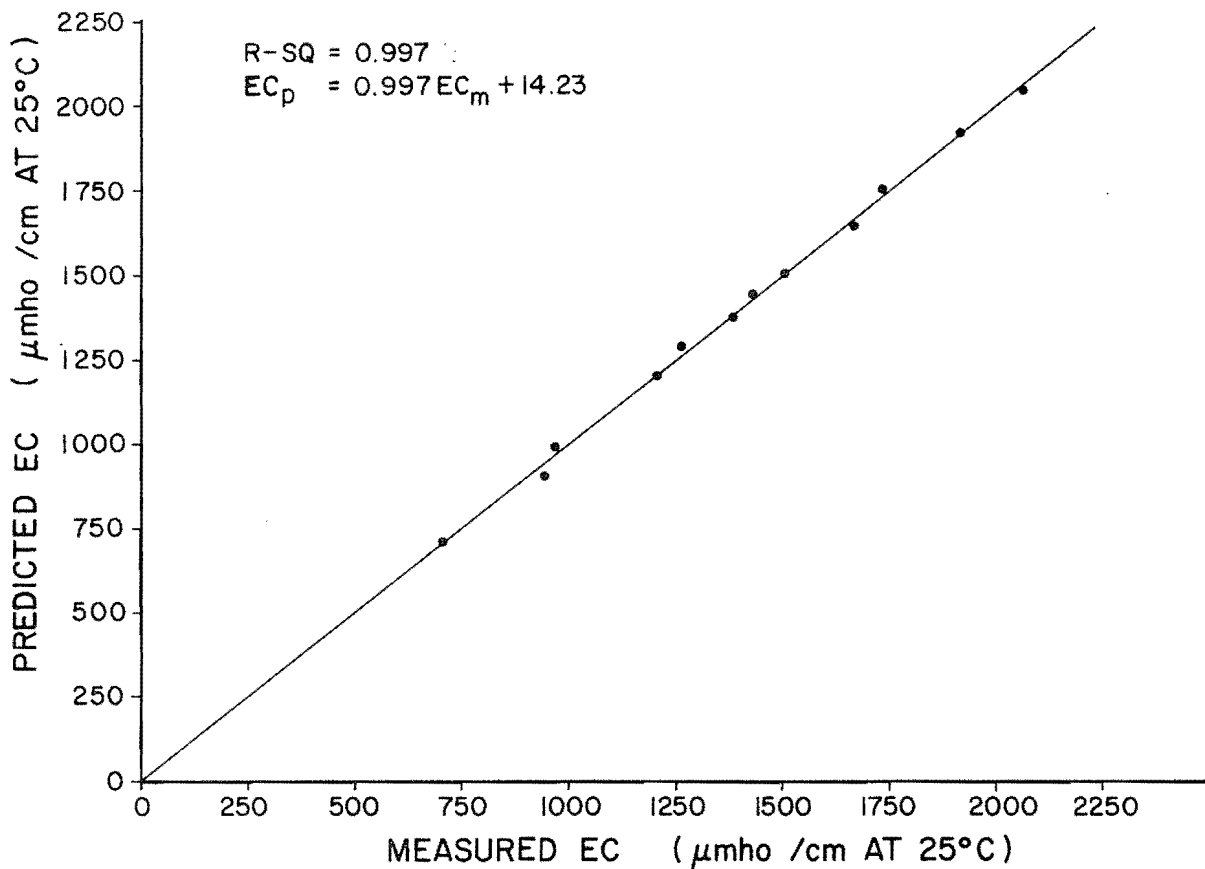


Figure 40. The linear regression of predicted and measured values of EC using Equation 74 (Experimental Set I, Table 10).

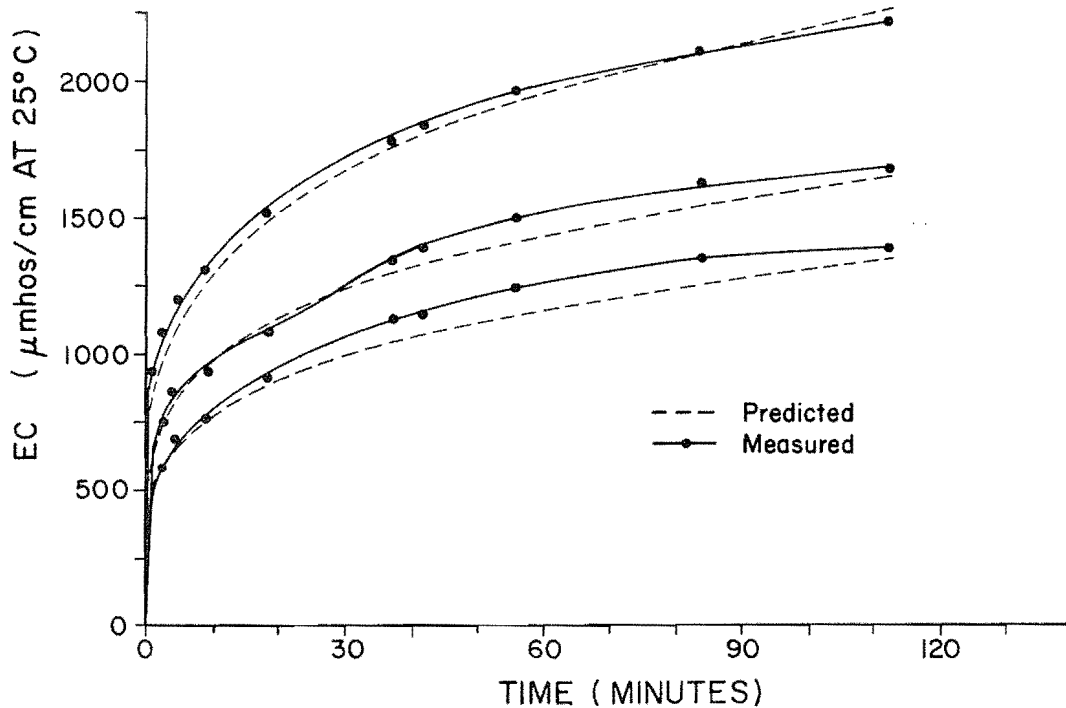


Figure 41. Comparison of predicted and measured EC using Equation 74 on data from a replicated run (Experimental Set I, Table 10).

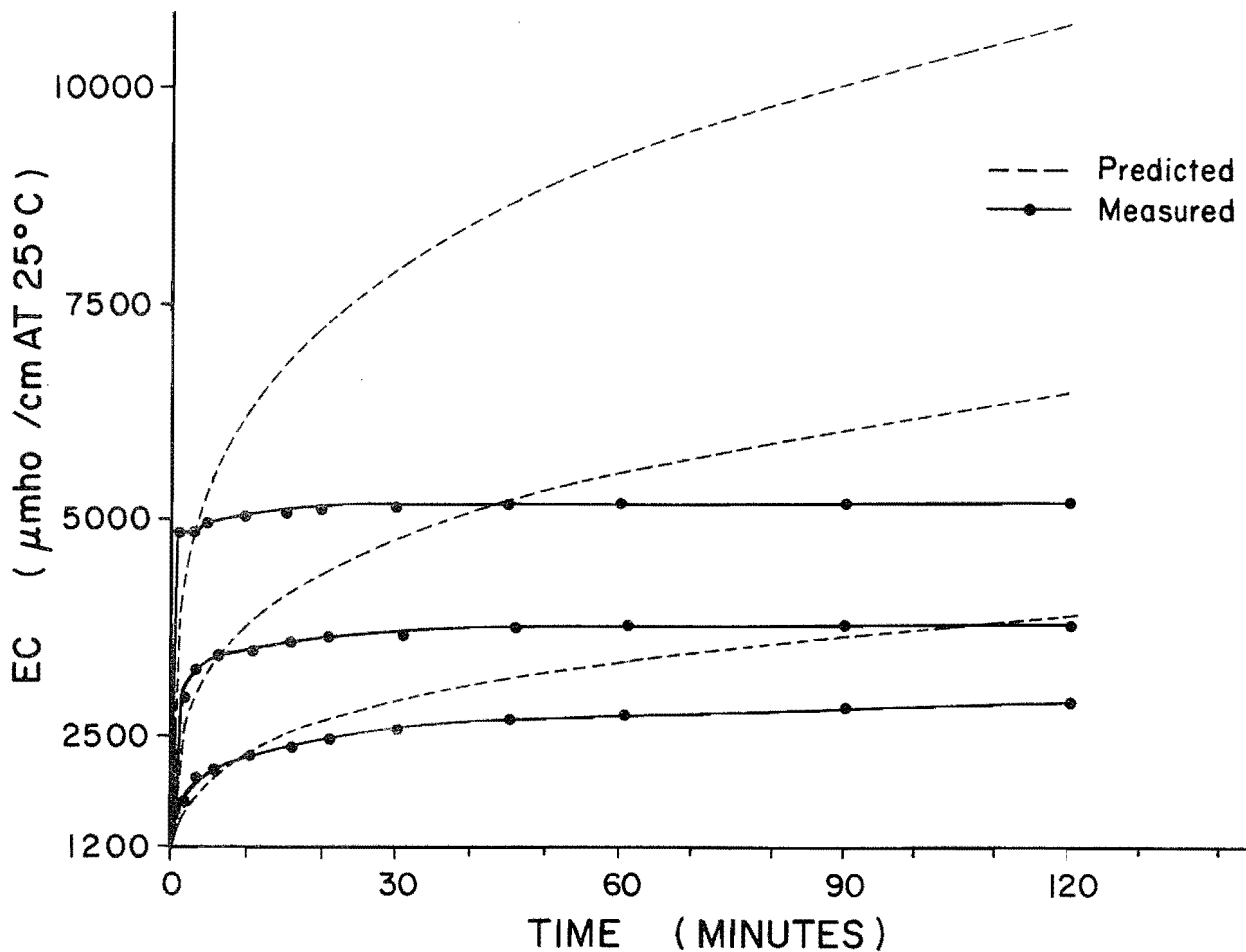


Figure 42. Comparison of predicted and measured EC values using Equation 74 over a higher dilution factor range of 0.05-0.2 (Experimental Set I, Table 10).

multiplication requires parallel lines for results plotted on a log-log scale. The difference in salt release rates between higher and lower dilutions prevented the Pi terms from producing parallel lines on log-log plots throughout the entire range of 0.01-0.2, but it was possible to separate the range into three zones within which the lines are approximately parallel. Separate coefficients for three ranges of the dilution factor (0.001-0.02, 0.02-0.1, and 0.1-0.2) were derived from the experimental data and tabulated in Table 18.

The experimental data taken in the dilution factor range 0.1-0.2 were then used for verification of Equation 74 with the coefficients given in Table 18. From the comparison shown on Figure 43, the prediction improved significantly. The r^2 increased from 0.570 to 0.981

(Figures 42 and 43). Figure 44 shows similar results for a dilution factor of 0.05.

Performance of Equation 74 with Smaller Particle Sizes

The predictive capability of Equation 74 was also examined for particle sizes smaller than the 0.75 mm in the experimental data used in its development. Additional experimental runs (Experimental Set I, Table 10) with soil samples of size fraction $0.125 < d < 0.5$ mm, six different dilution factors ranging from 0.001 to 0.02, and three different mixing velocities (0.43 to 0.96 fps) were conducted. The experimentally measured EC's were compared those predicted using Equation 74 and the coefficients from Table 18 with the results in Table 19. The results verify

Table 18. Coefficients in Equation 74 as determined for different ranges of the dilution factor (Experimental Set I, Table 10).

| Coefficients | Dilution Factor (δ) Range | | |
|--------------|------------------------------------|--------------------------|-------------------------|
| | $0.001 < \delta \leq 0.02$ | $0.02 < \delta \leq 0.1$ | $0.1 < \delta \leq 0.2$ |
| k | 0.048 | 0.090 | 0.419 |
| a | 0.745 | 0.604 | 0.660 |
| b | 0.222 | 0.123 | 0.020 |

Table 19. Data on predictability of EC from Equation 74 for smaller particle sizes.

| Particle Size Fraction | Mixing Velocity (fps) | Dilution Factor: | Coefficients of Determination, r^2 , Resulting from a Linear Regression of EC_p on EC_m | | | | | |
|------------------------|-----------------------|------------------|---|-------|-------|-------|--------|-------|
| | | | 0.001 | 0.002 | 0.004 | 0.01 | 0.0133 | 0.02 |
| $0.125 < d < 0.5$ mm | 0.430 | | 0.912 | 0.996 | 0.996 | 0.992 | 0.987 | 0.979 |
| | 0.655 | | 0.993 | 0.985 | 0.995 | 0.981 | 0.967 | 0.986 |
| | 0.960 | | 0.998 | 0.995 | 0.981 | 0.985 | 0.966 | 0.991 |

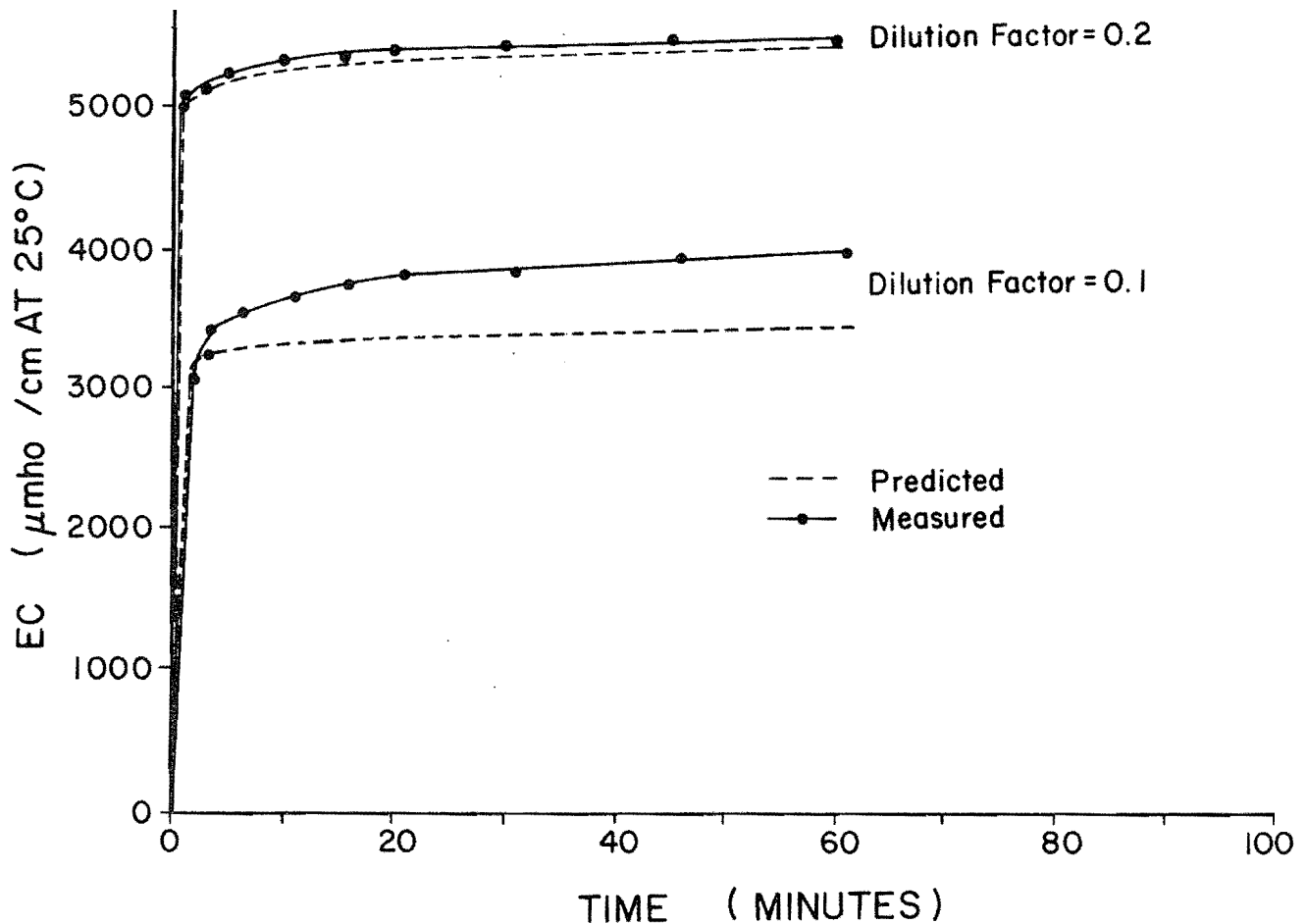


Figure 43. Comparison of predicted and measured EC using Equation 74 on dilution factor range 0.1-2.0 (Experimental Set I, Table 10).

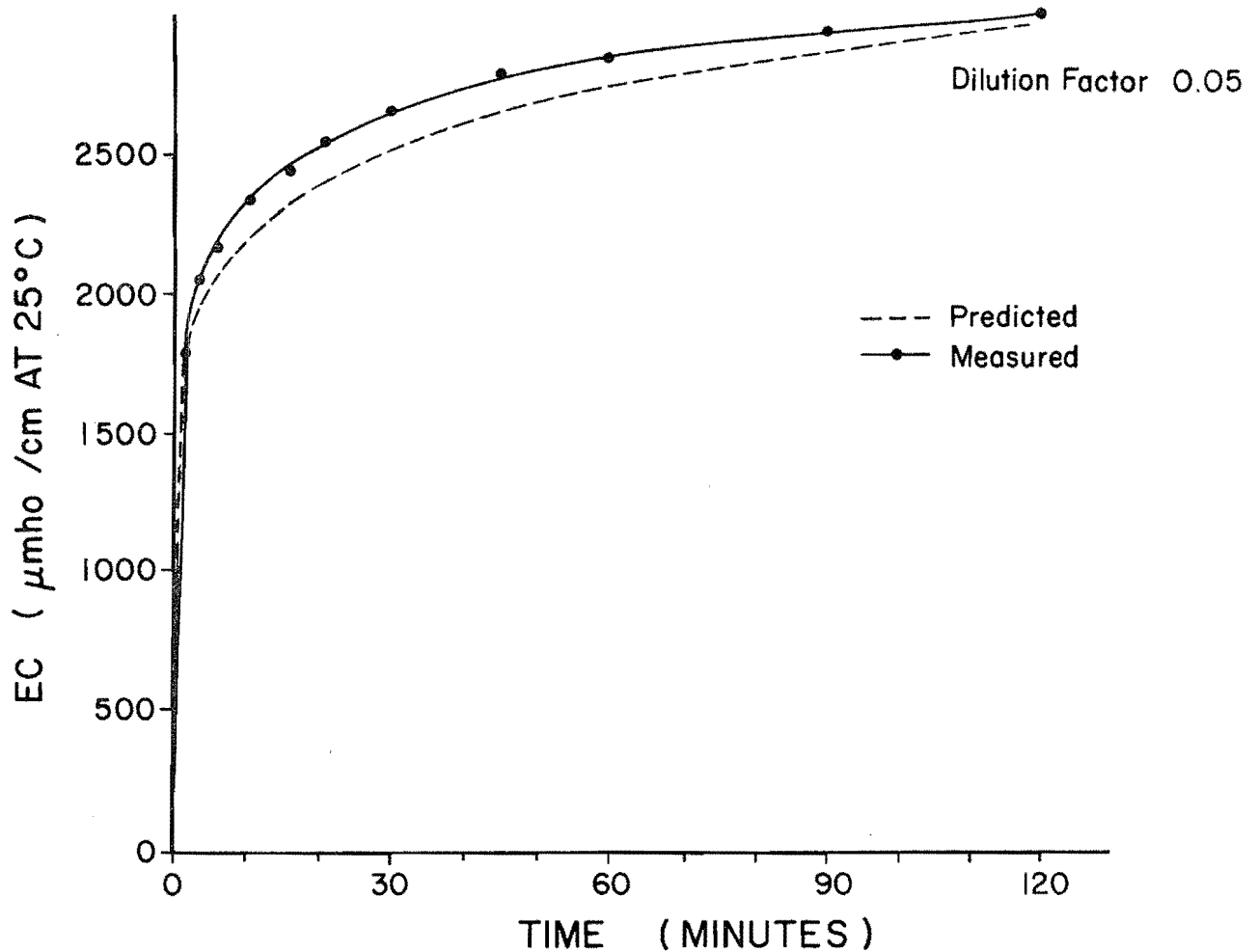


Figure 44. Comparison of predicted and measured EC using Equation 74 with coefficients: $k = 0.09$, $a = 0.604$, and $b = 0.123$ (Experimental Set I, Table 10).

the applicability of Equation 74 for these smaller particles.

Extrapolation of Equation 74 to Larger Systems

An attempt was made to test Equation 74 using experimental data obtained with the mixing tank apparatus. This was considered important because Equation 74 was developed based on experimental data obtained from the multiple stirrer apparatus. A test of its applicability to a larger system, such as the mixing tank, might provide important information about how well the equation extrapolates to the release of salt from sediments carried by a river system.

The only particle size fraction used in the mixing tank (Table 10) was $d < 2$ mm, but particle size varied considerably within the range. Equation 74 utilizes an average (D_{50}) particle size, which varies widely in natural soils. A second goal of this experiment was to investigate how well the median size of a natural soil sample represents a size range as far as salt release is concerned.

Figure 45 shows a comparison of values predicted by Equation 74 with data collected in the mixing tank. The coefficients of determination, r^2 , resulting from linear regression between the predicted and measured values of EC using Equation 74 ranged between 0.789-

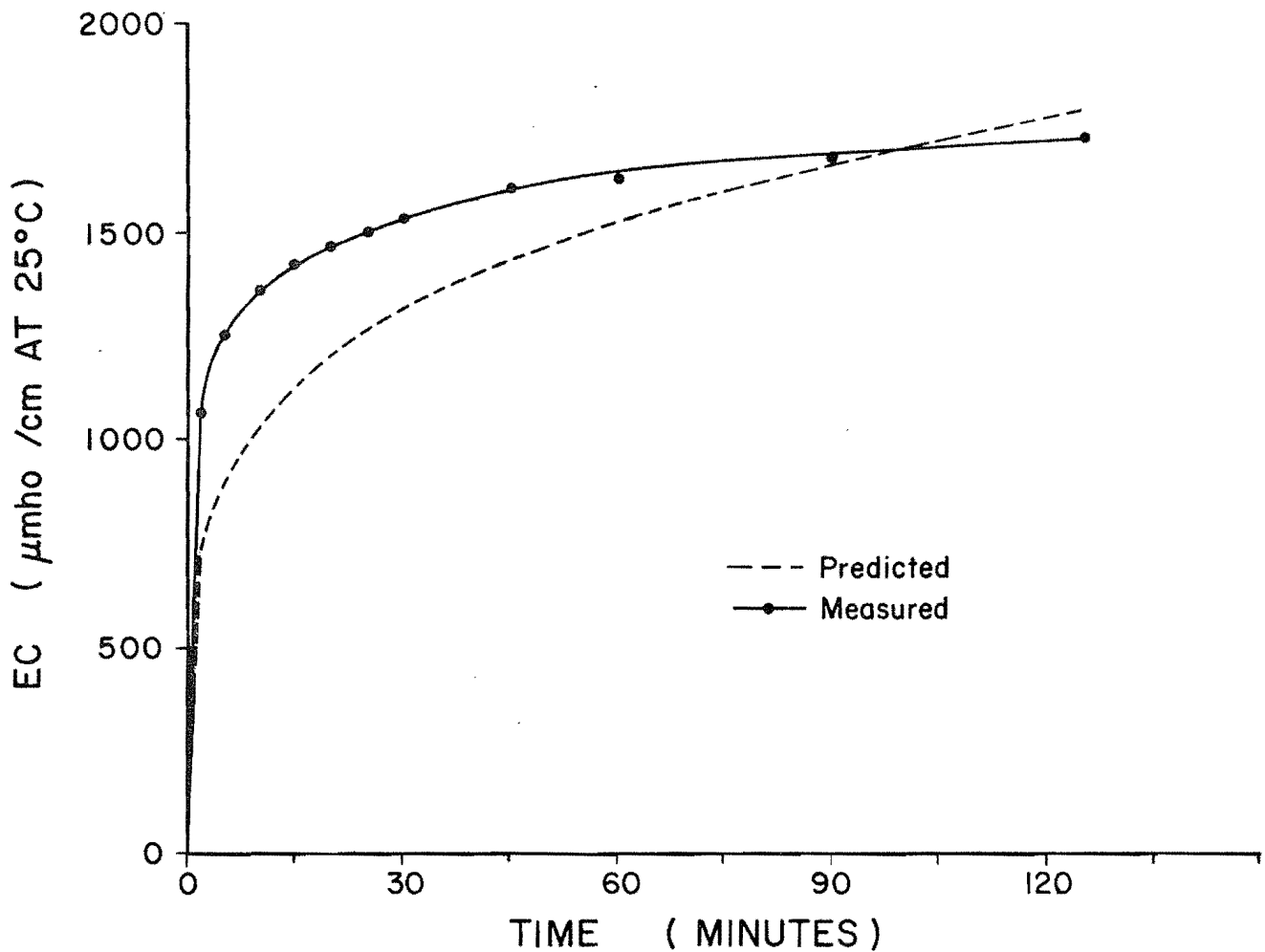


Figure 45. Comparison of the predicted and measured EC using Equation 74 applied to data obtained from the mixing tank apparatus (Experimental Set A, Table 10).

0.901. In conclusion, Equation 74 provides reasonable results for extrapolating from small laboratory mixing systems to larger natural systems with heterogeneous particle sizes.

Performance of Equation 74 in Initially Saline Solutions

Equation 74 was also tested using experimental data with initially saline solutions. Figure 46 shows Equation 74 to predict the EC values well up to an initial EC (EC_0) of 1125 $\mu\text{mho/cm}$ at 25°C. Equation 74 did not predict well for solutions with EC_0 values beyond about 1500 mho/cm at 25°C as by the comparison for a solution with EC_0 of 2125 $\mu\text{mho/cm}$ at 25°C. The good

prediction below 1500 $\mu\text{mho/cm}$ at 25°C is further indication of the additive affect of the sulfate sodium and sodium chloride solution up to a certain value. In conclusion, although Equation 74 does not include EC_0 as a variable, it may be applied to sediment-water solutions with EC_0 values up to 1500 mho/cm at 25°C by simply applying the equation to the data and adding EC_0 to the resulting EC value.

Testing Equation 79 and Its Comparison with Equation 74

Equation 79 was used to predict EC values from experimental runs conducted with solutions of sodium sulfate instead

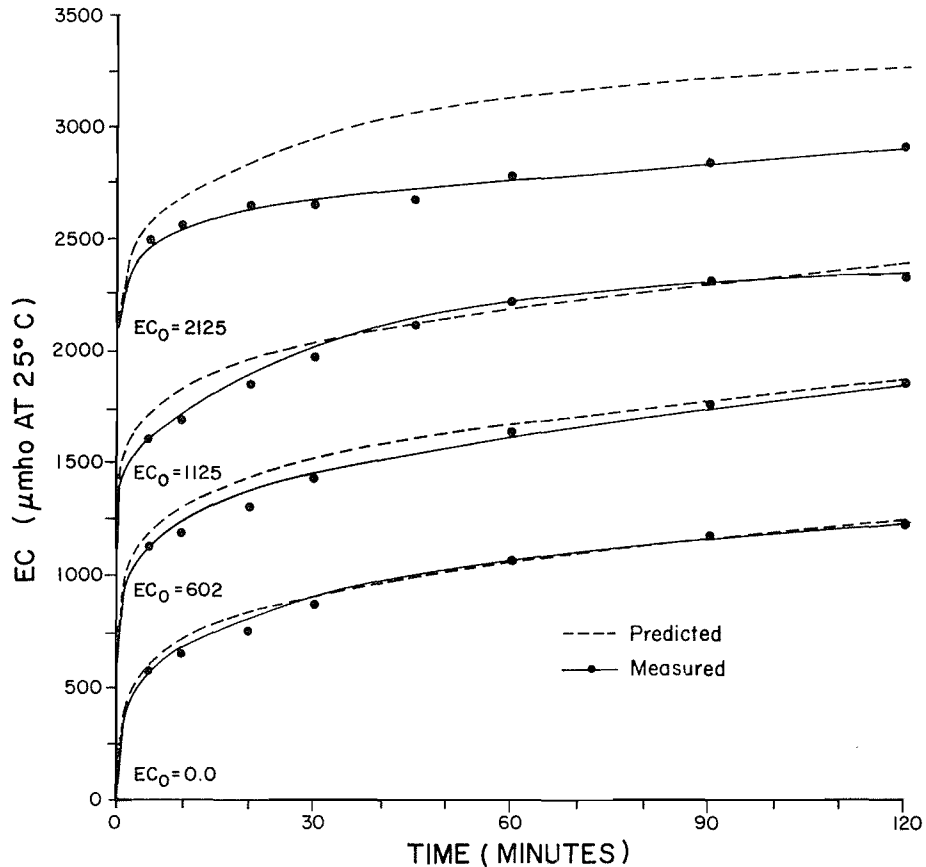


Figure 46. Comparison of measured EC with values predicted using Equation 74 for deionized water solutions with initial ECs of 602, 1125, and 2125 $\mu\text{mho/cm}$ at 25°C (Experimental Set I, Table 10).

of deionized water. The initial EC ranged from 600 to 8000 $\mu\text{mho/cm}$ at 25°C . Figure 47 shows the measured values of EC, the values predicted by Equation 79, and the values predicted by Equation 74 in solutions with four different levels of initial salinity and three different dilution factors.

Equation 74 did not predict well at these higher EC_0 's. In contrast, Equation 79 predicts well for all three dilution factors. Figure 48 shows EC values predicted by Equation 79 as plotted against the measured values using the experimental data from the entire spectrum of initial EC. The solid line denotes perfect fit. A linear regression resulted in a r^2

value of 0.99 for the experimental data. Equation 79 did not produce good results for solutions with initial EC below 1500 $\mu\text{mho/cm}$ at 25°C .

Chapter Summary

Equation 74, using the coefficient values in Table 18 for various dilution factor ranges, was found to do a good job of estimating the electrical conductivity in sediment water solutions beginning from deionized water or by adding the initial electrical conductivity to waters with initial values as high as 1500 $\mu\text{mho/cm}$ at 25°C . Equation 79 can be used for initial values as high as 8000 $\mu\text{mho/cm}$. The equations only apply in the presence of mixing.

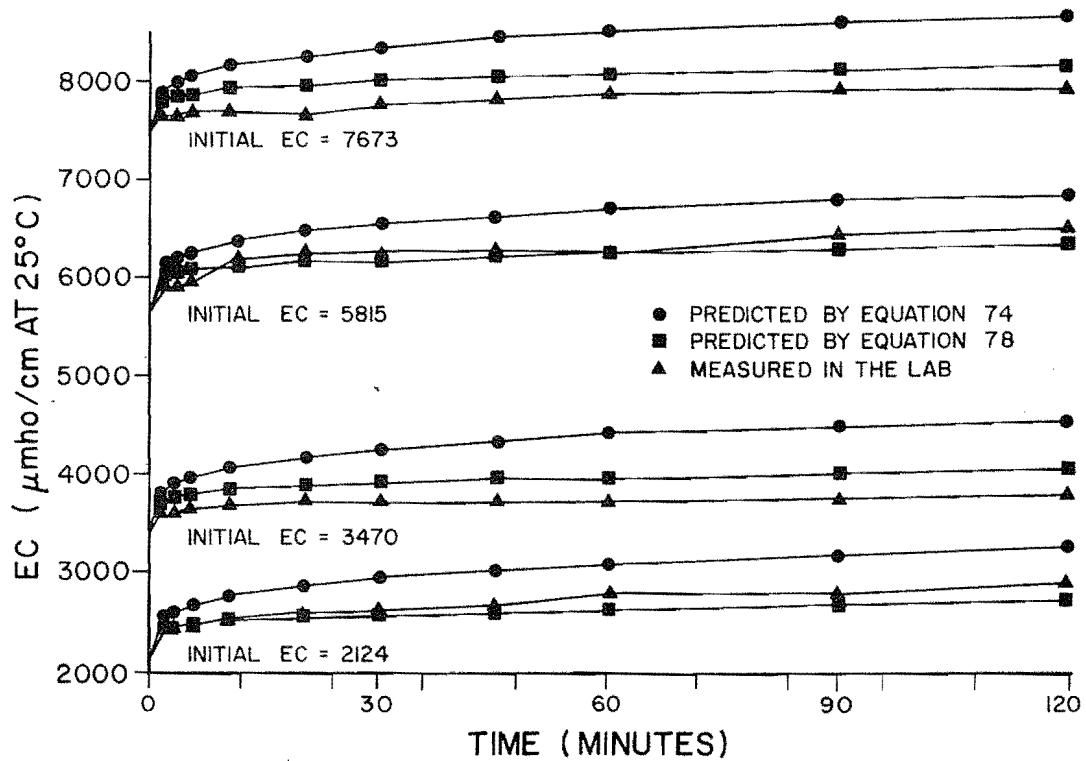


Figure 47. Comparison of predicted and measured EC using Equations 74 and 78 (Experimental Set I, Table 10).

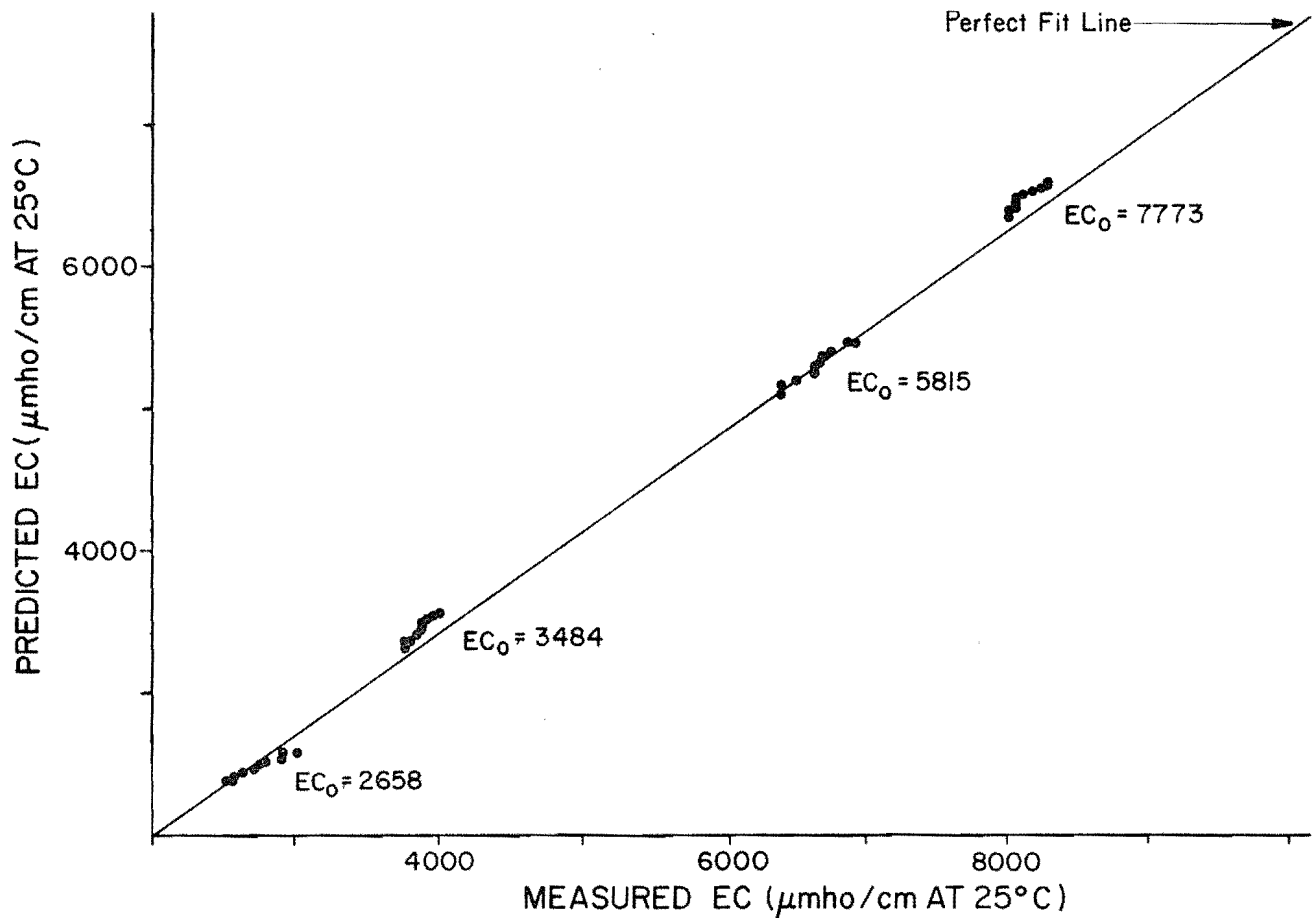


Figure 48. Comparison of predicted and measured EC using Equation 78 in the four different saline solutions (Experimental Set I, Table 10).

CHAPTER X

SALT-SEDIMENT MODEL: DEVELOPMENT AND APPLICATION

Introduction

This chapter describes use of the salt release equations in the development and application of a salt-sediment model designed to simulate the release of salt from suspended sediments in a stream channel. The water and sediment entering the stream channel were estimated from the Watershed Erosion and Sediment Transport (WEST) model (Leytham and Johanson 1979). The salt release equations were incorporated into the WEST model to estimate diffuse salinity loading in both overland flow and in the stream channel. The overall salt-sediment model was applied to a sub-watershed within the Price River Basin for the purposes of demonstrating application of the model and of quantifying salt release from suspended sediments as a diffuse source of salinity in the study area.

General Requirements of the Salt-Sediment Model

The salt-sediment model requires two phases with the following components:

- 1) Land phase:
 - a) hydrology component: simulating overland and sub-surface flow
 - b) erosion component: simulating sediment washoff from land surface
 - c) salinity component: using salt sediment equations to

estimate salt release from the suspended sediments

- 2) Channel phase:
 - a) hydraulic component: routing the flow of water in the stream
 - b) transport component: routing the suspension and deposition of suspended sediment load in the stream
 - c) salinity component: using salt sediment equations to estimate the amount of salt released from the suspended sediments

Figure 49 is a schematic of the general requirements of the salt-sediment model. Channel bank scour and its contribution to the suspended sediment load were not included because it was found that these materials yield insignificant amounts of salt as compared with the sediment material originating from land surface erosion (Figure 21).

Selection of the Watershed Erosion and Sediment Transport (WEST) Model

The literature review of sediment transport models resulted in the selection of the Watershed Erosion and Sediment Transport model (WEST model) developed by Hydrocomp Inc. (Leytham and Johanson 1979) because of features pertinent in satisfying the general requirements listed above. WEST is composed of a) The ARM model (Agricultural Runoff Management model by Donigian et

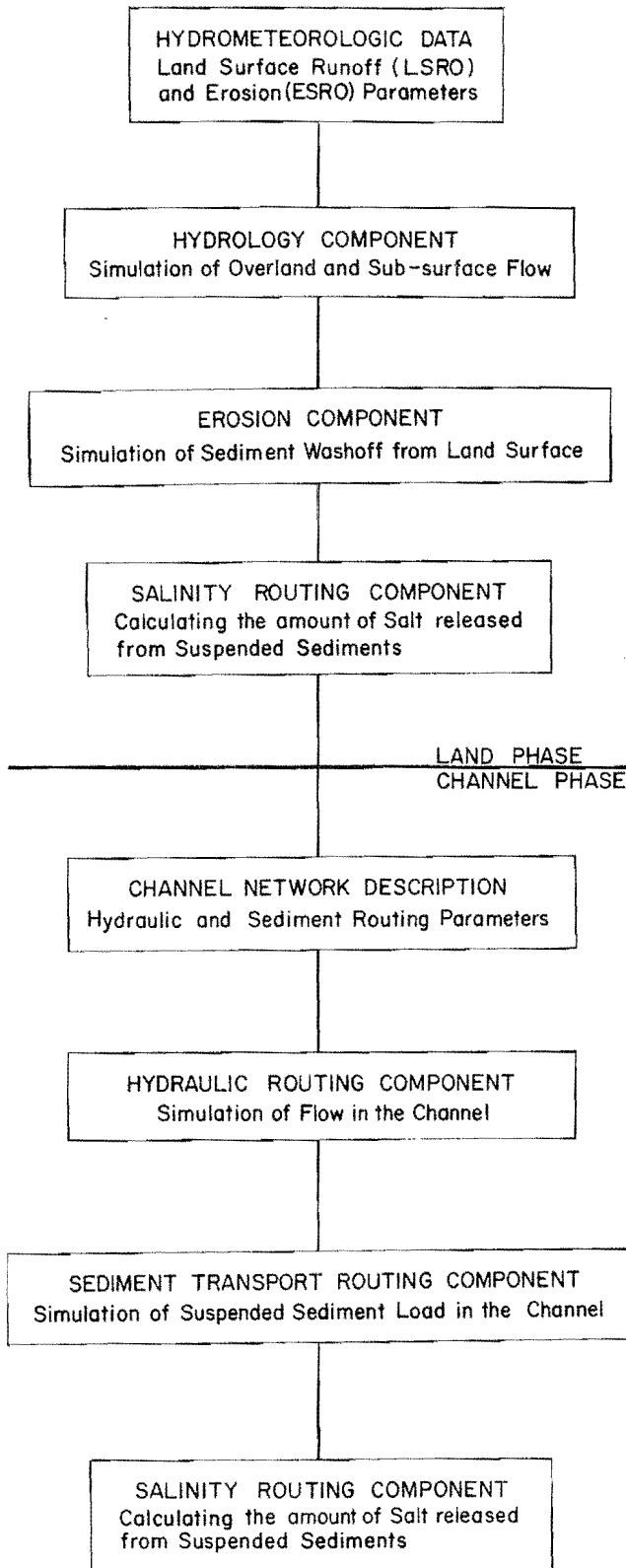


Figure 49. General requirements of the salt sediment model.

al. (1977)) and b) the CHANL model. The two models are linked by the data management system illustrated in Figure 50. The ARM model, which operates the land phase, includes hydrology and sediment production components.

The hydrology component of the ARM model is a modified version of the Stanford Watershed model (Crawford and Linsley 1966). One modification is the areal zone concept based on the infiltration capacity. The watershed is divided into five zones, each representing 20 percent of the total area (Figure 51). Schematically, Figure 51 shows that zone 1 will infiltrate much less water than zone 5, conversely, zone 5 will provide less overland flow than zone 1. This zonal concept attempts to simulate the areal variation in sediment loss due to variations in overland flow. This feature was found useful for the purpose of modeling salinity resulting from the eroded material because the areal variation in infiltration results in source areas or zones which generate more overland flow. Overland flow is important because it controls the production of sediment from the land surface and, consequently, the amount of salt released from the sediments.

The sediment production component of the ARM model simulates sheet erosion based on a model developed by Negev (1967). He found that conventional soil erosion equations such as the Universal Soil Loss Equation do not work well because they do not directly account for the effects of runoff. Sheet erosion mechanism requires overland flow. Negev simulated the entire spectrum of the erosion processes.

The component processes of sheet and rill erosion pertain to 1) detachment of soil fines (silt and clay) by raindrop impact, and 2) pick-up and transport by overland flow. These processes are represented in the ARM model by

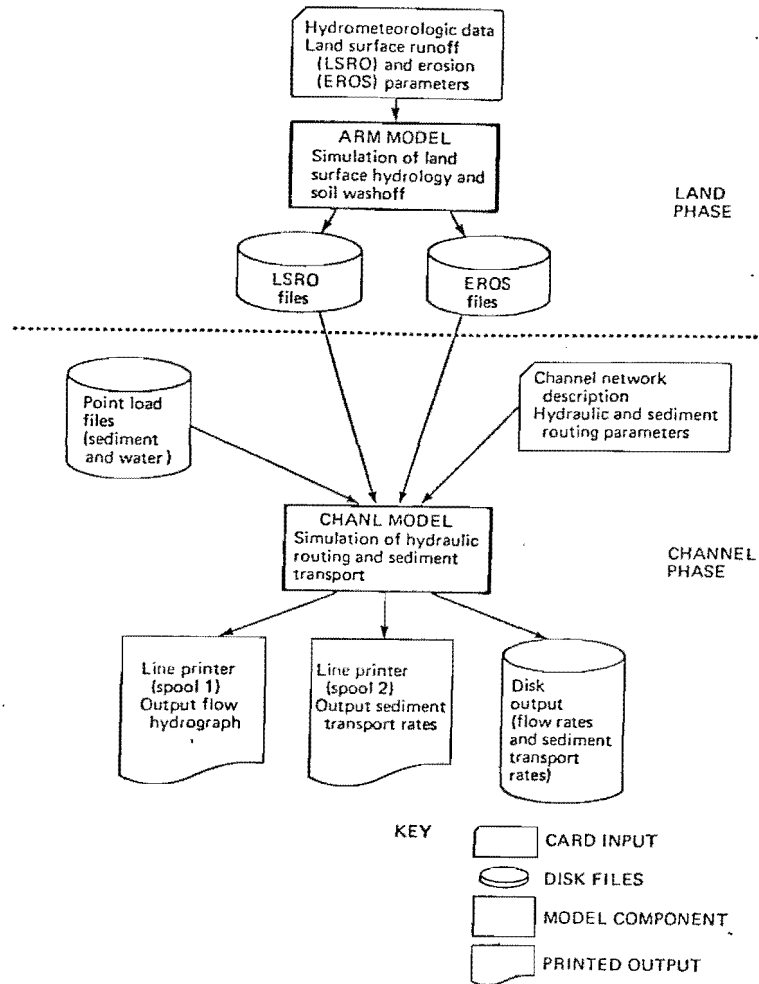


Figure 50. WEST model data management system (adapted from Leytham and Johanson 1979).

Soil fines detachment:

$$R_t = (1 - C_T) A P_t^B \quad . . . \quad (80)$$

C_T = fraction of vegetal cover as a function of time, T , within the growing season

Soil fines transport:

$$S_t = \begin{cases} F O_t^E, & S_t \leq SR_t \quad . . . \quad (81) \\ SR_t, & S_t > SR_t \quad . . . \quad (82) \end{cases}$$

A = detachment coefficient for soil properties

P_t = precipitation during the time interval (mm)

B = exponent for soil detachment

S_t = transport of fines by overland flow (tonnes/ha)

in which

R_t = soil fines detached during time interval t (tonnes/ha)

E = exponent for fines transport by overland flow

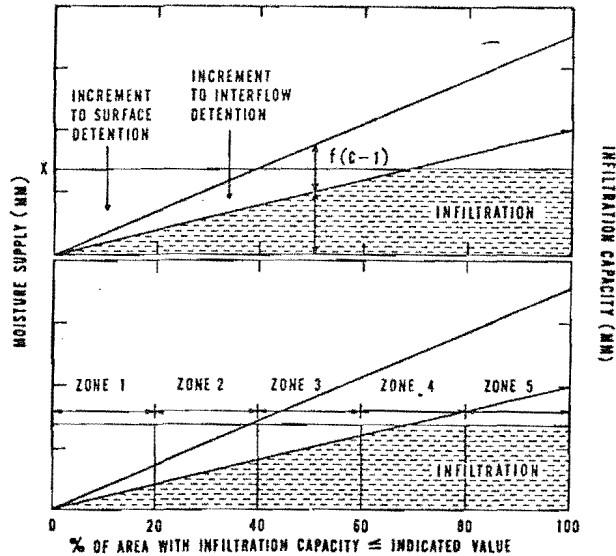


Figure 51. Source-zones superimposed on the infiltration capacity function.

F = coefficient of transport

SR_t = reservoir of soil fines at the beginning of the time interval, t (tonnes/ha)

O_t = overland flow occurring during the time interval, t , (mm)

In applying these equations, the soil detachment (R_t) during each time interval is calculated using Equation 80 and added to the total fines storage (SR_t). Next, the total transport capacity of the overland flow (S_t) is determined by Equation 81. Sediment is assumed to be transported at the capacity rate if sufficient fines are available, otherwise the amount of fines in transport is limited by the fines storage, SR_t , as described by Equation 81. The sediment loss to the waterway in each time interval is calculated

using Equation 82 based on the fraction of total overland flow that reaches the stream. A land surface flow routing technique determines the overland flow contribution to the stream in each time interval. After the fines storage is reduced by the sediment loss to the stream, the simulation moves to the next time interval. The sediment that does not reach the stream is treated as part of the fines storage and is available for transport in the next time interval.

The ARM model operates on a short time interval (5 or 15 minutes). This was also found to be appropriate for the simulation of salt release from eroded material using the equations derived in this study with contact time in minutes. Although ARM is a continuous simulation model, it can also be used to simulate single events if the initial hydrologic storage conditions can be estimated.

The CHANL model is a one-dimensional model for simulating the movement of water and sediment through the stream network. Hydraulic routing is performed using kinematic wave equations. Sediment routing is performed by explicitly modeling the advection of sediment and the scour and deposition of both cohesive and cohesionless material (Figure 52).

The estimate used in the model for potential or ultimate concentration of the cohesionless sediments is based on a technique developed by Ackers and White (1973). The theoretical basis of the method is described together with assumptions and restrictions by White (1972). The method has been extensively tested on both field and laboratory data and its performance compares favorably with that of other techniques (Leytham and Johanson 1979).

The deposition of clay and silt fractions (cohesive material) is estimated by modifying graphical solutions which Brown (1967) derived from work by Camp (1943) to incorporate work by Einstein (1968) and Owen (1969).

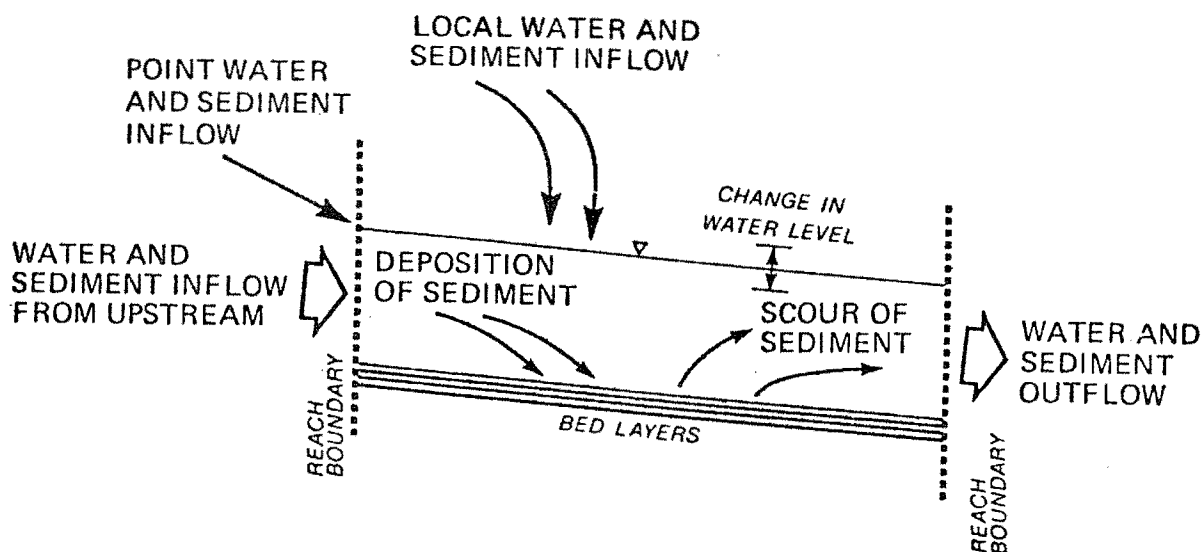


Figure 52. Processes simulated in a reach (after Leytham and Johanson 1979).

Modification of the WEST Model

Only selected components of the WEST model were necessary for this study:

1) The ARM model: Only the LANDS and SEDT subprograms were used in the land phase of salt sediment model. The other subprograms model movement of pesticides and nutrients and snowmelt and were excluded. The necessary changes were made to interface the SEDT and LANDS subprograms with the salt-release submodel discussed below.

2) The CHANL model: The hydraulic routing subprogram was adapted in the channel phase of the salt-sediment model. The sediment transport subprogram was modified to include transport of suspended sediments originating from land erosion only. Bed load transport was excluded.

The modified models were interfaced with the salt-release submodel and linked by a data management system to constitute the overall salt-sediment

model. The formulation of the salt-release submodel is described in the following section.

Salt-Release Submodel

The salt release submodel, designated SALTSD, calculates the salt released from suspended sediments in both overland and channel flows. In the land phase, overland flow and sediment production are simulated at each time interval from a unit area of the watershed. SALTSD is interfaced with the LANDS and SEDT components of LANDHYD in such a way that the simulated sediment mass and overland flow are used to calculate the dilution factor on a weight basis. The velocity of the overland flow is also used in the salt-sediment equation (Equation 74) and is limited to a maximum value equal to the settling velocity of the median particle size (D_{50}) of the surface soil. The TDS is estimated from EC by:

$$TDS = .746 EC \quad (83)$$

in which

TDS = total dissolved solids (mg/l)
(gm^{-3})

EC = electrical conductivity
($\mu\text{mho/cm}$ at 25°C)

Dixon (1978) derived this equation from samples taken from Coal Creek, in the Price River Basin. The TDS is used to estimate weight of salt per unit area. At the end of each time interval, the loading per unit area is input to the CHANNEL phase and an accumulated total is printed.

The SALTSD submodel operates somewhat differently in the channel phase. The initial EC of the channel (EC_0) is used to determine whether Equation 74 or 79 is employed to estimate the salt release from sediment in the channel. In contrast, in the land phase no initial EC is needed because overland flow is modeled to reach the stream within each model time interval. The channels receive inputs from the land phase. Amounts are estimated per unit area and accumulated by using the subarea of each reach as a multiplier to the runoff, sediment mass, and salt mass per unit area. The accumulated salt at the start of the simulation process becomes the basis for estimating the initial EC for a reach. The outflow from reach 1 becomes the inflow for reach 2, and similarly the electrical conductivity of reach 1 becomes the initial EC of reach 2, and so on along the stream channel.

Basic Assumptions for the Salt-Release Submodel

The following assumptions were made in order to utilize the salt-release submodel in the salt-sediment model:

1. Only soil materials which are washed off the land surface by the actions of rainfall and overland flow are included in the salt-release submodel.

2. Snowmelt runoff is assumed to be an unimportant soil washoff mechanism and therefore not considered as generating eroded material.

3. The scoured channel bank and bed materials are assumed to yield negligible salt and therefore excluded from the salinity calculations.

4. The mixing velocity in the salt release equations is taken as the velocity of the overland flow or channel flow as long as the sediment load is in suspension. If these velocities exceed the settling velocity of the suspended material, the velocity used in the salt release equations is limited to the settling velocity. The magnitude of the settling velocity depends on the particle size and flow characteristics.

5. Material deposited in the stream channel is assumed to be only a small percentage of the total suspended material and, therefore, is excluded from the salinity routing.

6. The dilution factor is assumed to equal the ratio of suspended material discharge to the flow volume, on a weight basis, over a model time interval.

7. Equation 74 can be used for initial EC values, EC_0 , less than $1500 \mu\text{mho/cm}$, and Equation 79 can be used for EC_0 values beyond that limit up to 8 mmho/cm .

8. The electrical conductivity of the sediment/water solutions, as predicted by the empirical equations, is related to the TDS using Equation 83; and the amount of salt, on a weight basis, is calculated by converting flow discharge to volume and multiplying that by TDS over a model time interval.

9. Any salt release occurring after a contact time of 2 hours is ignored. This is based on the observation that more than 90 percent of the salt associated with the suspended sedi-

ments was diffused under the laboratory conditions in a 2-hour period.

10. The spatial variability of the soil material upland of the watershed is assumed to be adequately accounted for by dividing the watershed into "segments," each with uniform salinity characteristics represented by its saturation extract EC.

Considerations in Applying the Salt-Sediment Model

General

Figures 53 and 54 show the organization of the two models as linked together by a data management system. Operational considerations in applying the salt-sediment model are described below.

Land Simulation Phase (LANDHYD)

For applying the salt-sediment model, a watershed is spatially divided into "segments," and LANDHYD is applied to each segment. Segments are visualized as areas of land with uniform physical properties. Input consists of hydro-meteorologic data (rainfall, potential evaporation) and physical characteristics of the system. The inputs are transformed to time series of land surface runoff (LSRO), land surface erosion (EROS), and salt release from the sediments (SRSD), a series for each segment. LSRO is the depth of runoff, both surface and subsurface, flowing into the stream channel. EROS is the mass of sediment washoff per unit area, and SRSD is the mass of salt released from the sediment per unit area and reaching the stream system in a model

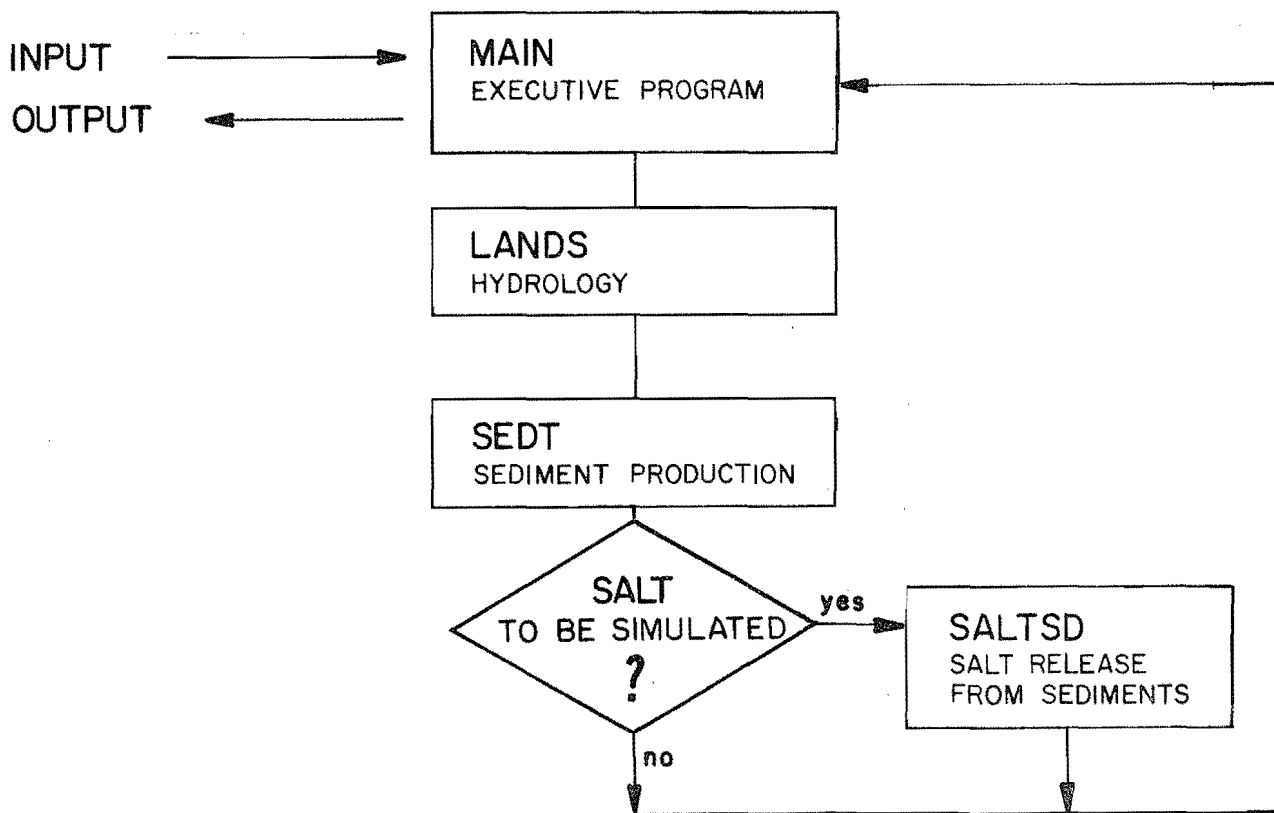


Figure 53. Organization of the LANDHYD (land phase) of the salt-sediment model.

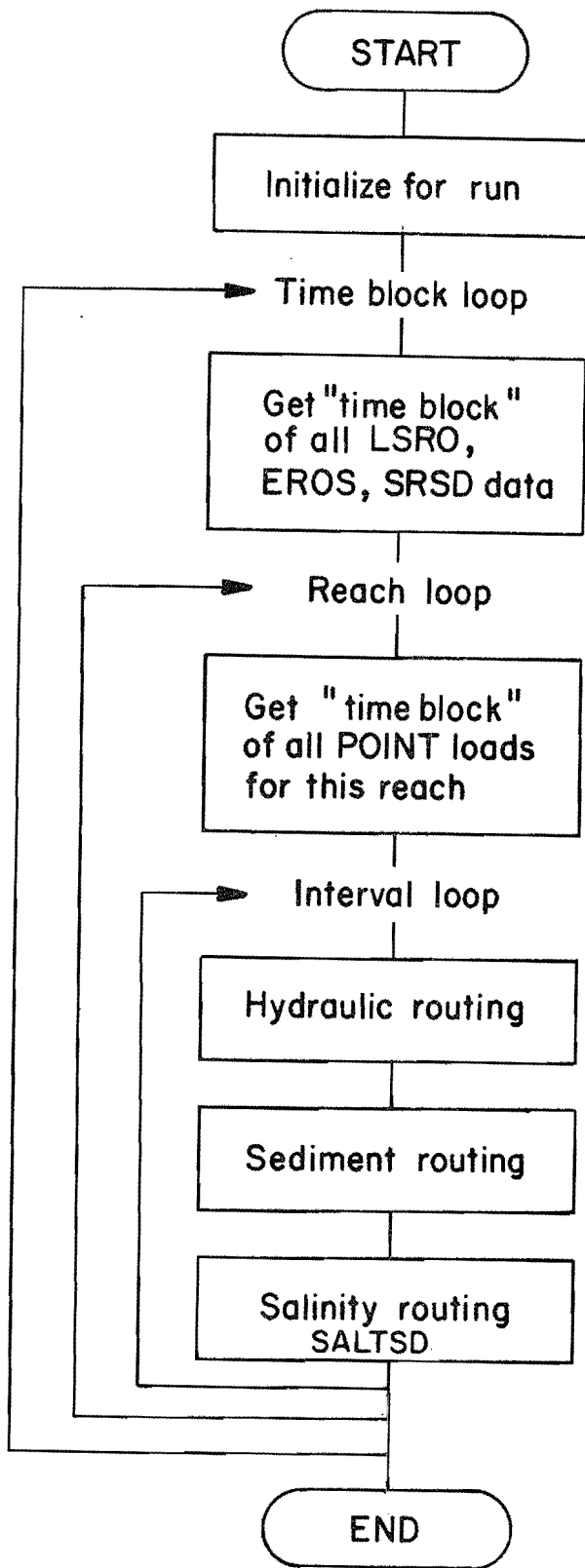


Figure 54. Organization of CHANNEL (channel phase) of the salt-sediment model.

time interval. The sediment algorithms estimate the total mass of sediment washed from the land surface in each time interval but give no indication of the particle size distribution. The median diameter, D_{50} , of the land surface material with size fraction of $d < 2$ mm was taken as a reasonable approximation for use in the salt release equations.

Channel Phase Simulation (CHANNEL)

The CHANNEL model estimates the amount of salt being released from suspended material and simulates water, sediment, and salt movement through the stream channel system (Nezafati 1982). It uses a tree-like structure of "reaches" to represent the principal water courses and routes movements of water, sediment, and salt through these reaches to the basin outlet. Allowance is provided for both point and diffuse loads.

The CHANNEL model calculates flow discharges, sediment transport rates, and movements of released salt at specified points in the system. Reach outflow is computed for every time interval and becomes the inflow to the reach downstream. A maximum concentration of suspended sediment is estimated for the flow characteristics at each time interval (Ackers and White 1973). A suspended sediment load that would otherwise exceed this concentration is assumed deposited and does not enter the salinity release or routing.

Listings of both the LANDHYD and CHANNEL models, and sample inputs and outputs are found in Nezafati (1982, Appendix B).

Application of the Salt-Sediment Model in the Price River Basin

General

Application of the model to the entire Price River Basin was not fea-

sible due to the lack of observed data for calibration and verification. In particular, most of the suspended sediment data are based on grab samples, consist of monthly concentrations, have no size distribution analysis, and do not necessarily correspond to discrete storm events. Better data exist for some subcatchments.

Ephemeral channels in the basin were monitored by Riley et al. (1982a, 1982b). Automatic recording devices were used to measure water flows, sediment, and total dissolved solids moving in these channels, and data were obtained for this study. For one such ephemeral channel, Coal Creek (Figure

55), has been studied. Dixon (1978) took soil samples and recorded single storm events and salinity measurements. He also applied his hydro-salinity model in order to estimate salt loading from the overland flow. Application of the salt-sediment model to Coal Creek would both indicate the salinity contribution of suspended sediments and provide additional information for comparison with Dixon's results.

Subwatershed Selection

The salt-sediment model was applied to a subwatershed within the Coal Creek subbasin which had been instrumented

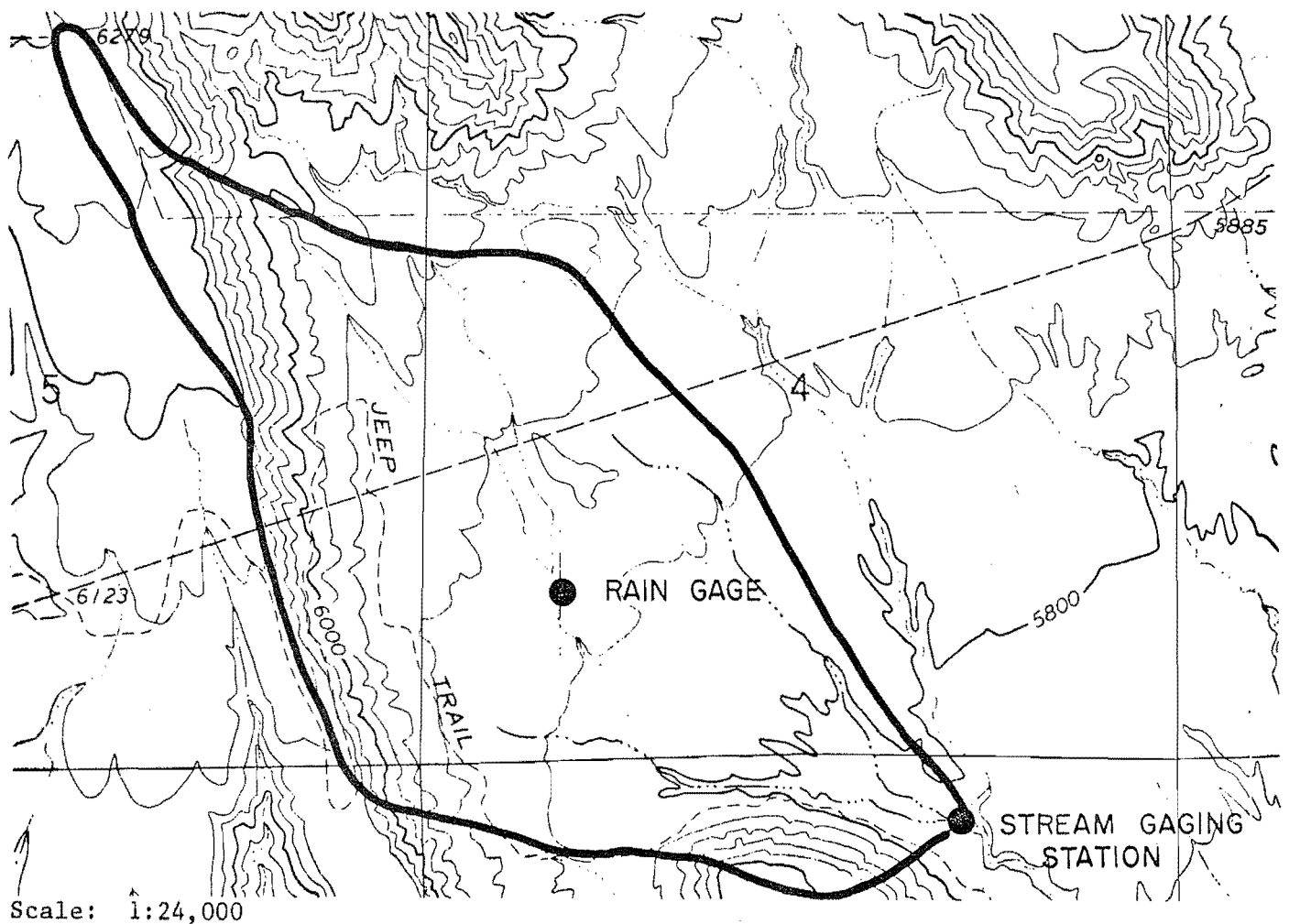


Figure 55. Subwatershed in the Coal Creek subbasin.

with a control section, an automatic water level recorder, and an automatic water quality sampler (Peckins 1981). Figure 55 shows the configuration of the subwatershed and the locations of the recording rain gage and the stream gaging site. Data obtained for selected storm events on runoff, total suspended sediments, and electrical conductivity are given in Table 20.

Model Calibration

Rainfall charts were used to prepare 5-minute rainfall data for the land phase of the model. Daily potential evaporation data were obtained from a USGS weather station at Scofield Reservoir, located about 60 miles to the west of the study subwatershed and the only measurement location for evaporation data in the Price River Basin.

The land hydrology model was calibrated for two storms (values in Table 21). Figure 56 compares measured with simulated flows for a storm of

18 mm which occurred on August 25, 1980. The simulated hydrograph quite closely follows the shape of the measured hydrograph, and the volume difference is less than 5 percent. The calibrated model was also used to simulate runoff from a storm of 10 mm occurring on July 18, 1978. However, since this storm occurred earlier in the year it was necessary to change the values of two parameters, namely, the initial lower soil moisture storage (LZS), and length of overland flow (L). Figure 57 is a comparison of measured and simulated flows as the result of using 2.5 centimeters and 45.7 meters for LZS and L, respectively, as compared with 12.7 centimeters and 91.4 meters used for the August storm. The soil moisture content has higher in July 1978 than it was for the storm in August 1980.

Model Results

The salt-sediment model was run for the two storms with the results shown

Table 20. Coal Creek flow, sediment and salinity data for two storms.

| Time (Min) | Flow cfs | Suspended Sediment (mg/l) | EC ^a µmho/cm | Time (Min) | Flow cfs |
|----------------------|-----------------|---------------------------|-------------------------|------------------------|----------|
| <u>July 18, 1978</u> | | | | <u>August 25, 1980</u> | |
| 1 | 15 | 90,000 | 845 | 1 | 11 |
| 2 | 16 | 77,420 | 932 | 2 | 21 |
| 3 | 16 | 96,290 | 1,166 | 3 | 44 |
| 4 | 17 | 79,630 | 1,296 | 12 | 81 |
| 12 | 42 | 132,700 | 1,417 | 20 | 300 |
| 20 | 28 ^b | - | - | 28 | 56 |
| 28 | 24 ^b | - | - | 44 | 15 |
| 36 | 14 ^b | - | - | 60 | 8 |
| 44 | 6 | 60,550 | 1,272 | 76 | 7 |
| 60 | 2 | 53,350 | 1,781 | 100 | 6 |
| 76 | 2 | 58,250 | 1,562 | 124 | 5 |

^aField measurement (does not correspond to the time of sampling).

^bAdjusted.

Source: Peckins (1981).

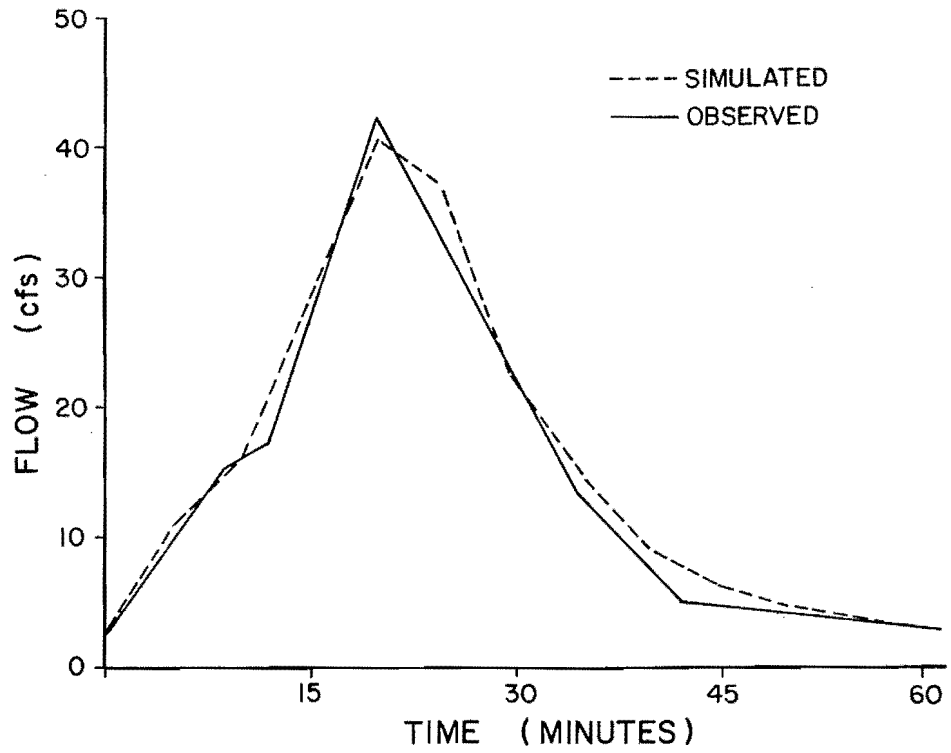


Figure 56. Comparison of observed and simulated flows from a storm on August 25, 1980.

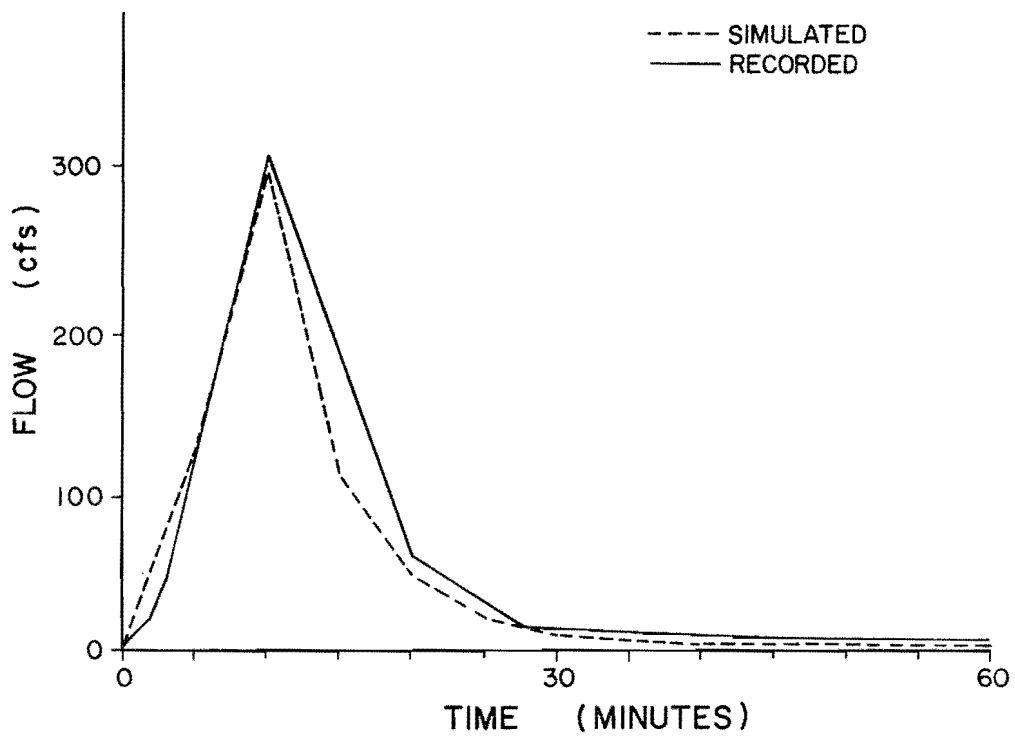


Figure 57. Comparison of observed and simulated flows from a storm on July 18, 1978.

in Figures 58 and 59. The salt load released from suspended sediments was predicted for each storm and amounted to 385 kg km⁻² and 214 kg km⁻² for the storms in 1978 and 1980, respectively.

Table 21. Parameter values calibrated for LANDHYD.

| Parameter ^a | Value (English Units) |
|------------------------|-----------------------------|
| UZSN | 0.05 |
| LZSN | 8.00 |
| INFIL | 0.40 |
| INTER | 0.05 |
| COVMAX | 0.05 |
| IRC | 0.00 |
| NN | 0.20 |
| L | 150.00 |
| SS | 0.04 |
| A | 0.00 |
| UZS | 0.00 |
| LZS | 12.00 |
| SGW | 0.00 |
| GWS | 0.00 |
| KV | 0.00 |
| K24L | 0.00 |
| KK24 | 0.00 |
| ICS | 0.00 |
| OFS | 0.00 |
| IFS | 0.00 |
| K24EL | 0.00 |
| KK24 | 0.00 |
| JRER | 5.30 |
| KRER | 0.24 |
| JSER | 2.00 |
| KSER | 0.30 |
| SRERI | 1.98 |

^aFor the parameter definitions see Nezafati (1982).

The higher estimate was extrapolated to estimate the total salt load released from sediment in the Price River Basin. Based on records of 37 years, an average of four storms occur annually in the Price River Basin (Rao 1982). The salt load per unit area was extrapolated to the entire Coal Creek subbasin by assuming that the modeled area was representative. The annual salt load extrapolated this way amounted to 8.5 x 10⁵ kg from Coal Creek.

These results were then extrapolated to salt load estimates for the Price River at Woodside. Dixon (1978) estimated that the Coal Creek subbasin contained about 55.6 km² of undivided Mancos Shales out of a total for the Price River Basin (Ponce 1975) of 1211 km². Extrapolating by the ratio of these two areas of 21.8 gives an annual salt load of 1.86 x 10⁶ kg released from suspended sediments at Woodside. Ponce (1975) estimated the total annual salt load at Woodside as 3.678 x 10⁸ kg. Therefore, less than one percent of the annual salt load in the Price River Basin is estimated to be released from suspended sediments.

Comparison of Results

The salt load from overland flow and natural channels has been estimated by Ponce (1975), White (1977), Dixon (1978), and Riley et al. (1980). Table 22 compares their results with those obtained in this study. Although none of these studies separate out salt loading from suspended material, the salt-sediment model seems to estimate within the ranges of the previous studies.

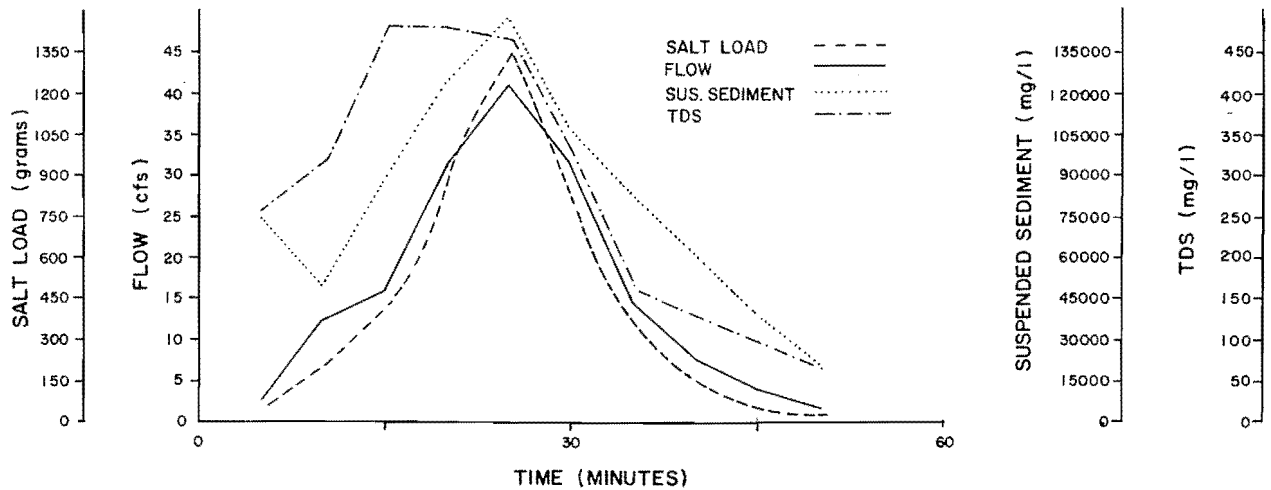


Figure 58. Flow, suspended sediment, TDS, and salt load predicted by model for storm on August 25, 1980.

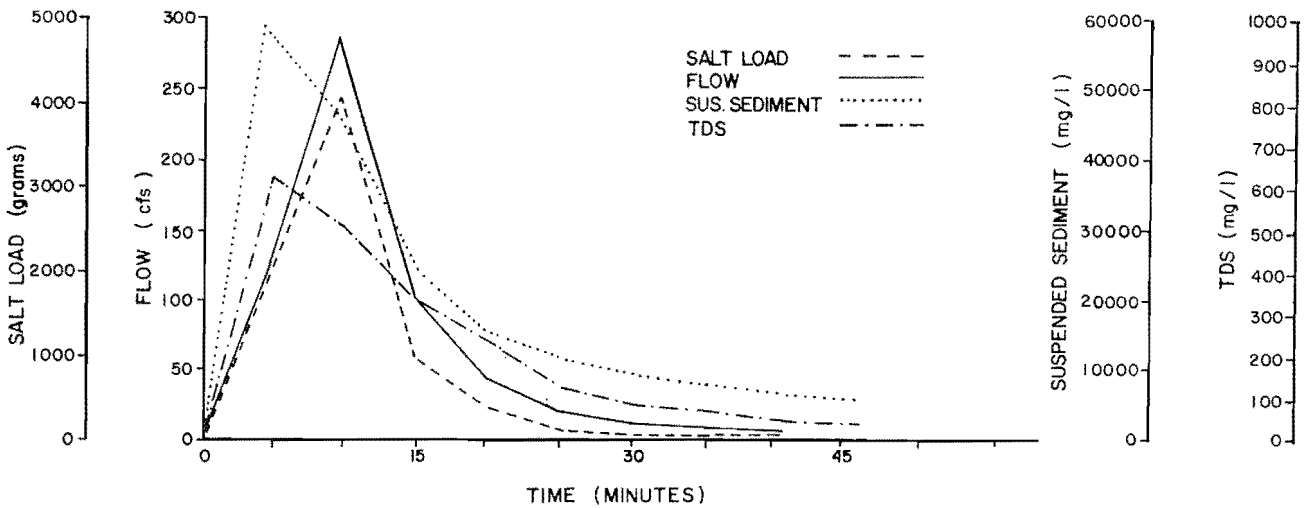


Figure 59. Flow, suspended sediment, TDS, and salt load predicted by model for storm on July 18, 1978.

Table 22. Comparison of the estimated percentage of total annual salt load at Woodside with respect to source.

| Source | Percent of Salt Load at Woodside | | | | |
|---------------------------------|----------------------------------|--------------|--------------|--------------|---------------------|
| | This Study | Ponce (1975) | White (1977) | Dixon (1978) | Riley et al. (1980) |
| Overland flow | - | 0.50 | - | 5.70 | 2.10 |
| Overland flow (eroded material) | 0.38 | - | - | - | - |
| 1st order channels | 0.12 | - | 3.40 | 0.74 | 1.10 |
| 2nd order channels | - | - | - | 0.36 | 0.36 |
| 3rd order channels | - | - | - | 0.23 | 0.23 |
| 4th order channels | - | - | - | 0.09 | 0.09 |
| Totals | 0.50 | 0.50 | 3.40 | 7.12 | 3.88 |

CHAPTER XI

SUMMARY, CONCLUSIONS, AND RECOMMENDATIONS

Summary

Overview

The principal processes causing salts to move from underground formations into streamflow are 1) dissolution from the soil surface during runoff events, 2) transpiration of soil water leaving salt residuals, 3) efflorescence left by evaporating seepage and then dissolved by subsequent runoff, 4) dissolution with weathering of fixed bed channels, 5) salts released by sediments entering the channel from sheet, gully, and bank erosion, and 6) deep percolation through saline aquifer reaching the stream as base flow. Previous studies have shown processes 1, 2, and 4 to be minor salt sources in the Price River Basin. This study examined processes 3 and 5 and found them to be similarly small (though efflorescence seems to contribute considerably more salts than do the other sources). This leaves waters percolating through aquifers containing soluble salts and emerging as base flow as the probable source of perhaps most of the salt loading from natural lands. No one has tried quantifying salt loading from sediments entering the stream through bank cutting or sloughing or as the bed material is ground in transit, but these sources are probably minor.

Study of Salt Efflorescence

Studies of salt efflorescence as a source of salinity in the Price River Basin were conducted by field observation and instrumentation, laboratory experiments, and mathematical modeling.

In the field, near saturation moisture conditions were observed below salt efflorescence crusts in many places. Electrical conductivity (EC) of the soil-water saturating the channel bed material varied from 35 mmho/cm to above 45 mmho/cm. Sodium and sulfate were the major ions. Salt efflorescence densities varied between 0.14 and 0.36 g/cm². Field data indicated that salt efflorescence accumulates for the first 10-15 days after a storm washes off earlier efflorescence. After this period, the rate of accumulation of efflorescence is negligible.

Soil columns were used to grow efflorescence artificially under controlled conditions in the laboratory. Moisture content and salt concentrations were monitored at different depths during the growth of efflorescence. The data obtained were used to verify the mathematical model developed for simulating the formation of salt efflorescence.

A water flow-salt transport model was developed and verified against the field and laboratory data. A chemical equilibrium submodel was later interfaced with the water flow-salt transport model. The model satisfactorily predicted water content, salt concentration profiles and efflorescence crust densities. Model extrapolation estimated that no more than 7.5 percent of the total salt loading in the Price River Basin is associated with salt efflorescence.

Study of Salt Release from Sediment

Salt release from suspended sediments was studied in the laboratory using sediment material obtained from various locations in the Price River Basin. The experimental procedure was to record the increase of electrical conductivity (EC) in a sediment/water solution while varying the dilution factor, defined as the ratio of sediment to water on a weight basis; particle size; mixing velocity; and initial EC.

The Buckingham Pi Theorem was employed to derive relationships expressing the EC of a sediment water system as a function of the controlling factors. The results were presented in two salt release equations, one excluding the effect of initial EC and the other providing for initially saline solutions. These solutions were created using NaCl and Na₂SO₄, the predominant salts in waters of the study area.

Additional laboratory experiments were performed to collect data to validate the salt release equations. The results showed that it was necessary to divide the dilution factor into three ranges of 0.001-0.02, 0.02-0.1, and 0.1-0.2 and separately calibrate the predictive equation for each range. The equations showed good predictive capability over the ranges of the variables on which their development was based.

The salt release equations provided a basis for assessment of salt release from eroded material in a river basin. The equations were incorporated into an adapted version of the Watershed Erosion and Sediment Transport (WEST) model. The resulting salt-sediment model was applied to a small tributary of Coal Creek for the purpose of assessing the importance of salinity resulting from sediments originating from upland erosion in the land and channel phases. The modeling assumed that 1) overland flow and stream velocity provide reason-

able approximations of the mixing velocity of sediment water solutions provided the sediment load is still in suspension, and 2) the dilution factors in the salt-sediment equations can be approximated by the ratio of suspended sediment to flow volume, on a weight basis, over each modeling interval.

The hydrologic submodel was calibrated for two selected storms. The salt loading from the two storm events amounted to 385 kg km⁻² and 214 kg km⁻², respectively. Extrapolation to the entire Price River Basin led to an estimate that about 0.50 percent of the total annual salt load of 3.7 x 10⁸ kg at Woodside, as estimated by Ponce (1975), is released from suspended sediments.

Conclusions

Study of Salt Efflorescence

The conditions favorable to the accumulation of salt efflorescence are highly saline water just below the soil surface and a source of heat for vaporizing the water. Readily soluble salt efflorescence accumulates in nearly all stream channels in the Price River Basin. Additional efflorescence occurs in poorly drained areas such as depressions, stagnant water ditches and areas with shallow water tables.

Field data indicate that the salt efflorescence forms over the first 10-15 days after a storm washes off the earlier efflorescence. After this period, the efflorescence forms a salt crust that acts as a physical barrier to further soil-water evaporation.

Observations from aerial photography suggest that the source of saline water for efflorescence in ephemeral streams is the infiltration of water from an earlier storm rather than local subsurface inflow. This was not confirmed by field data.

An expected value of salt efflorescence crust density at the time of a storm, 0.12 g/cm^2 , was computed by fitting an exponential probability distribution for the time interval between consecutive summer storms in the Price River Basin. This density was used with an average number of four storms per year and a proportional fraction of the total basin area underlain by undivided Mancos Shales to extrapolate that salt efflorescence contributes no more than 7.5 percent of the total salt loading in the Price River Basin. Because of assumptions that all the salt efflorescence is washed off during every storm, no salt is leached back into the soil, and all the salts picked up are carried by the storm to the mouth of the Price River, the above percentage may be an overestimate. It does, however, neglect salt efflorescence movement by off season storms and spring snowmelt.

Study of Salt Release from Sediment

Salt release from suspended sediments from the in-channel and channel bank material are believed to be minor salt contributors to the Price River. Most of the salt originally associated with in-channel material seems to be released before it reaches the stream, principally during its transport by overland flow. The channel bank material was shown to have a salt release rate that was rapid in the first few minutes but quickly decreased to almost zero. The soil washed into the channel was found to be the most significant salinity contributing sediment material.

Dilution factor, particle size, mixing velocity, and initial electrical conductivity (i.e., initial salinity) are the most important factors controlling salt release from the suspended sediments. The effects of dilution, particle size, and initial EC were found to be similar in that higher sediment concentrations, smaller particle sizes, and higher initial saline

solutions all work to lower concentration gradient. The system approaches equilibrium more rapidly than it does with lower sediment concentrations, coarser particle size, and lower initial EC. The study further indicated that salt release from suspended sediment is diffusion-controlled.

The accelerated salt release rate in the higher mixing velocities is believed to be due to the reduction caused by turbulent mixing of the thickness of the stagnant boundary layer during the dissolution process. The slow process of Fickian diffusion toward the solid/liquid interface is replaced by more rapid turbulent diffusion away from the suspended particles.

Particle size degradation resulting from mixing at higher velocities could not be measured. New particle size measuring methods are needed to determine the extent of particle size degradation.

The salt-release rate from studied sediment-water systems in solutions containing NaCl and Na_2SO_4 did not change up to an ionic strength of 0.019 M. This indicated an additive effect of these solutions on the salt release up to that ionic strength.

The equations derived by application of the Buckingham Pi Theorem to estimate salt release from sediment as a function of the above factors provided excellent predictive capabilities. They agree reasonably well with the chemical and physical explanations of salt release processes reported in other studies.

Application of the salt-sediment model to the Coal Creek subbasin and extrapolation of the results over the Price River Basin showed that only 0.50 percent of the estimated total salt load at Woodside is contributed by suspended sediments originating from upland areas of the study area. Consequently, one would expect the total salt release from

suspended sediments to be less than 1 percent of the total salt load in the Price River.

Recommendations

Past studies of the salt loading of the Price River and other Colorado tributaries, including this study, have largely focused on salt loading at the land surface, whether from overland flow or within the channels. This study adds to the others in concluding that these surface salt sources produce a relatively small fraction of the total loading. Future salt loading studies need to go underground. They need to quantify and examine the flow lines of water movement from mountain source and valley floor recharge areas to points of emergence as base flow in the larger stream channels. They need to investigate the aquifers and their soluble salt content.

Water use changes that redirect major flow paths through underground formations with high soluble salt contents can at this point be hypothesized as the single human water management practice that increases salt loading most. Consequently, the salinity control measures most likely to be effective are those that reduce flow rates through these formations. The top priority for future studies should be in mapping formations and flowlines and determining how flowlines are inadvertently or purposely altered by water use changes, wells, canal leakage, mining, etc.

A second subject deserving further investigation is salt-sediment transport. Very little is known about transport dynamics as sharp crested cloud-burst hydrographs move down ephemeral streams. Studies should examine salt-sediment transport dynamics hydraulically in terms of amounts and distances of movement during a given storm and chemically as ions interact. On a large scale, we know next to nothing about when salinity control measures in the Price River Basin might have any

effect at Imperial Dam. Better understanding of salt-sediment transport dynamics may well be useful in water management applications moving salt transport away from times with high concentrations.

Specifically to salt efflorescence, future field experiments should be statistically designed to verify the hypotheses made in this study regarding the growth of salt efflorescence and the processes bringing it to a halt. This should be done by direct measurement of salt accumulations rather than through indirect EC measurements. Field research is also needed to determine what happens to salt efflorescence washed from the surface and to estimate the percentage of salt efflorescence that is leached back into the channel bed material during storm events and thus does not contribute to stream salinity.

As to salt-sediment modeling, the lack of basinwide data for model calibration, limitations of the model, and the complexity of the interacting natural processes make it difficult to consider the findings of this study conclusive. More careful modeling of salt-sediment loading in the Price River Basin and fuller model development for applications at other locations where this process may be relatively more important are needed.

The Buckingham Pi Theorem could be applied to quantify the release of individual ions while considering the effects of common ions and indifferant salt. This method could also be applied to the salt-release data from soil material and the salt transport by water movement through the soil profile. The resulting mathematical relationships could be used to develop a submodel to simulate the salt contribution from subsurface flow.

The salt-sediment model could be further expanded by addition of a salt efflorescence component. In this way the direct salt contribution from

channel bank material could be included in the salinity routing. Expansion of the salt-sediment model could also call for a chemical precipitation-dissolution submodel to cover the chemical precipitation and dissolution of lime and gypsum.

Attention needs to be given to bank erosion during storm events and sloughing because of prolonged seepage. The

resulting sediments would be largely coarse materials and add to stream bed load. The salt content of these sediments may be high because the seepage water causing sloughing may well also cause efflorescence. Also bank sloughing is normally concentrated at a few problem locations that may well be much less expensive to correct (should they be creating a salt loading problem) than more diffuse salt sources.

SELECTED BIBIOLGRAPHY

- Ackers, P., and W. R. White. 1973. Sediment transport: New approach and analysis. Proceedings, American Society of Civil Engineers 99 (HY11):2041-2060.
- Adams, F. 1971. Ionic concentrations and activities in soil solutions. Soil Sci. Soc. Amer. Proc. 35:420-426.
- Andersen, J. C., and A. P. Kleinman. 1978. Salinity management options for the Colorado River. UWRL/P-78/03. Utah Water Research Laboratory, Logan, Utah. June.
- Bagnold, R. A. 1966. An approach to the sediment transport problem from general physics. U.S. Geological Survey Professional Paper 422-I, Washington, D. C.
- Bishop, A. A., Simons, D. B., and E. V. Richardson. 1965. Total bed material transport. Proceedings Paper 4266, Journal of Hydraulics Division, American Society of Civil Engineers Vol. 91, No. HY2.
- Blackman, W. C., Jr., J. V. Rouse, G. R. Schillinger, and W. H. Shafer, Jr. 1973. Mineral pollution in the Colorado River Basin. Journal of Water Pollution Control Federation 45(7):1517-1557. July.
- Bowles, D. S., W. J. Grenney, J. J. Jurinak, and J. Paul Riley. 1977. In channel salt-sediment relationships in the Colorado River Basin. A research proposal submitted to the Director, OWRT, Department of the Interior, Washington, D. C.
- Bresler, E. 1973. Simultaneous transport of solute and water under transient unsaturated flow conditions. Water Resour. Res. 9:975-986.
- Bresler, E., and R. J. Hanks. 1969. Numerical method for estimating simultaneous flow of water and salt in unsaturated soils. Soil Sci. Soc. Amer. Proc. 33:827-832.
- Brooks, R. H., and A. T. Corey. 1964. Hydraulic properties of porous media. Hydrology Papers, Colorado State Univ. 3:1027.
- Brown, C. B. 1950. Sediment transportation. In H. Rouse (Ed.). Engineering hydraulics. Wiley, N.Y.
- Brown, C. B. 1967. Sediment transportation, p. 811-814. In H. Rouse (Ed.). Engineering Hydraulics. John Wiley, New York.
- Bruce, G. H., D. W. Peaceman, H. H. Rachford, Jr., and J. D. Rice. 1953. Calculations of unsteady-state gas flow through porous media. Trans. Amer. Inst. of Mining and Met. Engrs. 198:79-92.
- Buckingham, E. 1915. Model experiments and forms of empirical equations. Transactions, American Society of Mechanical Engineers Vol. 37.
- Cameron, D. R., and A. Klute. 1977. Convective-dispersive solute transport with a combined equilibrium and kinetic adsorption model. Water Resources Res. 13:183-188.

- Camp, T. R. 1943. The effects of turbulence on retarding settling. Proceedings of the Second Hydraulics Conference, Bulletin No. 27. University of Iowa, Iowa City, Iowa. pp. 307-317.
- Campbell, G. S. 1974. A simple method for determining unsaturated conductivity from moisture retention data. Soil Sci. 117(6):311-314.
- CH2M Hill. 1982. Quality of water, Colorado River Basin. Progress Report No. 10. CH2M Hill.
- Chadwick, G. 1978. Hydrosalinity modeling in the Price River Basin. M.S. Thesis. College of Engineering, Utah State University, Logan, Utah.
- Childs, S. W., and R. J. Hanks. 1975. Model of soil salinity effects on crop growth. Soil Sci. Soc. Amer. Proc. 39:617-622.
- Clinton, M. J. 1980. Letter response. August 14.
- Colby, B. R., and C. H. Hembree. 1955. Computations of total sediment discharge, Niobara River near Cody, Nebraska. U. S. Geological Survey, Water Supply Paper 1357.
- Cooper, R. H., and Peterson, A. S. 1970. Discussion of "Coordination in mobile-bed hydraulics," by Thomas Blench. Proceedings Paper 7497, American Society of Civil Engineers, Journal of the Hydraulics Division 96(HY9):1880-1888. September.
- Cordova, R. M. 1964. Hydrogeologic reconnaissance of part of the headwaters area of the Price River, Utah. Water Resources Bulletin 14, Utah Geological and Mineralogical Survey.
- Crank, J. 1975. Mathematics of diffusion. Second Edition, Clarendon Press, Oxford.
- Crank, J., and P. Nicolson. 1947. A practical method for numerical evaluation of solutions of partial differential equations of the heat-conduction type. Proc. Cambridge Phil. Soc. 43:50-67.
- Darab, K., J. Csillag, and I. Pinter. 1980. Studies on the ion composition of salt solutions and of saturation extracts of salt affected soils. Geoderma 23:95-111.
- Dixon, L. S. 1978. A mathematical model of salinity uptake in natural channels transversing Mancos shale badlands. Ph.D. dissertation. Utah State University, Logan, Utah.
- Donigian, A.S., Jr., and N. H. Crawford. 1976. Modeling pesticides and nutrients on agricultural lands. EPA 600/2-76-043. U. S. Environmental Protection Agency, Washington, D. C.
- Donigian, A. S., Jr., et al. 1977. Agricultural runoff management (A) model, version II: Refinement and testing. U. S. Environmental Protection Agency, Washington, D.C.
- DuBoys, M. P. 1879. Etudes du regime et l'action exercee par les eaux sur un lit a fond de Gravier indefiniment affouilable. Annales de ponts et chaussées, Ser. 5, Vol. 18, pp. 141-195. (original not seen).
- Dutt, G. R., M. J. Schaffer, and W. J. Moore. 1972. Computer simulation model of dynamic bio-physicochemical processes in soils. Univ. Arizona Agri. Exp. Stn. Tech. Bull. No. 196.
- Einstein, H. A. 1942. Formulas for the transportation of bed load, Transactions of the American Society of Civil Engineers, Vol. 107.

- Einstein, H. A. 1950. The bed-load function for sediment transportation in open channel flows. United States Department of Agriculture, Technical Bulletin 1026. p. 71.
- Einstein, H. A. 1968. Deposition of suspended particles in a gravel bed. Proceedings of the American Society of Civil Engineers 94(HY5): 1197-1205.
- Erh, K. T. 1972. Application of the spline function to soil science. Soil Sci. 114:333-338.
- Feltis, R. D. 1966. Water from bedrock in the Colorado River plateau of Utah. U. S. Geological Survey in cooperation with the Utah Oil and Gas Conservation Commission. Technical Publication 15, Utah State Engineer.
- Foster, J. E., and L. D. Meyer. 1975. Mathematical simulation of upland erosion by fundamental erosion mechanics. U. S. Agricultural Research Service, Department of Agriculture, ARS-S-40.
- Foster, G. R., L. D. Meyer, and C. A. Onstad. 1977. An erosion equation derived from basic erosion principles. Transactions of the American Society of Agricultural Engineers 20(4).
- Frissel, M. J., and P. Poelstra. 1967. Chromatographic transport through soils. I. Theoretical Evaluations. Plant and Soil 26:285-301.
- Gardner, W. R. 1959. Solutions of the flow equation for the drying of soils and other porous media. Soil Sci. Soc. Amer. Proc. 23:183-187.
- Gardner, W. R., and M. Fireman. 1957. Laboratory studies of evaporation from soil columns in the presence of a water table. Soil Sci. 85:244-249.
- Gifford, G. F., R. H. Hawkins, J. J. Jurinak, S. L. Ponce, and J. P. Riley. 1975. Effects of land processes on diffuse sources of salinity in the Upper Colorado River Basin. Report to the Bureau of Land Management and Bureau of Reclamation, U.S. Department of the Interior. Utah Agricultural Experiment Station, Utah State University, Logan, Utah.
- Gilbert, K. G. 1914. The transportation of debris by running water. U. S. Geological Survey, Professional Paper 86.
- Glueckauf, E. 1955. Theory of chromatography Part 9. The "Theoretical Plate" concept in column separations. Trans Faraday Soc. 51:34-44.
- Graf, W. 1971. Hydraulics of sediment transport. McGraw-Hill Book Company, New York.
- Griffin, R. A., and J. J. Jurinak. 1973. Estimation of activity coefficients from the electrical conductivity and sulfate on ionic systems and soil extracts. Soil Science. 116:26-30.
- Haan, C. T. 1977. Statistical methods in hydrology. The Iowa State University Press, Ames, Iowa.
- Hanks, R. J., and S. A. Bowers. 1962. Numerical solution of the moisture flow equation for infiltration into layered soils. Soil Sci. Soc. Amer. Proc. 26:530-534.
- Hornsby, A.G., and J.M. Davidson. 1973. Solution and adsorbed fluometuron concentration distribution in a water-saturated soil: experimental and predicted evaluation. Soil Sci. Soc. Amer. Proc. 37:823-828.
- Hyatt, M. L., J. P. Riley, M. L. McKee, and E. K. Israelsen. 1970. Computer simulation of the hydrologic-

- salinity flow system within the Upper Colorado River Basin. Utah Water Research Laboratory, PRWG54-1, Utah State University, Logan, Utah.
- Iorns, W. V., C. H. Hembree, and G. L. Oakland. 1965. Water resources of the upper Colorado River Basin. Technical Report Professional Paper 441. U. S. Geological Survey.
- Jackson, R. D. 1972. On the calculation of hydraulic conductivity. Soil Sci. Soc. Amer. Proc. 36:380-382.
- Jeppson, R. W., G. L. Ashcroft, A. L. Huber, G. V. Skogerboe, and J. M. Bagley. 1968. Hydrologic Atlas of Utah. Utah Water Research Laboratory, Utah State University, Logan, Utah.
- Jurinak, J. J., J. C. Whitmore, and R. J. Wagenet. 1977. Kinetics of salt release from a saline soil. Soil Science Society of America Journal 41:721-724.
- Jury, W. A., and P. F. Pratt. 1980. Estimation of the salt burden of irrigation drainage water. J. Env. Quality 9:141-146.
- Kalinske, A. A. 1947. Movement of sediment as bed load in rivers. Transactions, American Geophysical Union 28(4).
- Kemper, W. D., and J. C. Van Schaik. 1966. Diffusion of salts in clay-water systems. Soil Sci. Soc. Amer. Proc. 30:534-540.
- Kerssen, P., M. J., Ad Prins, and L. C. van Rijn. 1979. Model for suspended sediment transport. Proceedings, American Society of Civil Engineers, Division of Hydraulics, No. HY5. May.
- Kerssen, P. M. J., L. C. van Rijn, and N. J. van Wijngaarden. 1977. International Association for Hydraulics Research. Paper A15, Seventeenth Congress. pp. 113-120.
- Kirda, C., D. R. Nielsen, and J. W. Biggar. 1973. Simultaneous transport of chloride and water during infiltration. Soil Sci. Soc. Amer. Proc. 37:339-345.
- Klute, A. 1952. Some theoretical aspects of the flow of water in unsaturated soils. Soil Sci. Soc. Amer. Proc. 16:144-148.
- Klute, A., R. D. Whisler, and E. J. Scott. 1965. Numerical solution of the nonlinear diffusion equation for water flow in a horizontal soil column of finite length. Soil Sci. Soc. Amer. Proc. 29:353-358.
- Lapidus, L., and N. R. Amundson. 1952. Mathematics of adsorption in beds. 6: The effect of longitudinal diffusion in ion-exchange and chromatographic columns. J. Phys. Chem. 56:984-988.
- Lai, S. H., and J. J. Jurinak. 1971. Numerical approximation of cation exchange in miscible displacement through soil columns. Soil Sci. Soc. Amer. Proc. 35:894-899.
- Lai, S.H., and J.J. Jurinak. 1972. Cation adsorption in one-dimensional flow through soils: A numerical solution. Water Resour. Res. 8:99-107.
- Lane, E. W., and A. A. Kalinske. 1941. Engineering calculations of suspended sediment. American Geophysical Union, Transactions. pp. 603-607.
- Laronne, J. B., and S. A. Schumm. 1977. Evaluation of the storage of diffuse sources of salinity in the upper Colorado River Basin. Report #27, Environmental Resources Center, Colorado State University, Fort Collins.

- Lelliavsky, S. 1955. An Introduction to Fluvial Hydraulics. Dover Publications, Inc., New York. (original not seen).
- Leytham, K. M., and R. C. Johanson. 1979. Watershed erosion and sediment transport model. Environmental Research Laboratory, Office of Research and Development, U.S. Environmental Protection Agency, Athens, Georgia 30605.
- Malekuti, A. A. 1975. Role of vegetation in the process of diffuse salt movement from rangelands. M.S. Thesis, USU, Logan, Utah.
- Malekuti, A. A., and G. F. Gifford. 1978. Native vegetation as a source of diffuse salt within the Colorado River Basin. Water Resources Bulletin, 14(1):195-205.
- Maletic, J.T. 1972. Colorado River water quality improvement program. Paper presented at Wyoming Interdepartmental Water Conference, Cheyenne. Oct. 17.
- McNeal, B. L., J. D. Oster, and J. T. Hatcher. 1970. Calculation of electrical conductivity from solution composition data as an aid to in-situ estimation of soil salinity. Soil Sci. 110:405-415.
- Melamed, D., R.J. Hanks, L.S. Willardson. 1977. Model of salt flow in soil with a source-sink term. Soil Sci. Soc. Amer. J. 41:29-33.
- Mundorff, J. C. 1972. Reconnaissance of chemical quality of surface water and fluvial sediment in the Price River Basin, Utah. Technical Publication No. 39. State of Utah, Department of Natural Resources.
- Murphy, G. 1950. Similitude in Engineering. Ronald Press, New York.
- Negev, M. A. 1967. A sediment model on a digital computer. Technical Report No. 76. Department of Civil Engineering, Stanford University, Stanford, California. 109 pp.
- Nezafati, H. 1981. Salt release from suspended sediments as a source of Colorado River salinity. PhD Dissertation, Utah State University, Logan, Utah.
- Nielsen, D. R., and J. W. Biggar. 1963. Miscible displacement III. Theoretical considerations. Soil Sci. Soc. Amer. Proc. 26:216-221.
- Nielsen, D. R., J. W. Biggar, and C. S. Simmons. 1980. Mechanisms of solute transport in soils.
- Nordin, C. F. 1970. Suspended load. Presented at the Institute of River Mechanics, Fort Collins, Colorado, June 15-26.
- Olsen, S. R., and W. D. Kemper. 1968. Movement of nutrients to plant roots. Adv. in Agron. 20:91-151.
- Onstad, C. A., and G. R. Foster. 1975. Erosion modeling on a watershed. Trans., ASCE, 18(3).
- Oster, J. D., and J. D. Rhoads. 1975. Calculated drainage water compositions and salt burdens resulting from irrigation with river waters in Western United States. J. Env. Quality 4:73-79.
- Owen, M. W. 1969. Deposition of suspended particles in a gravel bed. (Discussion of paper by H. A. Einstein). Proc. Am. Soc. Civ. Eng. 95(HY3):1085-1087.
- Owens, M. J., and N. V. M. Odd. 1970. A mathematical model of the effect of a tidal barrier on siltation in an estuary. Proceedings of International Conference on Utilization of Tidal Power. Halifax, Nova Scotia, May 25-29.
- Peckins, B. K. 1981. The potential of water and salt yields from overland flow on public lands in the Price

- River Basin. M.S. Thesis. Utah State University, Logan, Utah.
- Peterson, S. R. 1979. Kinetics of salt release from Mancos derived soils. Master's Thesis, Utah State University, Logan.
- Ponce, L. S. 1975. Examination of a non-point source loading function for the Mancos shale wildlands of the Price River Basin, Utah. PhD Dissertation, Utah State Univ., Logan, Utah.
- Porter, L. K., W. D. Kemper, R. J. Jackson, and B. A. Stewart. 1960. Chloride diffusion in soils as influenced by moisture content. *Soil Sci. Soc. Amer. Proc.* 24:460-463.
- Rao, B. K. 1982. A water flow-salt transport model to simulate salt efflorescence in the ephemeral channels of Price River. PhD Dissertation, Utah State University, Logan, Utah.
- Remson, I., R. L. Drake, S. S. McNeary, and E. M. Wallo. 1965. Vertical drainage of an unsaturated soil. *Proc. Amer. Soc. Civil Engineers. J. Hydraul. Div.* 91(HY1):55-74.
- Richards, L. A. 1931. Capillary conduction of liquids in porous medium. *Physics* 1:318-333.
- Richards, L. A. Editor. 1954. Diagnosis and improvement of saline and alkali soils. U.S. Department of Agriculture, *Agricultural Handbook* No. 60.
- Richtmyer, R. D. 1957. Difference methods for initial-value problems. Interscience Publishers, New York.
- Riley, J. P., D. S. Bowles, D. G. Chadwick, and W. J. Grenney. 1979. Preliminary identification of Price River Basin salt pick-up and transport processes. *Water Resources Bulletin* 15(4):984-995.
- Riley, J. P., D. G. Chadwick, L. S. Dixon, W. J. Grenney, and E. K. Israelsen. 1980. A study of salt uptake in natural channels transversing Mancos shale in the Price River basin, Utah. Utah Water Research Laboratory, Logan, Utah.
- Riley, J. P., D. G. Chadwick, Jr., L. S. Dixon, L. D. James, W. J. Grenney, and E. K. Israelsen. 1982a. Salt uptake in natural channels traversing Mancos Shales in the Price River Basin, Utah. UWRL/P-82/02, Utah Water Research Laboratory, Logan, Utah.
- Riley, J. P., E. K. Israelsen, W. N. McNeill, and B. Peckins. 1982b. Potential of water and salt yields from surface runoff on public lands in the Price River Basin. UWRL/P-82/01, Utah Water Research Laboratory, Logan, Utah.
- Robbins, C. W. 1979. A salt transport and storage model for calcareous soils that may contain gypsum. PhD Dissertation, Utah State University, Logan, Utah.
- Robbins, C. W., J. J. Jurinak, and R. J. Wagenet. 1980a. Calculating cation exchange in a salt transport model. *Soil Sci. Soc. Amer. J.* 44:1195-2000.
- Robbins, C. W., R. J. Wagenet, and J. J. Jurinak. 1980b. A combined salt-transport chemical equilibrium model for calcareous and gasiferous soils. *Soil Sci. Soc. Amer. J.* 44:1191-1194.
- Rouse, H. 1937. Modern conceptions of the mechanics of turbulence. *Transactions of the American Society of Civil Engineers* Vol. 102.
- Rubin, J. 1966. Theory of rainfall uptake by soils initially drier than their field capacity and its

- applications. *Water Resources Res.* 2:739-749.
- Rubin, J. 1968. Theoretical analysis of two-dimensional, transient flow of water in unsaturated and partly unsaturated soils. *Soil Sci. Soc. Amer. Proc.* 32:607-615.
- Schoklitsch, A. 1914. *Über Schleppekraft und eschiebebeweyneng.* Engelmann, Leipzig (original not seen).
- Schoklitsch, A. 1930. *Handbuck des wasserbes springer*, Vienna. (2nd Edition), 1950. English translation 1937 by S. Shulits.
- Shields, A. 1936. *An Wendung des Ahnlichkeits Mechanik and Turbulenzforschung auf die Geschiebebewegung.* Mitteil. Prems. Versuchsans Wasser, Ero, Schiffsbau, Berlin. No. 26. (original not seen).
- Shen, H. W. 1970. Total sediment load. Presented at the Institute of River Mechanics, Fort Collins, Colorado, June 15-26.
- Shen, H. W. 1979. Reviews of geophysics and space physics. *American Geophysical Union* 17(6).
- Shirley, F. D., and L. J. Lane. 1978. A sediment yield equation from an erosion simulation model. *Proc. of Arizona Sec. of AWRA and Hydrol. Sec. of Ariz. Academy of Sci., Flagstaff, Arizona.* April.
- Simons, D. B., and R. M. Li. 1976. Procedure for estimating model parameters of a mathematical model. *USDA Forest Service, Rocky Mtn. For. and Range Exp. Sta.* April.
- Simons, D. B., R. M. Li, and M. A. Stevens. 1975. Developments of models for predicting water and sediment routing and yield from storms on small watersheds. *USDA Forest Service, Rocky Mountain Forest and Range Exp. Sta.* August.
- Simons, D. B., R. M. Li, and T. J. Ward. 1977. Estimation of parameters that describe channel geometry for watershed modeling. *USDA Forest Service, Rocky Mountain Forest and Range Exp. Sta.* December.
- Simons, D. B., E. V. Richardson, et al. 1965. Bedload equations for ripples and dunes. *U. S. Geological Survey Professional Paper* 462-H. 9 p.
- Smith, R. E. 1976. Simulation erosion dynamics with a deterministic distributed watershed model. *Proc. 3rd Fed. International Sediment Conf., U. S. Water Resources Council.*
- Snedecor, G. W. 1967. *Statistical methods.* 5th Edition. The Iowa State College Press, Ames, Iowa.
- Straub, L. G. 1936. Transportation of sediment in suspension. *Civil Engineering, American Society of Civil Engineers*, 6(3).
- Stumm, W., and J. J. Morgan. 1970. *Aquatic chemistry.* Wiley Interscience, New York. 583 p.
- Tanji, K. K., L. D. Doneen, G. V. Ferry, and R. S. Ayers. 1972. Computer simulation analysis on reclamation of salt-affected soils in San Joaquin Valley, California. *Soil Sci. Soc. Amer. Proc.* 36:127-133.
- Tillotson, W. R. 1979. Simulation of soil-water and nitrogen fluxes under cropped situations. *M.S. Thesis, Utah State University, Logan, Utah.*
- Tywniuk, N. 1969. Unsteady flow simulation on the south Saskatchewan River. *M.S. Thesis, University of Saskatchewan at Saskatoon, Saskatchewan, Canada.*
- USDA. 1969. Diagnosis and improvement of saline and alkali soils. *Agriculture Handbook* No. 60.

- USDI. 1978. The effects of surface disturbance on the salinity of public lands in the Upper Colorado River Basin. 1977 Status Report, Bureau of Reclamation. p. 83, 86.
- USDI. 1979. Quality of water, Colorado River Basin. Progress Report No. 9. January.
- Utah State University. 1975. Colorado River regional assessment study. Part II. Utah Water Research Laboratory, Utah State University, Logan, Utah.
- Van de Pol, R. M., P. J. Wierenga, and D. R. Nielsen. 1977. Solute movement in a field soil. *Soil Sci. Soc. Amer. J.* 41:10-13.
- Van Der Molen, W. H. 1955. Desalinization of saline soils as a column process. *Soil Sci.* 81:19-27.
- Vanoi, V. A. 1977. Sedimentation engineering. Manual 54. American Society of Civil Engineers.
- VanGenuchten, M. Th., and R. W. Cleary. 1979. Movement of solutes in soil: computer simulated and laboratory results, p. 349-386. In G. H. Bolt (ed.). *Soil chemistry: bio physico-chemical models.* Elsevier Scientific Publ. Co., Amsterdam.
- VanGenuchten, M. Th., J. M. Davidson, and P. J. Wierenga. 1974. An evaluation of kinetic and equilibrium equations for the prediction of pesticide movement through porous media. *Soil Sci. Soc. Amer. Proc.* 38:29-35.
- Wagenet, R. J. 1982. Principles of salt movement in soils. In *Chemical Mobility and Reactivity in Soil Systems.* Special Publication, American Society of Agronomy.
- Wagenet, R. J., and J. J. Jurinak. 1977. Spatial variability of soluble salt content in a Mancos shale watershed. *Soil Science* 126(6):342-349.
- Warrick, A. W., J. W. Biggar, and D. R. Nielsen. 1971. Simultaneous solute and water transfer for an unsaturated soil. *Water Resour. Res.* 7:1216-1225.
- Weast, R. C. 1975. *Handbook of Physics and Chemistry.* CRS Press, Inc. 55th edition.
- White, R. B. 1977. Salt production from micro-channels in the Price River Basin, Utah. M.S. Thesis, Utah State University, Logan, Utah.
- White, W. R. 1972. Sediment transport in channels: a general function. Report INT-104, Hydraulics Research Station, Wallingford, England.
- Whitmore, J. C. 1976. Some aspects of the salinity of Mancos shale and Mancos derived soils. M.S. Thesis, Utah State University, Logan, Utah. 69 p.
- Williams, J. S. 1975. The natural salinity of the Colorado River. Utah Water Research Laboratory, Occasional Paper 7, Utah State University, Logan, Utah.
- Williams, T. R. 1978. A sediment graph. *Water Research Research* 14(4).
- Wischmeier, W. H., and D. D. Smith. 1965. Predicting rainfall-erosion losses from cropland east of the Rocky Mountains. *Agric. Handbook* No. 282. U.S. Department of Agriculture, Washington, D.C.
- Wischmeier, W. H., and D. D. Smith. 1978. Predicting rainfall erosion losses--a guide to conservation planning. *Agriculture Handbook* No. 537, U.S. Department of Agriculture, Wash., D.C. Nov.
- Woolhiser, D. A., and P. H. Blinco. 1975. Watershed sediment yield--a stochastic approach. U.S. Agricultural Research Service, Department of Agriculture, AR5-5-40. June.

Appendix A

Water Content and Chemical Analysis Data

For the 27-Column Experiment

Water Content (cm^3/cm^3)

| Day | Section | Sample #1 | Sample #2 | Sample #3 |
|-----|---------|-----------|-----------|-----------|
| 1 | 0-2 cm | 0.27 | 0.31 | 0.34 |
| 1 | 2-5 | 0.32 | 0.32 | 0.32 |
| 1 | 5-10 | 0.31 | 0.32 | 0.32 |
| 1 | 20-30 | 0.34 | 0.37 | 0.36 |
| 1 | 40-45 | 0.29 | 0.33 | 0.32 |
| 2 | 0-2 cm | 0.35 | 0.33 | 0.23 |
| 2 | 2-5 | 0.35 | 0.31 | 0.31 |
| 2 | 5-10 | 0.30 | 0.33 | 0.33 |
| 2 | 20-30 | 0.35 | 0.32 | 0.31 |
| 2 | 40-45 | 0.33 | 0.35 | 0.31 |
| 3 | 0-2 cm | 0.32 | 0.39 | 0.28 |
| 3 | 2-5 | 0.28 | 0.28 | 0.31 |
| 3 | 5-10 | 0.31 | 0.29 | 0.32 |
| 3 | 20-30 | 0.31 | 0.33 | 0.35 |
| 3 | 40-45 | 0.29 | 0.34 | 0.31 |
| 4 | 0-2 cm | 0.27 | 0.33 | 0.30 |
| 4 | 2-5 | 0.30 | 0.29 | 0.32 |
| 4 | 5-10 | 0.31 | 0.30 | 0.28 |
| 4 | 20-30 | 0.32 | 0.31 | 0.30 |
| 4 | 40-45 | 0.29 | 0.28 | 0.29 |
| 5 | 0-2 cm | 0.28 | 0.29 | 0.26 |
| 5 | 2-5 | 0.30 | 0.31 | 0.29 |
| 5 | 5-10 | 0.30 | 0.32 | 0.31 |
| 5 | 20-30 | 0.31 | 0.34 | 0.35 |
| 5 | 40-45 | 0.33 | 0.32 | 0.33 |
| 7 | 0-2 cm | 0.26 | 0.25 | 0.30 |
| 7 | 2-5 | 0.26 | 0.28 | 0.29 |
| 7 | 5-10 | 0.31 | 0.30 | 0.31 |
| 7 | 20-30 | 0.33 | 0.34 | 0.33 |
| 7 | 40-45 | 0.31 | 0.33 | 0.33 |
| 11 | 0-2 cm | 0.19 | 0.22 | 0.23 |
| 11 | 2-5 | 0.23 | 0.26 | 0.25 |
| 11 | 5-10 | 0.25 | 0.27 | 0.26 |
| 11 | 20-30 | 0.28 | 0.28 | 0.33 |
| 11 | 40-45 | 0.28 | 0.29 | 0.27 |

Calcium, Ca²⁺ (meq/l)

| Day | Section | Sample #1 | Sample #2 | Sample #3 |
|-----|---------|-----------|-----------|-----------|
| 1 | 0-2 cm | 36.96 | 25.71 | 25.02 |
| 1 | 2-5 | 27.33 | 30.84 | 26.85 |
| 1 | 5-10 | 30.60 | 30.80 | 26.04 |
| 1 | 20-30 | 24.22 | 23.22 | 18.71 |
| 1 | 40-45 | 25.89 | 22.75 | 23.47 |
| 2 | 0-2 cm | 33.30 | 24.95 | 48.82 |
| 2 | 2-5 | 27.41 | 25.92 | 27.16 |
| 2 | 5-10 | 27.74 | 25.69 | 25.90 |
| 2 | 20-30 | 20.61 | 25.11 | 25.98 |
| 2 | 40-45 | 26.01 | 21.20 | 28.33 |
| 3 | 0-2 cm | 26.83 | 26.67 | 30.30 |
| 3 | 2-5 | 27.63 | 29.60 | 26.71 |
| 3 | 5-10 | 23.27 | 31.33 | 22.53 |
| 3 | 20-30 | 23.57 | 22.75 | 21.40 |
| 3 | 40-45 | 34.99 | 23.42 | 23.27 |
| 4 | 0-2 cm | 37.29 | 23.27 | 33.47 |
| 4 | 2-5 | 35.93 | 27.13 | 24.59 |
| 4 | 5-10 | 28.99 | 24.49 | 28.34 |
| 4 | 20-30 | 23.25 | 23.40 | 26.07 |
| 4 | 40-45 | 23.40 | 37.25 | 28.70 |
| 5 | 0-2 cm | 23.95 | 38.21 | 49.06 |
| 5 | 2-5 | 29.94 | 25.25 | 25.89 |
| 5 | 5-10 | 28.96 | 26.51 | 24.35 |
| 5 | 20-30 | 23.18 | 23.02 | 25.69 |
| 5 | 40-45 | 22.46 | 24.46 | 24.48 |
| 7 | 0-2 cm | 52.16 | 46.28 | 29.15 |
| 7 | 2-5 | 30.60 | 28.86 | 25.34 |
| 7 | 5-10 | 26.80 | 28.64 | 25.92 |
| 7 | 20-30 | 21.09 | 26.43 | 22.88 |
| 7 | 40-45 | 23.49 | 20.56 | 24.95 |
| 11 | 0-2 cm | 80.27 | 37.09 | 36.70 |
| 11 | 2-5 | 33.92 | 31.14 | 32.25 |
| 11 | 5-10 | 31.90 | 38.18 | 45.46 |
| 11 | 20-30 | 31.90 | 27.66 | 30.36 |
| 11 | 40-45 | 24.40 | 26.38 | 29.53 |

Magnesium, Mg²⁺ (meq/l)

| Day | Section | Sample #1 | Sample #2 | Sample #3 |
|-----|---------|-----------|-----------|-----------|
| 1 | 0-2 cm | 416.26 | 34.15 | 123.76 |
| 1 | 2-5 | 266.38 | 325.95 | 266.54 |
| 1 | 5-10 | 390.62 | 354.87 | 227.36 |
| 1 | 20-30 | 233.94 | 127.35 | 109.00 |
| 1 | 40-45 | 64.59 | 56.76 | 58.54 |
| 2 | 0-2 cm | 172.40 | 196.61 | 453.88 |
| 2 | 2-5 | 164.34 | 235.57 | 228.77 |
| 2 | 5-10 | 190.41 | 230.54 | 176.04 |
| 2 | 20-30 | 93.85 | 190.88 | 241.22 |
| 2 | 40-45 | 133.92 | 93.92 | 94.74 |
| 3 | 0-2 cm | 222.01 | 251.73 | 107.88 |
| 3 | 2-5 | 157.83 | 282.05 | 92.93 |
| 3 | 5-10 | 149.75 | 197.89 | 83.91 |
| 3 | 20-30 | 113.05 | 125.86 | 70.70 |
| 3 | 40-45 | 151.25 | 130.41 | 74.44 |
| 4 | 0-2 cm | 591.63 | 276.01 | 354.15 |
| 4 | 2-5 | 245.80 | 143.99 | 164.73 |
| 4 | 5-10 | 266.54 | 131.76 | 199.46 |
| 4 | 20-30 | 133.88 | 134.09 | 115.83 |
| 4 | 40-45 | 109.84 | 166.35 | 291.07 |
| 5 | 0-2 cm | 227.52 | 547.37 | 634.82 |
| 5 | 2-5 | 257.65 | 216.35 | 210.62 |
| 5 | 5-10 | 292.20 | 254.35 | 182.63 |
| 5 | 20-30 | 194.46 | 190.51 | 182.77 |
| 5 | 40-45 | 120.11 | 161.78 | 161.94 |
| 7 | 0-2 cm | - | 822.11 | 439.78 |
| 7 | 2-5 | 380.82 | 332.82 | 226.88 |
| 7 | 5-10 | 139.42 | 202.70 | 187.40 |
| 7 | 20-30 | 129.83 | 129.01 | 139.87 |
| 7 | 40-45 | 135.87 | 98.12 | 151.37 |
| 11 | 0-2 cm | 367.20 | - | 965.16 |
| 11 | 2-5 | 257.42 | 162.40 | 288.84 |
| 11 | 5-10 | 245.92 | 429.66 | 302.26 |
| 11 | 20-30 | 341.00 | 289.12 | 321.07 |
| 11 | 40-45 | 149.00 | 128.04 | 99.90 |

Sodium, Na⁺ (meq/l)

| Day | Section | Sample #1 | Sample #2 | Sample #3 |
|-----|---------|-----------|-----------|-----------|
| 1 | 0-2 cm | 1802.25 | 1352.07 | 567.13 |
| 1 | 2-5 | 991.34 | 1306.29 | 1187.48 |
| 1 | 5-10 | 1742.15 | 1303.30 | 941.99 |
| 1 | 20-30 | 641.72 | 432.62 | 391.48 |
| 1 | 40-45 | 227.69 | 200.09 | 206.34 |
| 2 | 0-2 cm | 855.66 | 1004.79 | 1838.24 |
| 2 | 2-5 | 661.16 | 935.34 | 815.09 |
| 2 | 5-10 | 764.11 | 978.56 | 561.12 |
| 2 | 20-30 | 344.50 | 583.14 | 816.63 |
| 2 | 40-45 | 421.27 | 281.86 | 300.55 |
| 3 | 0-2 cm | 855.00 | 959.40 | 359.17 |
| 3 | 2-5 | 581.00 | 1093.65 | 281.47 |
| 3 | 5-10 | 560.28 | 547.17 | 240.32 |
| 3 | 20-30 | 416.73 | 434.98 | 198.85 |
| 3 | 40-45 | 474.27 | 322.39 | 245.41 |
| 4 | 0-2 cm | 2375.29 | 847.81 | 1563.01 |
| 4 | 2-5 | 903.01 | 788.36 | 714.45 |
| 4 | 5-10 | 843.85 | 449.47 | 703.11 |
| 4 | 20-30 | 421.38 | 430.63 | 377.99 |
| 4 | 40-45 | 321.58 | 560.81 | 1153.14 |
| 5 | 0-2 cm | 1411.81 | 2246.27 | 3400.84 |
| 5 | 2-5 | 1007.40 | 804.70 | 782.06 |
| 5 | 5-10 | 1113.54 | 961.30 | 652.46 |
| 5 | 20-30 | 547.79 | 662.31 | 556.77 |
| 5 | 40-45 | 287.08 | 421.38 | 421.79 |
| 7 | 0-2 cm | 3538.36 | 2712.16 | 1732.07 |
| 7 | 2-5 | 824.78 | 1252.73 | 790.46 |
| 7 | 5-10 | 602.23 | 793.40 | 703.82 |
| 7 | 20-30 | 457.65 | 440.22 | 453.56 |
| 7 | 40-45 | 413.09 | 278.38 | 421.93 |
| 11 | 0-2 cm | 5002.00 | 3903.20 | 3969.00 |
| 11 | 2-5 | 1087.02 | 691.04 | 1357.20 |
| 11 | 5-10 | 1160.00 | 1675.80 | 1320.90 |
| 11 | 20-30 | 1870.00 | 759.20 | 1037.90 |
| 11 | 40-45 | 522.00 | 413.22 | 318.57 |

Potassium, K⁺ (meq/l)

| Day | Section | Sample #1 | Sample #2 | Sample #3 |
|-----|---------|-----------|-----------|-----------|
| 1 | 0-2 cm | 13.13 | 6.81 | 23.78 |
| 1 | 2-5 | 9.49 | 11.40 | 9.97 |
| 1 | 5-10 | 25.08 | 13.31 | 18.46 |
| 1 | 20-30 | 76.95 | 45.78 | 41.34 |
| 1 | 40-45 | 68.39 | 60.10 | 61.98 |
| 2 | 0-2 cm | 10.85 | 11.00 | 15.51 |
| 2 | 2-5 | 18.05 | 13.61 | 10.99 |
| 2 | 5-10 | 15.33 | 14.38 | 13.04 |
| 2 | 20-30 | 46.30 | 47.21 | 29.20 |
| 2 | 40-45 | 61.92 | 66.29 | 72.07 |
| 3 | 0-2 cm | 11.68 | 13.38 | 86.95 |
| 3 | 2-5 | 20.81 | 14.32 | - |
| 3 | 5-10 | 29.13 | 86.07 | 58.15 |
| 3 | 20-30 | 48.01 | 47.57 | 63.13 |
| 3 | 40-45 | 57.14 | 68.45 | 69.42 |
| 4 | 0-2 cm | 17.28 | 17.86 | 16.71 |
| 4 | 2-5 | 8.59 | 25.40 | 16.69 |
| 4 | 5-10 | 10.23 | 26.16 | 26.05 |
| 4 | 20-30 | 48.31 | 47.57 | 50.36 |
| 4 | 40-45 | 73.37 | 49.29 | 17.22 |
| 5 | 0-2 cm | 12.28 | 39.79 | 25.97 |
| 5 | 2-5 | 14.73 | 21.74 | 13.39 |
| 5 | 5-10 | 15.55 | 21.19 | 19.44 |
| 5 | 20-30 | 55.70 | 40.34 | 41.85 |
| 5 | 40-45 | 69.05 | 78.04 | 78.12 |
| 7 | 0-2 cm | 54.00 | 22.46 | 34.88 |
| 7 | 2-5 | 14.71 | 12.86 | 23.51 |
| 7 | 5-10 | 21.37 | 13.91 | 23.96 |
| 7 | 20-30 | 39.40 | 38.47 | 40.84 |
| 7 | 40-45 | - | 65.72 | 67.77 |
| 11 | 0-2 cm | 31.54 | 89.35 | 32.26 |
| 11 | 2-5 | 25.62 | 20.38 | 17.52 |
| 11 | 5-10 | 18.68 | - | 24.40 |
| 11 | 20-30 | 60.00 | 73.63 | - |
| 11 | 40-45 | 76.70 | 55.10 | 80.03 |

Chloride, Cl⁻ (meq/l)

| Day | Section | Sample #1 | Sample #2 | Sample #3 |
|-----|---------|-----------|-----------|-----------|
| 1 | 0-2 cm | 125.40 | 71.32 | 46.77 |
| 1 | 2-5 | 68.68 | 94.16 | 91.70 |
| 1 | 5-10 | 128.31 | 92.76 | 54.55 |
| 1 | 20-30 | 43.58 | 19.81 | 27.08 |
| 1 | 40-45 | 16.96 | 14.90 | 15.37 |
| 2 | 0-2 cm | 57.34 | 67.00 | 103.50 |
| 2 | 2-5 | 43.10 | 58.44 | 64.81 |
| 2 | 5-10 | 53.84 | 56.82 | 39.90 |
| 2 | 20-30 | 15.84 | 38.57 | 49.74 |
| 2 | 40-45 | 20.50 | 13.68 | 13.14 |
| 3 | 0-2 cm | 57.69 | 54.66 | 23.19 |
| 3 | 2-5 | 33.88 | 84.46 | 17.22 |
| 3 | 5-10 | 34.60 | 25.71 | 13.28 |
| 3 | 20-30 | 26.23 | 27.60 | 12.16 |
| 3 | 40-45 | 31.21 | 16.26 | 16.82 |
| 4 | 0-2 cm | 153.27 | 45.09 | 128.10 |
| 4 | 2-5 | 63.36 | 28.43 | 25.76 |
| 4 | 5-10 | 61.20 | 22.32 | 48.27 |
| 4 | 20-30 | 20.05 | 21.90 | 24.75 |
| 4 | 40-45 | 12.69 | 27.41 | 85.62 |
| 5 | 0-2 cm | 236.57 | 180.52 | 70.74 |
| 5 | 2-5 | 94.44 | 80.40 | 64.41 |
| 5 | 5-10 | 74.45 | 78.63 | 48.50 |
| 5 | 20-30 | 24.77 | 48.32 | 43.89 |
| 5 | 40-45 | 10.60 | 34.68 | 30.06 |
| 7 | 0-2 cm | - | 294.34 | 135.41 |
| 7 | 2-5 | 78.85 | 141.94 | 79.96 |
| 7 | 5-10 | 45.59 | 61.12 | 57.27 |
| 7 | 20-30 | 32.60 | 25.62 | 30.62 |
| 7 | 40-45 | 22.71 | 15.22 | 30.30 |
| 11 | 0-2 cm | 135.86 | 186.32 | 268.38 |
| 11 | 2-5 | 91.01 | 82.77 | 96.86 |
| 11 | 5-10 | 78.18 | 115.16 | 102.94 |
| 11 | 20-30 | 67.20 | 80.29 | 55.10 |
| 11 | 40-45 | 18.90 | 33.17 | 15.43 |

Sulfate, $\text{SO}_4^{=}$ (meq/l)

| Day | Section | Sample #1 | Sample #2 | Sample #3 |
|-----|---------|-----------|-----------|-----------|
| 1 | 0-2 cm | 2143.19 | 1347.42 | 692.92 |
| 1 | 2-5 | 1225.86 | 1580.31 | 1399.14 |
| 1 | 5-10 | 2060.13 | 1609.52 | 1159.30 |
| 1 | 20-30 | 933.25 | 609.18 | 533.45 |
| 1 | 40-45 | 369.61 | 324.80 | 334.95 |
| 2 | 0-2 cm | 1014.87 | 1170.35 | 2252.95 |
| 2 | 2-5 | 827.86 | 1152.00 | 1017.20 |
| 2 | 5-10 | 943.75 | 1192.35 | 736.20 |
| 2 | 20-30 | 489.42 | 807.77 | 1063.29 |
| 2 | 40-45 | 622.61 | 449.59 | 482.55 |
| 3 | 0-2 cm | 1057.83 | 1196.51 | 561.10 |
| 3 | 2-5 | 753.39 | 1335.16 | 439.99 |
| 3 | 5-10 | 727.82 | 836.75 | 391.63 |
| 3 | 20-30 | 575.13 | 603.56 | 341.91 |
| 3 | 40-45 | 686.44 | 528.41 | 395.71 |
| 4 | 0-2 cm | 2868.22 | 1119.85 | 1839.24 |
| 4 | 2-5 | 1129.97 | 956.45 | 894.69 |
| 4 | 5-10 | 1088.41 | 609.57 | 908.69 |
| 4 | 20-30 | 606.78 | 613.79 | 545.50 |
| 4 | 40-45 | 515.50 | 786.27 | 1404.50 |
| 5 | 0-2 cm | 1438.98 | 2691.12 | 4039.96 |
| 5 | 2-5 | 1215.28 | 987.65 | 967.55 |
| 5 | 5-10 | 1375.79 | 1184.72 | 830.38 |
| 5 | 20-30 | 796.36 | 867.87 | 763.19 |
| 5 | 40-45 | 488.09 | 650.98 | 656.27 |
| 7 | 0-2 cm | 5347.37 | 3308.68 | 2100.48 |
| 7 | 2-5 | 1172.06 | 1485.32 | 986.22 |
| 7 | 5-10 | 744.23 | 977.52 | 883.83 |
| 7 | 20-30 | 615.37 | 608.52 | 626.53 |
| 7 | 40-45 | 608.08 | 447.56 | 635.71 |
| 11 | 0-2 cm | 6305.26 | 5713.36 | 4735.08 |
| 11 | 2-5 | 1311.99 | 822.19 | 1599.06 |
| 11 | 5-10 | 1378.78 | 2062.12 | 1590.44 |
| 11 | 20-30 | 2291.80 | 1068.91 | 1468.77 |
| 11 | 40-45 | 783.10 | 589.57 | 512.93 |

Electrical Conductivity, EC (mmhos/cm @ 25°C)*

| Day | Section | Sample #1 | Sample #2 | Sample #3 |
|-----|---------|-----------|-----------|-----------|
| 1 | 0-2 cm | 88.50 | - | 50.60 |
| 1 | 2-5 | 70.00 | 83.80 | 44.60 |
| 1 | 5-10 | 90.80 | 77.10 | 63.00 |
| 1 | 20-30 | 60.60 | 43.00 | 45.00 |
| 1 | 40-45 | - | 25.20 | - |
| 2 | 0-2 cm | 55.00 | 70.00 | 62.10 |
| 2 | 2-5 | 52.00 | 64.30 | 59.90 |
| 2 | 5-10 | 59.60 | - | 48.40 |
| 2 | 20-30 | 35.50 | 49.00 | 67.10 |
| 2 | 40-45 | 41.30 | 30.80 | 26.10 |
| 3 | 0-2 cm | 60.20 | 72.10 | - |
| 3 | 2-5 | 41.90 | - | 30.10 |
| 3 | 5-10 | 44.50 | 44.50 | 28.10 |
| 3 | 20-30 | 39.40 | 41.30 | 29.00 |
| 3 | 40-45 | 42.60 | 32.80 | 28.80 |
| 4 | 0-2 cm | 87.50 | 62.10 | 82.10 |
| 4 | 2-5 | 55.40 | 33.60 | 49.00 |
| 4 | 5-10 | 63.60 | 39.40 | 51.30 |
| 4 | 20-30 | 38.90 | 40.70 | 37.00 |
| 4 | 40-45 | 32.70 | 39.90 | - |
| 5 | 0-2 cm | - | 95.40 | 91.80 |
| 5 | 2-5 | 63.20 | - | 56.00 |
| 5 | 5-10 | 68.00 | 63.50 | 53.50 |
| 5 | 20-30 | 50.30 | 56.90 | 51.90 |
| 5 | 40-45 | 34.00 | 40.60 | - |
| 7 | 0-2 cm | 102.00 | 88.90 | 85.40 |
| 7 | 2-5 | 50.80 | 71.60 | 57.40 |
| 7 | 5-10 | 40.60 | 53.50 | 52.10 |
| 7 | 20-30 | 44.90 | 42.40 | 44.10 |
| 7 | 40-45 | 40.80 | 33.80 | 41.60 |
| 11 | 0-2 cm | 104.00 | 95.00 | 102.00 |
| 11 | 2-5 | 60.50 | 48.40 | 68.10 |
| 11 | 5-10 | 64.70 | 75.40 | 67.40 |
| 11 | 20-30 | 91.80 | 58.70 | 33.00 |
| 11 | 40-45 | 45.40 | 40.90 | 71.10 |

*EC data are measured for the saturation extracts.

Appendix B

Experimental Data

Table B.1. Experimental Set A. EC (in $\mu\text{mho}/\text{cm}$ @ 25°C) of soil/water solutions in different dilutions: $d < 2$ mm, and velocity = 1 fps.

| Time (minutes) | Dilution δ | | | | | | | | |
|------------------|-------------------|-------------|------|-------------|-------------|------|-------------|-------------|------|
| | 1:10 | | | 1:20 | | | 1:40 | | |
| | Replicate 1 | Replicate 2 | Mean | Replicate 1 | Replicate 2 | Mean | Replicate 1 | Replicate 2 | Mean |
| 0 | 304 | 304 | 304 | 328 | 330 | 329 | 285 | 287 | 286 |
| 0.5 | 2859 | 2759 | 2809 | 1500 | 1564 | 1532 | | | |
| 1 | 2985 | 3231 | 3108 | 1652 | 1796 | 1724 | | | |
| 2 | 3118 | 3250 | 3184 | 1805 | 2020 | 1915 | 489 | 511 | 500 |
| 5 | 3689 | 3717 | 3703 | 2125 | 2165 | 2145 | 651 | 713 | 682 |
| 10 | 3880 | 3910 | 3895 | 2289 | 2435 | 2362 | 781 | 923 | 852 |
| 15 | 3921 | 3995 | 3958 | 2389 | 2565 | 2477 | 968 | 1144 | 1056 |
| 30 | 4047 | 4125 | 4086 | 2651 | 2789 | 2720 | 1316 | 1506 | 1411 |
| 60 | 4048 | 4150 | 4099 | 2620 | 3152 | 2886 | 1511 | 1651 | 1581 |
| 75 | - | - | - | 2685 | 3189 | 2937 | 1539 | 1665 | 1602 |
| 90 | - | - | - | 2685 | 3189 | 2937 | 1598 | 1704 | 1651 |
| 120 | 4088 | 4212 | 4150 | 2715 | 3209 | 2962 | 1611 | 1733 | 1672 |
| 180 | 4178 | 4250 | 4214 | - | - | - | | | |
| 240 | 4189 | 4265 | 4227 | - | - | - | | | |
| EC _{eq} | 4190 | 4270 | 4230 | 2714 | 3210 | 2962 | 1678 | 1900 | 1789 |

Table B.2. Experimental Set B. EC ($\mu\text{mho}/\text{cm}$ @ 25°C) of soil/water solutions in different mixing velocities: $\delta = 1:75$, $d < 2$ mm.

| Time (minutes) | Mixing Velocity (fps) | | | | | | | | | | | | | | |
|------------------|-----------------------|-------------|------|-------------|-------------|------|-------------|-------------|------|-------------|-------------|------|-------------|-------------|------|
| | 0.0 | | | 0.3 | | | 0.7 | | | 1 | | | 2 | | |
| | Replicate 1 | Replicate 2 | Mean | Replicate 1 | Replicate 2 | Mean | Replicate 1 | Replicate 2 | Mean | Replicate 1 | Replicate 2 | Mean | Replicate 1 | Replicate 2 | Mean |
| 0 | 323 | 323 | 323 | 364 | 364 | 364 | 345 | 345 | 345 | 335 | 335 | 335 | 342 | 342 | 342 |
| 1 | 328 | 360 | 344 | 651 | 645 | 648 | 626 | 744 | 700 | 706 | 742 | 724 | 721 | 755 | 738 |
| 2 | 330 | 368 | 349 | 681 | 741 | 711 | 725 | 785 | 755 | 798 | 812 | 805 | 776 | 834 | 805 |
| 4 | 326 | 388 | 357 | 712 | 760 | 736 | 800 | 820 | 810 | 900 | 844 | 872 | 802 | 888 | 845 |
| 9 | 330 | 412 | 371 | 718 | 778 | 748 | 840 | 860 | 850 | 1005 | 895 | 950 | 910 | 968 | 939 |
| 16 | 396 | 416 | 406 | 735 | 787 | 761 | 902 | 900 | 901 | 1010 | 1082 | 1046 | 1110 | 1036 | 1073 |
| 25 | 400 | 424 | 412 | 756 | 790 | 773 | 950 | 1050 | 1000 | 1160 | 1226 | 1193 | 1140 | 1115 | 1165 |
| 36 | 412 | 482 | 447 | 781 | 777 | 779 | 1040 | 1080 | 1100 | 1198 | 1270 | 1234 | 1214 | 1198 | 1284 |
| 49 | 431 | 529 | 480 | 781 | 777 | 779 | 1100 | 1200 | 1150 | 1234 | 1313 | 1274 | 1248 | 1300 | 1274 |
| 64 | 482 | 536 | 509 | 780 | 792 | 786 | 1190 | 1210 | 1200 | 1280 | 1388 | 1334 | 1290 | 1378 | 1334 |
| 81 | 512 | 548 | 530 | 780 | 792 | 786 | 1210 | 1290 | 1250 | 1300 | 1396 | 1348 | 1310 | 1378 | 1344 |
| 100 | 548 | 554 | 551 | 780 | 792 | 786 | 1210 | 1290 | 1250 | 1300 | 1396 | 1349 | 1310 | 1378 | 1344 |
| 121 | 552 | 590 | 571 | 780 | 792 | 786 | 1210 | 1290 | 1250 | 1300 | 1396 | 1348 | 1310 | 1378 | 1344 |
| EC _{eq} | 770 | 850 | 810 | 780 | 792 | 786 | 1210 | 1290 | 1250 | 1300 | 1396 | 1348 | 1310 | 1378 | 1344 |

Table B.3. Experimental Set C. EC ($\mu\text{mho}/\text{cm}$ @ 25°C) of channel material/water solutions: velocity = 0.96 fps.

| Time (minutes) | d < 0.074 mm | | | | | | 0.074 < d < 0.125 mm | | | | | | 0.125 < d < 0.5 mm | | | | | |
|-------------------|----------------|----------------|------|----------------|----------------|------|----------------------|----------------|------|----------------|----------------|------|--------------------|----------------|------|----------------|----------------|------|
| | Dilution | | | | | | | | | | | | | | | | | |
| | 1:100 | | | 1:50 | | | 1:5 | | | 1:10 | | | 1:5 | | | 1:10 | | |
| | Replicate 1 | Replicate 2 | Mean | Replicate 1 | Replicate 2 | Mean | Replicate 1 | Replicate 2 | Mean | Replicate 1 | Replicate 2 | Mean | Replicate 1 | Replicate 2 | Mean | Replicate 1 | Replicate 2 | Mean |
| 0 | 0 | 0 | 0 | 0 | 0 | 0 | 0 | 0 | 0 | 0 | 0 | 0 | 0 | 0 | 0 | 0 | 0 | 0 |
| 1 | - | - | - | 1183 | 1219 | 1201 | 1200 | 1032 | 1116 | - | - | - | 1421 | 1253 | 1337 | - | - | - |
| 2 | 696 | 724 | 710 | - | - | - | - | - | - | 700 | 602 | 651 | - | - | - | 685 | 805 | 744 |
| 4 | - | - | - | 1191 | 1239 | 1215 | 1210 | 1070 | 1140 | - | - | - | 1425 | 1275 | 1350 | - | - | - |
| 5 | 696 | 724 | 710 | - | - | - | - | - | - | 705 | 597 | 651 | - | - | - | 700 | 858 | 779 |
| 10 | - | - | - | 1206 | 1260 | 1233 | 1225 | 1077 | 1151 | 710 | 616 | 663 | 1524 | 1430 | 1477 | - | - | - |
| 11 | - | - | - | - | - | - | - | - | - | - | - | - | - | - | - | 798 | 900 | 849 |
| 12 | 703 | 739 | 721 | - | - | - | - | - | - | - | - | - | - | - | - | - | - | - |
| 26 | - | - | - | 1216 | 1272 | 1244 | 1265 | 1107 | 1186 | 711 | 615 | 663 | 1600 | 1494 | 1547 | 830 | 950 | 890 |
| 28 | 715 | 751 | 733 | - | - | - | - | - | - | - | - | - | - | - | - | - | - | - |
| 45 | 723 | 753 | 738 | 1247 | 1289 | 1268 | 1262 | 1110 | 1186 | 725 | 625 | 675 | 1695 | 1539 | 1617 | 874 | 1010 | 942 |
| 60 | 723 | 753 | 738 | 1262 | 1296 | 1279 | 1238 | 1110 | 1174 | 720 | 630 | 675 | 1670 | 1540 | 1605 | 895 | 1035 | 965 |
| 90 | 723 | 753 | 738 | 1262 | 1296 | 1279 | 1245 | 1139 | 1192 | 715 | 635 | 675 | 1665 | 1545 | 1605 | 900 | 1030 | 965 |
| 120 | 723 | 753 | 738 | 1262 | 1296 | 1279 | 1244 | 1140 | 1192 | 715 | 635 | 675 | 1665 | 1545 | 1605 | 900 | 1030 | 965 |
| EC _{eq} | 723 | 753 | 738 | 1262 | 1296 | 1279 | - | - | - | - | - | - | - | - | - | - | - | - |

Table B.4. Experimental Set D. EC ($\mu\text{mho/cm}$ @ 25°C) of soil/water solutions in various dilutions: $0.5 < d < 1.0$ mm, and velocity = 0.96 fps.

| Time (minutes) | Dilution | | | | | | | | | | | | | | | | | |
|-------------------|----------------|----------------|------|----------------|----------------|------|----------------|----------------|------|----------------|----------------|------|----------------|----------------|------|----------------|----------------|------|
| | 1:5 | | | 1:10 | | | 1:20 | | | 1:50 | | | 1:75 | | | 1:100 | | |
| | Replicate 1 | Replicate 2 | Mean |
| 0 | 0 | 0 | 0 | 0 | 0 | 0 | 0 | 0 | 0 | 0 | 0 | 0 | 0 | 0 | 0 | 0 | 0 | 0 |
| 0.5 | | | | | | | | | | | | | | | | 395 | 331 | 363 |
| 1 | 5121 | 5057 | 5089 | - | - | - | - | - | - | 715 | 665 | 690 | 520 | 574 | 547 | - | - | - |
| 2 | - | - | - | 3108 | 3028 | 3068 | 1786 | 1710 | 1748 | - | - | - | 579 | 633 | 606 | - | - | - |
| 2.5 | | | | | | | | | | | | | | | | | | |
| 3 | 5153 | 5083 | 5118 | - | - | - | - | - | - | 1065 | 789 | 927 | - | - | - | - | - | - |
| 3.5 | - | - | - | 3450 | 3398 | 3424 | 2127 | 1985 | 2056 | - | - | - | - | - | - | - | - | - |
| 4 | | | | | | | | | | | | | | | | 589 | 529 | 559 |
| 4.5 | | | | | | | | | | 1108 | 794 | 951 | 665 | 715 | 690 | - | - | - |
| 5 | 5212 | 5250 | 5231 | - | - | - | - | - | - | - | - | - | - | - | - | - | - | - |
| 6 | - | - | - | 3561 | 3549 | 3555 | 2216 | 2136 | 2176 | - | - | - | - | - | - | - | - | - |
| 10 | 5342 | 5312 | 5327 | - | - | - | - | - | - | - | - | - | - | - | - | - | - | - |
| 10.5 | | | | | | | | | | | | | | | | 698 | 614 | 656 |
| 11 | - | - | - | 3716 | 3596 | 3656 | 2359 | 2337 | 2348 | 1286 | 1092 | 1189 | 764 | 876 | 820 | - | - | - |
| 15 | | | | | | | | | | | | | 872 | 912 | 892 | 739 | 687 | 713 |
| 15.5 | 5489 | 5211 | 5350 | - | - | - | - | - | - | 1319 | 1277 | 1248 | - | - | - | - | - | - |
| 16 | - | - | - | 3769 | 3721 | 3745 | 2531 | 2369 | 2450 | - | - | - | - | - | - | - | - | - |
| 20 | 5568 | 5244 | 5406 | - | - | - | - | - | - | 1398 | 1338 | 1368 | 941 | 979 | 960 | 798 | 762 | 780 |
| 21 | - | - | - | 3843 | 3789 | 3816 | 2586 | 2526 | 2556 | - | - | - | - | - | - | - | - | - |
| 25 | | | | | | | | | | 1478 | 1354 | 1416 | 1069 | 983 | 1026 | 868 | 776 | 822 |
| 30 | 5628 | 5244 | 5436 | - | - | - | 2715 | 2613 | 2664 | 1519 | 1457 | 1488 | 1108 | 1004 | 1056 | 916 | 836 | 876 |
| 31 | - | - | - | 3894 | 3786 | 3840 | - | - | - | - | - | - | - | - | - | - | - | - |
| 45 | 5630 | 5314 | 5472 | - | - | - | 2803 | 2789 | 2796 | 1689 | 1611 | 1650 | 1278 | 1134 | 1206 | 1058 | 910 | 984 |
| 46 | - | - | - | 3986 | 3886 | 3936 | - | - | - | - | - | - | - | - | - | - | - | - |
| 60 | - | - | - | - | - | - | 2881 | 2831 | 2856 | 1786 | 1646 | 1716 | 1312 | 1280 | 1296 | 1129 | 983 | 1056 |
| 61 | 5635 | 5325 | 5480 | 4005 | 3947 | 3976 | - | - | - | - | - | - | - | - | - | - | - | - |
| 90 | 5635 | 5325 | 5480 | 4005 | 3955 | 3980 | 2991 | 2913 | 2952 | 2009 | 1783 | 1896 | 1456 | 1376 | 1416 | 1254 | 1086 | 1170 |
| 120 | 5635 | 5325 | 5480 | 4005 | 3959 | 3984 | 3056 | 2972 | 3014 | 2125 | 1967 | 2046 | 1624 | 1446 | 1535 | 1298 | 1114 | 1206 |
| EC _{eq} | 5636 | 5325 | 5481 | 4000 | 3960 | 3980 | 3100 | 2990 | 3045 | 2300 | 2292 | 2296 | 1700 | 1564 | 1632 | 1400 | 1196 | 1285 |

Table B.5. Experimental Set E. EC ($\mu\text{mho/cm @ } 25^{\circ}\text{C}$) as affected by particle size fraction, channel material, dilution 1:30, and $v = 0.96 \text{ fps}$.

| Time (minutes) | Particle Size Fraction (mm) | | | | | | | | | | | | | | | | | |
|-------------------|-----------------------------|----------------|------|----------------|----------------|------|-----------------|----------------|------|------------------|----------------|------|-----------------|----------------|------|----------------|----------------|------|
| | d < 0.074 | | | 0.5 < d < 0.85 | | | 1.0 < d < 1.651 | | | 1.651 < d < 3.92 | | | 3.92 < d < 7.92 | | | d < 7.92 | | |
| | Replicate 1 | Replicate 2 | Mean | Replicate 1 | Replicate 2 | Mean | Replicate 1 | Replicate 2 | Mean | Replicate 1 | Replicate 2 | Mean | Replicate 1 | Replicate 2 | Mean | Replicate 1 | Replicate 2 | Mean |
| 0 | 0 | 0 | 0 | 0 | 0 | 0 | 0 | 0 | 0 | 0 | 0 | 0 | 0 | 0 | 0 | 0 | 0 | 0 |
| 2 | 1385 | 1615 | 1500 | 610 | 530 | 570 | 512 | 428 | 470 | 512 | 358 | 435 | 465 | 353 | 409 | 200 | 204 | 202 |
| 5 | 1485 | 1635 | 1560 | 645 | 595 | 620 | 545 | 455 | 500 | 555 | 475 | 515 | 500 | 460 | 480 | 325 | 375 | 350 |
| 10 | 1555 | 1645 | 1600 | 715 | 685 | 700 | 700 | 660 | 680 | 675 | 525 | 600 | 550 | 480 | 515 | 365 | 395 | 380 |
| 15 | 1555 | 1645 | 1600 | 745 | 675 | 710 | 715 | 695 | 705 | | | | | | | | | |
| 16 | | | | | | | | | | 700 | 528 | 614 | - | - | - | - | - | - |
| 17 | | | | | | | | | | - | - | - | 615 | 585 | 600 | - | - | - |
| 18 | | | | | | | | | | - | - | - | - | - | - | 435 | 395 | 415 |
| 30 | 1555 | 1625 | 1590 | 760 | 680 | 720 | 800 | 760 | 780 | | | | | | | | | |
| 31 | | | | | | | | | | 735 | 625 | 680 | - | - | - | - | - | - |
| 31.5 | | | | | | | | | | - | - | - | 645 | 575 | 610 | - | - | - |
| 32 | | | | | | | | | | - | - | - | - | - | - | 445 | 415 | 430 |
| 45 | 1535 | 1625 | 1580 | 775 | 705 | 740 | 825 | 775 | 800 | | | | | | | | | |
| 46 | | | | | | | | | | 745 | 635 | 690 | 695 | 605 | 650 | 446 | 430 | 438 |
| 60 | 1535 | 1625 | 1580 | 800 | 700 | 750 | 805 | 775 | 790 | 750 | 650 | 700 | - | - | - | - | - | - |
| 62 | | | | | | | | | | - | - | - | 715 | 645 | 680 | 445 | 435 | 440 |
| 105 | 1550 | 1570 | 1560 | 800 | 700 | 750 | 815 | 795 | 805 | 750 | 650 | 700 | 715 | 645 | 680 | 445 | 433 | 439 |
| 120 | 1550 | 1510 | 1530 | 800 | 700 | 750 | 805 | 795 | 800 | 750 | 650 | 700 | 715 | 645 | 680 | 450 | 446 | 448 |
| EC _{eq} | 1650 | 1610 | 1630 | 1000 | 920 | 960 | 940 | 860 | 900 | 780 | 720 | 750 | 745 | 715 | 730 | 530 | 490 | 510 |

Table B.6. Experimental Set F. EC ($\mu\text{mho}/\text{cm}$ @ 25°C) measurements of soil/water solutions of different particle size fractions.

| Time (minutes) | Particle Size Fraction (mm) Mixed in 0.96 fps and Dilution Factor 1:20 | | | | | | Particle Size Fraction (mm) Mixed in 0.43 fps and Dilution Factor 1:20 | | | | | |
|------------------|---|----------------|------|------------------|----------------|------|---|----------------|------|------------------|----------------|------|
| | 0.175 < d < 0.5 | | | 0.85 < d < 1.651 | | | 0.175 < d < 0.5 | | | 0.85 < d < 1.651 | | |
| | Replicate 1 | Replicate 2 | Mean | Replicate 1 | Replicate 2 | Mean | Replicate 1 | Replicate 2 | Mean | Replicate 1 | Replicate 2 | Mean |
| 0 | 0 | 0 | 0 | 0 | 0 | 0 | 0 | 0 | 0 | 0 | 0 | 0 |
| 1 | | | | | | | 513 | 465 | 489 | 569 | 539 | 554 |
| 2 | 693 | 721 | 707 | 951 | 1027 | 989 | | | | | | |
| 5 | 835 | 883 | 859 | 1020 | 1220 | 1120 | 587 | 489 | 538 | 603 | 593 | 598 |
| 10 | 951 | 983 | 967 | 1125 | 1375 | 1250 | 601 | 541 | 571 | 751 | 629 | 690 |
| 15 | 989 | 1075 | 1032 | 1205 | 1425 | 1315 | 609 | 543 | 576 | 762 | 652 | 707 |
| 20 | 997 | 1177 | 1087 | 1289 | 1471 | 1380 | | | | | | |
| 25 | 1009 | 1209 | 1109 | 1315 | 1511 | 1413 | 721 | 659 | 690 | 829 | 779 | 804 |
| 30 | 1056 | 1226 | 1141 | 1389 | 1481 | 1435 | 758 | 676 | 717 | 876 | 842 | 859 |
| 45 | 1105 | 1373 | 1239 | 1425 | 1651 | 1538 | 879 | 719 | 799 | 908 | 896 | 902 |
| 60 | 1205 | 1393 | 1299 | 1552 | 1708 | 1630 | 903 | 869 | 886 | 1043 | 903 | 973 |
| 90 | 1286 | 1388 | 1337 | 1652 | 1838 | 1745 | 1023 | 945 | 984 | 1084 | 1068 | 1076 |
| 120 | | | | | | | 1097 | 1015 | 1065 | 1172 | 1110 | 1141 |
| 125 | 1245 | 1423 | 1359 | 1795 | 1945 | 1870 | | | | | | |
| 150 | | | | | | | 1125 | 1071 | 1098 | 1185 | 1145 | 1163 |
| 155 | 1350 | 1432 | 1391 | 1845 | 2022 | 1935 | | | | | | |
| 180 | | | | | | | 1125 | 1071 | 1098 | 1206 | 1186 | 1196 |
| 210 | | | | | | | 1165 | 1075 | 1120 | 1256 | 1222 | 1239 |
| 240 | 1359 | 1445 | 1402 | 1990 | 2130 | 2060 | 1191 | 1135 | 1163 | 1289 | 1277 | 1283 |
| 280 | 1362 | 1464 | 1413 | 1998 | 2144 | 2071 | | | | | | |
| 300 | 1362 | 1464 | 1413 | 2005 | 2157 | 2081 | | | | | | |
| 332 | | | | | | | 1230 | 1216 | 1223 | 1425 | 1357 | 1391 |
| 360 | | | | | | | 1235 | 1221 | 1228 | 1467 | 1359 | 1413 |
| EC _{eq} | 1375 | 1517 | 1446 | 2156 | 2194 | 2174 | 1450 | 1420 | 1435 | 1700 | 1604 | 1652 |

Table B.6. Continued.

| Time (minutes) | Particle Size Fraction (mm) Mixed in 0.43 fps and Dilution Factor 1:20 | | | | | | Particle Size Fraction (mm) Mixed in 0.96 fps and Dilution Factor 1:20 | | | | | |
|------------------|---|----------------|------|----------------|----------------|------|---|----------------|------|----------------|----------------|------|
| | d < 0.074 | | | d < 1.981 | | | d < 0.074 | | | d < 1.981 | | |
| | Replicate 1 | Replicate 2 | Mean | Replicate 1 | Replicate 2 | Mean | Replicate 1 | Replicate 2 | Mean | Replicate 1 | Replicate 2 | Mean |
| 0 | 0 | 0 | 0 | 0 | 0 | 0 | 0 | 0 | 0 | 0 | 0 | 0 |
| 1 | 810 | 756 | 783 | 541 | 589 | 565 | | | | | | |
| 2 | | | | | | | 1953 | 1853 | 1903 | 1125 | 987 | 1065 |
| 5 | 958 | 788 | 873 | 626 | 678 | 652 | 2308 | 2214 | 2261 | 1312 | 1188 | 1250 |
| 10 | 1456 | 1370 | 1413 | 661 | 709 | 685 | 2416 | 2346 | 2381 | 1416 | 1302 | 1359 |
| 15 | 1562 | 1482 | 1522 | 761 | 869 | 815 | 2415 | 2389 | 2402 | 1498 | 1350 | 1424 |
| 20 | | | | | | | 2468 | 2358 | 2413 | 1519 | 1415 | 1467 |
| 25 | 1806 | 1672 | 1739 | 867 | 915 | 891 | 2480 | 2410 | 2445 | 1589 | 1411 | 1500 |
| 30 | 1819 | 1735 | 1777 | 892 | 1000 | 946 | 2506 | 2450 | 2478 | 1605 | 1461 | 1533 |
| 45 | 1905 | 1857 | 1881 | 1042 | 1100 | 1071 | 2519 | 2481 | 2500 | 1697 | 1521 | 1609 |
| 60 | 1905 | 1857 | 1881 | 1054 | 1206 | 1130 | 2519 | 2481 | 2500 | 1712 | 1548 | 1630 |
| 90 | 2116 | 2058 | 2087 | 1247 | 1319 | 1283 | 2516 | 2464 | 2490 | 1786 | 1584 | 1685 |
| 120 | 2189 | 2137 | 2163 | 1262 | 1456 | 1359 | | | | | | |
| 125 | | | | | | | 2516 | 2464 | 2490 | 1815 | 1641 | 1728 |
| 150 | 2201 | 2191 | 2196 | 1356 | 1506 | 1431 | | | | | | |
| 155 | | | | | | | 2516 | 2464 | 2490 | 1886 | 1636 | 1761 |
| 180 | 2309 | 2229 | 2269 | 1395 | 1561 | 1478 | 2500 | 2394 | 2447 | 1889 | 1643 | 1766 |
| 210 | 2316 | 2250 | 2283 | 1432 | 1612 | 1522 | 2500 | 2460 | 2480 | 1916 | 1748 | 1832 |
| 240 | 2342 | 2268 | 2305 | 1493 | 1659 | 1576 | 2500 | 2460 | 2480 | 1919 | 1755 | 1837 |
| 300 | | | | | | | 2515 | 2467 | 2491 | 1925 | 1759 | 1842 |
| 330 | | | | | | | 2492 | 2468 | 2480 | 1938 | 1746 | 1842 |
| 332 | 2358 | 2316 | 2337 | 1603 | 1701 | 1652 | | | | | | |
| 360 | 2405 | 2335 | 2370 | 1648 | 1786 | 1717 | | | | | | |
| EC _{eq} | 2650 | 2534 | 2592 | 1880 | 1990 | 1935 | 2550 | 2496 | 2523 | 2050 | 1820 | 1935 |

Table B.6. Continued.

| Time (minutes) | Particle Size (mm) Channel Material Dilution 1:5, in the Absence of Mixing | | | | | | | | | Particle Size (mm) Dilution = 1:10 | | | | | | | | |
|-------------------|---|----------------|------|-------------------|----------------|------|-----------------|----------------|------|------------------------------------|----------------|------|-------------------|----------------|------|-----------------|----------------|------|
| | d < 0.074 | | | 0.074 < d < 0.125 | | | 0.125 < d < 0.5 | | | d < 0.074 | | | 0.074 < d < 0.125 | | | 0.125 < d < 0.5 | | |
| | Replicate 1 | Replicate 2 | Mean | Replicate 1 | Replicate 2 | Mean | Replicate 1 | Replicate 2 | Mean | Replicate 1 | Replicate 2 | Mean | Replicate 1 | Replicate 2 | Mean | Replicate 1 | Replicate 2 | Mean |
| 0 | 0 | 0 | 0 | 0 | 0 | 0 | 0 | 0 | 0 | 0 | 0 | 0 | 0 | 0 | 0 | 0 | 0 | 0 |
| 1 | 200 | 150 | 175 | 265 | 211 | 238 | 110 | 70 | 90 | 140 | 106 | 123 | 136 | 104 | 120 | 100 | 86 | 93 |
| 3 | 312 | 224 | 268 | 300 | 236 | 268 | 185 | 105 | 145 | 140 | 116 | 128 | 136 | 120 | 128 | 100 | 88 | 94 |
| 5 | | | | | | | | | | 165 | 149 | 157 | 174 | 164 | 169 | 215 | 169 | 192 |
| 6 | 355 | 245 | 300 | 350 | 278 | 314 | 245 | 181 | 213 | | | | | | | | | |
| 10 | 365 | 297 | 331 | 370 | 280 | 325 | 400 | 332 | 366 | 192 | 158 | 175 | 215 | 203 | 209 | 300 | 188 | 244 |
| 15 | | | | | | | | | | 254 | 170 | 212 | 215 | 193 | 204 | 298 | 190 | 244 |
| 16 | 410 | 298 | 354 | 398 | 346 | 372 | 400 | 250 | 325 | | | | | | | | | |
| 25 | | | | | | | | | | 300 | 212 | 256 | 225 | 217 | 221 | 312 | 222 | 267 |
| 26 | 415 | 283 | 349 | 390 | 354 | 372 | 390 | 210 | 340 | | | | | | | | | |
| 45 | | | | | | | | | | 390 | 280 | 335 | 255 | 233 | 244 | 365 | 227 | 296 |
| 46 | 444 | 312 | 378 | 510 | 466 | 488 | 425 | 413 | 419 | | | | | | | | | |
| 60 | | | | | | | | | | 385 | 285 | 355 | 285 | 249 | 267 | 400 | 298 | 349 |
| 61 | 585 | 381 | 483 | 515 | 473 | 494 | 495 | 435 | 465 | | | | | | | | | |
| Time (hours) | | | | | | | | | | | | | | | | | | |
| 20 | 1100 | 876 | 988 | 915 | 713 | 814 | 1080 | 896 | 988 | 712 | 568 | 640 | 565 | 481 | 523 | 815 | 651 | 733 |
| 65 | 1410 | 1242 | 1326 | 1300 | 1130 | 1215 | 1635 | 1385 | 1512 | 890 | 738 | 814 | 745 | 615 | 680 | 1100 | 946 | 1023 |
| 93 | 1425 | 1301 | 1363 | 1385 | 1341 | 1363 | 1745 | 1571 | 1658 | 950 | 732 | 841 | 785 | 647 | 716 | 1115 | 953 | 1034 |
| 119 | 1490 | 1350 | 1420 | 1350 | 1262 | 1306 | 1915 | 1721 | 1818 | 950 | 754 | 852 | 790 | 642 | 716 | 1135 | 1023 | 1079 |
| 143 | 1600 | 1400 | 1500 | 1465 | 1375 | 1420 | 2100 | 1876 | 1988 | 951 | 753 | 852 | 800 | 676 | 738 | 1207 | 1155 | 1181 |
| 256 | 1800 | 1688 | 1744 | 1700 | 1572 | 1636 | 2350 | 2150 | 2250 | 1100 | 910 | 1005 | 900 | 782 | 841 | 1400 | 1270 | 1335 |
| 280 | 1810 | 1690 | 1750 | 1715 | 1557 | 1636 | 2463 | 2305 | 2385 | 1155 | 947 | 1051 | 910 | 794 | 852 | 1426 | 1300 | 1363 |

Table B.7. Experimental Set E. EC ($\mu\text{mho/cm}$ @ 25°C) of soil/water solutions as affected by particle size and mixing velocity: dilution 1:20.

| Time (minutes) | Particle Size (mm) $v = 0.43$ fps | | | | | | Particle Size (mm) $v = 0.96$ fps | | | | | |
|----------------|-----------------------------------|----------------|------|-------------------|----------------|------|-----------------------------------|----------------|------|-------------------|----------------|------|
| | 0.107 < d < 0.175 | | | 0.175 < d < 0.417 | | | 0.107 < d < 0.175 | | | 0.175 < d < 0.417 | | |
| | Replicate 1 | Replicate 2 | Mean | Replicate 1 | Replicate 2 | Mean | Replicate 1 | Replicate 2 | Mean | Replicate 1 | Replicate 2 | Mean |
| 0 | 0 | 0 | 0 | 0 | 0 | 0 | 0 | 0 | 0 | 0 | 0 | 0 |
| 1 | 685 | 745 | 715 | 450 | 580 | 515 | 1700 | 1500 | 1600 | 815 | 659 | 737 |
| 3 | 764 | 814 | 789 | 485 | 585 | 535 | 1845 | 1725 | 1785 | 990 | 840 | 915 |
| 5 | 825 | 895 | 860 | 541 | 615 | 578 | 2015 | 1857 | 1936 | 1055 | 885 | 970 |
| 10 | 1245 | 1385 | 1315 | 585 | 635 | 610 | 2160 | 2000 | 2080 | 1100 | 990 | 1045 |
| 20 | 1510 | 1710 | 1610 | 640 | 690 | 665 | 2185 | 2035 | 2110 | 1200 | 1072 | 1136 |
| 30 | 1590 | 1780 | 1685 | 710 | 780 | 745 | 2362 | 2110 | 2236 | 1315 | 1175 | 1245 |
| 60 | 1645 | 1809 | 1727 | 810 | 960 | 915 | 2485 | 2289 | 2387 | 1425 | 1343 | 1384 |
| 75 | 1727 | 1845 | 1786 | 920 | 1100 | 1010 | 2510 | 2320 | 2415 | 1465 | 1365 | 1415 |
| 90 | 1845 | 1985 | 1915 | 1000 | 1100 | 1050 | 2540 | 2320 | 2430 | 1500 | 1420 | 1460 |
| 120 | 1892 | 2000 | 1946 | 1050 | 1150 | 1100 | 2540 | 2390 | 2465 | 1545 | 1475 | 1510 |

Table B.8. Experimental Set H. EC ($\mu\text{mho/cm}$ @ 25°C) of soil/water solutions as affected by initial EC (EC_0) and dilution factor: $v = 0.96$ fps and $0.5 < d < 1$ mm.

| $\text{EC}_0 \approx 0$ | | | | | | | | | |
|-------------------------|-------------|-------------|------|-------------|-------------|------|-------------|-------------|------|
| Dilution: | 1:100 | | | 1:75 | | | 1:50 | | |
| Time (minutes) | Replicate 1 | Replicate 2 | Mean | Replicate 1 | Replicate 2 | Mean | Replicate 1 | Replicate 2 | Mean |
| 0 | 20 | 20 | 20 | 0 | 0 | 0 | 0 | 0 | 0 |
| 1 | 398 | 486 | 442 | 684 | 548 | 616 | 1000 | 860 | 930 |
| 3 | 541 | 645 | 593 | 798 | 714 | 756 | 1125 | 1039 | 1082 |
| 5 | 658 | 714 | 686 | 914 | 808 | 861 | 1245 | 1155 | 1200 |
| 11 | 735 | 786 | 762 | 1015 | 845 | 930 | 1385 | 1243 | 1314 |
| 20 | 814 | 1000 | 907 | 1160 | 1004 | 1082 | 1596 | 1428 | 1512 |
| 40 | 1056 | 1200 | 1128 | 1415 | 1259 | 1337 | 1875 | 1683 | 1779 |
| 45 | 1064 | 1216 | 1140 | 1485 | 1283 | 1384 | 1935 | 1739 | 1837 |
| 60 | 1188 | 1300 | 1244 | 1600 | 1400 | 1500 | 2000 | 1930 | 1965 |
| 90 | 1295 | 1415 | 1355 | 1708 | 1548 | 1628 | 2116 | 2070 | 2093 |
| 120 | 1336 | 1500 | 1418 | 1785 | 1657 | 1721 | 2245 | 2151 | 2198 |

| $\text{EC}_0 \approx 1100$ | | | | | | | | | |
|----------------------------|-------------|-------------|------|-------------|-------------|------|-------------|-------------|------|
| Dilution: | 1:100 | | | 1:75 | | | 1:50 | | |
| Time (minutes) | Replicate 1 | Replicate 2 | Mean | Replicate 1 | Replicate 2 | Mean | Replicate 1 | Replicate 2 | Mean |
| 0 | 1125 | 1125 | 1125 | 1113 | 1113 | 1113 | 1113 | 1113 | 1113 |
| 1 | 1417 | 1605 | 1511 | 1445 | 1623 | 1534 | 1900 | 1758 | 1829 |
| 3 | 1500 | 1700 | 1600 | 1515 | 1711 | 1613 | 2100 | 1944 | 2022 |
| 5 | 1523 | 1725 | 1624 | 1639 | 1815 | 1727 | 2145 | 2013 | 2079 |
| 10 | 1623 | 1785 | 1704 | 1690 | 1900 | 1795 | 2200 | 2140 | 2170 |
| 20 | 1746 | 1986 | 1866 | 1877 | 2085 | 1981 | 2450 | 2342 | 2396 |
| 30 | 1840 | 2100 | 1970 | 2042 | 2150 | 2096 | 2600 | 2422 | 2511 |
| 45 | 1946 | 2200 | 2073 | 2100 | 2300 | 2200 | 2700 | 2530 | 2615 |
| 60 | 2063 | 2315 | 2189 | 2158 | 2450 | 2304 | 2815 | 2599 | 2707 |
| 90 | 2170 | 2400 | 2285 | 2316 | 2500 | 2408 | 2912 | 2688 | 2800 |
| 120 | 2195 | 2409 | 2302 | 2424 | 2550 | 2487 | 3000 | 2784 | 2892 |

| $\text{EC}_0 \approx 600$ | | | | | | | | | |
|---------------------------|-------------|-------------|------|-------------|-------------|------|-------------|-------------|------|
| Dilution: | 1:100 | | | 1:75 | | | 1:50 | | |
| Time (minutes) | Replicate 1 | Replicate 2 | Mean | Replicate 1 | Replicate 2 | Mean | Replicate 1 | Replicate 2 | Mean |
| 0 | 602 | 602 | 602 | 602 | 602 | 602 | 602 | 602 | 602 |
| 1 | 1035 | 965 | 1000 | 1150 | 1100 | 1125 | 1515 | 1325 | 1420 |
| 3 | 1125 | 1033 | 1079 | 1235 | 1207 | 1221 | 1612 | 1456 | 1534 |
| 5 | 1195 | 1056 | 1130 | 1287 | 1213 | 1250 | 1665 | 1515 | 1590 |
| 10 | 1234 | 1128 | 1181 | 1512 | 1328 | 1420 | 1798 | 1632 | 1715 |
| 20 | 1412 | 1262 | 1337 | 1650 | 1444 | 1547 | 1945 | 1823 | 1884 |
| 30 | 1512 | 1372 | 1442 | 1745 | 1605 | 1675 | 2045 | 1921 | 1983 |
| 45 | 1614 | 1450 | 1532 | 1945 | 1683 | 1814 | 2206 | 2074 | 2140 |
| 60 | 1725 | 1531 | 1628 | 2015 | 1753 | 1884 | 2300 | 2142 | 2221 |
| 90 | 1800 | 1688 | 1744 | 2185 | 1815 | 2000 | 2450 | 2324 | 2387 |
| 120 | 1900 | 1762 | 1831 | 2208 | 1920 | 2064 | 2600 | 2432 | 2516 |

| $\text{EC}_0 \approx 2100$ | | | | | | | | | |
|----------------------------|-------------|-------------|------|-------------|-------------|------|-------------|-------------|------|
| Dilution: | 1:100 | | | 1:75 | | | 1:50 | | |
| Time (minutes) | Replicate 1 | Replicate 2 | Mean | Replicate 1 | Replicate 2 | Mean | Replicate 1 | Replicate 2 | Mean |
| 0 | 2100 | 2148 | 2124 | 2200 | 2094 | 2147 | 2100 | 2104 | 2102 |
| 1.5 | - | - | - | - | - | - | 2715 | 2851 | 2783 |
| 2 | - | - | - | 2585 | 2685 | 2635 | - | - | - |
| 2.5 | 2402 | 2550 | 2476 | - | - | - | - | - | - |
| 3 | 2498 | 2500 | 2499 | 2652 | 2800 | 2726 | 2811 | 2915 | 2863 |
| 5 | - | - | - | 2683 | 2815 | 2749 | 2835 | 2935 | 2885 |
| 6 | 2425 | 2595 | 2510 | - | - | - | - | - | - |
| 10 | 2541 | 2615 | 2578 | 2685 | 2835 | 2760 | 2973 | 3025 | 2999 |
| 20 | 2616 | 2700 | 2658 | 2826 | 2900 | 2863 | 3063 | 3185 | 3124 |
| 30 | 2646 | 2750 | 2698 | 2875 | 2965 | 2920 | 3184 | 3200 | 3192 |
| 45 | 2652 | 2800 | 2726 | 2944 | 3100 | 3022 | 3238 | 3350 | 3294 |
| 60 | 2780 | 2900 | 2840 | 2978 | 3200 | 3089 | 3338 | 3410 | 3374 |
| 90 | 2811 | 2915 | 2863 | 3110 | 3250 | 3180 | 3371 | 3445 | 3408 |
| 120 | 2893 | 3015 | 2954 | 3244 | 3300 | 3272 | 3444 | 3600 | 3522 |

Table B.8. Continued.

| EC ₀ ≈ 2600 | | | | | | | | | |
|------------------------|-------------|-------------|------|-------------|-------------|------|-------------|-------------|------|
| Dilution: | 1:100 | | | 1:75 | | | 1:50 | | |
| Time (minutes) | Replicate 1 | Replicate 2 | Mean | Replicate 1 | Replicate 2 | Mean | Replicate 1 | Replicate 2 | |
| 0 | 2600 | 2740 | 2670 | 2600 | 2648 | 2624 | 2600 | 2716 | 2658 |
| 1 | - | - | - | - | - | - | 2951 | 3115 | 3033 |
| 1.5 | - | - | - | 2890 | 2950 | 2920 | - | - | - |
| 2 | 2734 | 2900 | 2817 | - | - | - | - | - | - |
| 3 | 2777 | 2925 | 2851 | 2897 | 2965 | 2931 | 2999 | 3135 | 3067 |
| 5 | 2801 | 2935 | 2868 | 2933 | 2975 | 2954 | 3110 | 3250 | 3180 |
| 10 | - | - | - | 2974 | 3000 | 2987 | 3116 | 3268 | 3192 |
| 11 | 2885 | 2965 | 2925 | - | - | - | - | - | - |
| 20 | - | - | - | 3021 | 3045 | 3033 | 3128 | 3278 | 3203 |
| 21 | 2900 | 2984 | 2942 | - | - | - | - | - | - |
| 30 | 2908 | 3000 | 2954 | 3033 | 3055 | 3044 | 3166 | 3310 | 3238 |
| 45 | 2952 | 3000 | 2976 | 3059 | 3075 | 3067 | 3193 | 3395 | 3294 |
| 60 | 2983 | 3015 | 2999 | 3059 | 3075 | 3067 | 3200 | 3388 | 3294 |
| 90 | 3021 | 3045 | 3033 | 3080 | 3100 | 3090 | 3200 | 3388 | 3294 |
| 120 | 3020 | 3058 | 3039 | 3080 | 3100 | 3090 | 3200 | 3388 | 3294 |

| EC ₀ ≈ 5800 | | | | | | | | | |
|------------------------|-------------|-------------|------|-------------|-------------|------|-------------|-------------|------|
| Dilution: | 1:100 | | | 1:75 | | | 1:50 | | |
| Time (minutes) | Replicate 1 | Replicate 2 | Mean | Replicate 1 | Replicate 2 | Mean | Replicate 1 | Replicate 2 | |
| 0 | 5800 | 5830 | 5815 | 5800 | 5830 | 5815 | 5800 | 5830 | 5815 |
| 1 | 6000 | 6094 | 6047 | 6260 | 6300 | 6280 | 6450 | 6342 | 6396 |
| 3 | 5994 | 6100 | 6047 | 6250 | 6310 | 6280 | 6750 | 6508 | 6629 |
| 5 | 6054 | 6158 | 6106 | 6342 | 6450 | 6396 | 6790 | 6584 | 6687 |
| 11 | 6261 | 6415 | 6338 | 6426 | 6600 | 6513 | 6900 | 6672 | 6786 |
| 20 | 6307 | 6485 | 6396 | 6420 | 6606 | 6513 | 6995 | 6693 | 6844 |
| 30 | 6300 | 6492 | 6396 | 6462 | 6680 | 6571 | 7100 | 6706 | 6903 |
| 45 | 6300 | 6492 | 6396 | 6500 | 6642 | 6571 | 7100 | 6706 | 6903 |
| 60 | 6300 | 6492 | 6396 | 6578 | 6680 | 6629 | 7100 | 6706 | 6903 |
| 90 | 6492 | 6650 | 6571 | 6690 | 6800 | 6745 | 7155 | 6885 | 7020 |
| 120 | 6558 | 6700 | 6629 | 6751 | 6855 | 6803 | 7155 | 6885 | 7020 |

| EC ₀ ≈ 3500 | | | | | | | | | |
|------------------------|-------------|-------------|------|-------------|-------------|------|-------------|-------------|------|
| Dilution: | 1:100 | | | 1:75 | | | 1:50 | | |
| Time (minutes) | Replicate 1 | Replicate 2 | Mean | Replicate 1 | Replicate 2 | Mean | Replicate 1 | Replicate 2 | |
| 0 | 3500 | 3440 | 3470 | 3500 | 3460 | 3480 | 3500 | 3468 | 3484 |
| 1 | 3700 | 3684 | 3692 | 3715 | 3669 | 3692 | 4085 | 3831 | 3958 |
| 3 | 3710 | 3674 | 3692 | 3885 | 3787 | 3836 | 4150 | 3880 | 4015 |
| 5 | 2765 | 2707 | 2736 | 3900 | 3794 | 3847 | 4235 | 3953 | 4094 |
| 10 | 3815 | 3747 | 3781 | 3950 | 3822 | 3886 | 4285 | 3995 | 4140 |
| 20 | 3850 | 3778 | 3814 | 4000 | 3850 | 3925 | 4315 | 4055 | 4185 |
| 30 | 3850 | 3756 | 3803 | 3978 | 3850 | 3914 | 4315 | 4077 | 4196 |
| 45 | 3850 | 3800 | 3825 | 4050 | 3900 | 3975 | 4365 | 4095 | 4230 |
| 60 | 3885 | 3809 | 3847 | 4050 | 3900 | 3975 | 4385 | 4155 | 4270 |
| 90 | 3915 | 3869 | 3892 | 4085 | 3921 | 4003 | 4390 | 4160 | 4275 |
| 120 | 3986 | 3886 | 3936 | 4100 | 4018 | 4059 | 4400 | 4172 | 4286 |

| EC ₀ ≈ 7700 | | | | | | | | | |
|------------------------|-------------|-------------|------|-------------|-------------|------|-------------|-------------|------|
| Dilution: | 1:100 | | | 1:75 | | | 1:50 | | |
| Time (minutes) | Replicate 1 | Replicate 2 | Mean | Replicate 1 | Replicate 2 | Mean | Replicate 1 | Replicate 2 | |
| 0 | 7700 | 7646 | 7673 | 7700 | 7646 | 7773 | 7700 | 7646 | 7773 |
| 1 | 7895 | 7785 | 7840 | 7915 | 7875 | 7895 | 8150 | 7974 | 8062 |
| 3 | 7900 | 7802 | 7851 | 8100 | 7912 | 8006 | 8215 | 8019 | 8117 |
| 5 | 7985 | 7805 | 7895 | 8155 | 7969 | 8062 | 8286 | 8060 | 8173 |
| 10 | 7965 | 7825 | 7895 | 8200 | 8034 | 8117 | 8450 | 8230 | 8340 |
| 20 | 7960 | 7830 | 7895 | 8200 | 8034 | 8117 | 8400 | 8280 | 8340 |
| 30 | 8000 | 7902 | 7951 | 8250 | 8096 | 8173 | 8400 | 8280 | 8340 |
| 46 | 8055 | 7957 | 8006 | 8350 | 8218 | 8284 | 8565 | 8337 | 8451 |
| 60 | 8100 | 8024 | 8062 | 8350 | 8218 | 8284 | 8560 | 8342 | 8451 |
| 90 | 8155 | 8081 | 8118 | 8550 | 8352 | 8451 | 8600 | 8414 | 8507 |
| 120 | 8155 | 8081 | 8118 | 8600 | 8414 | 8507 | 8635 | 8489 | 8562 |

Table B.9. Experimental Set I. EC ($\mu\text{mho/cm}$ @ 25°C) of soil/water solutions: particle size fraction $0.125 < d < 0.5$ mm.

| Dilution, $v = 0.96$ fps | | | | | | | | | | | | | | | | | | |
|--------------------------|-------------|-------------|-------|-------------|-------------|-------|-------------|-------------|-------|-------------|-------------|------|-------------|-------------|------|-------------|-------------|------|
| 1:1000 | | | 1:500 | | | 1:250 | | | 1:100 | | | 1:75 | | | 1:50 | | | |
| Time (minutes) | Replicate 1 | Replicate 2 | Mean | Replicate 1 | Replicate 2 | Mean | Replicate 1 | Replicate 2 | Mean | Replicate 1 | Replicate 2 | Mean | Replicate 1 | Replicate 2 | Mean | Replicate 1 | Replicate 2 | Mean |
| 0 | 0 | 0 | 0 | 0 | 0 | 0 | 0 | 0 | 0 | 0 | 0 | 0 | 0 | 0 | 0 | 0 | 0 | 0 |
| 1 | 68 | 76 | 72 | 118 | 86 | 102 | 116 | 144 | 130 | 515 | 335 | 425 | 612 | 518 | 565 | 715 | 685 | 700 |
| 3 | 78 | 102 | 90 | 128 | 112 | 120 | 155 | 179 | 167 | 534 | 416 | 475 | 646 | 564 | 605 | 950 | 810 | 880 |
| 5 | 84 | 112 | 98 | 142 | 122 | 132 | 186 | 274 | 230 | 625 | 515 | 570 | 715 | 585 | 650 | 985 | 875 | 930 |
| 10 | 105 | 125 | 115 | 161 | 125 | 143 | 200 | 300 | 250 | 660 | 550 | 605 | 735 | 615 | 675 | 1100 | 880 | 990 |
| 15 | 116 | 134 | 125 | 170 | 130 | 150 | 226 | 310 | 268 | 695 | 625 | 660 | 745 | 695 | 720 | 1215 | 935 | 1075 |
| 20 | 126 | 138 | 132 | 175 | 145 | 160 | 244 | 312 | 278 | 725 | 675 | 700 | 800 | 750 | 775 | 1235 | 975 | 1105 |
| 30 | 148 | 156 | 152 | 181 | 153 | 167 | 250 | 346 | 298 | 765 | 695 | 730 | 835 | 765 | 800 | 1256 | 1104 | 1180 |
| 45 | 151 | 189 | 170 | 195 | 165 | 180 | 295 | 375 | 335 | 850 | 750 | 800 | 925 | 885 | 905 | 1315 | 1205 | 1260 |
| 60 | 169 | 201 | 185 | 206 | 174 | 190 | 304 | 382 | 343 | 875 | 775 | 825 | 1015 | 935 | 975 | 1380 | 1230 | 1305 |
| 75 | 179 | 215 | 197 | 215 | 185 | 200 | 321 | 385 | 353 | 915 | 845 | 880 | 1075 | 945 | 1010 | 1500 | 1300 | 1400 |
| 90 | 184 | 236 | 210 | 216 | 204 | 210 | 325 | 395 | 360 | 955 | 845 | 900 | 1110 | 1030 | 1070 | 1500 | 1300 | 1400 |
| 120 | 195 | 245 | 220 | 216 | 224 | 220 | 340 | 400 | 370 | 955 | 845 | 900 | 1120 | 1080 | 1100 | 1500 | 1300 | 1400 |

137

Table B.9. Continued.

| Dilution, $v = 0.655$ fps | | | | | | | | | | | | | | | | | | |
|---------------------------|-------------|-------------|-------|-------------|-------------|-------|-------------|-------------|-------|-------------|-------------|------|-------------|-------------|------|-------------|-------------|------|
| 1:1000 | | | 1:500 | | | 1:250 | | | 1:100 | | | 1:75 | | | 1:50 | | | |
| Time (minutes) | Replicate 1 | Replicate 2 | Mean | Replicate 1 | Replicate 2 | Mean | Replicate 1 | Replicate 2 | Mean | Replicate 1 | Replicate 2 | Mean | Replicate 1 | Replicate 2 | Mean | Replicate 1 | Replicate 2 | Mean |
| 0 | 0 | 0 | 0 | 0 | 0 | 0 | 0 | 0 | 0 | 0 | 0 | 0 | 0 | 0 | 0 | 0 | 0 | 0 |
| 1 | 76 | 44 | 60 | 117 | 73 | 95 | 205 | 123 | 164 | 412 | 298 | 355 | 384 | 492 | 438 | 789 | 693 | 741 |
| 3 | 94 | 56 | 75 | 129 | 93 | 111 | 258 | 156 | 207 | 481 | 355 | 408 | 450 | 562 | 506 | 894 | 816 | 855 |
| 5 | 98 | 62 | 80 | 130 | 104 | 117 | 261 | 175 | 218 | 496 | 380 | 438 | 575 | 625 | 600 | 983 | 843 | 913 |
| 10 | 101 | 73 | 87 | 126 | 122 | 124 | 280 | 204 | 242 | 512 | 406 | 459 | 596 | 698 | 647 | 1002 | 876 | 939 |
| 20 | 107 | 85 | 96 | 134 | 142 | 138 | 298 | 238 | 268 | 536 | 466 | 501 | 678 | 782 | 730 | 1100 | 986 | 1043 |
| 30 | 113 | 93 | 103 | 136 | 156 | 146 | 313 | 261 | 287 | | | | | | | | | |
| 45 | 126 | 102 | 114 | 148 | 170 | 159 | 345 | 285 | 315 | 685 | 567 | 626 | 761 | 845 | 803 | 1195 | 1099 | 1147 |
| 60 | 132 | 108 | 120 | 148 | 172 | 160 | 358 | 304 | 331 | 698 | 596 | 647 | 772 | 896 | 834 | 1216 | 1182 | 1199 |
| 75 | 138 | 114 | 126 | 165 | 191 | 178 | 364 | 320 | 342 | 715 | 641 | 678 | 794 | 916 | 855 | 1285 | 1167 | 1226 |
| 90 | 138 | 118 | 128 | 165 | 197 | 181 | 381 | 333 | 357 | 715 | 641 | 678 | 825 | 917 | 871 | 1286 | 1176 | 1231 |
| 120 | 138 | 126 | 132 | 168 | 212 | 190 | 385 | 345 | 365 | 715 | 689 | 702 | 835 | 917 | 876 | 1289 | 1235 | 1262 |

Table B.9. Continued.

| Time (minutes) | Dilution, $v = 0.43$ fps | | | | | | | | | | | | | | | | | |
|-------------------|--------------------------|----------------|------|----------------|----------------|------|----------------|----------------|------|----------------|----------------|------|----------------|----------------|------|----------------|----------------|------|
| | 1:1000 | | | 1:500 | | | 1:250 | | | 1:100 | | | 1:75 | | | 1:50 | | |
| | Replicate 1 | Replicate 2 | Mean | Replicate 1 | Replicate 2 | Mean | Replicate 1 | Replicate 2 | Mean | Replicate 1 | Replicate 2 | Mean | Replicate 1 | Replicate 2 | Mean | Replicate 1 | Replicate 2 | Mean |
| 0 | 0 | 0 | 0 | 0 | 0 | 0 | 0 | 0 | 0 | 0 | 0 | 0 | 0 | 0 | 0 | 0 | 0 | 0 |
| 1 | 72 | 48 | 60 | 112 | 68 | 90 | 135 | 159 | 147 | 253 | 371 | 312 | 365 | 505 | 435 | 646 | 714 | 680 |
| 3 | 81 | 63 | 72 | 115 | 97 | 106 | 164 | 176 | 170 | 301 | 395 | 348 | 405 | 515 | 460 | 662 | 738 | 700 |
| 5 | 96 | 64 | 80 | 126 | 107 | 116 | 175 | 189 | 182 | 315 | 405 | 360 | 422 | 518 | 470 | 699 | 751 | 725 |
| 10 | 98 | 76 | 87 | 136 | 124 | 130 | 198 | 218 | 208 | 340 | 428 | 384 | 426 | 560 | 493 | 752 | 798 | 775 |
| 15 | 102 | 84 | 93 | 149 | 133 | 141 | 215 | 235 | 225 | 381 | 437 | 409 | 575 | 625 | 600 | 780 | 820 | 800 |
| 20 | 106 | 84 | 95 | 168 | 134 | 151 | 221 | 251 | 236 | 393 | 451 | 422 | 575 | 625 | 600 | 848 | 912 | 880 |
| 30 | 109 | 85 | 97 | 176 | 140 | 158 | 237 | 269 | 253 | 392 | 482 | 437 | 605 | 655 | 630 | 875 | 925 | 900 |
| 45 | 112 | 86 | 99 | 186 | 164 | 175 | 251 | 289 | 270 | 425 | 495 | 460 | 645 | 715 | 680 | 915 | 965 | 940 |
| 60 | 113 | 87 | 100 | 195 | 169 | 182 | 281 | 295 | 288 | 500 | 580 | 540 | 655 | 745 | 700 | 960 | 980 | 970 |
| 75 | 113 | 91 | 102 | 201 | 183 | 192 | 284 | 312 | 298 | 551 | 589 | 570 | 655 | 745 | 700 | 985 | 995 | 990 |
| 90 | 116 | 94 | 105 | 205 | 195 | 200 | 292 | 316 | 304 | 540 | 600 | 590 | 665 | 755 | 710 | 1005 | 1015 | 1010 |
| 120 | 116 | 104 | 110 | 216 | 204 | 210 | 312 | 298 | 315 | 600 | 640 | 620 | 700 | 800 | 750 | 1020 | 1040 | 1030 |

138

Table B.9. Continued.

| Time (minutes) | Dilution, $v = 0.96$ fps and $0.5 < d < 1$ mm | | | | | | | | | | | | | | | | | |
|-------------------|---|----------------|------|----------------|----------------|------|----------------|----------------|------|----------------|----------------|------|----------------|----------------|------|----------------|----------------|------|
| | 1:5 | | | 1:10 | | | 1:20 | | | 1:50 | | | 1:75 | | | 1:100 | | |
| | Replicate 1 | Replicate 2 | Mean | Replicate 1 | Replicate 2 | Mean | Replicate 1 | Replicate 2 | Mean | Replicate 1 | Replicate 2 | Mean | Replicate 1 | Replicate 2 | Mean | Replicate 1 | Replicate 2 | Mean |
| 0 | 0 | 0 | 0 | 0 | 0 | 0 | 0 | 0 | 0 | 0 | 0 | 0 | 0 | 0 | 0 | 0 | 0 | 0 |
| 1 | 5000 | 5200 | 5100 | 3100 | 3020 | 3060 | 1850 | 1650 | 1750 | 685 | 715 | 700 | 610 | 490 | 550 | 384 | 332 | 358 |
| 3 | 5030 | 5210 | 5120 | 3500 | 3320 | 3410 | 2150 | 1950 | 2050 | 1015 | 845 | 930 | 745 | 605 | 675 | - | - | - |
| 5 | 5160 | 5300 | 5230 | 3650 | 3450 | 3550 | 2310 | 2050 | 2180 | 1024 | 876 | 950 | 764 | 616 | 690 | 684 | 516 | 600 |
| 10 | 5165 | 5485 | 5325 | 3700 | 3620 | 3660 | 2450 | 2250 | 2350 | 1295 | 1105 | 1200 | 900 | 750 | 825 | 745 | 575 | 660 |
| 20 | 5305 | 5495 | 5400 | 3845 | 3735 | 3790 | 2685 | 2415 | 2550 | 1425 | 1325 | 1375 | 1052 | 878 | 965 | 845 | 705 | 775 |
| 30 | 5380 | 5500 | 5440 | 3915 | 3755 | 3835 | 2700 | 2620 | 2660 | 1515 | 1441 | 1478 | 1150 | 990 | 1070 | 945 | 815 | 880 |
| 45 | 5425 | 5515 | 5470 | 4000 | 3860 | 3930 | 2815 | 2775 | 2795 | 1724 | 1566 | 1645 | 1285 | 1115 | 1200 | 1015 | 965 | 990 |
| 60 | 5445 | 5535 | 5490 | 4035 | 3895 | 3965 | 2915 | 2805 | 2860 | 1812 | 1638 | 1725 | 1350 | 1250 | 1300 | 1100 | 1030 | 1065 |
| 90 | 5445 | 5535 | 5490 | 4045 | 3915 | 3980 | 2985 | 2915 | 2950 | 2000 | 1800 | 1900 | 1450 | 1362 | 1406 | 1215 | 1145 | 1180 |
| 120 | 5445 | 5535 | 5490 | 4050 | 3910 | 3980 | 3050 | 2990 | 3020 | 2115 | 1985 | 2050 | 1600 | 1430 | 1515 | 1247 | 1185 | 1216 |

Table B.9. Continued.

| Dilution, $v = 0.96$ fps, and EC Saturation Extract, $4500 \mu\text{mho/cm}$ @ 25°C | | | | | | | | | | | | | | | | | | |
|---|----------------|----------------|------|----------------|----------------|------|----------------|----------------|------|----------------|----------------|------|----------------|----------------|------|----------------|----------------|------|
| Time (minutes) | 1:1000 | | | 1:500 | | | 1:250 | | | 1:100 | | | 1:75 | | | 1:50 | | |
| | Replicate 1 | Replicate 2 | Mean |
| 0 | 0 | 0 | 0 | 0 | 0 | 0 | 0 | 0 | 0 | 0 | 0 | 0 | 0 | 0 | 0 | 0 | 0 | 0 |
| 1 | 5 | 15 | 10 | 26 | 12 | 18 | 20 | 40 | 30 | 56 | 86 | 71 | 100 | 82 | 91 | 136 | 120 | 128 |
| 3 | 6 | 16 | 12 | 30 | 14 | 22 | 29 | 45 | 37 | 60 | 98 | 79 | 110 | 84 | 97 | 146 | 128 | 137 |
| 5 | 10 | 18 | 14 | 30 | 18 | 24 | 30 | 50 | 40 | 64 | 100 | 82 | 112 | 90 | 101 | 152 | 130 | 141 |
| 10 | 12 | 22 | 17 | 35 | 25 | 30 | 39 | 55 | 47 | 69 | 105 | 87 | 120 | 88 | 104 | 155 | 135 | 145 |
| 20 | 15 | 25 | 20 | 38 | 28 | 33 | 40 | 58 | 49 | 70 | 110 | 90 | 120 | 96 | 108 | 160 | 138 | 149 |
| 30 | 16 | 28 | 22 | 40 | 28 | 34 | 45 | 55 | 50 | 71 | 110 | 91 | 120 | 98 | 109 | 160 | 140 | 150 |
| 60 | 19 | 31 | 25 | 42 | 32 | 37 | 45 | 61 | 53 | 76 | 110 | 93 | 122 | 100 | 111 | 160 | 146 | 153 |

Appendix C

Data For Analysis of Summer Storms in
the Price River Basin

Thirty-seven years of data for summer storms in the Price River Basin available from U.S. Weather Bureau Climatological reports were used. Days on which precipitation equals or exceeds 0.25 inches is considered as a storm that produces runoff based on the study by Peckins (1981). The data were measured at Price (Latitude 39 36' N., Longitude 110 38'W., Elevation 5,560') from 1941 to June 1957, at Price Game Farm (Latitude 30 37'N., Longitude 110 50'W., Elevation 5,580') from July 1957 to May 1969 and at Price Warehouses (Latitude 39 37' N., Longitude 110 50'W., Elevation 5,560') from June 1969 onward.

| <u>Year</u> | <u>Number of Storms</u> | <u>Interval Between Storms in Days</u> |
|-------------|-------------------------|--|
| 1941 | 4 | 3, 16, 42 |
| 1942 | 0 | |
| 1943 | 0 | |
| 1944 | 3 | 14, 24 |
| 1945 | 2 | 60 |
| 1946 | 2 | 2 |
| 1947 | 5 | 88, 1, 11, 1 |
| 1948 | 4 | 19, 5, 28 |
| 1949 | 11 | 11, 6, 1, 7, 7, 1, 14, 1, 1, 33 |
| 1950 | 3 | 1, 20 |
| 1951 | 5 | 19, 18, 42, 1 |
| 1952 | 6 | 5, 12, 64, 1, 18 |
| 1953 | 3 | 13, 3 |
| 1954 | 5 | 21, 12, 18, 9 |
| 1955 | 3 | 11, 7 |
| 1956 | 2 | 19 |
| 1957 | 6 | 8, 3, 17, 1, 4 |
| 1958 | 3 | 2, 94 |
| 1959 | 5 | 49, 20, 15, 6 |
| 1960 | 2 | 87 |
| 1961 | 5 | 30, 12, 1, 14 |
| 1962 | 2 | 25 |
| 1963 | 5 | 60, 1, 13, 8 |
| 1964 | 6 | 1, 1, 19, 20, 45 |
| 1965 | 10 | 2, 26, 5, 1, 7, 14, 11, 14, 20 |
| 1966 | 4 | 10, 10, 21 |
| 1967 | 8 | 3, 2, 14, 7, 33, 9, 7 |
| 1968 | 4 | 75, 12, 6 |
| 1969 | 9 | 31, 9, 7, 27, 6, 24, 1, 11 |
| 1970 | 4 | 3, 47, 30 |
| 1971 | 4 | 60, 43, 8 |
| 1972 | 1 | |
| 1973 | 6 | 1, 43, 6, 30, 1 |
| 1974 | 0 | 31, 20, 8, 1, 13, 1 |
| 1975 | 7 | 31, 20, 8, 1, 13, 1 |
| 1976 | 2 | 108 |
| 1977 | 8 | 2, 10, 40, 16, 1, 1, 1 |